2007

The anatomy of a coastal bay/lake system

Michelle Greene
Louisiana State University and Agricultural and Mechanical College

THE ANATOMY OF A COASTAL BAY/LAKE SYSTEM

A Thesis

Submitted to the Graduate Faculty of the
Louisiana State University and
Agricultural and Mechanical College
in partial fulfillment of the
requirements for the degree of
Master of Science

In

The Department of Oceanography and Coastal Sciences

By
Michelle Greene
B.S., University of Washington, 1995
December, 2007

ACKNOWLEDGEMENTS

I would like to thank my major advisor, Dr. Harry Roberts, for being patient with me during the completion of this project and not losing hope that I would indeed finish. In addition, I would like to thank my advisory committee, Dr. Charles Wilson and Dr. Nan Walker, for providing valuable feedback. Funds for collection of geophysical data for this project were provided by the Louisiana Department of Natural Resources and the Louisiana Sea Grant College Program (Gulf Oyster Industry Program).

Thank you to Floyd Demers for all of his assistance developing my sediment sampler and preparing and assisting with my field sampling cruise and laboratory analysis. Thank you to Walker Winans for allowing me to use his computer program processing keys and Yvonne Allen for assisting me with data processing and GIS requirements. Thanks to my eternally optimistic friend Susanne Hoeppner for invaluable field work assistance and statistical input.

Last, but definitely not least, I would like to thank my loving husband, Sean and my beautiful son, Liam Indigo for graciously enduring seconded positions in exotic locations like Kazakhstan and tolerating hours of daycare to allow me the time necessary to finish my degree.

TABLE OF CONTENTS

LIST OF TABLES

LIST OF FIGURES

ABSTRACT

A comprehensive and integrated approach involving sedimentology, shallow surface geophysics and radio-chemistry was used to understand lakebed sediment dynamics in Little Lake. This methodology attempted to (1) define the morphology and origin of the lake, (2) understand the variability in lake-bottom sediments, (3) assess short-term and long-term sediment accumulation rates, and (4) image lakebed features.

Subbottom chirp, single beam echo sounder, and side scan sonar data were collected to define hydrographic depths, lateral variability in seabed sediment type, lakebed features, and shallow subsurface structure. Sediment samples were taken at representative locations throughout the lake and particle size distributions were determined. Radionuclide dating was performed on selected samples to gain an understanding of lake sediment accumulation rates.

The results indicate the lake formed as a consequence of subsidence and the amalgamation of four sub-basins to form the current lake extent. The distribution of surface sediment is controlled by basin morphology and in situ relic channel/levee deposits. The surface sediment in Little Lake is organic rich clay near tidal channels (from erosion of tidal channel banks), silt near the perimeter of the lake (winnowing by shallow wave action), and sand in the center of the lake (erosion of relic channels).

The shallow surface sediments showed three discernable accumulation layers defined as (1) short-term, < 200 days, Be-7 in the upper few centimeters with a potential riverine source, (2) event deposition, days to weeks, constant excess Pb-210 activity up to 10 cm thick interpreted as a storm deposit (Isidore and Lili, 2002) and (3) long-term, 150 years, excess Pb-210 with classic decay, 1-5 mm/year accumulation rates.

Identified lakebed features include bottom scars, marine pipelines, channels and shell beds. Bottom scars cover approximately 25% of the lake bottom and are preserved in silts and clays whereas sands are mostly devoid of recognizable scars.

This thesis is the first comprehensive study of a coastal lake/bay and represents a baseline dataset for future studies trying to understand the affects of the Davis Pond River Diversion restoration project on lakebed sediment dynamics. Data indicate that the Davis Pond River Diversion has not significantly affected Little Lake.

CHAPTER 1 INTRODUCTION/LITERATURE REVIEW

Introduction

The evolution of coastal Louisiana during the Holocene has resulted in a complex and extremely dynamic geologic system. The main depositional/geologic features comprising coastal Louisiana consist of a series of six delta complexes which formed as a result of major Mississippi River avulsions throughout the past 6000-8000 years (Frazier, 1967; Roberts, 1997). The formation of these delta complexes built the framework upon which modern sedimentation and geologic processes are occurring.

The natural evolutionary cycle of a delta complex consists of regressive and transgressive phases (Roberts, 1997). The initial fluvial dominated delta building phase persists for approximately 1000 to 1500 years. At this point, most of the river discharge is diverted down a more hydraulically efficient route to form a new delta complex. One modern example of this process is the present day Atchafalaya diversion of Mississippi River water and sediment to the central Louisiana coast. Following a relatively short period of stability (50-100 years), the transgressive marine-dominated phase will dominate and sediment supply is greatly diminished (Roberts, 1997). Sediments previously deposited during delta building phases subside and are reworked by wave action at the seaward perimeter of the once active delta and eventually form barrier island chains and submerged shoals (Penland et al., 1988; Roberts, 1997; Scrunton, 1960). Geologic evidence from each phase of this delta cycle can be found within the various delta complexes, subdeltas, and deltaic plain environments of coastal Louisiana.

One of the most highly publicized topics pertaining to Louisiana is coastal land loss. It is incumbent upon coastal scientists and engineers to dissect this issue with the aide of revised technological approaches that integrate geochemistry, geophysics, geotechnics, and hydrography. Louisiana is currently experiencing approximately 90% of the nation's coastal wetland loss

(Barras et al., 2003). The causes of land loss are numerous and include both natural and man-induced processes (Coleman et al., 1998). The socioeconomic and environmental implications of diminishing coastal lands are tremendous and include financial losses due to flooding, reduced quality of drinking water, disruptions to established urban and suburban infrastructure, loss of essential fisheries and wildlife habitat, and loss of protection from storms and hurricanes (Pilkey et al., 1989).

Coastal land loss is difficult to quantify owing to its on-going and dynamic nature. Therefore, knowledge of sediment accumulation rates and an understanding of the processes that control sediment accumulation are necessary for making informed predictions of future land loss trends and essential for restoration projects designed to maintain and re-establish the coastal marshlands. Figure 1.1 illustrates historical and recent land loss (post Hurricane Katrina and Rita) for Little Lake, the study site for this thesis.

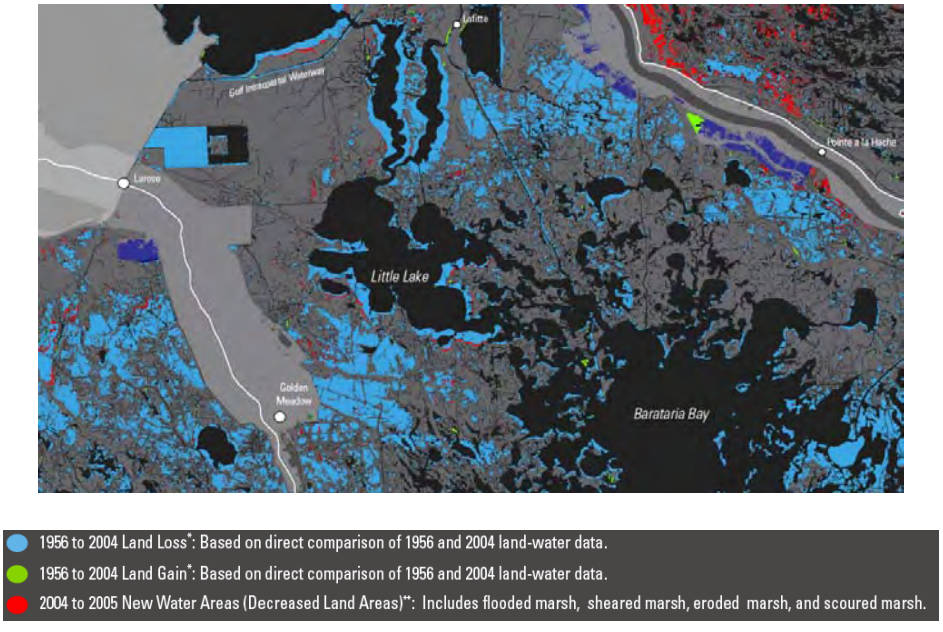

Figure 1.1. Historical and recent land loss for the study site, Little Lake, Barataria Basin (Barras, 2006).

Situation and Need

After decades of study, biologists, geologists, and engineers agree that sediment addition is the only true large-scale solution to land loss in coastal Louisiana. As such, numerous maintenance and restoration projects have been planned for reversing the land loss trends. Some of the most expansive and economically significant restoration projects have been the development and implementation of freshwater river diversions (Boesch et al., 1994). The diversions are designed to mimic spring floods, which deliver water, nutrients, and sediment to the interdistributary basins in order to maintain and build coastal marshlands. One of the questions of primary interest deals with the impact of diverted sediments on the characteristically shallow bays and lakes within the Louisiana deltaic plain. The necessity to monitor and evaluate environmental and ecological impacts of freshwater diversions is imperative. Essential baseline datasets for coastal bays and lakes are critical for successful assessment and monitoring of diversion-based restoration projects.

Given the current need for large restoration efforts in coastal Louisiana and the universal lack of baseline geologic and high resolution bathymetric data for Louisiana's coastal bays and lakes, this study was developed to provide a template for future data collection, so that we can develop a uniform baseline of bay-bottom data against which future change can be measured. This study was developed to gain a well-documented understanding of the basic geologic framework for one shallow lake in upper Barataria Bay. The goal of the study is to identify important bay-bottom characteristics that define the sub-environments of this shallow-water area. Given that no comprehensive studies of this nature have been conducted in the past, this study attempts to establish basic scientific methodologies and associated datasets for understanding and documenting geologic conditions in Louisiana's coastal lake/bay systems.

Little Lake

The study area is Little Lake, a shallow coastal lake. It is located within Jefferson and LaFourche Parishes in the Barataria Basin, Southeastern Louisiana (Fig. 1.2). This site is part of the interdistributary basin between the old LaFourche and modern Mississippi River levee systems. The study site consists of a shallow water area of approximately 125 km^2 and is centrally located in microtidal, well-mixed Barataria Bay. The exact manner in which these characteristically shallow lakes are formed has not been thoroughly investigated and is not the primary focus of this thesis; however, data collected for this thesis provides insight into the formation processes. The formation is likely linked to variations in local subsidence and compaction (Coleman, 1966). However, some researchers have postulated that subsidence associated with local faulting may be a formation mechanism (Coleman, 1966; Gagliano et al., 2003; Keucher, 1994).

The Barataria Estuary has various sources of freshwater input including precipitation, surface runoff via streams, three small Mississippi River diversion structures (Davis Pond, West Point a la Hache, and Naomi), and Atchafalaya River discharge through the Gulf Intracoastal Waterway (ICWW or GIWW) (Park, 2002; Snedden, 2006). Salinities in Little Lake measured over a 101 day time period (Dec. 22, 2002 to March 30, 2003) varied between nearly 0 ppt and 17 ppt with salinities showing a strong correlation to Atchafalaya River stage (Snedden, 2006). The largest restoration project currently underway in the Barataria Estuary is the Davis Pond Freshwater Diversion which was designed to prevent and combat the loss of coastal marshes by supplying freshwater, nutrients, and sediment to upper Barataria Basin. It is currently the largest freshwater diversion in Louisiana and the maximum design discharge rate is 10,650 cfs. Actual freshwater discharge rates, however, are determined based on hydrologic conditions and basin salinities (Fredine, 2003; USACE, 2003). Controlled releases of freshwater have occurred from

the Davis Pond Diversion structure between July 18, 2002 and present. The release of freshwater and suspended sediments has many potential long-term and short-term ecological and geological implications including changes to essential habitat. At present, we do not know the rates of change of geologic and sedimentary processes taking place within the shallow interdistributary basin lakes and bays. The baseline geologic data attained from this study will assist in future assessments of this region.

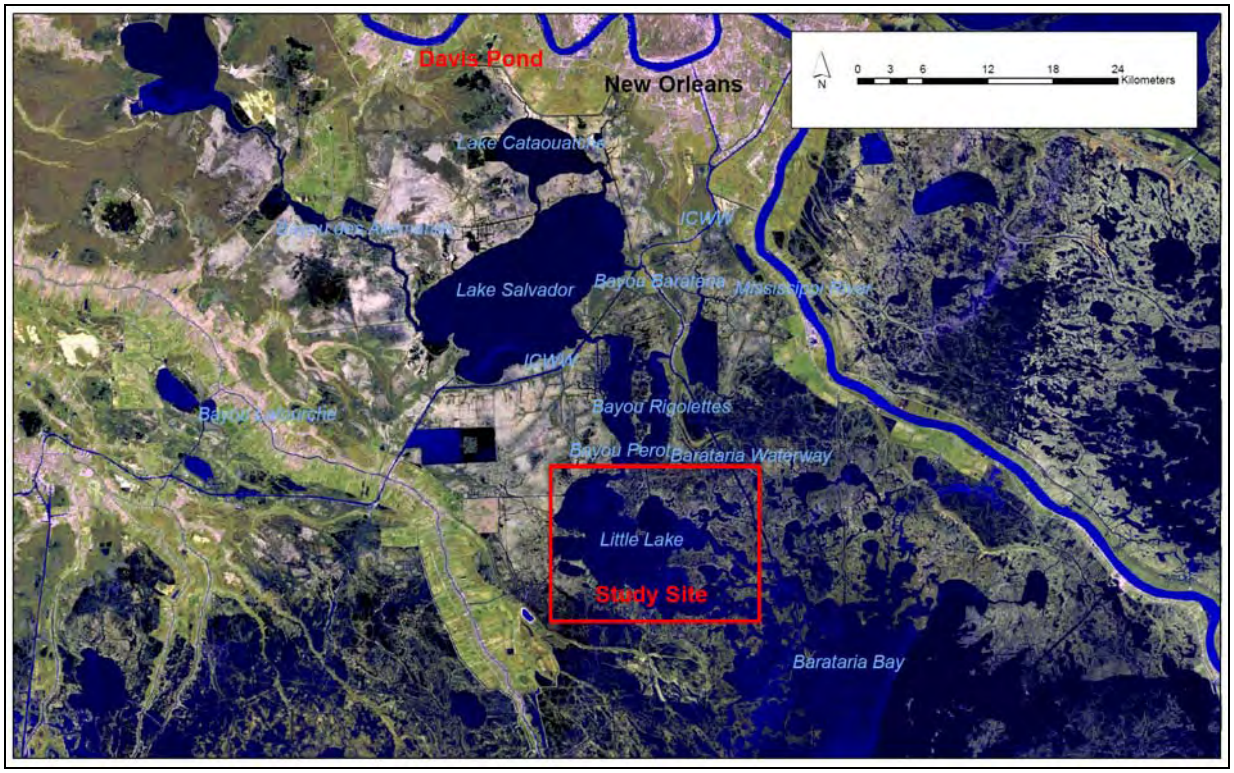

Figure 1.2. Project location, Little Lake, in relation to Davis Pond River Diversion and Barataria Basin.

The following chapters will include a qualitative and quantitative geologic assessment of Little Lake, focusing primarily on the lakebed surface. The information generated from this study will facilitate the assessment of lake-bottom variability, sediment type distributions and patterns, and shed light on the associated time scales of erosion and deposition within the limits of the analysis methods used.

Critical Research Questions - Rationale and Approach

Critical Research questions for this project include: 1) What is the origin of Little Lake and what is its lakebed morphology? 2) How does the lakebed morphology control or influence the surface sediment properties of Little Lake? 3) What are the sedimentary sequences, sediment accumulation characteristics (long and short-term), and the radionuclide signatures of the surface sediments in Little Lake? 4) Given the sediment characteristics, is the region currently impacted by the Davis Pond River Diversion? and 5) What acoustic features are present on the lakebed and do the acoustic characteristics of the lakebed correlate to the physical sediment properties?

These critical research questions were answered by 1) defining the bathymetry of the lake bed; 2) developing surface geologic maps of sediment properties 3) defining sedimentary sequences and determining present day (short-term) and historical (long-term) lake bottom sediment accumulation rates; 4) determining the spatial distribution of short-lived, riverine derived, radionuclide Be-7 activities and 5) conducting a qualitative and quantitative analysis of the acoustic side scan sonar mosaic. The above questions were addressed through the integrated analysis of geophysical datasets, sediment cores, sediment analysis, and radionuclide dating techniques. All of the data and data-reduction products derived from the study are now available as baseline information against which future change in Little Lake can be measured.

CHAPTER 2 LAKE BED MORPHOLOGY

Introduction

There is a lack of data available to characterize the seabed of the shallow lakes and bays of coastal Louisiana. Sounding data currently available from navigation charts is of low resolution, outdated, and largely inadequate for understanding much about the lake and bay bottom (Fig. 2.1). Knowledge of the detailed bathymetry of the coastal zone is essential, not only for safe navigation but also for understanding physical processes such as circulation, sediment accumulation patterns, and the interrelationships between the physical and biological processes. Management decisions regarding coastal land loss in Louisiana are at times based on information obtained from numerical models, which require high resolution bathymetric data as input. Efforts have been made to compile bathymetric data for the Barataria Basin and other regions of coastal Louisiana for modeling purposes, however, data are still sparse in many locations (Reyes, 2006).

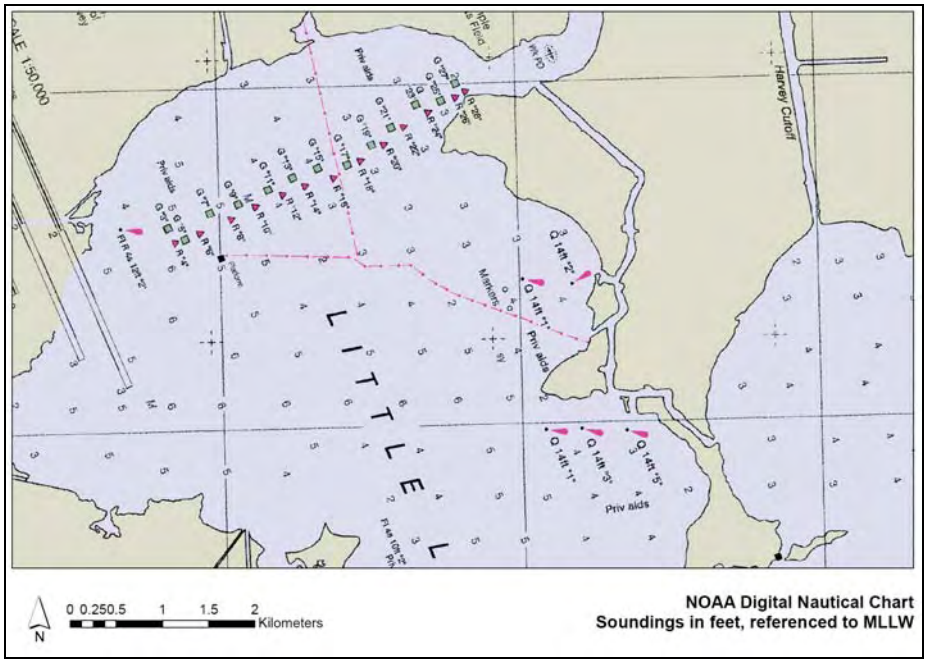

Figure 2.1. Bathymetric soundings in Little Lake available through NOAA website.

In addition to traditionally acquired bathymetric data, recent technological advances have made it possible for the acquisition of extremely accurate topographic and hydrographic datasets through the use of LIDAR (LIght Detection and Ranging) aerial surveys. However, turbid water common to the Mississippi delta limits this method of data collection. Topographic data, acquired by airborne LIDAR, is available for the coastal regions of Louisiana.

Utilizing software applications such as NOAA's VDATUM (Milbert and Hess, 2001), topographic elevations and bathymetric depths can be converted to a harmonious vertical frame of reference. The combination of high resolution topographic and bathymetric datasets allows for the seamless integration of land and water data into a single elevation model. These reasonably accurate, high resolution elevation models are critical to the management of Louisiana's coastline and for assessing elevation changes.

Objectives

The objective of this portion of the study is to determine the lakebed morphology and origin of Little Lake. A detailed bathymetric map and associated bathymetric surfaces for the lakebed were created. This high resolution baseline bathymetric dataset will facilitate an understanding of how the morphology of the basin relates to estuarine circulation, sediment distribution and accumulation, and the formative processes of coastal bay/lake systems.

Methods

The project objectives were accomplished through the use of hydrographic and geophysical datasets. The hydrographic and geophysical data for the Little Lake project were collected between June 15 and July 8, 1999. Data collected during this time frame included single beam echo-sounder data, dual frequency digital side scanning sonar data, and single channel subbottom chirp sonar data.

The geophysical datasets utilized for this study were collected onboard a 12.5 m (41 ft) LOA x 4.8 m (16 ft) wide Lafitte Skiff, the *M/V High Roller*. All horizontal positioning and associated datasets were collected with the use of an ASHTEC GPS system with differential positioning corrections provided by SATLOC, resulting in submeter horizontal accuracy. The GPS antenna was mounted midships. The geophysical instrumentation was mounted at various locations on the vessel and offsets were applied to the acquired GPS positions for generation of true acquisition position. A description of the data acquisition instrumentation and techniques is described by Roberts et al. (2000; 1999). Figures 2.2 and 2.3 illustrate the unique vessel configuration necessary for geophysical surveying in the shallow water environments of coastal Louisiana.

Single beam bathymetric soundings were acquired along east-west oriented tracklines throughout the entire study site (Fig. 2.4) with the use of a 200 kHz Odom Hydrotrac echosounder. The trackline spacing was approximately 150 m and soundings were extracted from the sonar file at approximately 20 s intervals resulting in an along-track sounding spacing of nearly 50 m and a total of 18,696 individual soundings. Since the echosounder transducer was centrally located on the vessel near the GPS antenna, no lateral offsets/corrections were applied to the horizontal sounding positions (Allen, 2003).

Various vertical offsets were applied to the raw bathymetric soundings (post-acquisition) to establish a standard vertical frame of reference, essential for incorporating and comparing the bathymetric data with other available datasets. First, a vertical offset was applied to all raw soundings to account for the transducer mounting location 0.3 m below the water surface. In addition, tidal offsets/corrections available from the nearest NOAA tide station 876124 Grand Isle, LA, were applied, resulting in a bathymetric dataset reduced to a Mean Lower Low Water vertical datum (MLLW). Figure 2.5 illustrates the location of the reference tide station in

relation to the study site. The NOAA water level/tide data were obtained from the NOAA Center for Operational Oceanographic Products and Services website (NOAA, 2006). Verified 6-minute interval water level data in meters above/below MLLW, UTC time, were downloaded from the above specified station. Water level fluctuations for the entire field program ranged from 0.10 m below MLLW to 0.54m above MLLW. However, geophysical survey operations occurred during high tide with water levels fluctuating between approximate 0.09 and 0.54 m above MLLW and averaging 0.35 m above MLLW (Fig. 2.6). The water level data and original bathymetric soundings were imported into Microsoft Access and a visual basic script was used to match tidal water level offsets values to the appropriate bathymetric soundings based on concurrent date and time.

A tool developed by the NOAA Office of Coast Survey and Geodetic Survey, VDATUM, allows for the transformations of tidally derived vertical datums, such as MLLW to orthometric datums such as NAVD88 and 3-dimensional datums such as WGS84 utilizing localized geoid models (NOAA, 2004). Although a vertical transformation model is available for portions of southern Louisiana, the entire Little Lake study site did not fall within the bounds of the VDATUM geodetic model. Therefore, a straight offset value of 0.167 m, obtained from the Grand Isle tidal station (Fig. 2.7), was applied to all soundings to convert the vertical datum from Mean Lower Low Water to NAVD 88, congruent with the vertical datum of the adjacent terrestrial LIDAR data available for this region. No vertical offsets were applied to compensate for the heave and squat/dynamic draft of the vessel, however, the 0.3 m initial offset reflects the transducer location at cruising speed of approximately 4.5 to 5.0 knots. Figure 2.8 illustrates various vertical offsets applied to the bathymetric dataset.

Corrected bathymetric soundings were verified utilizing cross section profiles in areas of data overlap. Potential errant soundings were deleted from the dataset and sounding data not

relevant to the Little Lake study site were removed. Spatial and summary statistical analysis was completed to determine tends in the dataset.

Figure 2.2. Instrument configuration associated with the survey vessel. Side scan sonar was mounted on the bow and the subbottom chirp fish was mounted on starboard side of the vessel.

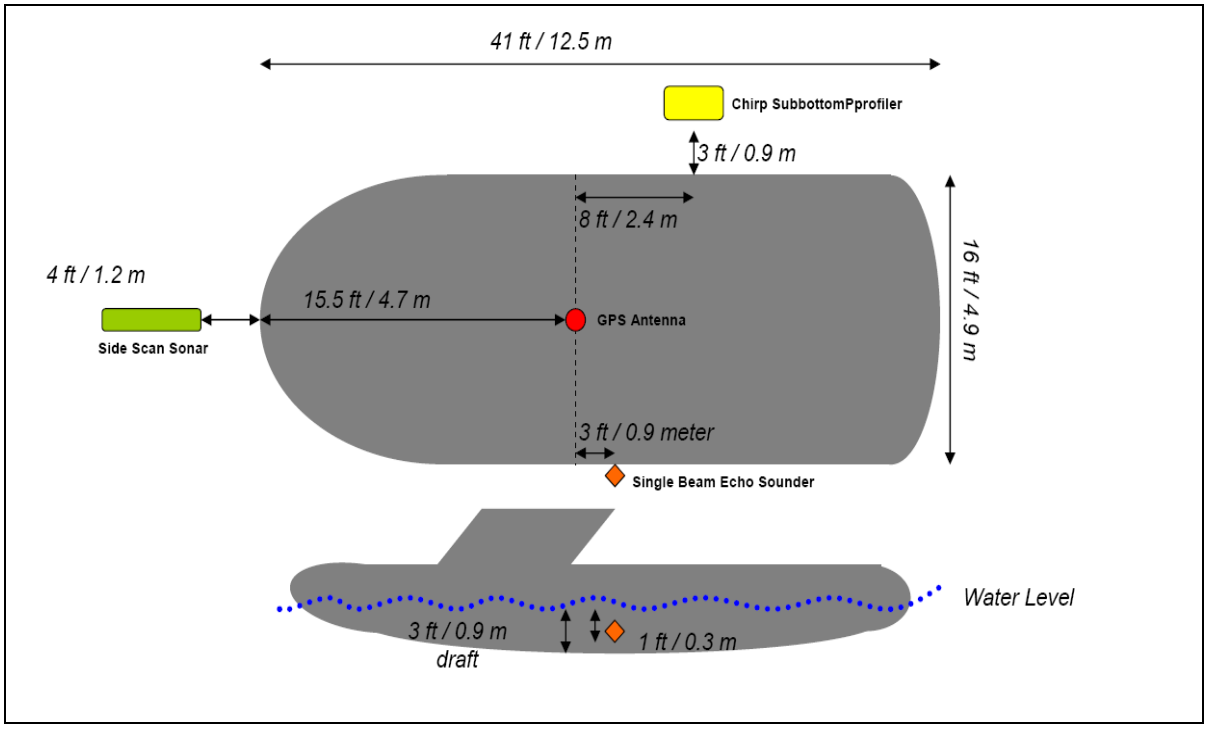

Figure 2.3. Geophysical survey vessel configuration and all offset measurements.

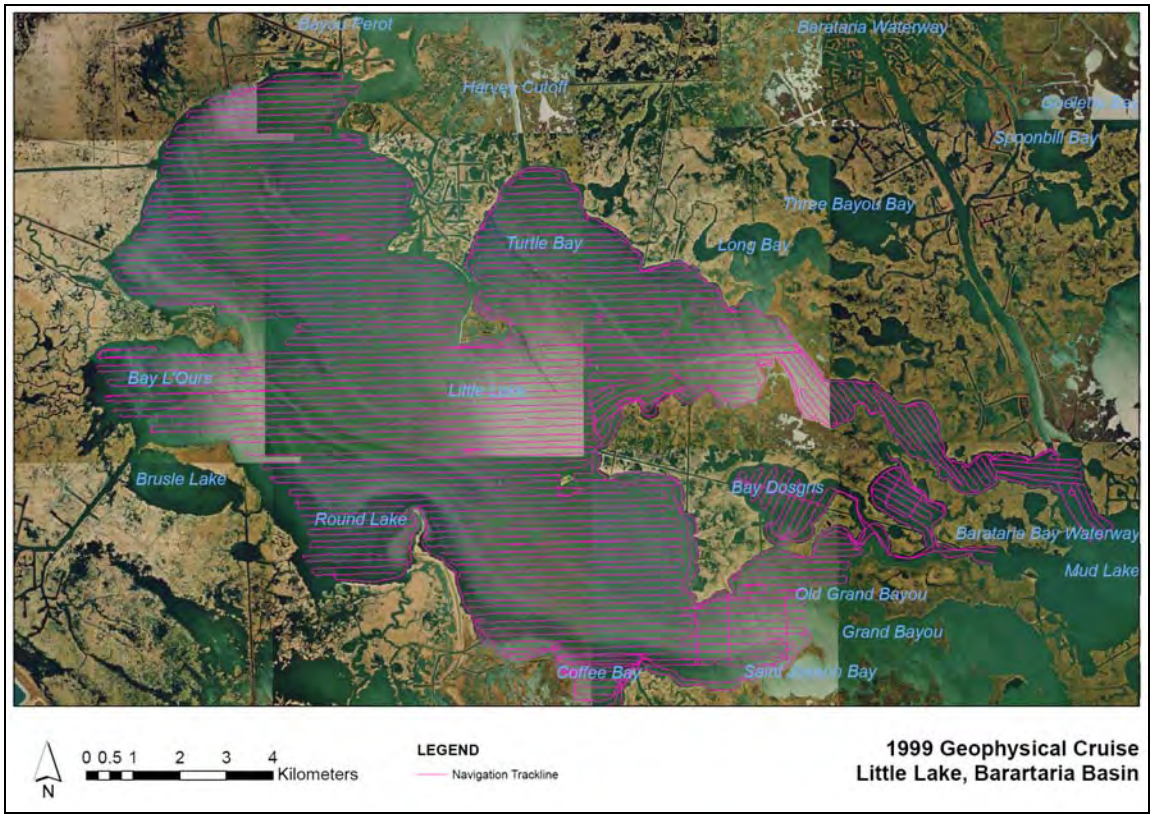

Figure 2.4. Survey vessel navigation tracklines.

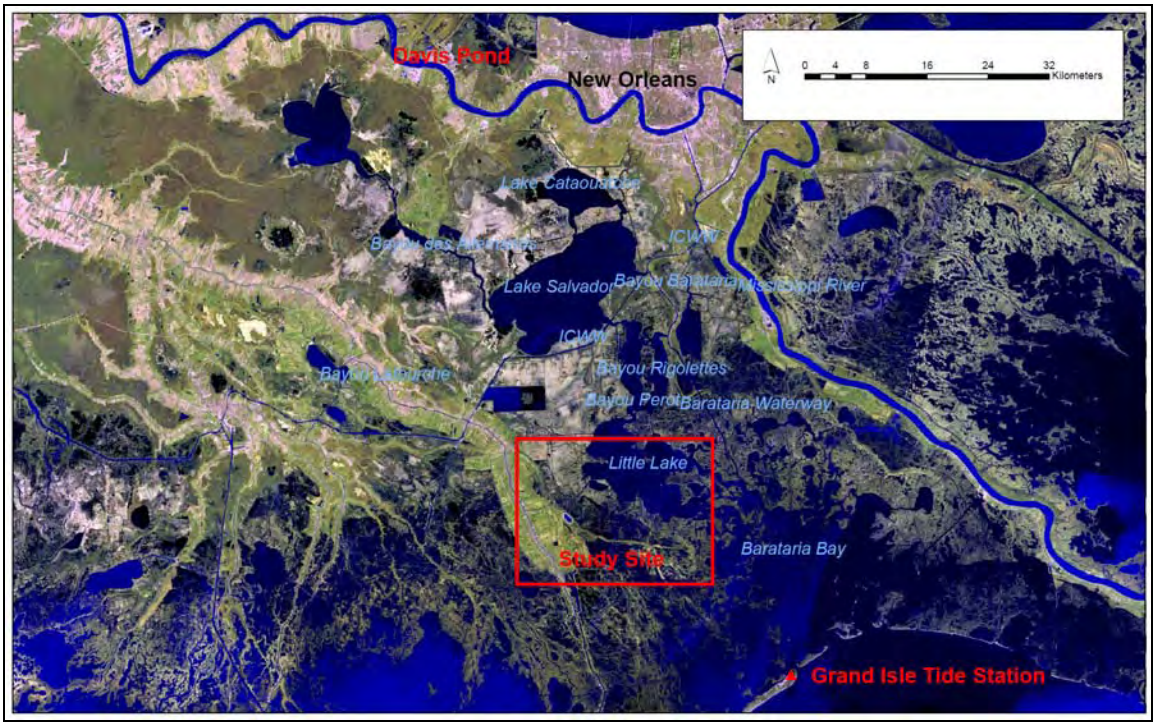

Figure 2.5. Tide station location in relation to Little Lake.

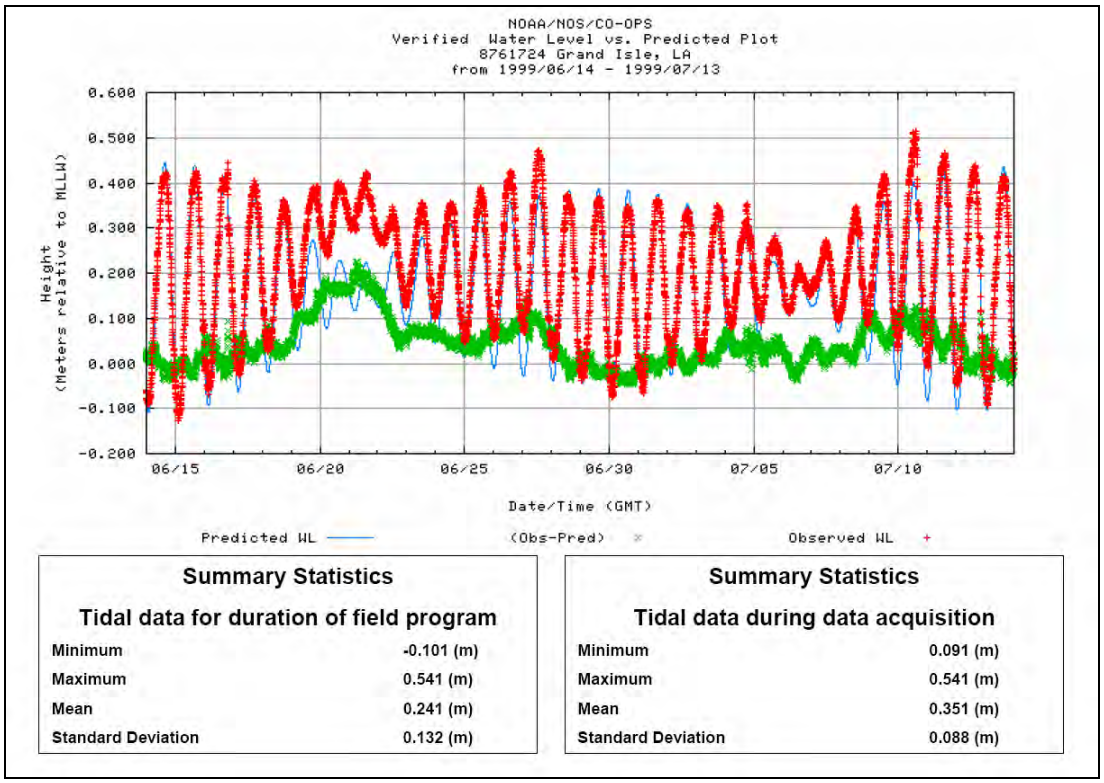

Figure 2.6. Tidal range data for June 14 – July 13th, 1999. Geophysical data acquisition occurred during high tide.

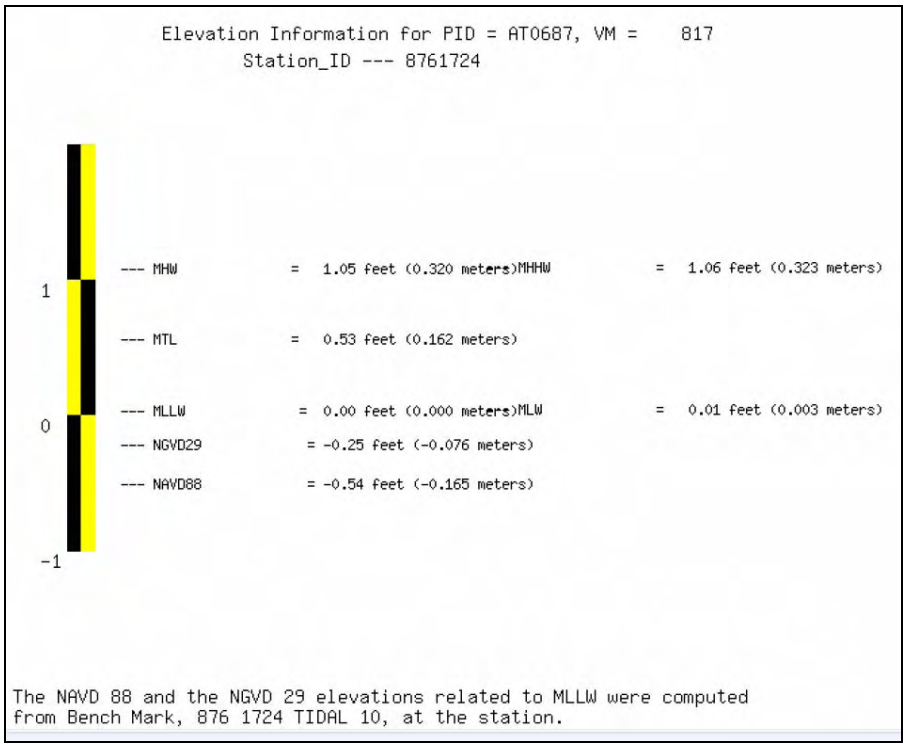

Figure 2.7. Elevation information for Grand Isle tide station.

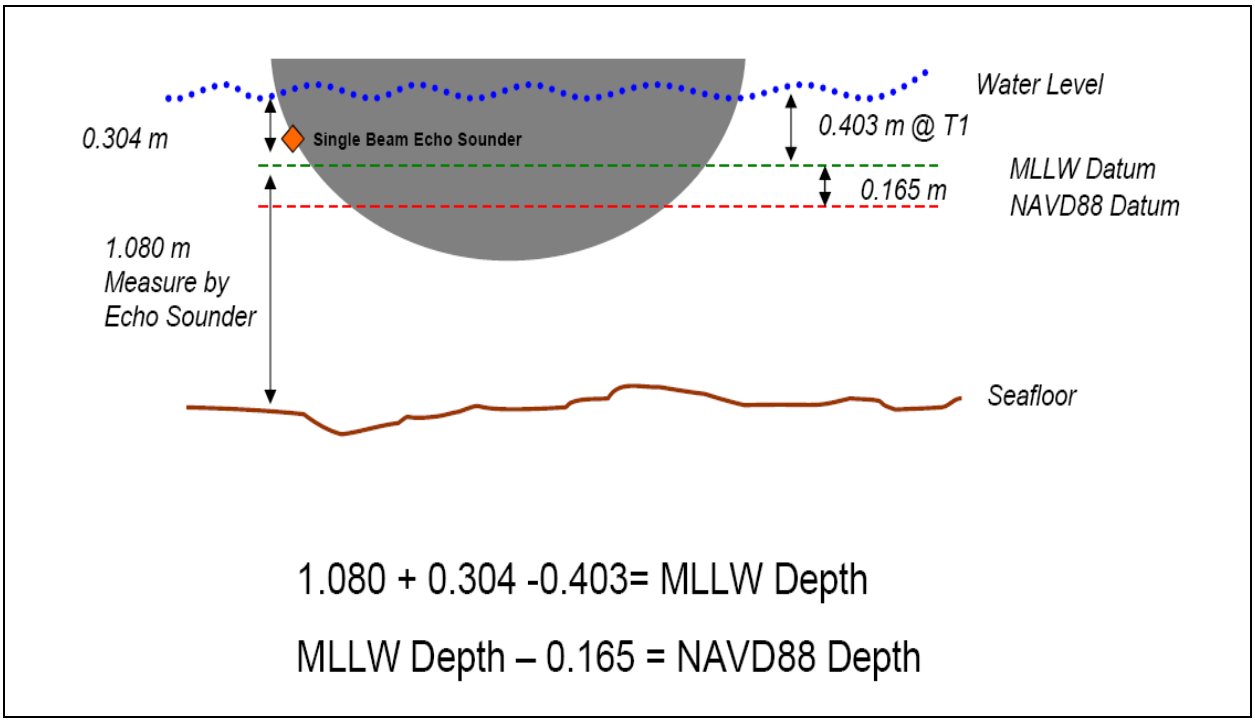

Figure 2.8. Vertical offsets applied to raw bathymetric soundings.

Bathymetric surfaces and contours were created from the corrected soundings. Originally, a Triangulated Irregular Network model (TIN) was utilized to create a bathymetric surface. A TIN model is a set of contiguous and non-overlapping triangles where sample points are connected by lines to create triangles. Each triangle represents a vertical plane with a specific slope and aspect. However, owing to sparse data density in the across-track direction and dense data in the along track direction, the TIN model was coarse and did make for an esthetically appealing or smooth surface model and contours. Therefore, kriging, a geostatistical approach that incorporates the spatial correlation between neighborhood points, was used to create a bathymetric surface. The krigged surface created using ESRI ArcMap Geostatistical Analyst was modeled using a spherical Semivariogram. Once a satisfactory bathymetric surface was obtained, bathymetric contours were created for Little Lake.

Results

Statistical Analysis

Summary statistics for the bathymetric soundings in the Little Lake study site indicate a tide corrected (MLLW) depth range between 0.02 m and 8.78 m (Fig. 2.9). The average water depth for the site is approximately 1.5 m. The data distribution is slightly positively skewed with more depths in the < 2 m range. A statistical test for normality (Shapiro-Wilk) could not be run on the dataset as a result of the large number of data points. The dataset was assumed to be normally distributed for the purpose of contouring.

Minimum	0.023
1st Quartile	1.137
Mean	1.495
Median	1.453
3rd Quartile	1.769
Maximum	8.780
Total N	18696
Standard Dev	0.634

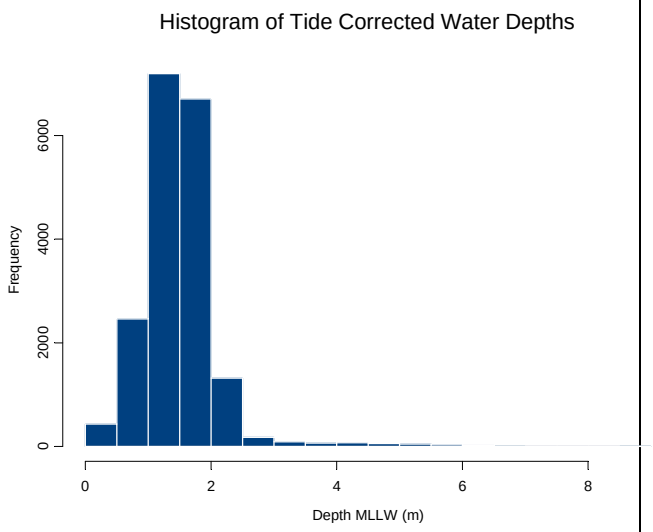

Figure 2.9. Summary Statistics for Water Depth (meters MLLW).

Bathymetric Surfaces

A snapshot of the resultant corrected bathymetric soundings is shown in Figure 2.10. This figure illustrates the difference in data density between the newly acquired bathymetric soundings and those soundings currently presented on the nautical chart for the region. The krigged bathymetric surface and contour map are also presented below (Figs 2.11 and 2.12).

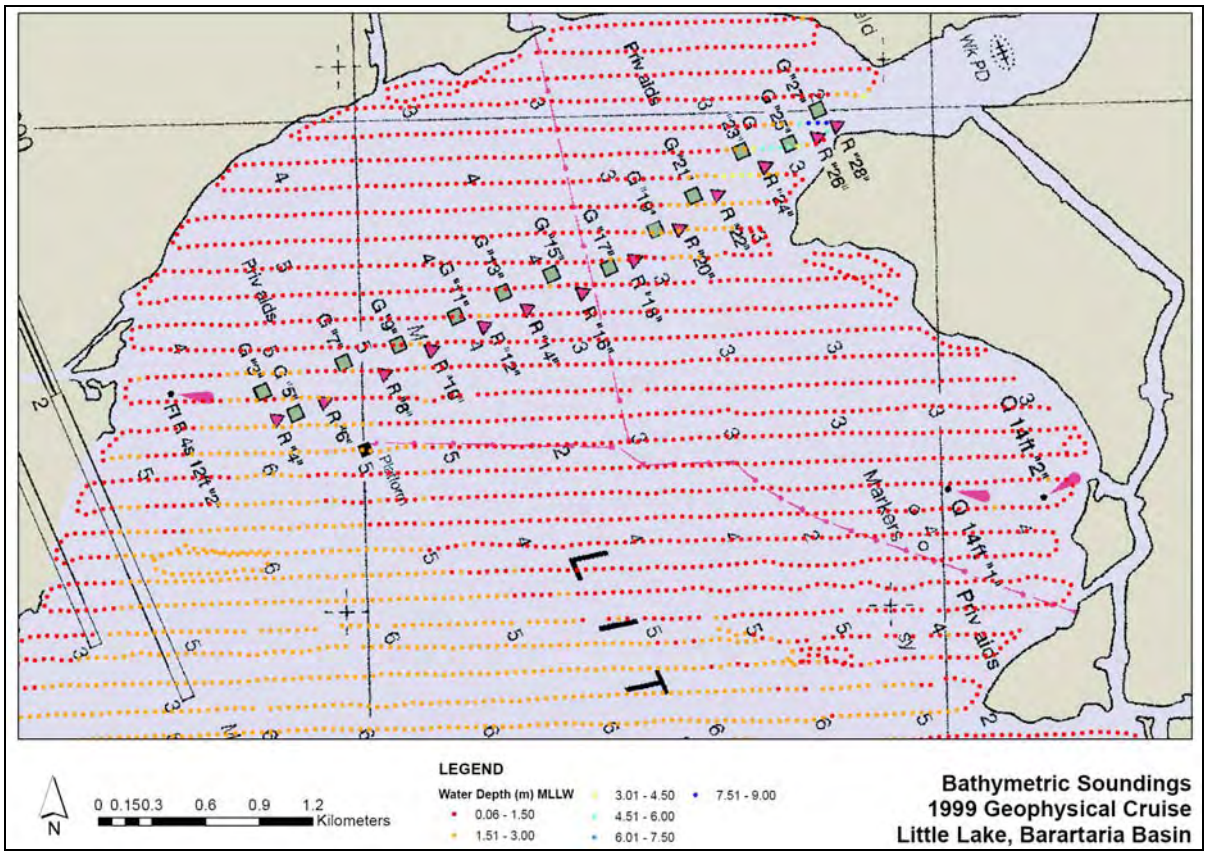

Figure 2.10. Resultant bathymetric soundings and sounding data available on NOAA nautical charts.

Lakebed Morphology

The morphology of Little Lake can be subdivided into various channels and basins (Fig. 2.13). There are three large tidal channels which input into the study site including a deep main channel (CHANNEL 1), draining Bayou Perot and Bayou Rigolettes, and two main sinuous tidal channels (CHANNEL 2 and CHANNEL 3), Bayou St. Denis and Grand Bayou, which lead into the eastern portion of Little Lake. In addition to these natural tidal channels, a large man-made canal (CANAL, Harvey Cutoff), enters the study site from the north into Turtle Bay. Four large basins comprise the bulk of the study site. These basins include, the North Basin, Central Basin, South Basin, and Turtle Bay Basin.

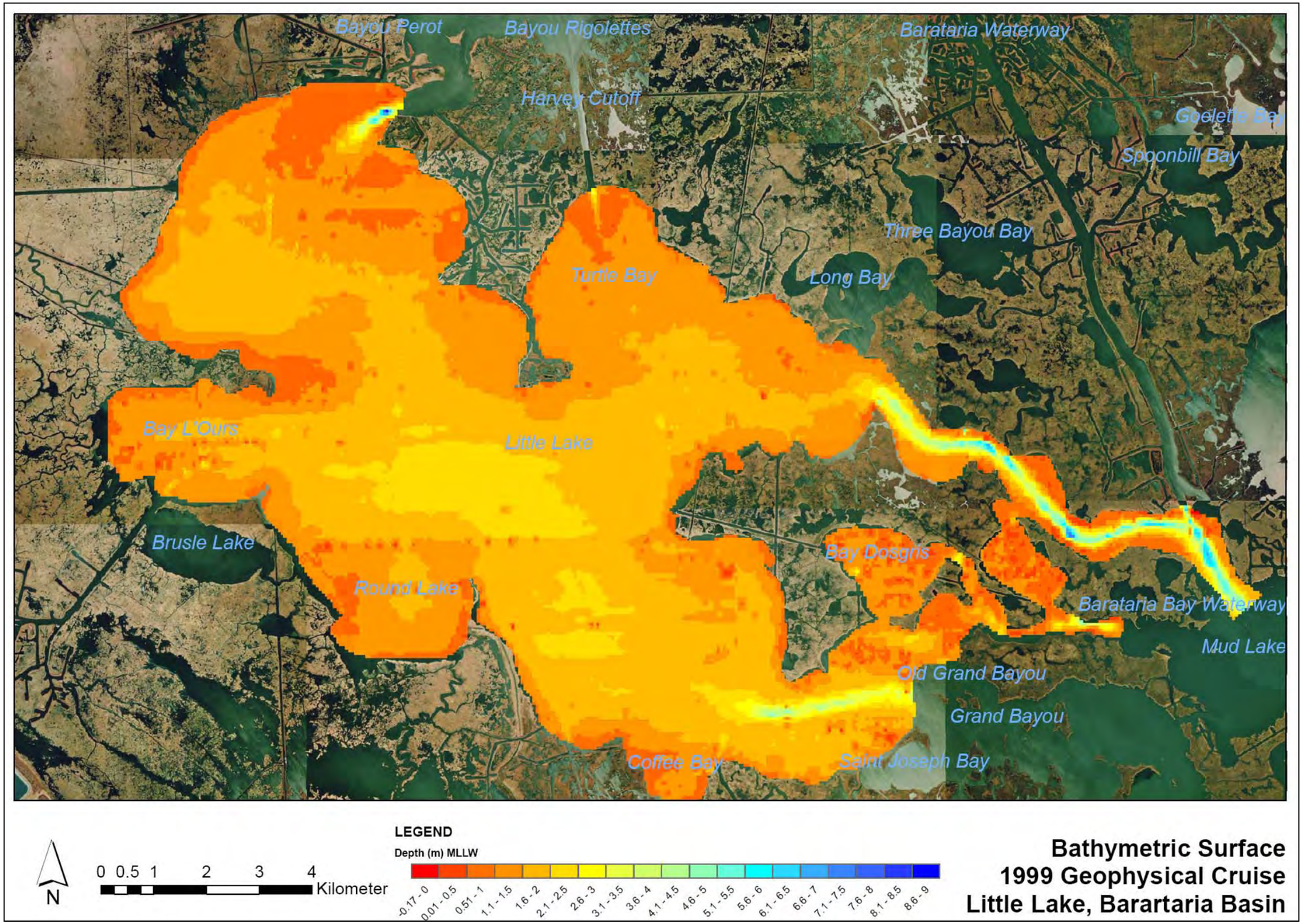

Figure 2.11. Final bathymetric surface referenced to MLLW. Color contour interval is 0.5 m.

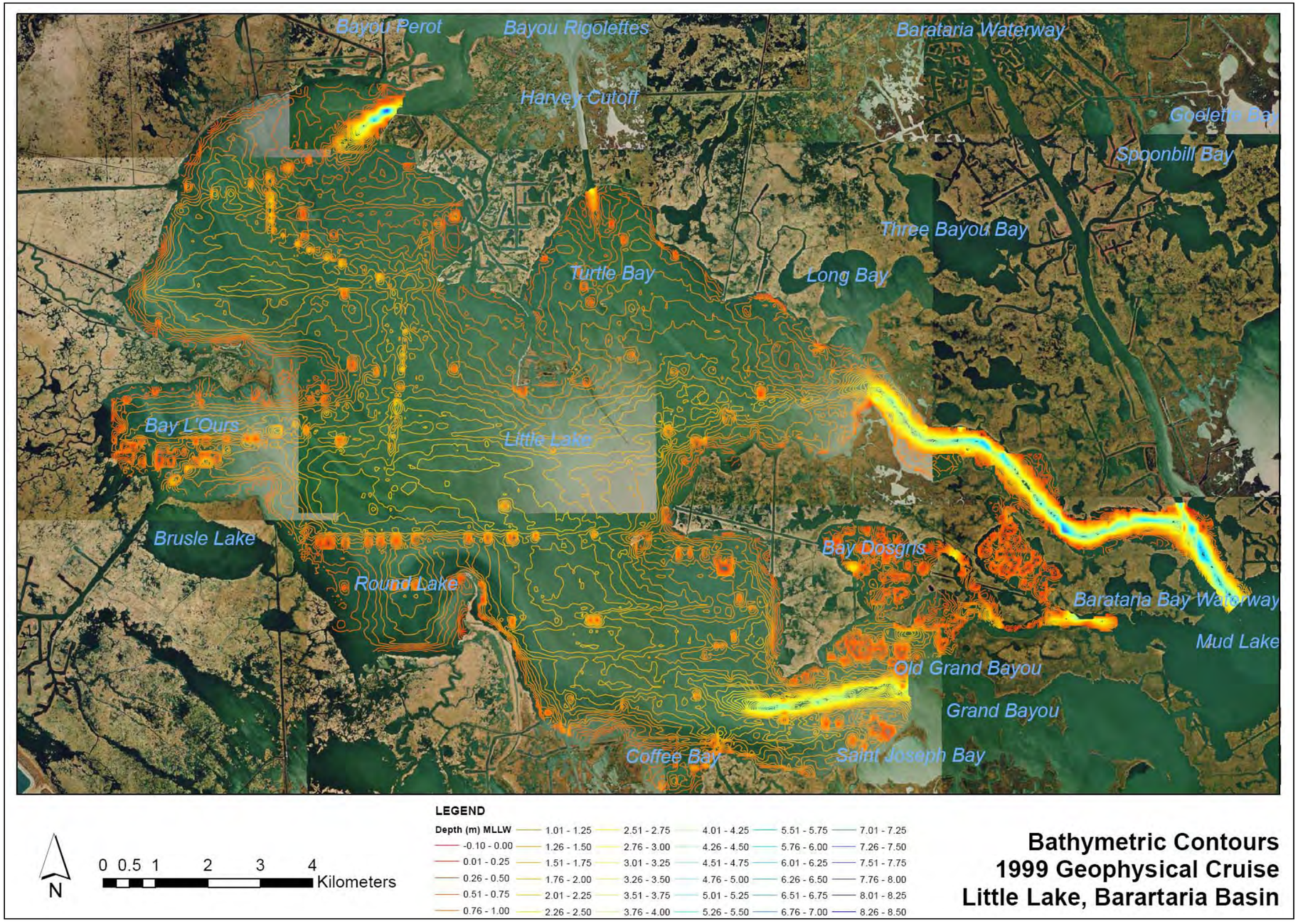

Figure 2.12. Final bathymetric contours referenced to MLLW. Contour interval is 0.25 m.

The deep main channel in the northern portion of the lake (CHANNEL 1) reaches a maximum depth of 8.5 m with a width and length of approximately 650 m and 1750 m, respectively (Fig. 2.13). The man-made canal (CANAL) which drains into Turtle Bay is narrower (approximately 300 m wide), greatly abbreviated (800 m in length), and only reaches a maximum depth of 3.3 m. The two channels in the eastern portion of the study site (CHANNEL 2 and CHANNEL 3) have maximum depths of 4.7 m and 7.1 m with the northern channel being the deeper of the two. The eastern channel lengths and widths vary from 3700-9000 m (length) and approximately 400-500 m (width).

The remaining regions of the lakebed can be categorized into various sub-basins, 1) North Basin, 2) Central Basin, 3) South Basin, and 4) Turtle Bay Basin (Fig. 2.13). These sub-basins are characterized as areas of relatively little bathymetric relief and comprise approximately 80 % of the lake area. Water depths in the North Basin range from nearly 0.0 to 2.6 m with an average depth of 1.4 m. The Central Basin ranges in water depth from nearly 0.0 to 2.7 m with an average depth of 1.6 m. The smaller South Basin has depths in the range of 0.0 to 2.2 m with an average depth of 1.5 m. The Turtle Bay basin ranges in depth from nearly 0.0 to 2.2 m with an average depth of 1.3 m.

Anthropogenic features were also identified in the bathymetric surfaces. These features include a series of pipelines that extend from the North Basin to the Central Basin. In addition, there are many shoal regions in the North and Central basins which could be associated with manmade features or perhaps prehistoric shell middens.

Summary

The detailed bathymetric data and contours reveal three main tidal channels and one larger man-made canal (Harvey Cutoff) as direct inputs into the lake. In addition, four main

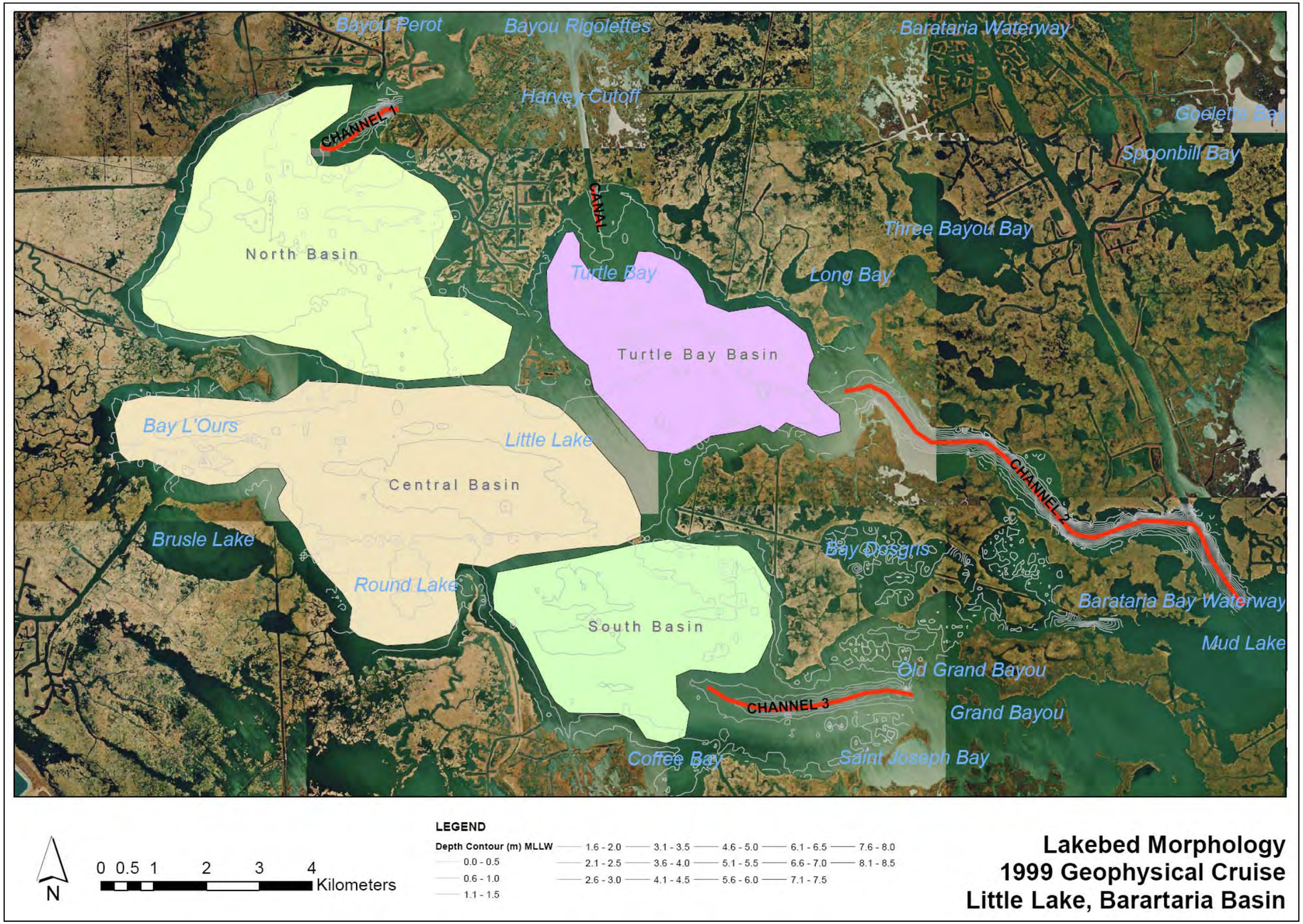

Figure 2.13. Little Lake lakebed morphology with basin and channels indicated.

sub-basins exist which make up the majority of the lakebed area. With the exception of a few manmade features such as pipelines or dredged channels, these four sub-basins exhibit very little bathymetric variability.

The formation of Little Lake appears to be the result of regional subsidence and a decrease in sediment supply combined with bank erosion, salt water intrusion (fresh marsh deterioration) and subsequent bank undercutting and channel enlargement. The submergence of adjacent marshland depressions also appears to be important. The bathymetric data define sub-basins within Little Lake that appear to have subsided, enlarged, fused and amalgamated to form the present lake. Figure 2.14 illustrates this process as Brusle Lake is amalgamated into the central portion of Little Lake from 1998 to 2005.

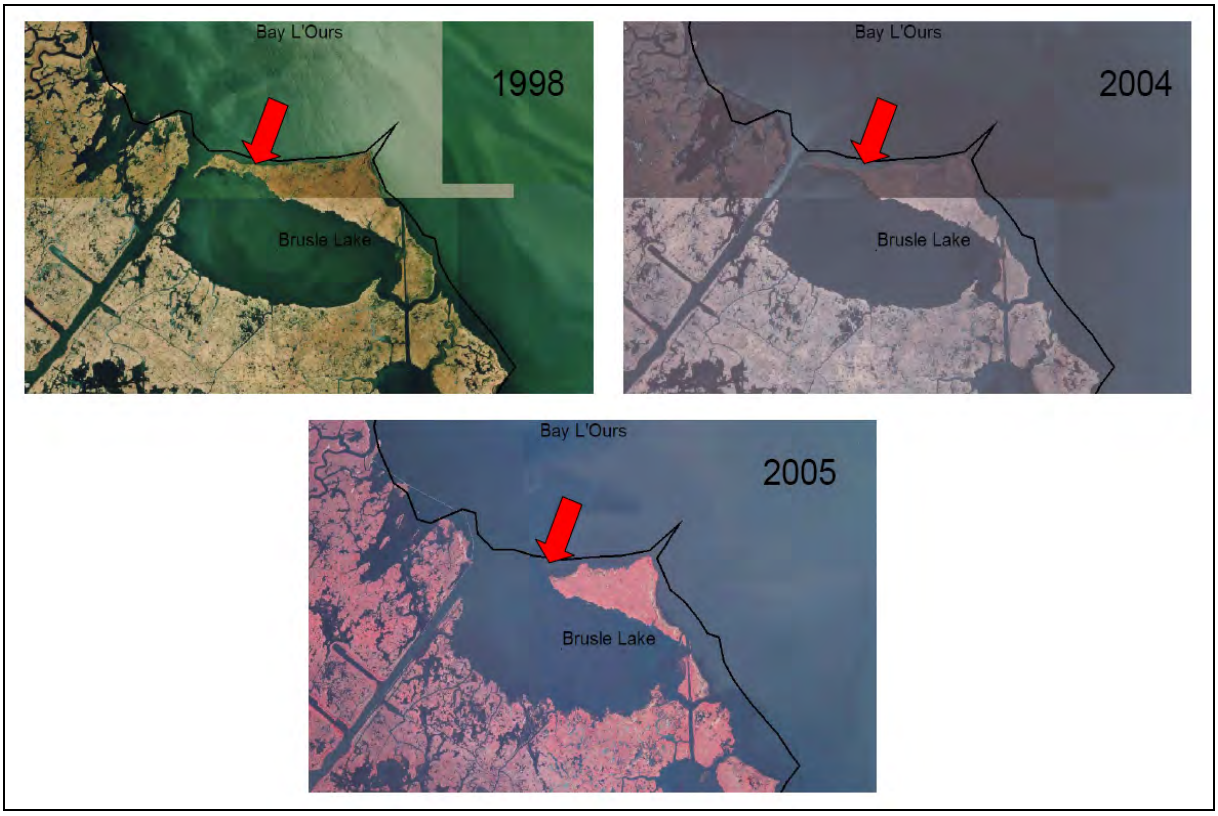

Figure 2.14. The amalgamation of Brusle Lake from 1998 to 2005.

CHAPTER 3 SPATIAL DISTRIBUTION OF SURFACE SEDIMENTS

Introduction

Currently, sediment suspension and deposition patterns in the shallow lakes and bays of coastal Louisiana are controlled mainly by long-term and short-term variability in basin morphology, sea level, river discharge, flooding, channel migration, dominant tidally-driven flows, wind-driven currents, and wave action associated with storm events (Dyer, 1995; Frey and Howard, 1986). Erosion of the lake margins and adjacent marshland also provide an important source of sediment to the lake. Changes in the hydrologic regime, either anthropogenically induced (large-scale restoration projects such as river diversions) or naturally occurring (storm events, increased water levels/flooding), have an impact by introducing, resuspending, and depositing sediments within these regions.

Recent studies of the effects of the Caernarvon River Diversion indicated suspended sediment concentrations entering the diversion structure from the Mississippi River ranged from 40 – 252 mg/l and averaged 118 mg/l (Lane, 2003; Lane et al., 1999). Seasonal fluctuations were observed with low concentrations in the late summer and early fall and high concentrations during the winter and spring (Lane, 2003; Lane et al., 1999). In addition, during large diversion pulses, sediments originating from the Caernarvon diversion were detected in the Breton Sound Estuary up to 10-15 km away (Lane, 2003). These seasonal and diversion-related fluctuations in suspended sediment concentration will affect the sediment distribution and accumulation rates in related down-basin shallow lakes and bays as recently shown by Wheelock (2003).

Objectives

The objective of this portion of the study is to determine how the lakebed morphology controls or influences the surface sediment properties within Little Lake. This objective was

accomplished through the compilation of physical sediment properties such as grain size, water and organic content, and estimated shell content.

Methods

Seabed Sampling

Sediment sampling in the field was driven by differences in lakebed acoustic response determined from analysis of the side scan sonar data. Utilizing the sonar imagery, a stratified random sampling technique was implemented to ensure that each sediment type, which exhibited a unique acoustic signature, was sampled. The stratified random sampling was derived from a sonar mosaic that was subsequently classified into six separate preliminary acoustic signatures based on a technique called Jenks Optimization or Natural Breaks (backscatter values of 0-40, 41-94, 95-125, 126-160, 161-202, 203-255). Sample locations where randomly chosen and included multiple locations within all six preliminary classes. The planned sample locations were entered as waypoints into ChartView Pro, a navigation software package used during the field sampling program.

Owing to the shallow water nature of the study site, surface sediment samples were collected with a sampling device which consisted of a long extendable pole, with an attached sampling cup. Figure 3.1 illustrates the sampling device.

Field sampling was undertaken between October 13, 2003 and October 16, 2003 onboard the 7.9m (26 ft) TwinVee Weekender, *Tiger 1*. Sampling operations were based out of the Lafitte Marina and took place during daylight hours. Surface sediment samples were acquired in shallow water utilizing the surface sediment sampler. Where depths prohibited the use of the surface sampler, a Van Veen grab sampler was utilized. Geographic sample locations were acquired and recorded with the use of a WAAS enabled GARMIN GPS-5 global positioning

system integrated with the navigation software. This GPS device typically produces a horizontal accuracy of ±3 m. Surface samples were acquired, homogenized, and split onboard the vessel and were placed in appropriate sample bags. Upon return to LSU, the samples were preserved in cold storage until further laboratory analysis was undertaken.

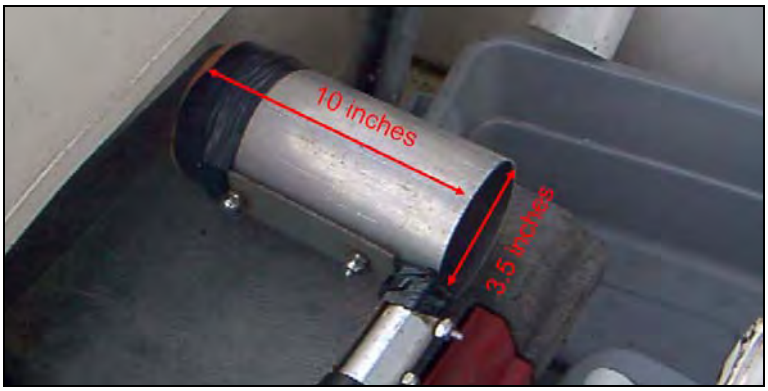

Figure 3.1. Surface sediment sampling device.

In addition to the surface and Van Veen sediment samples, additional surface sediment samples were obtained by homogenizing the top 3 cm of box cores collected during the same sampling cruise. The box cores were collected to determine sediment accumulation rates using radionuclide dating techniques and will be discussed in the subsequent chapters. Figure 3.2 illustrates the sample locations of all surface sediment acquired for this project.

Laboratory Analysis

Surface sediment samples were analyzed for total water and organic content, shell content, and grain size. An estimate of shell percentage was done prior to laboratory analysis by using visual percentage estimating diagrams commonly used in field geology (Compton, 1985). Water content was determined gravimetrically after placing each sediment sample in a 100°C drying oven until a constant weight was attained. Volatile solids (organics) were then determined by weight loss on ignition in a 400°C muffled furnace for 4 hours (Sawlan, 1976).

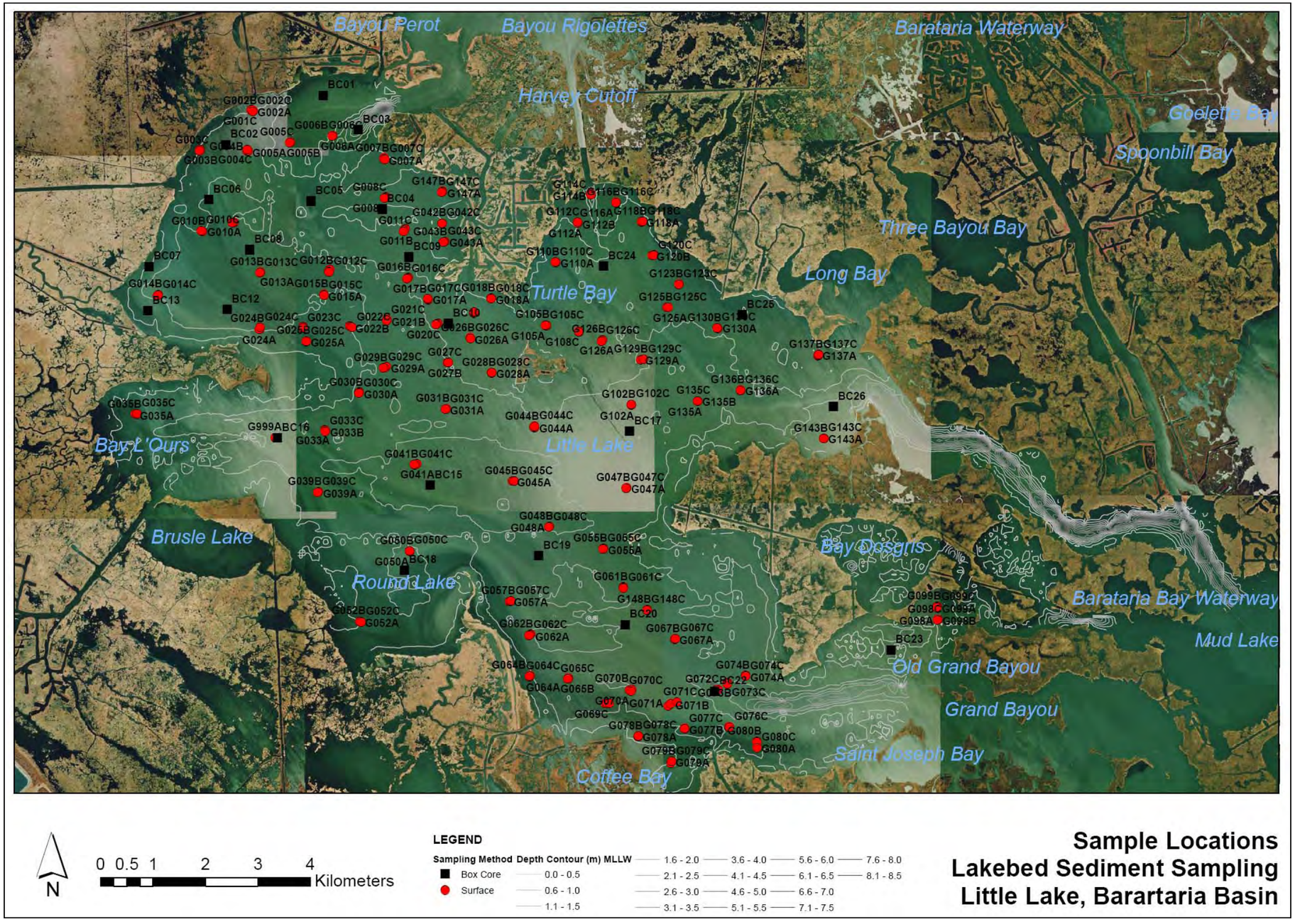

Figure 3.2. Surface sediment sample locations.

Prior to granulometric analysis, samples were pretreated with 30% hydrogen peroxide until no further evidence of organic digestion (Sawlan, 1976). Samples were placed in an ultra-sonic bath and then separated into a coarse (> medium sand) and fine fraction (< medium sand) by wet sieving through a 250 µm sieve. All particulate matter retained on the 250 µm sieve was noted (> medium sand, organics, shells) and the finer fraction was dispersed with one part 0.05% sodium metaphosphate (de-flocculent) and one part glycerin (increases viscosity) prior to granulometric analysis. Granulometric analysis of the fine fraction was completed with a Micromeritics ET-5100 Sedigraph particle analyzer (Coakley and Syvitski, 1991). Samples were analyzed for particles ranging in size from less than 250 µm (very fine sand) to less than 3.9 µm (clay). Total percentages of sand (250 µm – 62.5 µm), silt (62.5 µm – 3.9 µm), and clay (less than 3.9 µm) were calculated for each sample. Summary statistics were calculated for the resultant sand, silt, clay, water, mineral and shell content. The results were entered into a GIS and graduated symbol and contour maps were created to illustrate the spatial distribution of the various physical sediment properties within Little Lake. Iso-lines for sediment properties were created using the ESRI Geostatistical Analysis radial basis function with the following settings (Fig. 3.3).

Selected Method: Radial Basis Functions

Method Parameter(s):
- **Kernel Function:** Completely Regularized Spline
- **Anisotropy:**
  - **Angle:** 90.00
  - **Ratio:** 1.00

Parameter: 2.6024

Searching Neighborhood:
- **Neighbors to Include:** 15 (include at least 10)
- **Searching Ellipse:**
  - **Angle:** 0
  - **Major Semiaxis:** 4977.8
  - **Minor Semiaxis:** 4977.8
  - **Sector Mode:** 0

Figure 3.3. Surface sediment contouring model parameters.

Results

Physical Sediment Properties and Summary Statistics

Surface sediment sand content (250 μm – 62.5 μm) for Little Lake ranged from 0% to nearly 65%. Average sand content for the entire region was 18%. Figure 3.4 illustrates a non-normal, positively skewed distribution of sand content for all samples. The majority of the samples contained less than 30% sand.

The silt content of surface sediment samples varied for the region from a low of 2% to a high of 90%, averaging 50% throughout the study site. The data were normally distributed. Clay content of the surface sediment samples averaged 38% with values ranging from a minimum of 0% to maximum value of 97%.

Visual shell estimates encompassed the full spectrum ranging from samples with no shell content to samples with nearly 100% shell content. The average shell content for the region was approximately 11% with the bulk of sediment samples containing less than 10% shell (Fig. 3.5).

Moisture content for the surface sediment samples ranged from 26% to 84%. The average moisture content was 54%. Figure 3.6 illustrates the frequency of sediment moisture content for all samples from the study.

Organic content in the surface sediments ranged from 2% to 40%. The average organic content for all samples was 8% as illustrated on Figure 3.7. Table 3.1 summarized all of the measured physical sediment properties for the surface sediment samples collected in Little Lake.

Spatial Distribution of Sediment Properties

Graduated symbol and contour maps were created to illustrate the spatial distribution and local variability of the physical sediment properties discussed above. Regions of high sand content (greater than 30%) are confined mainly to the eastern portion of the Central Basin and

northwest margin of the South Basin (Fig. 3.8). Moderately high sand content (20-30%) is also present in the most northeastern portion of Turtle Bay Basin and gradually decreases along a northeast/southwest trend to less than 12%. The North Basin contains predominantly sediments with sand content between 10-20% while both eastern tidal channels (CHANNEL 2 and CHANNEL 3) have sediments which contain less than 10% sand.

The surface sediment silt content is more homogenous throughout the Little Lake study site (Fig. 3.9). There are a few isolated regions of high silt content such as the most northern portion of the Turtle Bay Basin (near the input CANAL) and portions of the North Basin and Central Basin, mostly restricted to the perimeter of these basins near the land water interface. The higher silt content in Turtle Bay illustrates a diminishing effect along a north/south trend with silt content ranging from a high of 60-70% at the most northern portion of the basin to lower silt content of 20-30% at the most southern portion the Turtle Bay Basin. The bulk of the North, Central, and South basins contain sediments predominantly comprising 40-50% silt.

The spatial distribution of surface sediment clay content is nearly the inverse of the sand content distribution (Fig. 3.10). Samples with the highest clay content are in and near the main tidal channels (CHANNEL1, CHANNEL2, and CHANNEL3). Low (10-20%) clay content is presented in the most northeastern portion of the Turtle Bay Basin and gradually increases along a northwest/southeast direction to 30-40%. This spatial pattern is the inverse of the sand distribution described previously. The lowest sediment clay content (10-30%) is observed in the Central and South basins. Again, the spatial distribution of sediment clay content inversely mimics the sediment sand content in all regions of the lake.

The spatial distribution of surface sediment water content is illustrated in Figure 3.11. Surface sediment water content is highest (greater than 60%) in the North Basin near

CHANNEL 1 and in the two eastern tidal channels (CHANNEL 2 and CHANNEL 3). Water content decreases from over 60% in the North Basin to between 33% and 50% in the Central and South basins. Water content is also lower (33%-50%) in the northern portion of the Turtle Bay Basin. Mineral content for the region inversely mimics the water content distribution with higher mineral content in regions of lower water content and vise versa (Fig. 3.12). Organic content is high in regions with relatively high water and clay content (Fig. 3.13). Elevated sediment organic content is observed at all three main tidal channel entry points into Little Lake and the organic content diminishes as the distance from the channel entry increases toward the Central Basin.

The spatial distribution of surface sediment shell content is a bit more varied (Fig. 3.14). Higher shell content (16-69%) is generally limited to the perimeter of the lakebed resulting in a large region of predominantly lower shell content (0-6%) within the main sub-basins.

Summary

The ebb tide 3-D hydrodynamic model for Little Lake is indicative of proportionally higher current velocities in the deep channels and lower current velocities in the large shallow basin regions (McCorquodale and Georgiou, 2006; Park, 2002) (Fig. 3.15). The boundary conditions for the above referenced hydrodynamic model included tidal forcing mechanisms and freshwater input via precipitation and Davis Pond river diversion input (assumed constant 1200cfs). Given the basin morphology and the associated hydrodynamic model, one would expect to find an accumulation of finer material in the large, central, relatively quiescent regions of the lake where lower currently velocities are predicted. Additionally, one would expect to find coarse material in the channels and proximal to the channel mouths where the predicted currently velocities are relatively high.

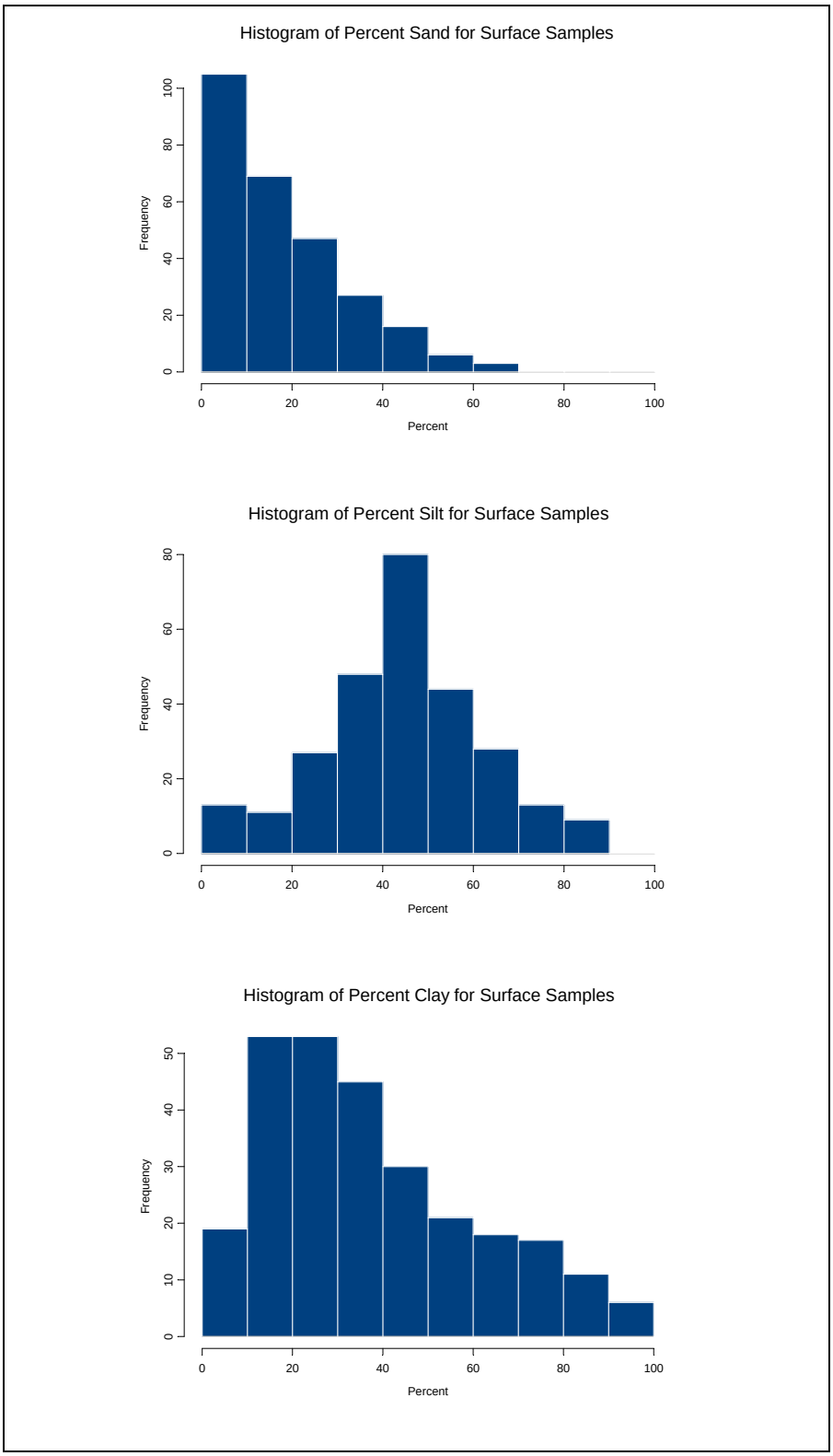

Figure 3.4. Surface sediment sand/silt/clay content histograms for Little Lake samples.

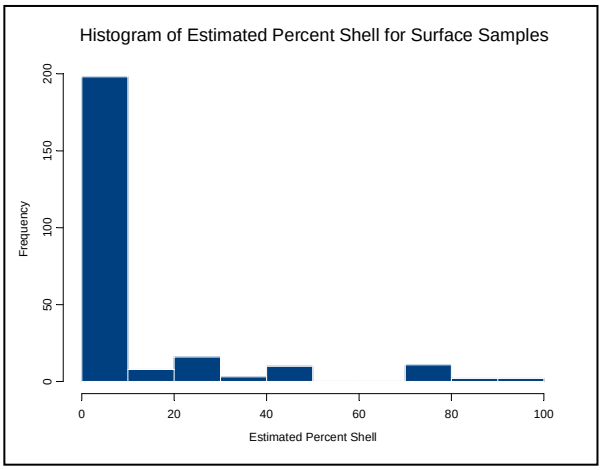

Figure 3.5. Surface sediment shell content histogram.

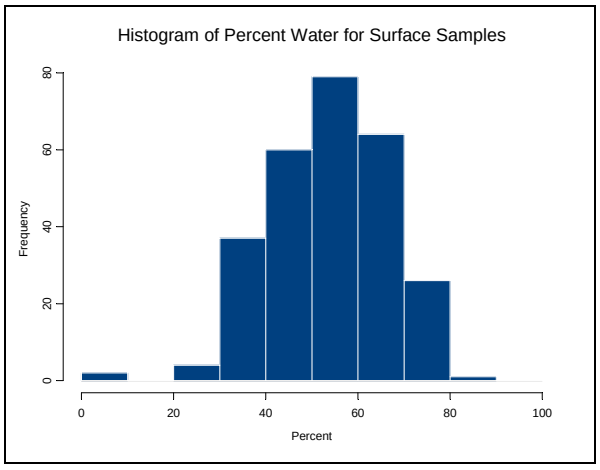

Figure 3.6. Surface sediment water content histogram.

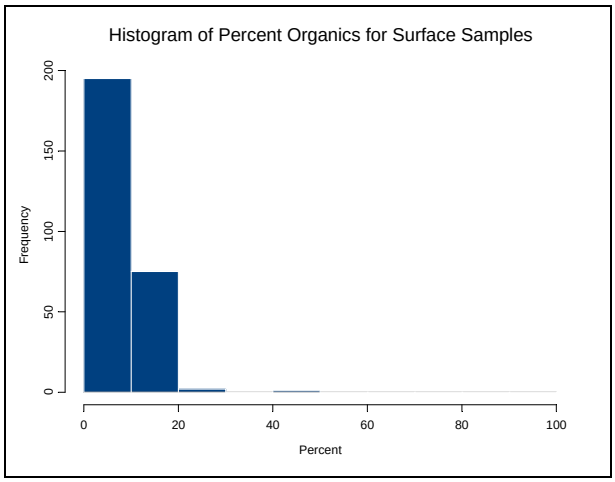

Figure 3.7. Surface sediment organic content histogram.

Table 3.1. Summary statistics for physical sediment properties (percent) for all Little Lake sediment samples.

	SAND	SILT	CLAY	WATER	ORGANIC	SHELL
N	272	272	272	271	271	250
Minimum	0	2	0	26	2	0
Median	13	45	32	55	7	0
Mean	18	45	38	54	8	11
Maximum	65	89	97	84	40	100

The actual distribution of surface sediment grain size within Little Lake was not as expected. Regions of higher coarse content (sand) were found in the shallow (< 2 m) Central Basin of the lake (low modeled current velocities), while higher fines content was observed in the three main tidal channels and near the channel mouths (high modeled current velocities). Considering the hydrodynamic model and the unexpected surface sediment distribution, it appears that the sediment dynamics are controlled by more than hydrodynamics. The distribution of surface sediment does not appear to be solely hydrodynamically controlled; however, local forcing mechanisms (wind-driven currents) and *in situ* sediment sources may be more active contributors than first envisioned.

The source of coarser material (sand/silt) observed in the Central Basin was identified through the analysis of the acoustic subbottom data. The subbottom data show multiple relic channel/levee systems in the vicinity of high surface sediment sand content (Fig. 3.16). These relic channel/levee systems are located stratigraphically above distributary mouth bar and channel sands of the Lafourche delta and can be identified on aerial photographs often terminating at the lake edge in the Central Basin (Fig. 3.17). Deposits from the relic channel/levee systems were likely reactivated to the surface by local dredging and predominant south-southeast winds create waves that resuspend and redistribute these relic deposits to the north (Fig. 3.18). In addition, the increased exposure (larger fetch) to physical processes in the Central Basin may result in the winnowing of fines.

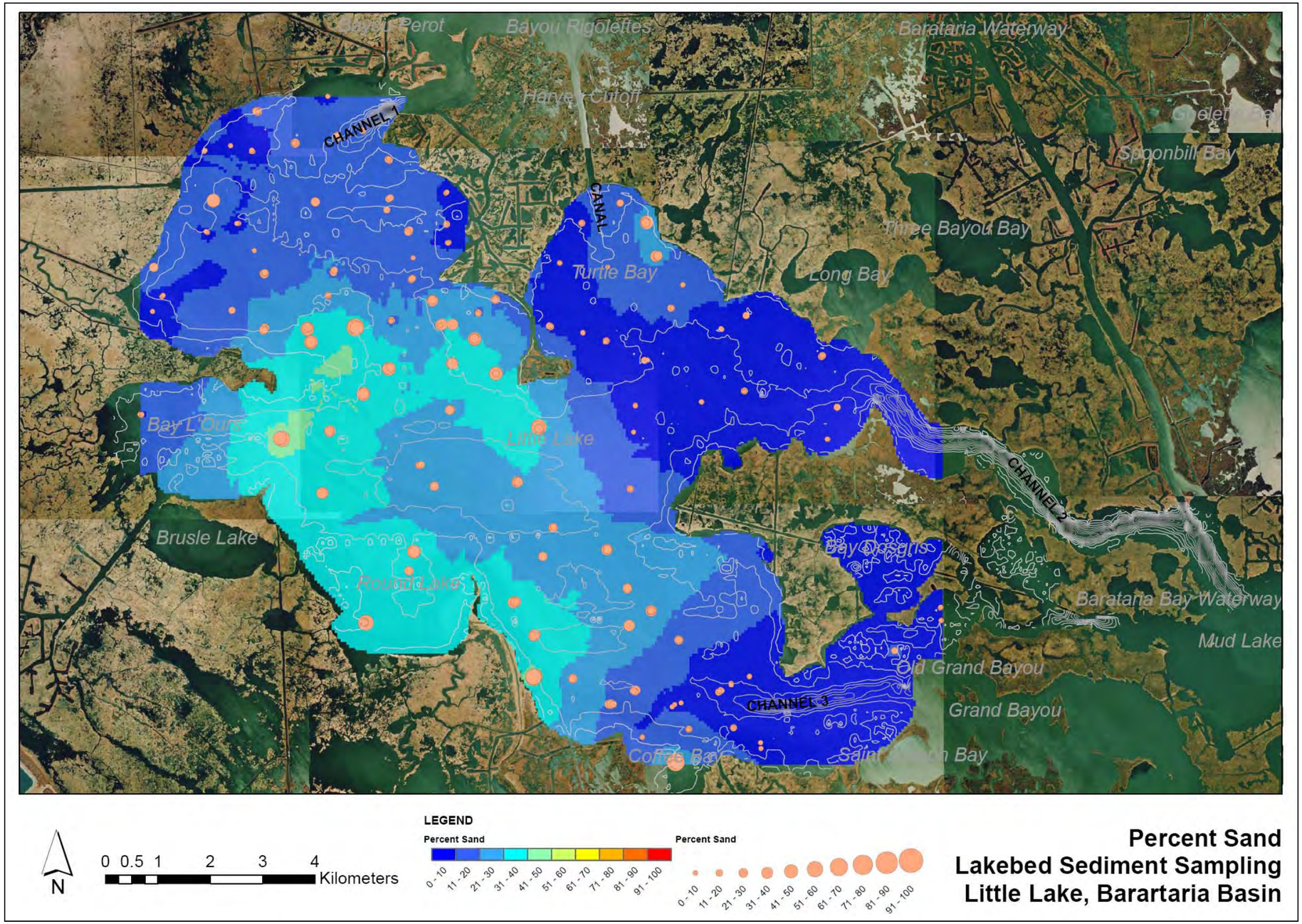

Figure 3.8. Surface sediment sand distribution.

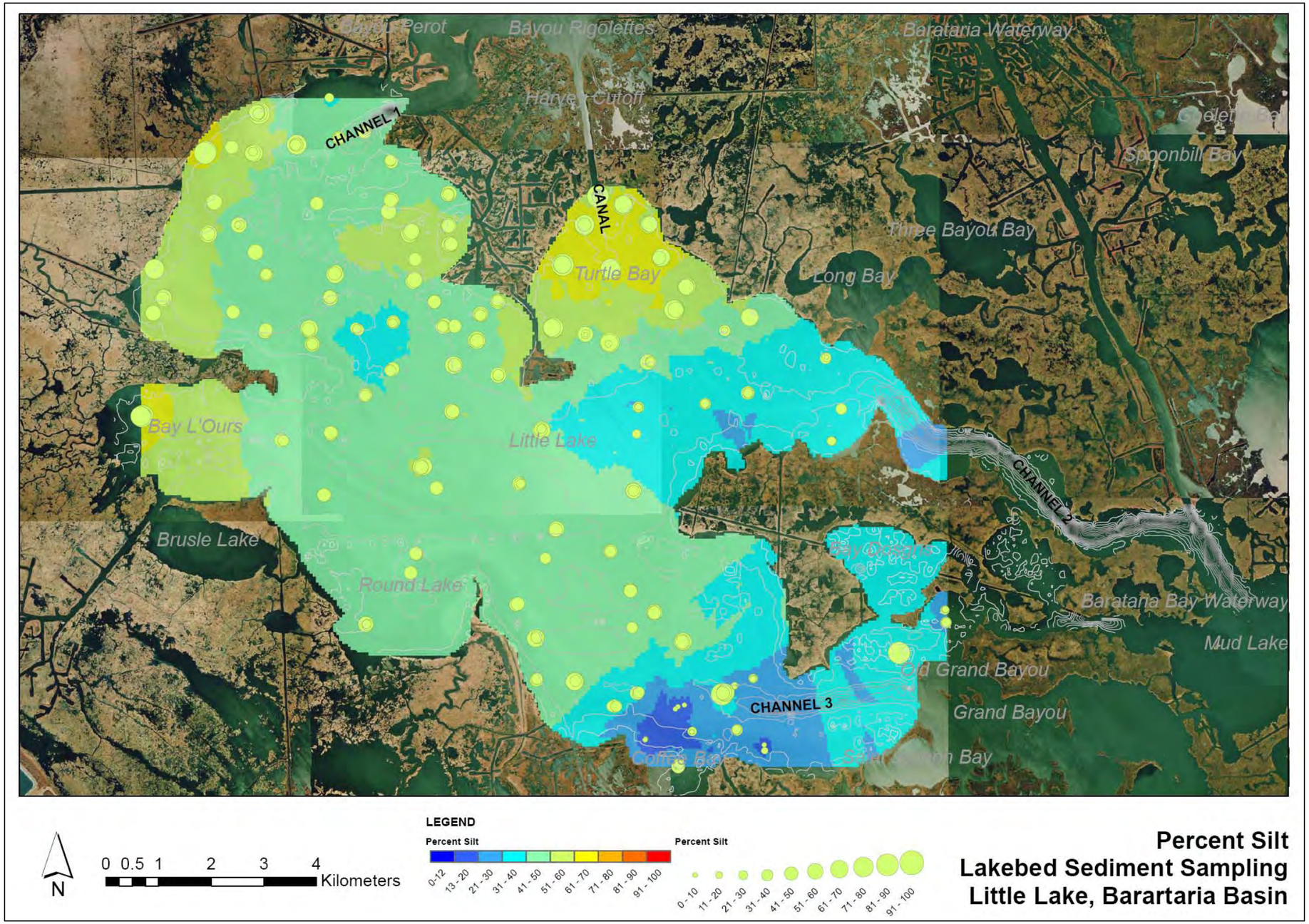

Figure 3.9. Surface sediment silt distribution.

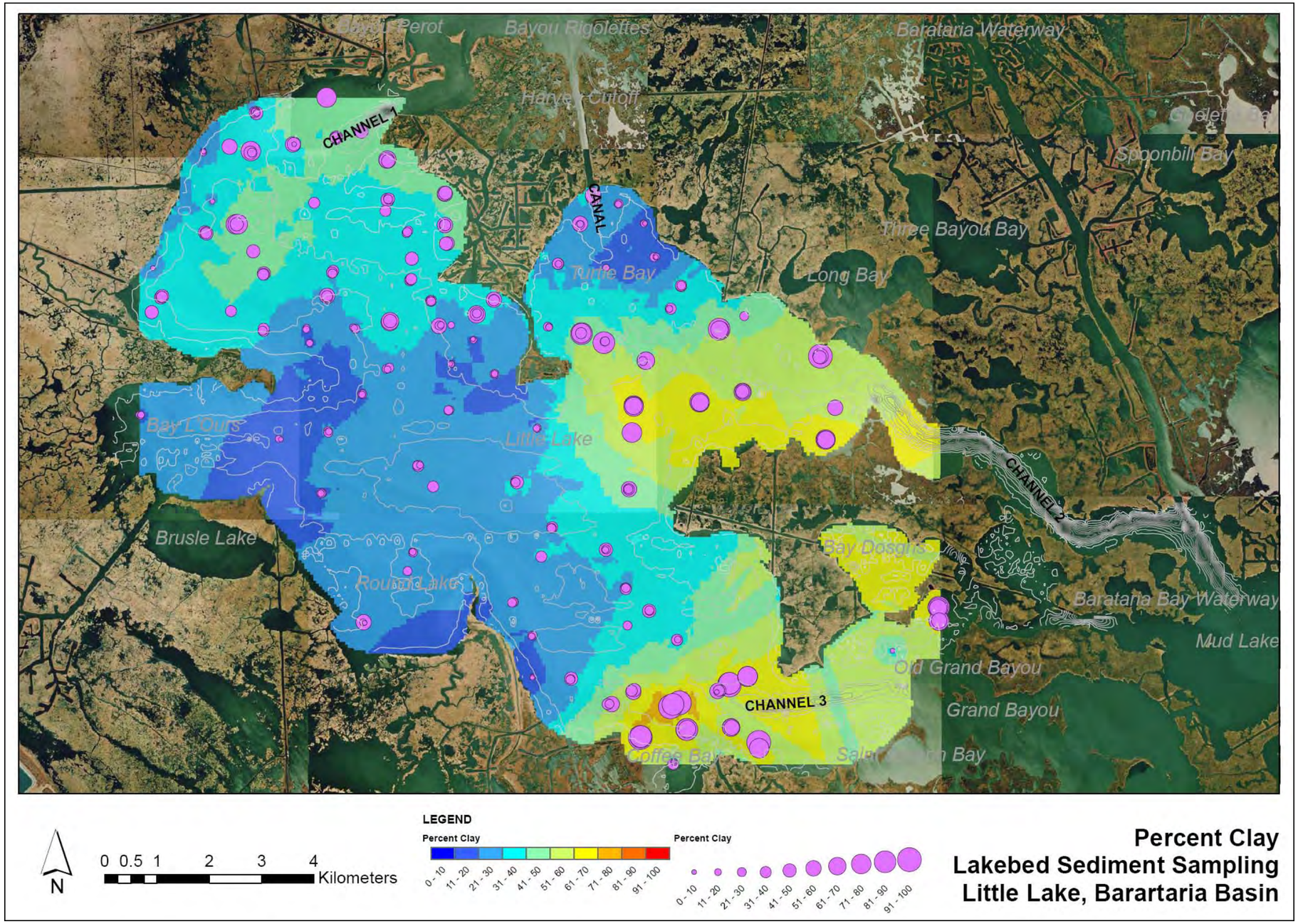

Figure 3.10. Surface sediment clay distribution.

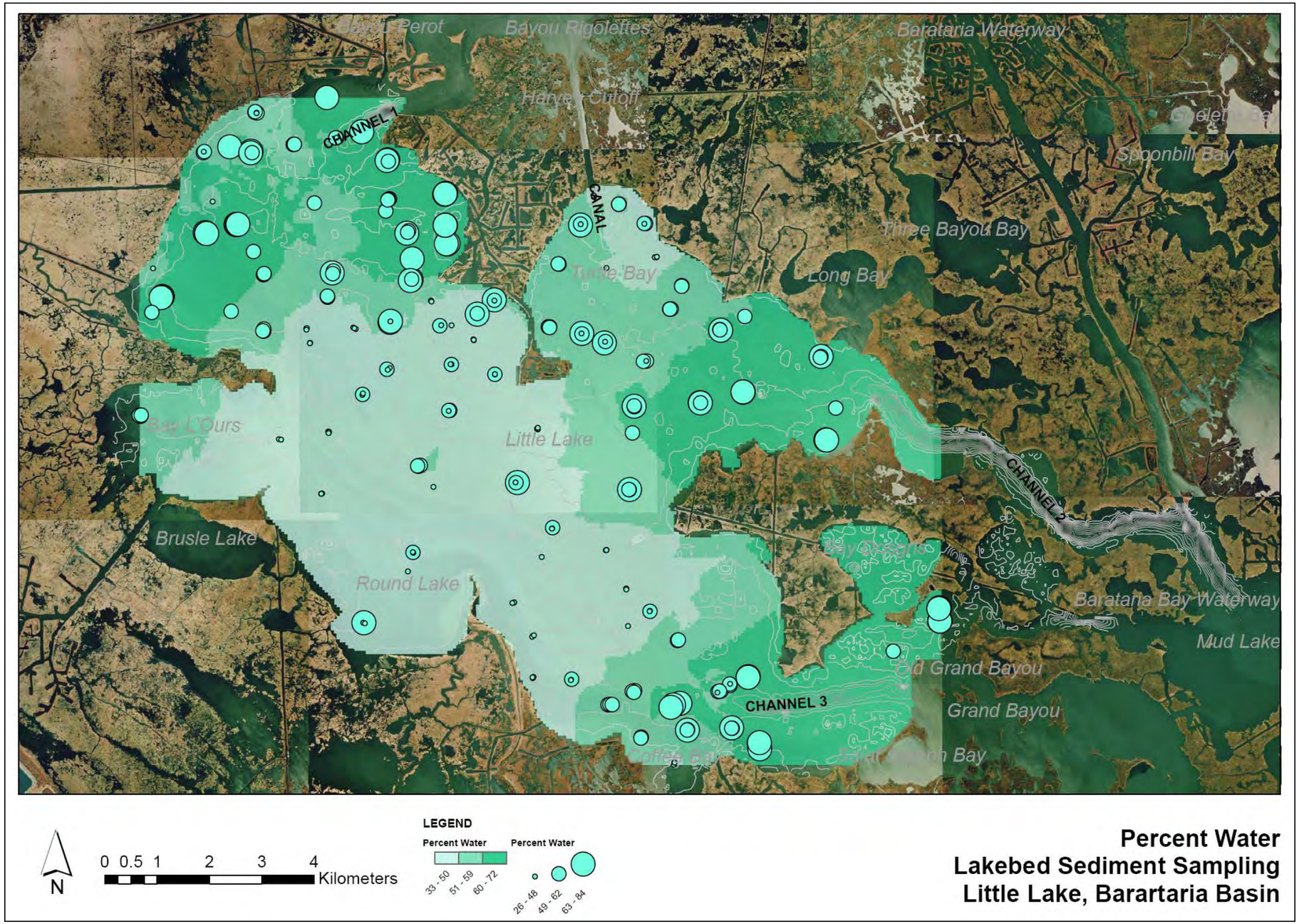

Figure 3.11. Surface sediment water content.

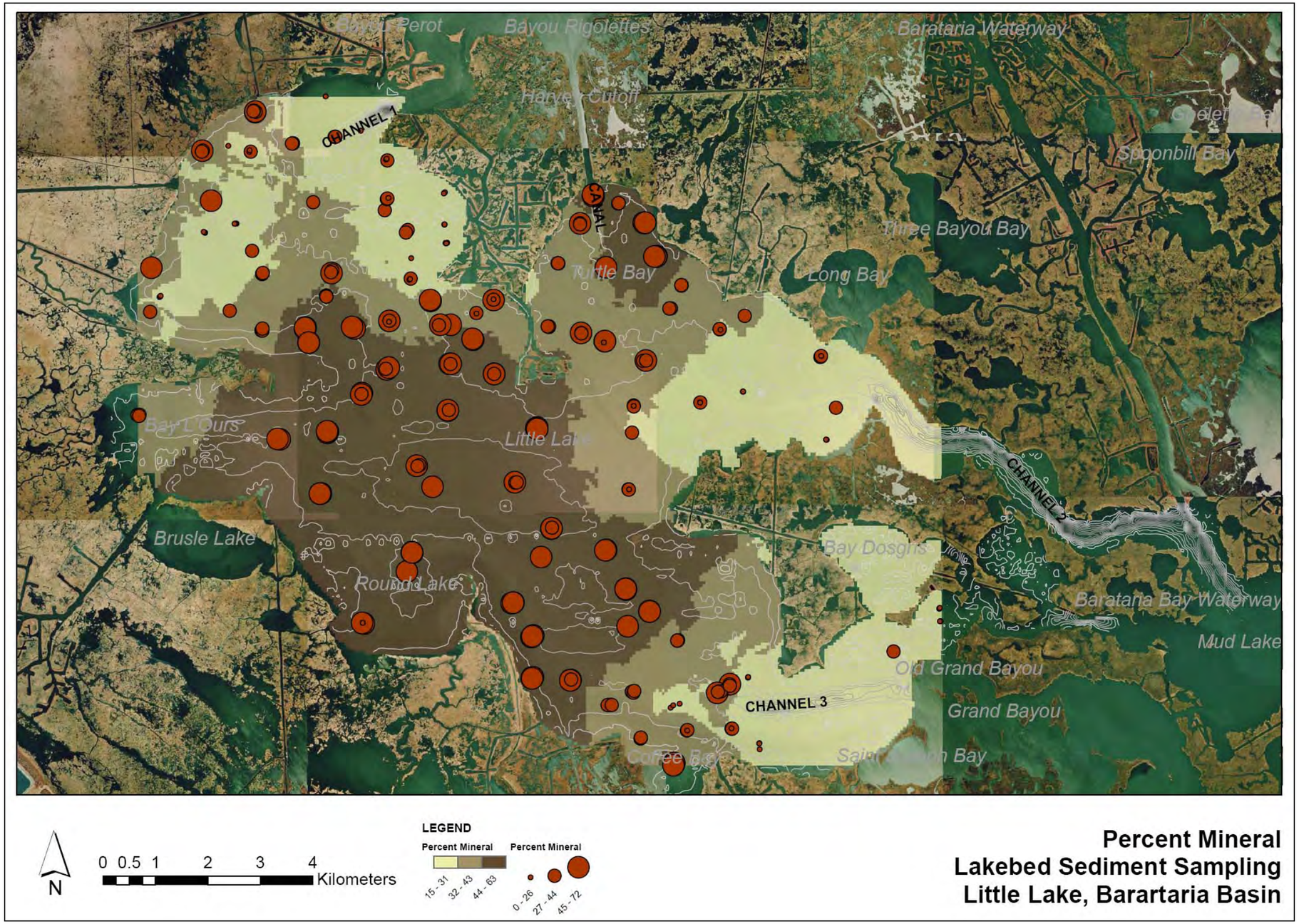

Figure 3.12. Surface sediment mineral content.

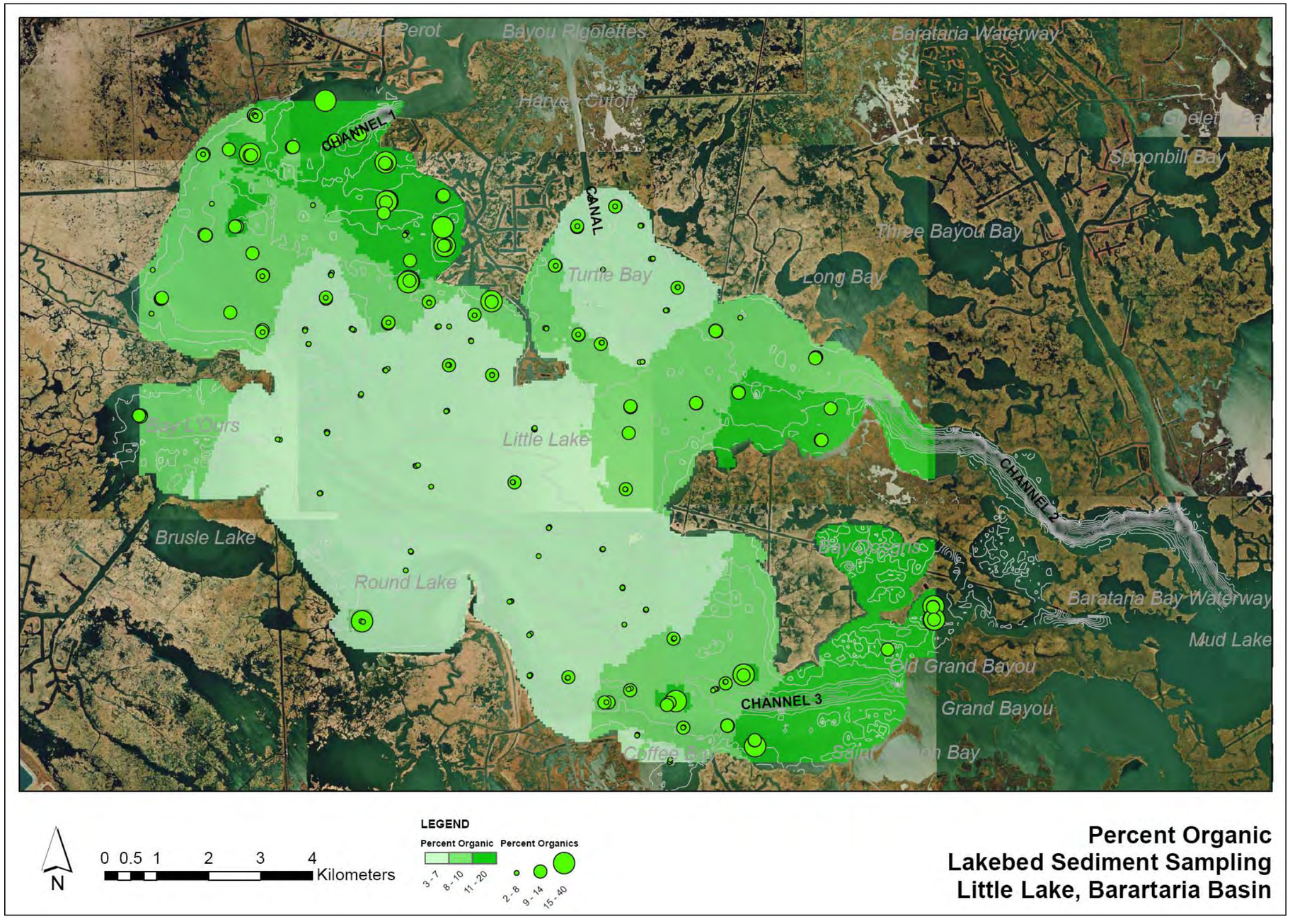

Figure 3.13. Surface sediment organic content.

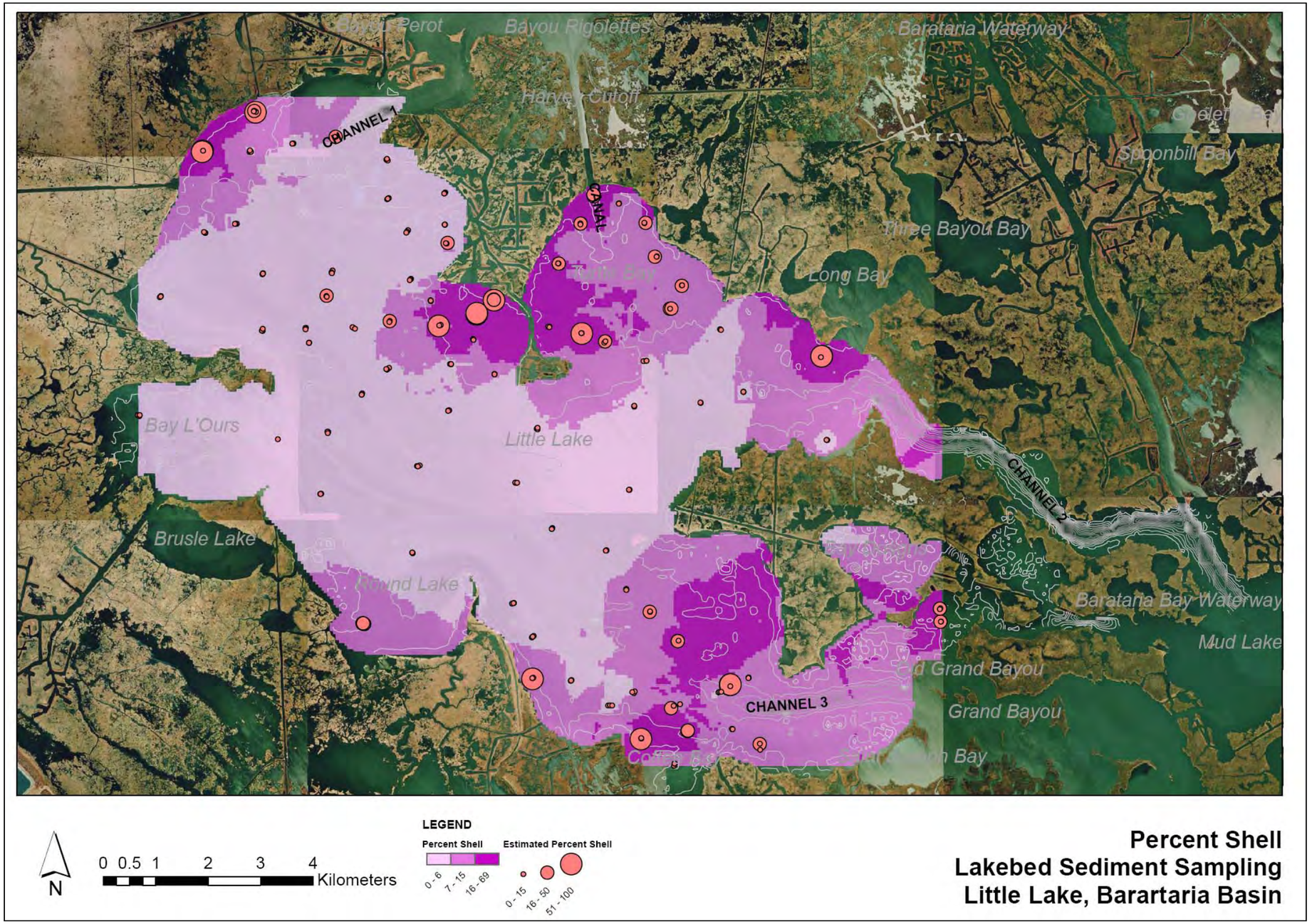

Figure 3.14. Surface sediment shell content.

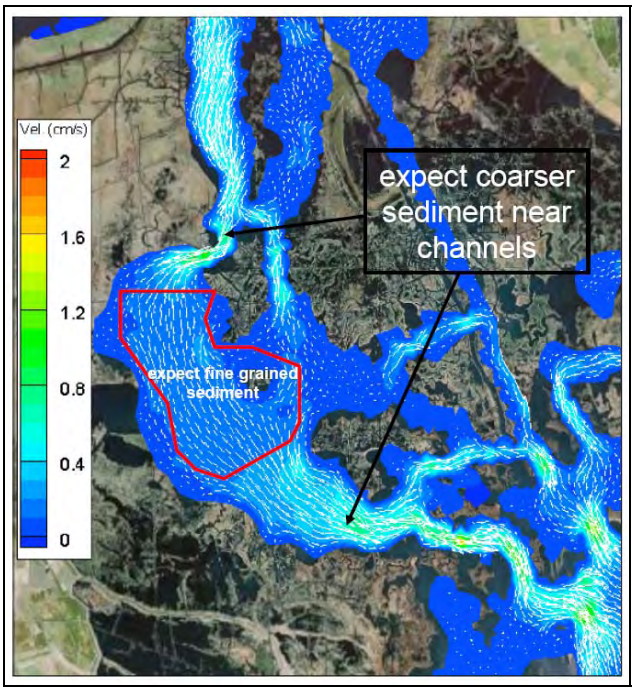

Figure 3.15. Hydrodynamic model of Little Lake showing current direction and magnitude during ebb tide (McCorquodale and Georgiou, 2006).

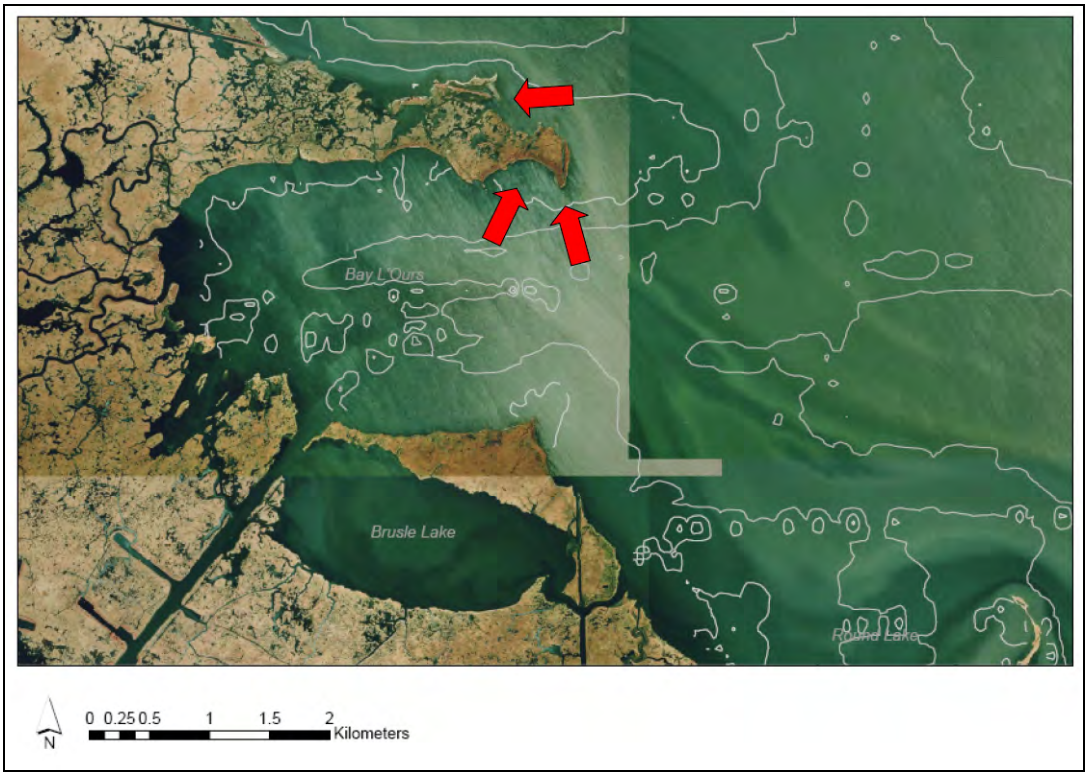

Figure 3.16. Relic channel/levee systems abbreviated at lake edge.

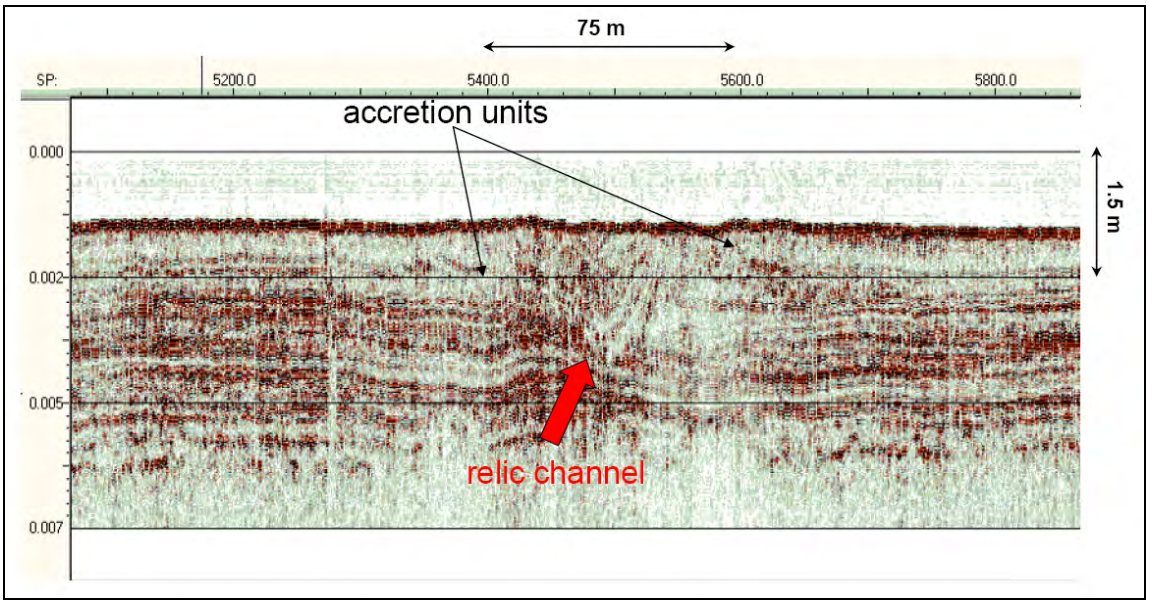

Figure 3.17. Chirp subbottom sonar data showing sand/silt rich relic channel and accretion units in the Central Basin.

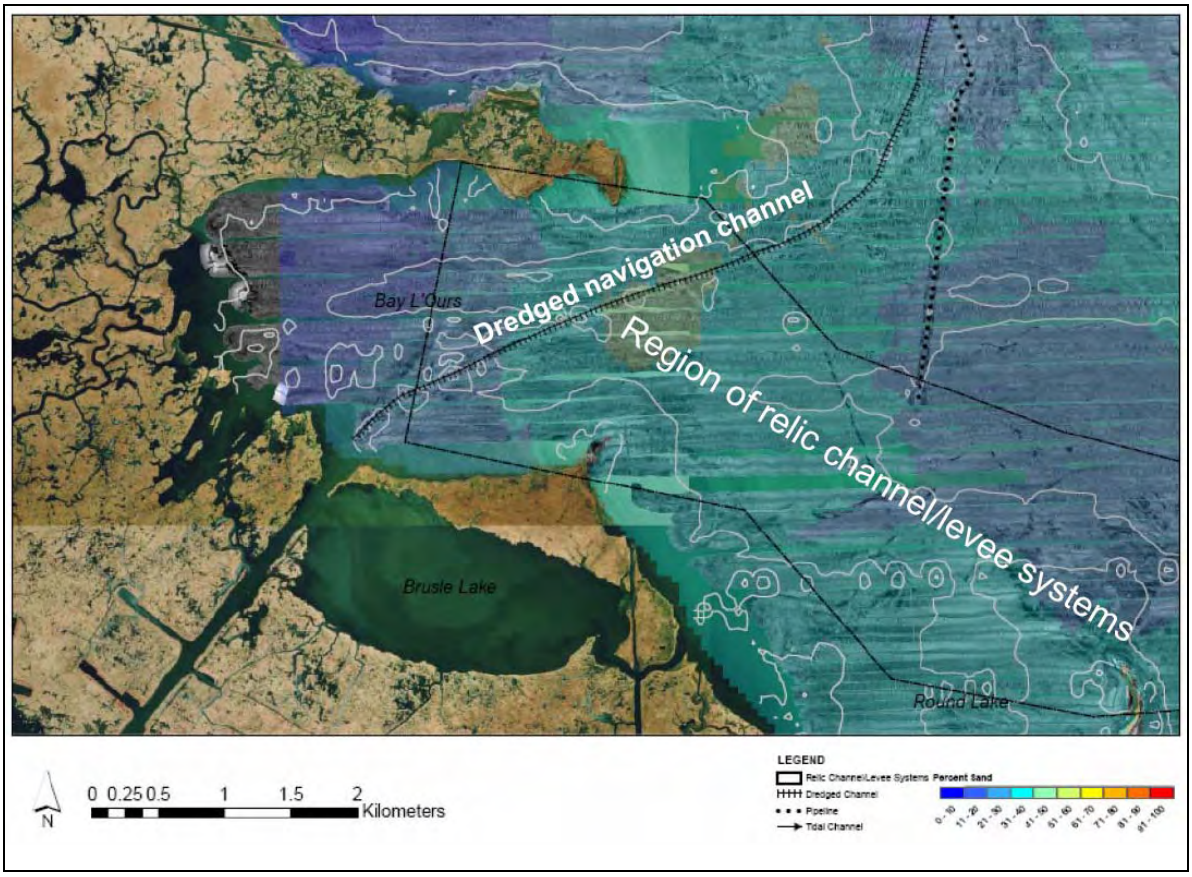

Figure 3.18. Reactivation and transport of relic sand/silt deposits via artificial dredging.

The three main tidal channels which enter the Little Lake study site are predominantly comprised of clay which indicates that no coarse material is input into the system through these points of entry. Bank erosion along these tidal passes and the entrainment of fine sediments and organic matter from adjacent marshlands is likely the source of the sediment. Storms erode the marsh and provide fine-grained sediments and organic debris. Marine vessel wakes exacerbate erosion of the channel margin banks. Transport of fine, organic rich sediment in and near all three main channels is interpreted as being driven by tidal exchange.

The distribution of surface sediments in the Turtle Bay basin is unique (Fig. 3.19). There is an increase in fines content (clay) and a decrease in coarser material (silt) with increasing distance from the man-made canal leading into Turtle Bay Basin (CANAL, Harvey Cutoff). Higher silt content is deposited near the canal mouth (sediment source) and the clay fraction increases as the distance away from the canal mouth increases. Based on surface sediment properties alone, the man-made canal, Harvey Cutoff, draining into the Turtle Bay basin, is interpreted as a source of sediment to the region.

In summary, fine sediment and organic material are deposited in Little Lake near the three main tidal channels via tidal exchange. The sediment and organic matter are entrained from bank/channel erosion and adjacent marshland during high water and tidal exchange. The sand in the Central Basin can be explained by the reactivation and transport of relic channel/levee deposits. Lastly, the Harvey Cutoff (CANAL) appears to be the entry point for silty material found in Turtle Bay Basin.

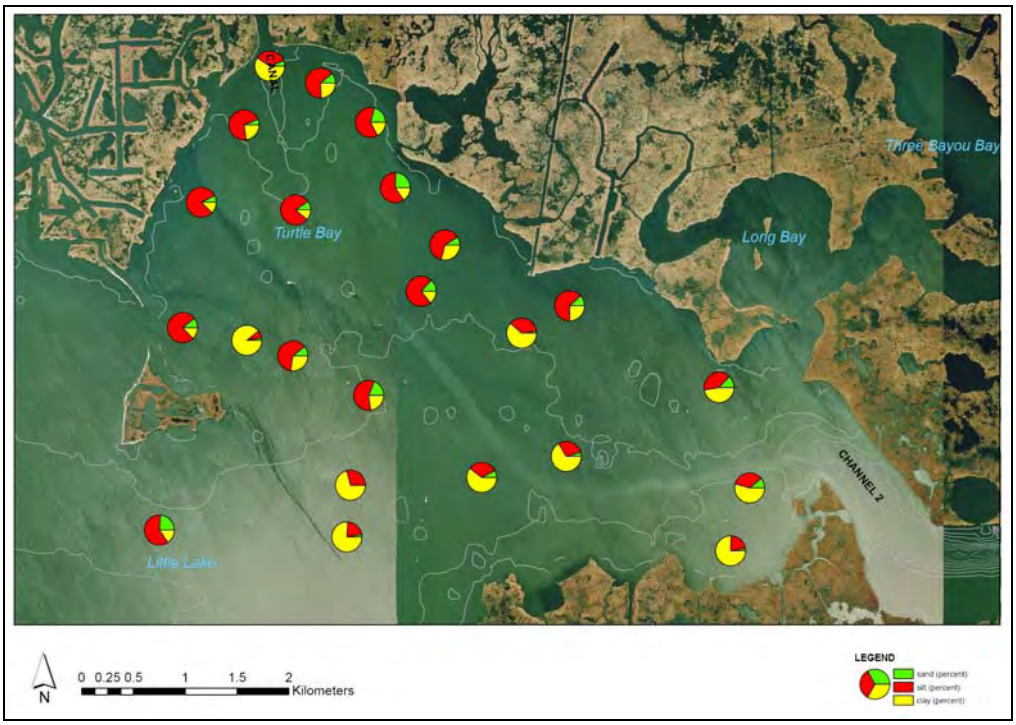

Figure 3.19. Turtle Bay silt/sand/clay pie chart illustrating decrease in silt content with increasing distance from mouth of Harvey Cutoff (CANAL).

CHAPTER 4 LAKE BED SEDIMENTATION ACCUMULATION

Introduction

Recent studies in both sediment-rich estuarine and continental-shelf marine environments have demonstrated the utility of Beryllium-7 (Be-7) as a tracer of fine-sediment deposition associated with river derived sources (Mullenbach and Nittrouer, 2000; Rotondo, 2004; Sommerfield et al., 1999). Studies using Be-7 have been undertaken to determine sediment accumulation rates, investigate sediment budgets by tracing fine sediment movement and short term storage in river channels, estimate river overbank deposit sedimentation, and to determine rates of water induced soil erosion on agriculture lands (Blake et al., 2002; Canuel et al., 1990; Walling et al., 1999). In freshwater systems, Be-7 can also be used as a reliable tracer of heavy metal pollutants due to similarities in particle adsorption behavior (Hawley et al., 1986).

Beryllium-7 is a particle-reactive radionuclide, which is formed in the atmosphere by cosmic ray spallation of atmospheric gas. It is transported to marine environments via atmospheric fallout and riverine sources. In most regions, riverine input of cosmogenic Be-7 is insignificant compared to that of atmospheric input. However, in regions where the ratio of drainage basin area to receiving basin surface area is large, riverine input can account for a significant portion of Be-7 input into the marine environment (Baskaran et al., 1997). The Mississippi River and its tributaries form the third largest drainage basin in the world and drain water from approximately 41% of the contiguous United States. Therefore, fluvial input is most likely a significant source of Be-7 to Louisiana's coastal bays and estuaries via bayous and canals connected directly or indirectly to the Mississippi or Atchafalaya Rivers. In addition, recently deposited riverine sediment on the inner shelf can be reactivated during storms and transported into coastal bays.

Since Beryllium-7 is formed exclusively in the atmosphere, has a short half-life ($t_{1/2}$ = 53.3 days), and is adsorbed to settling particles (strong affinity to inorganic clay particles), it has been used as a tracer of environmental processes in aqueous systems (Hawley et al., 1986). The usefulness of Be-7 as a tool to investigate short-term sedimentary processes in the freshwater bays and shallow lakes of the Louisiana deltaic plain is still decidedly underexplored.

Accurate sediment accumulation rates have been successfully determined in various oceanographic, coastal, marsh, and lacustrine settings utilizing radionuclides including Pb-210 ($t_{1/2}$=22 years), and Cs-137 ($t_{1/2}$=30.7 years) (Bentley et al., 2002; Bentley and Nittrouer, 1999; Dellapenna et al., 1998; Nittrouer et al., 1979). The naturally occurring radionuclide, Pb-210, is part of the Uranium-238 decay series. A few assumptions are necessary for the application of sediment dating utilizing measured excess Pb-210 activity. These assumptions include: 1) the atmospheric supply of Pb-210 is constant, 2) it is immediately adsorbed onto fine particulate matter in the water column, 3) there is not vertical mixing of Pb-210 in the sediment column, and 4) secular equilibrium is established between the parent and daughter products. Due to the longer half live of Pb-210 ($t_{1/2}$=22 years), sediment accumulation rates on the decadal scale can be determined using this methodology.

An anthropogenic product of nuclear fission, Cesium-137 (Cs-137), was released into the atmosphere during bomb testing in 1954, with a peak concentration occurring in 1963. The detection of a Cs-137 peak in sediments can be utilized to calculate the age of sediments and assuming a constant rate of accumulation, sediment accumulation rates can be determined. The Cs-137 sediment accumulation rates can be utilized as a comparison or validation for accumulation rates determined by utilizing the Pb-210 technique described above.

Information attained from this study establishes baseline radio-isotopic signatures concerning recent and historical sedimentation accumulations rates for Little Lake and provides important insights about existing sediment dynamics.

Objectives

The objectives of this portion of the study are to identify sedimentary sequences, determine the sediment accumulation characteristics (long and short-term) and radionuclide signatures of Little Lake sediments, and test for possible impacts of the Davis Pond River Diversion.

These objectives were accomplished by: (1) defining the structural and textural characteristics of sediment deposits in this shallow inter-distributary lake, (2) determining short-term (<200 days) and long-term (<150 years) sediment accumulation rates and radionuclide signatures in Little Lake using Be-7, and other natural and anthropogenic radionuclides including Pb-210 and Cs-137, and (3) demonstrating the effectiveness of Be-7 as a short-term sedimentologic tool in the shallow coastal lakes and bays of Louisiana by investigating the spatial variability of sediment-bound Be-7 in surface sediments. Box coring and radionuclide analysis were conducted.

Methods

Seabed Sampling

Utilizing a 24 x 24 x 38 cm Ocean Instruments, Inc. box core, sediment sampling commenced at pre-determined locations based on a simple random sampling fashion with more grid points situated in the northern portion of the lake and evenly spaced sample locations throughout the rest of the Little Lake. Field sampling took place between October 13, 2003 and

October 16, 2003 onboard a 7.9 m (26 ft) TwinVee Weekender, *Tiger 1*. Geographic sample locations were acquired and recorded with the use of a WAAS enabled GARMIN GPS-5 global positioning system integrated with the navigation software. Positional accuracy of this GPS device typically produces an accuracy of ±3 m. Once the box cores were acquired, each box core was sub-sampled using two 8 cm diameter PVC cores (Fig. 4.1). Upon return to LSU, the samples were placed in cold storage until further laboratory analysis. Figure 4.2 illustrates the box core sample locations.

Figure 4.1. Box core sampler and PVC subsampling.

Laboratory Analysis

The first sub-sample core of each box was extruded and sampled at 1 cm intervals. Specific 1 cm thick sub-samples were selected for analysis and water content was determined gravimetrically after placing each sediment sample in a 100°C drying over until a constant weight was attained. The dried sediment was homogenized by mortar and pestle and place in sealed plastic petri dishes. These samples were then analyzed for 20-24 hours by gamma spectroscopy to determine activities of Be-7 ($t_{1/2}$=52 days), Pb-210 ($t_{1/2}$=22 years), and Cs-137 ($t_{1/2}$=30.7 years) at the 477.7 KeV, 46.5 KeV and 661 KeV peaks. Detailed methods of these analyses are outlined in Bentley et al. (2002) and Sommerfield et al. (1999).

Figure 4.2. Box core sample locations.

Taking into consideration the assumptions discussed in the previous section , shallow subsurface sediment accumulation rates were calculated using Pb-210 and Cs-137 radiometric techniques described by Nittrouer et al. (1979). Accumulation rates were calculated from the Pb-210 activity by determining the least squares fit line of the natural log of excess Pb-210 activity versus core depth and solving for *s* (sedimentation rate) using the following equation (Nittrouer et al., 1979).

$$\ln A_{(z)} = \ln A_o - \lambda z / s$$ where λ= 0.031/year, A_o = surface activity, z=depth

If Cs-137 peaks were detected, accumulation rates were calculated from the Cs-137 activities assuming a constant sedimentation rate from the 1954 and 1963 time markers to present (DeLaune et al., 1989). Short-term sediment accumulation was determined using Be-7 activity and inventories (Sommerfield et al., 1999).

Sediment porosity was calculated from the sediment water content results assuming a particle density of 2.6 g/cm^3 (Berry and Reid, 1987). Utilizing the calculated porosity (ϕ) and assuming a mineral density (ρ_s) of 2.6 g/cm^3, the following equation was utilized to calculate Beryllium-7 inventories (I) for each 1 cm sample interval (Sommerfield et al., 1999).

$$I = \sum \rho_s X_i (1-\phi_i) A_i$$

The second box core sub-sample was thinly slabbed (1 cm thick) and digital X-radiograph images (16 bit) were acquired utilizing a Model PX-15HF portable veterinary X-ray machine and flat panel imaging system. High resolution core photographs were taken with a digital camera. Images from X-ray radiograph negatives were utilized to determine the presence of burrows and other sedimentary structures which may account for variations in the

radionuclide profiles. Sedimentary structures identified in the X-ray images were used to define the depositional environments in Little Lake (Coleman, 1966).

Results

Depositional Environments

Analysis of the box core X-radiographs and physical sediment properties revealed three distinct depositional sequences within Little Lake: 1) a massive mud, 2) interbedded silts and clays, and 3) a sand sequence. Figures 4.3, 4.5, and 4.6 illustrate the distinct differences observed in the sequences.

The massive mud sequence consisted of fine-grained material (brown silt and clay) with very little or no evidence of bedding or primary sedimentary structures. In the event bedding structures were visible on the X-radiographs, they were thin and largely unclear. Large intact shells and shell fragments are present throughout the cores. The shells appear to be located in clusters. The muddy sequences appears reasonably intact, however, a thorough inspection indicates some bioturbation. Cores that exhibited this type of depositional sequence included BC01, BC02, BC07, BC08, BC12, BC22, and BC26. The muddy sequence was identified mainly near the three tidal channel inlets. Figure 4.4 shows the location of the box cores and depositional sequence identified for each location.

An interbedded silt and clay sequence was identified in cores BC03, BC04, BC05, BC06, BC09, BC13, BC17, BC23, BC24, and BC25. All of these cores contain some parallel laminations of alternating fine and coarser material. The observed laminations are mostly intact and parallel, although there is some evidence of distorted, irregular, and lenticular types. Intact shells and shell fragments are observed in some of these cores and appear to be isolated to specific bedding layers. No direct evidence of burrowing was detected in the cores, although

some distorted bedding was visible in select cores. Some organic/peaty layers were also detected in this sequence. Figure 4.5 displays two of the cores that illustrate the above described sequence. The interbedded sequence was identified in the North, Turtle Bay, and South basins. The interbedded sequences were commonly found near stream and canal networks near the perimeter of the lake.

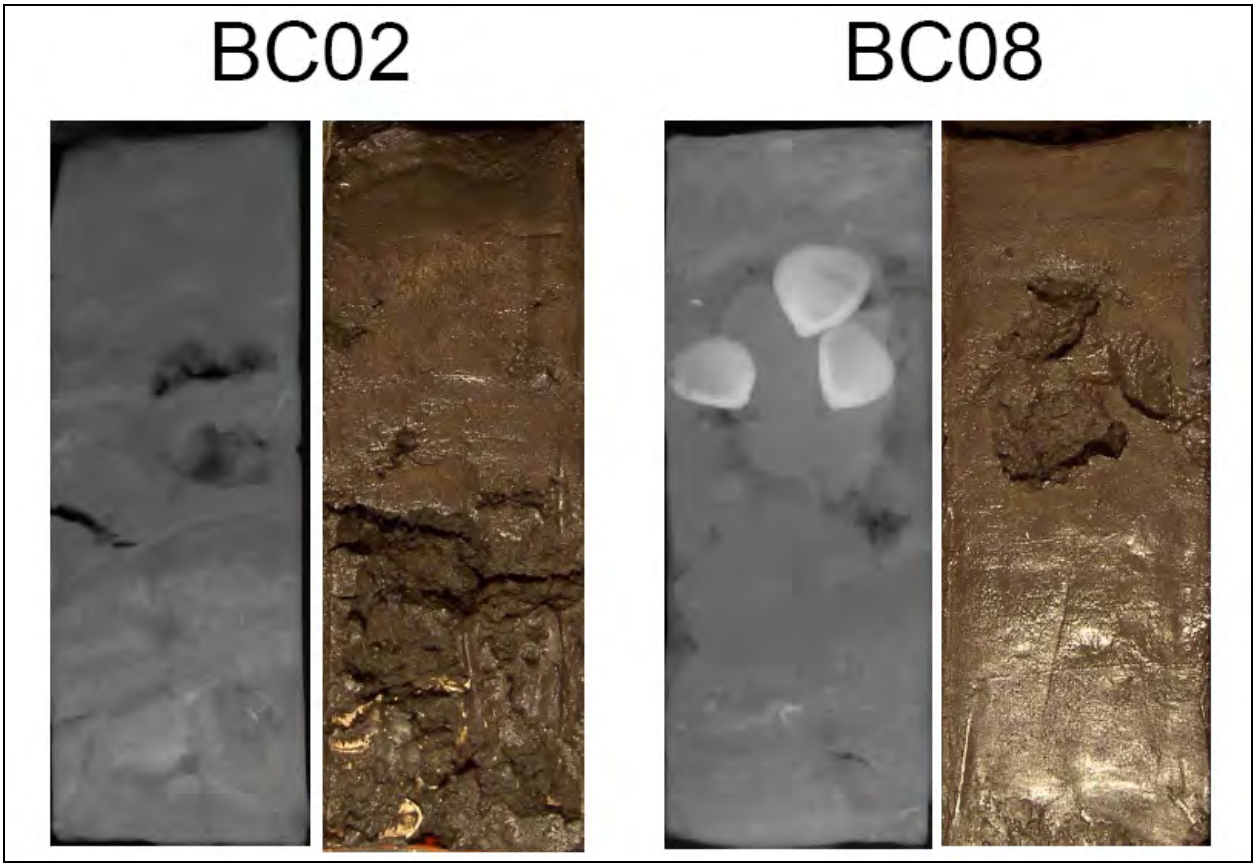

Figure 4.3. Two examples of the massive mud sequence.

A sandy sequence was observed in five of the Little Lake cores (BC10, BC15, BC16, BC18, BC19, BC20). The observed sands occurred in locations were core recovery was abbreviated due to the inability of the box corer to penetrate the seabed (shells or hard lakebed associated with sandy bottom sediments) or retain the sample in the coring apparatus. Cores

recovered from these regions averaged 10 cm in depth. Coarser grained particles were observed throughout these cores. Shells and shell fragments were present in most of the sandy cores. Bedding is visible in most of the cores, however the bedding appears to be highly distorted, flaser, wavy, and lentincular in nature. Bedding ranges in thickness from 1 mm to 10 cm. The sandy sequences occurred primarily in and near the Central Basin of Little Lake. Figure 4.6 illustrate two examples of this sediment type.

Short-term Sediment Accumulation

The temporal and spatial components of short-term sediment accumulation derived from Be-7 activities follow. Of the 23 box cores collected, 14 cores had appreciable Be-7 activity detected within the top 10 cm of the core. Activities and inventories of Be-7 ranged from 0.0 to 6.2 dpm/g and 0.0 to 3.8 dpm/cm^2 respectively, with the highest activities and inventories mainly confined to the top few centimeters of the cores.

The highest Be-7 activities were observed in cores obtained from the North Basin of Little Lake; specifically cores BC09, BC13, and BC04 (Fig. 4.7). Low detection or non-detection of Be-7 activity was found predominantly in the Central and South basins and the most southern portion of Turtle Bay Basin. Moderate Be-7 activity (2.6 dpm/g) was detected in Turtle Bay Basin, near the Harvey Cutoff canal mouth, and along the perimeter of the North Basin. Surface sediment in the Turtle Bay Basin, at location BC24, had one of the highest calculated Be-7 inventory values at 2.9 dpm/cm^2. High Be-7 activity identified in the surface sediments typically occurred within the interbedded sequences; however, some detectable Be-7 activity was also identified in the surface of the mud sequences. A very minor amount of Be-7 activity was found in some of the sandy sequences, however most surface material in the sandy sequence had no detectable Be-7 activity.

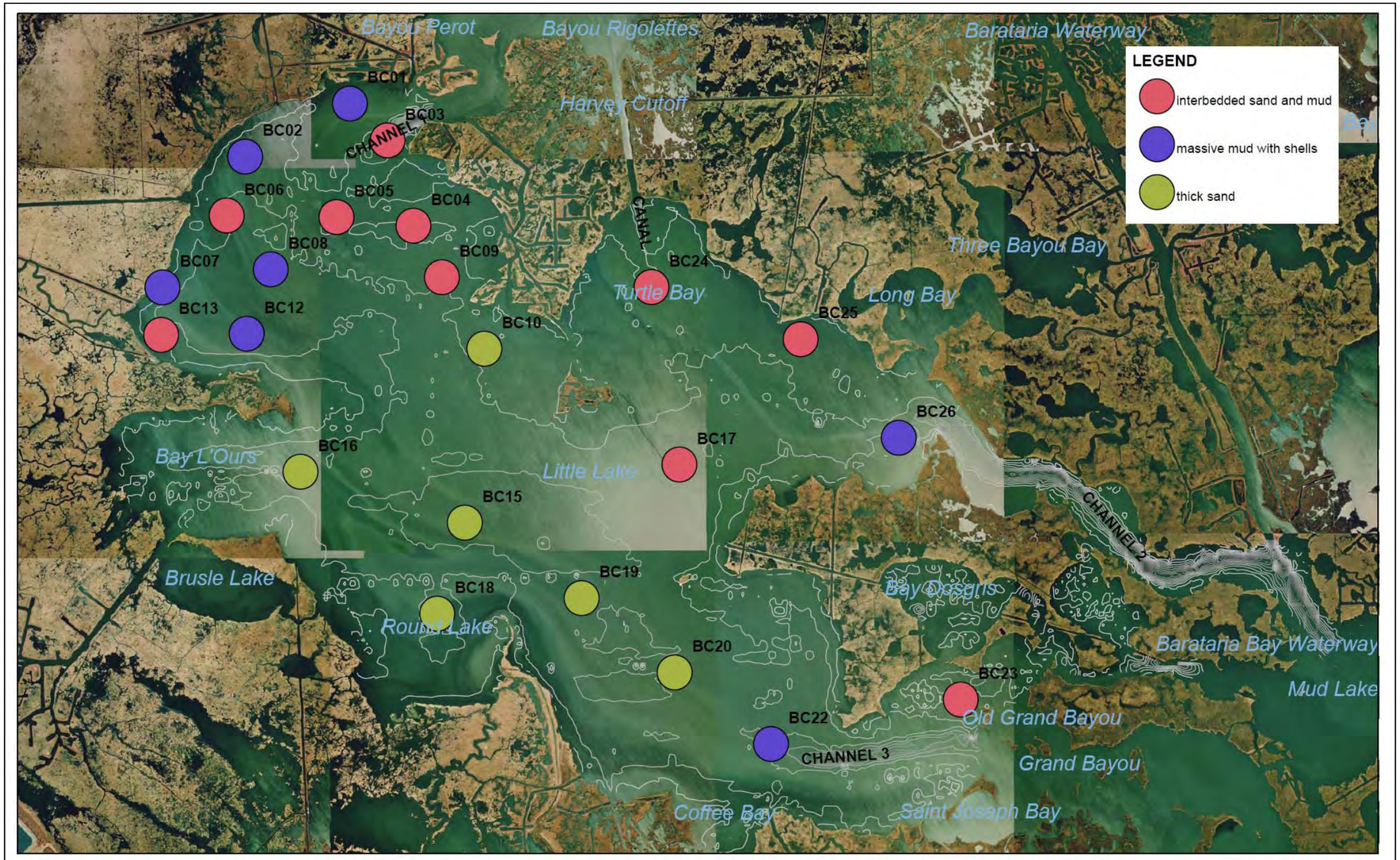

Figure 4.4. Depositional sequences identified in Little Lake.

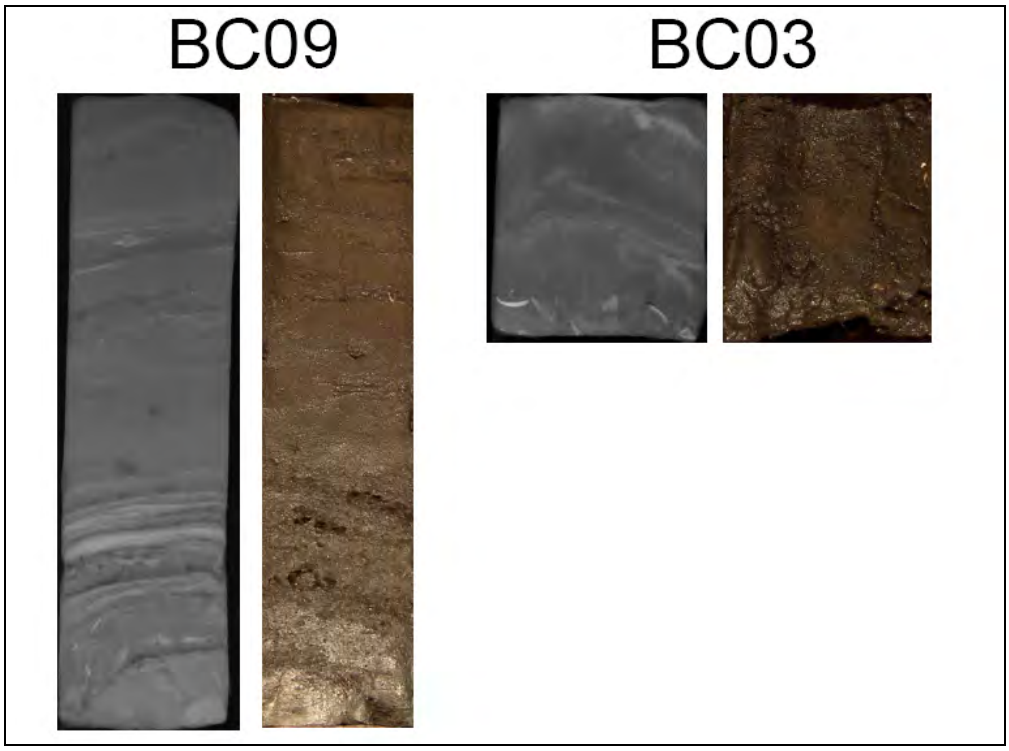

Figure 4.5. Two examples of the inter-bedded sequence.

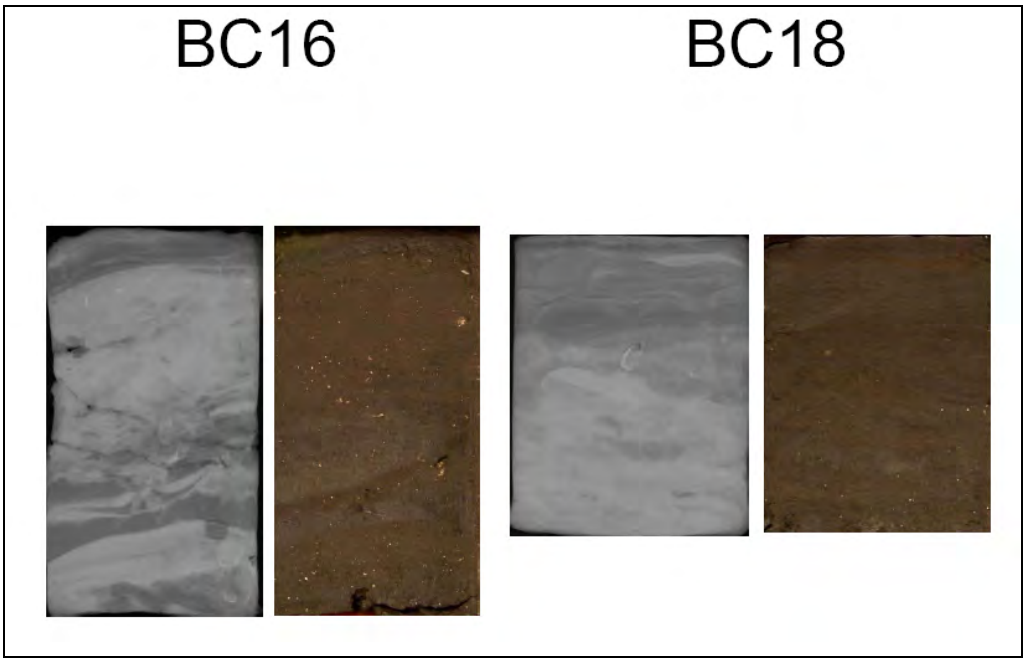

Figure 4.6. Two examples of the sandy sequence.

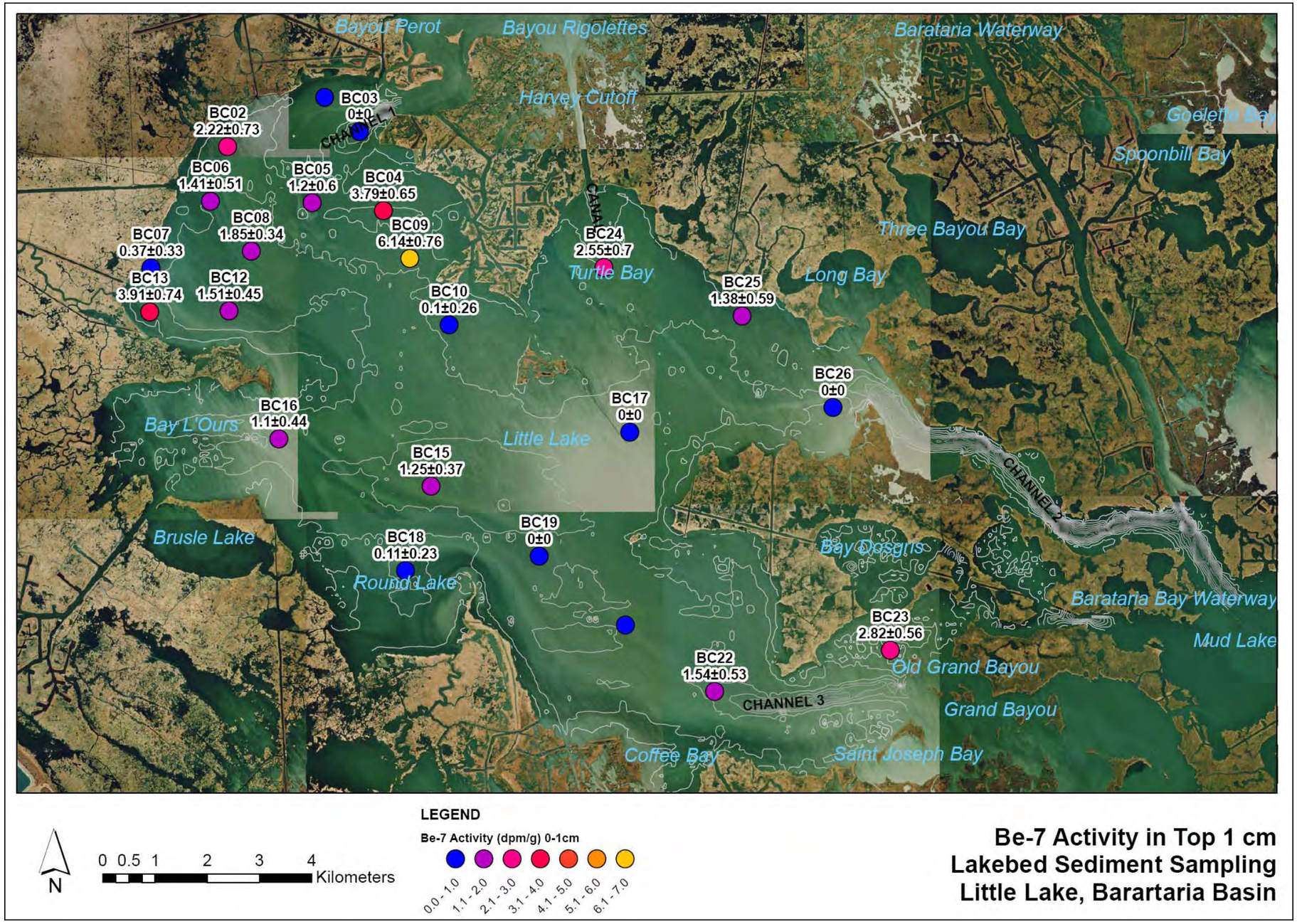

Figure 4.7. Detected Be-7 activity in the top 1 cm of each box core.

The maximum core depth of detectable Be-7 activity varied depending on which sequences was observed. The maximum depth of detection varied from zero to 1 (non-detectable or very little activity at all depths) in most of the sandy sequences, to approximately 4 cm depth detection, found primarily in the interbedded sequences. The mud sequence generally had a moderate Be-7 activity detection depth of 1-2 cm. A contour map, Figure 4.8, illustrates the spatial variability of the maximum Be-7 detection depth for the study site. The contoured data identify isolated hot spots of relatively deep down-core Be-7 detection. The Be-7 activity detection depth was greatest in the North Basin (2-4 cm) near stream/canal networks along the perimeter of the lake. The detection depth was the least (0-1 cm) in the Central Basin and South Basin where the sandy sequence predominated. Activities of Be-7 were detected at depths of 1-2 cm in the northern portion of the Turtle Bay Basin, near the Harvey Cutoff canal mouth.

Down-core Be-7 activity profiles and inventories for the three unique sequences (massive mud, inter-bedded, and sandy) are as presented below. The massive mud sequence (BC08) clearly shows diminishing Be-7 activity/inventory with depth with detectable levels in the 0-1 cm depth interval and nondetectable activities at depths beyond 1cm (Fig. 4.9). The inter-bedded sequence (BC09) also shows diminishing Be-7 activity/inventory with depth, however, activities are detected further down in the sequence. The sandy sequence (BC18) has no detectable Be-7 activity. However, some cores that have been classified as a sandy sequence show minimal Be-7 activity in the top centimeter of the core.

Long-term Sediment Accumulation

Long-term sediment accumulation results and radionuclide depth profiles for excess Pb-210 and Cs-137 are presented below for each type of sequence. The massive mud sequence (BC08) shows three distinct layers (Fig. 4.10). The upper most layer (0-1 cm) of the core is

interpreted as recently deposited riverine derived sediments based on the detectable Be-7 activity. The middle layer of core BC08 (2-9 cm) is either an event deposit or mixed sediments. The excess Pb-210 profile in this portion of the core is constant with depth which may indicate that the sediments were deposited contemporaneously during a flood or storm event or have been mixed by biological or physical processes. The lower layer (< 9 cm) of BC08 exhibits the classic radionuclide decay curve. The excess Pb-210 derived sediment accumulation rate for this layer is 5 mm/year. The three accumulation layers described above were also identified in other muddy sequences, including sample BC02. The calculated sediment accumulation rate for the lower accumulation layer in BC02 is 2 mm/year.

A similar, three layered accumulation pattern, was identified in the interbedded sequences. However, in most cases, the Be-7 enriched riverine derived sediments formed a thicker layer at the top of the core. The middle accumulation layer was identified as a region of fairly constant excess Pb-210 activity, indicating event deposition or mixing. The excess Pb-210 derived accumulation rate for the lower layer of core BC09 was 3mm/year.

Given the grain size and mineralogical content (quartz) of the sandy sequence, no Pb-210 derived sediment accumulation rates were calculated. Most excess Pb-210 profiles showed low detection values with little down-core variability. The Cs-137 profiles (Fig. 4.11) were reasonably constant with depth revealing no discernable peaks over the core length. No excess Cs-137 peaks were identified with confidence; therefore, Cs-137 was not used to validate the calculated excess Pb-210 accumulation rates. All radionuclide data and accumulation rates can be viewed in Appendix A.

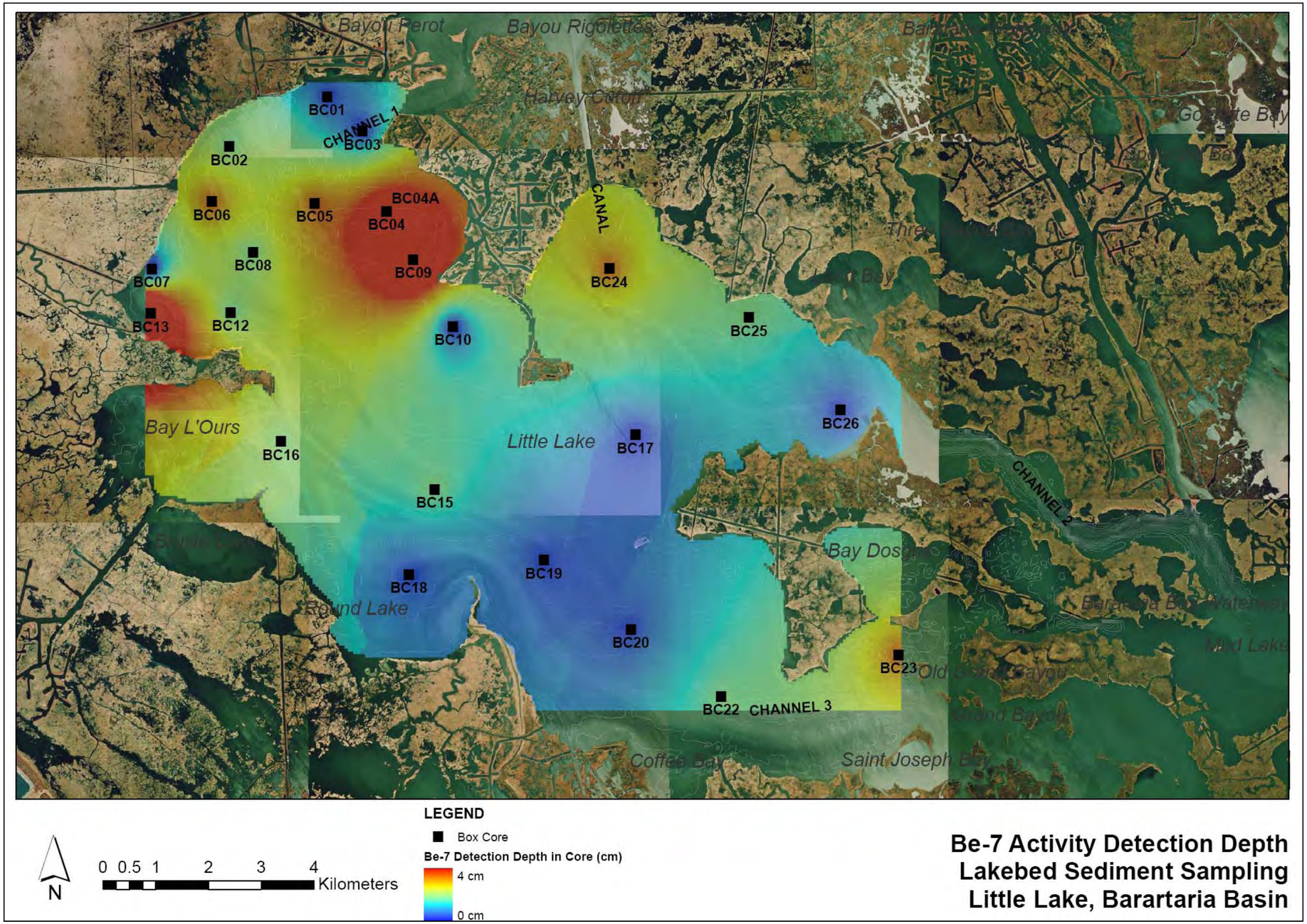

Figure 4.8. Maximum down-core depth of detectable Be-7 activity.

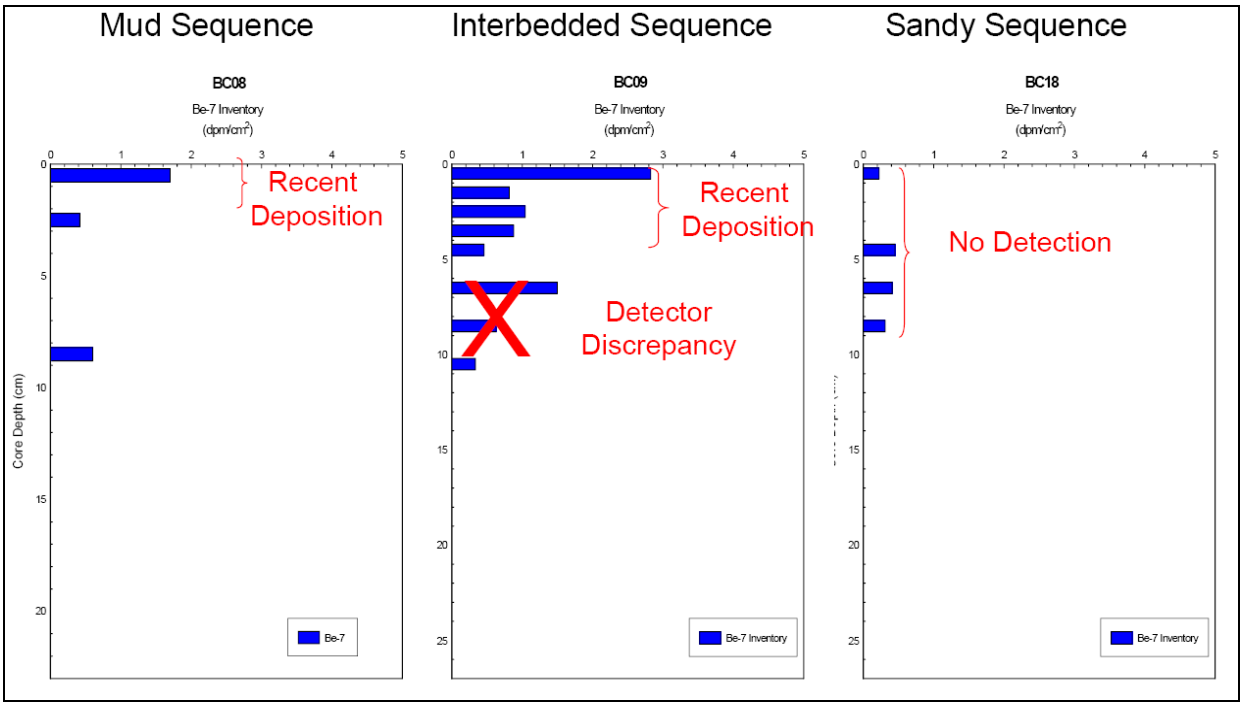

Figure 4.9. Be-7 inventory depth profile for mud, interbedded, and sandy sequences.

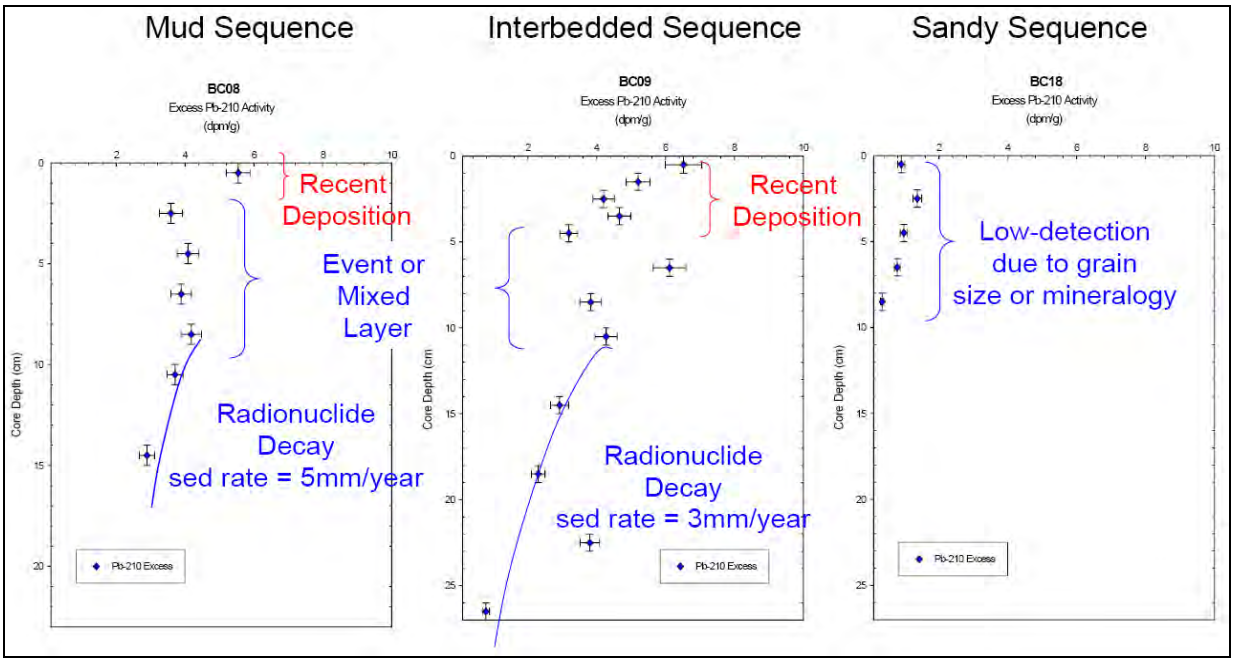

Figure 4.10. Excess Pb-210 activity depth profile for mud, interbedded, and sandy sequences.

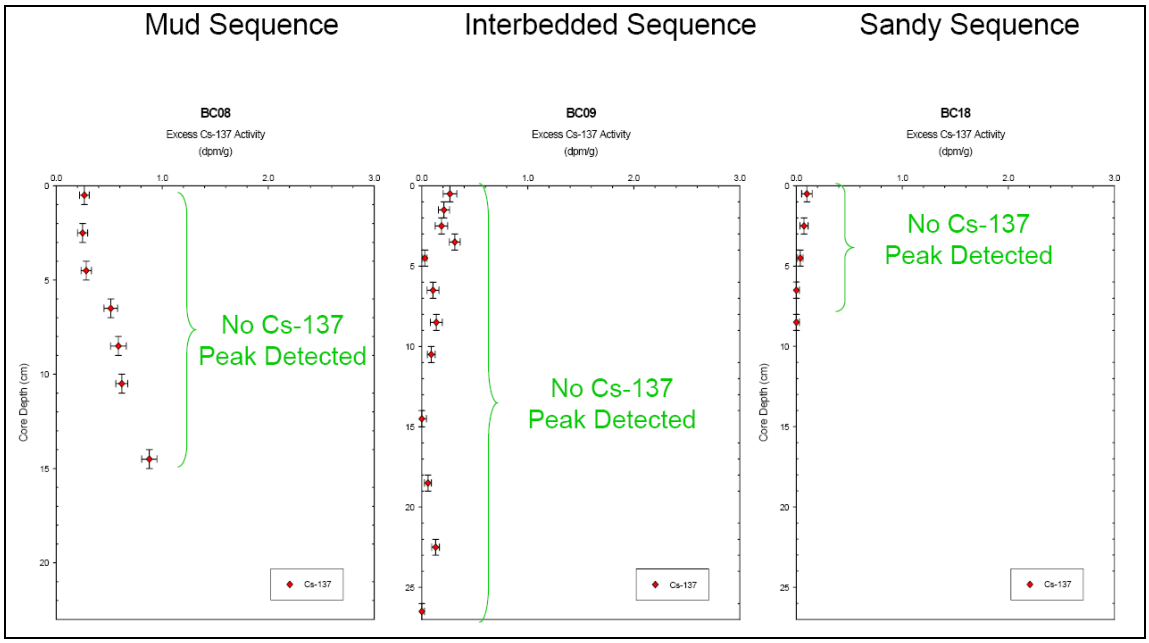

Figure 4.11. Cs-137 activity depth profile for mud, interbedded, and sandy sequences.

Summary

Three different depositional sequences were observed in the Little Lake region. The massive mud sequence was identified mainly in the North Basin, Turtle Bay Basin, and South Basin, occurred mainly near the main tidal channel mouths (CHANNEL 1, CHANNEL 2, and CHANNEL 3) and the deeper more quiescent regions of the lake. The inter-bedded sequence was observed throughout the study site but occurred primarily around the lake perimeter near localized entry points to the lake, such as stream and canal networks. The sand sequences occurred mainly in the Central Basin of Little Lake.

Beryllium-7 activity was detected in the muddy and interbedded sequences. While confined mainly to the top 1 cm of the muddy cores, Be-7 activity in the interbedded cores was detected down-core at depths up to 4 cm. Detectable Be-7 activity at the very top of the cores is interpreted as recent riverine derived sediment deposition (< 200 days). Visual inspection reveals that the highest Be-7 activities and maximum down-core depth of detection occurred

near the perimeter of the lake mostly near small tidal streams or man made canal networks (Fig. 4.12). Based on this geographic relationship, it is interpreted that certain dredged canal systems and tidal streams are localized sources of riverine sediments to the lake, where point source sedimentation is occurring and sediments do not disperse into the lake, far from the initial sediment source. The stream and canal networks identified in Figure 4.12 are indirectly connected to upstream riverine sources via the Intracoastal Waterway (ICWW), Bayou Barataria and Bayou Rigolettes (Fig 4.13). Causes of the increased sediment load at these localized sites are interpreted as the result of upstream flood waters entering the system.

Only a thin veneer of Be-7 was detected in the sandy sequence cores. The larger distance from the sandy cores to the riverine derived sediment source likely accounts for this result. Low Be-7 activities detected in the sandy sequence could be indicative a little or no recent deposition or purely a function of particle size and composition (less adsorption of Be-7 to coarser sand particle sizes, mostly comprised of quartz).

Given the enormity of the Davis Pond Diversion, it would not be prudent to dismiss the potential affects that this project will have on the short and long-term sediment distribution and accumulation rates in Little Lake. The diversion is designed to trap the majority of the suspended sediment particles into a ponding area close to the diversion discharge structure, and enhance the formation of marshes in this region. The remaining fine-grained suspended sediment is transported over a rock weir and into the inter-distributary lakes and bays of the Barataria Basin (Fredine, 2003). Satellite imagery in Figure 4.14 shows significant suspended sediment moving through the weir which will impact regions to the south. The project site, Little Lake, is centrally located within the Barataria Basin and the direct effects of river-derived suspended sediments in this region are largely unknown.

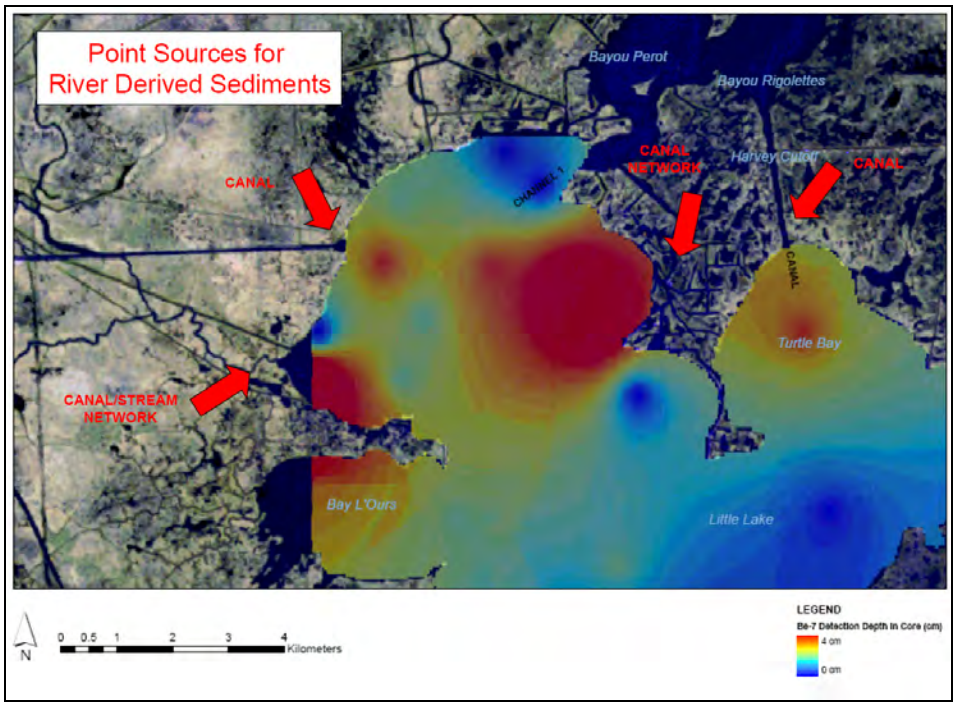

Figure 4.12. Canal and stream networks that serve as entry points for riverine sediments to Little Lake.

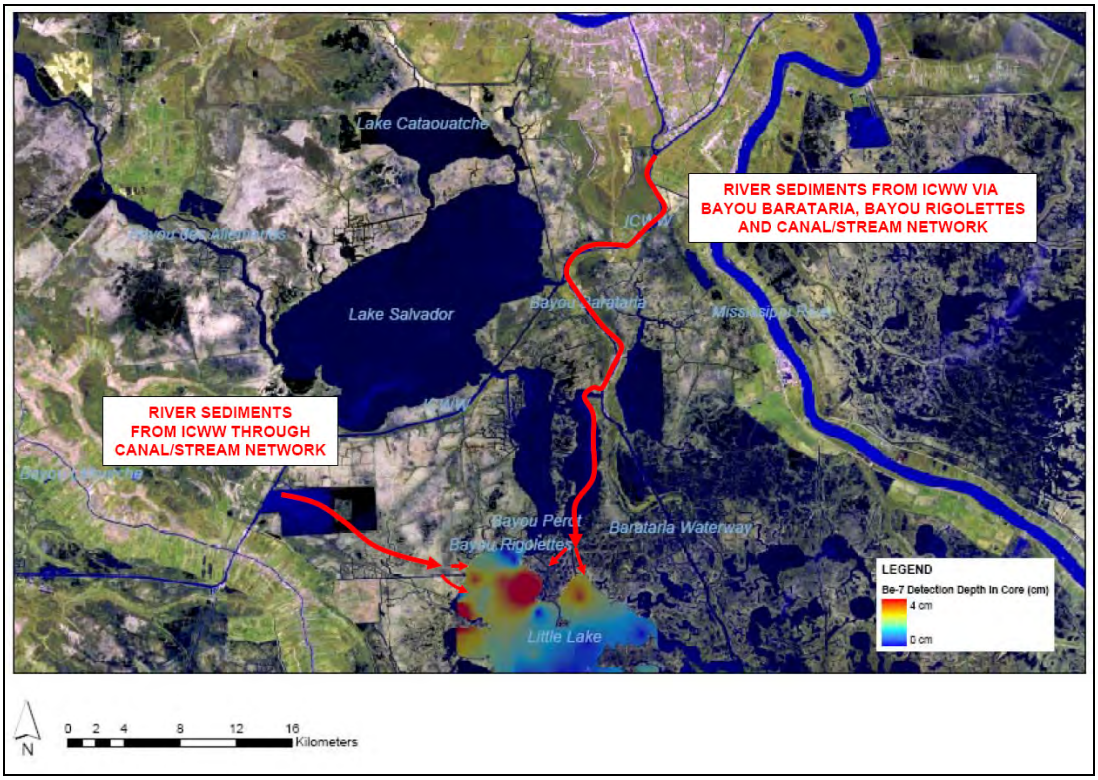

Figure 4.13. Transport pathways of riverine sediments into Little Lake.

Figure 4.14. Landsat imagery of Lake Cataouatche pre and post river diversion (left: 18 November 1999, right: 15 December 2003, two weeks after a full-capacity test-run of the structure, (2004). Note suspended sediment plume extending into Lake Cataouatche and beyond (Imagery courtesy of Nan Walker).

Figure 4.15 shows the freshwater release rates for the Davis Pond Diversion for the year of 2003 (Fredine, 2003). No freshwater discharge occurred during the sediment sample collection time period (Oct. 2003). If the diversion was supplying suspended sediments to Little Lake, the large release in April could potentially be detected in the cores. However, due to the geographic proximity of the identified Be-7 hotspots to the local features, such as man made canal and stream networks, it is most likely that these features are the source of localized Be-7 enriched surface sediments. The similarities in the sediment characteristics around all major tidal channels leading into Little Lake and lack of evidence to support a distinct Be-7 activity emanating from the northern tidal channel are indications that the Davis Pond River Diversion was not affecting the sediment distribution and accumulation patterns in Little Lake at the time of the study.

More research is necessary to assess the exact sources of the observed elevated Be-7 activities in this region and to determine if localized sources (canals, tidal streams),

Mississippi River derived sediments, or atmospherically supported Be-7 activities account for the patterns observed in this study. In addition, the affects of sediment grain size and mineralogy on Be-7 particle adsorption need to be more thoroughly addressed.

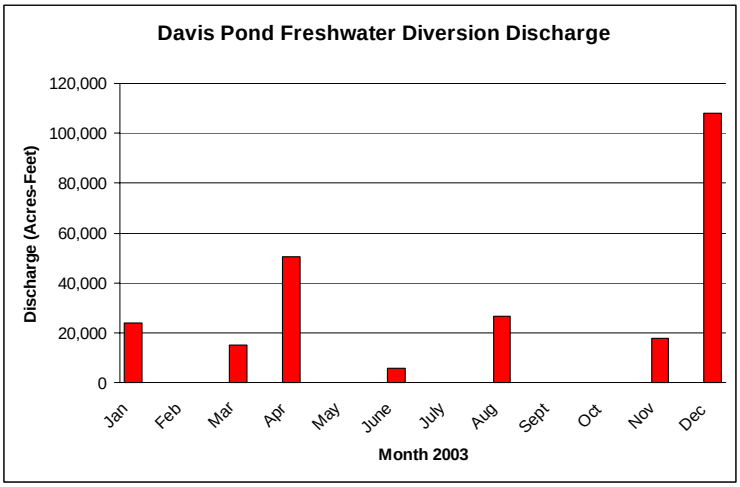

Figure 4.15. Davis Pond freshwater diversion discharge for 2003 (Fredine, 2003).

Utilizing the Be-7 and excess Pb-210 profiles, a three layered sediment accumulation pattern was identified in both the muddy and interbedded sequence cores. The top accumulation layer consisted of recently deposited riverine derived sediments as determined by detectable Be-7 activities. The middle accumulation layer exhibited a constant excess Pb-210 activity profile. The lack of variability in this layer may be indicative of event sedimentation or vertically mixed sediments. A classic excess Pb-210 radionuclide decay curve was detected in the lower layer of the cores. Excess Pb-210 derived sediment accumulation rates ranged from 1 to 5 mm/year for the study site.

Given the identified sequences and resultant radionuclide profiles, it is interpreted there are three time scales of deposition in the region. Most recently, short-term point source sedimentation (<200 days) linked to spring flooding is occurring near tidal streams and canal networks which are directly connected to upland river sources. Secondly, event sedimentation

(up to 10 cm thick) has occurred and is most likely due to storm or hurricane activity in the region or the physical/biological reworking of the sediments. Tropical Storm Isidore and Hurricane Lili made landfall in coastal Louisiana in late September and early October 2002. Tropical Storm Isidore passed directly over Little Lake while Hurricane Lili made landfall west of the study site (Fig. 4.16). These storm events could serve as the forcing mechanism for the event layers as offshore (4.5 m and 6 m water depth) current velocities measured for both storms exceeded 1 m/s @ 65 cm above the seabed (Allison et al., 2005). Water levels in Little Lake rose approximately 1 m during both of these storm events (Fig. 4.17) (USGS, 2007).

Lastly, long-term sediment accumulation has been identified down-core, preceding both the event and short-term deposition discussed above. Figure 4.18 is an overview of the surface sediment deposition patterns observed in Little Lake.

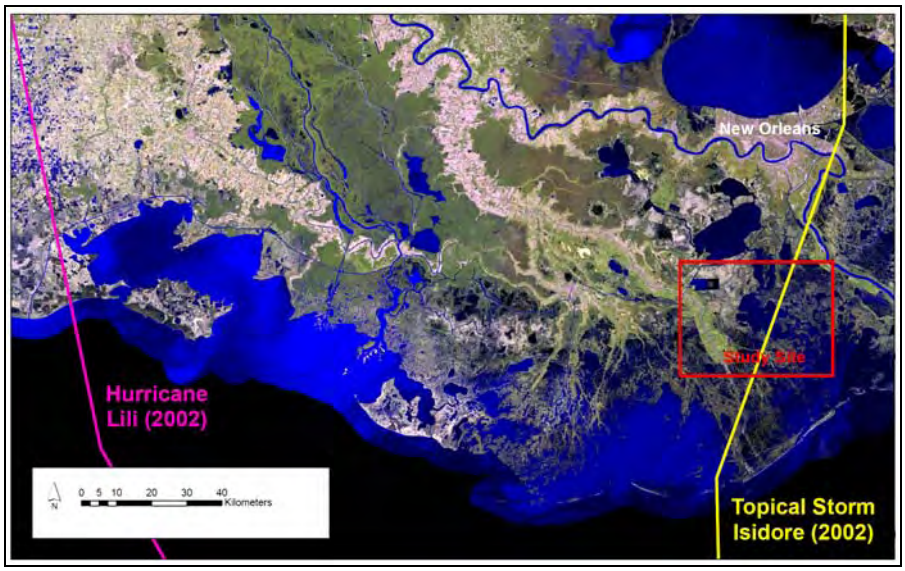

Figure 4.16. Hurricane Lili and Tropical Storm Isidore tracks relative to Little Lake.

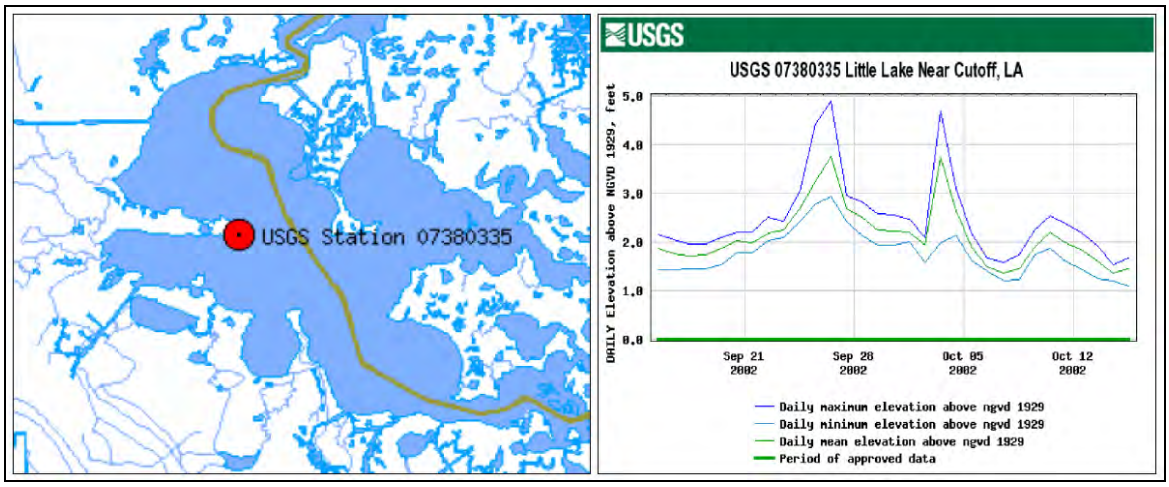

Figure 4.17. Water level data from USGS station in Little Lake during Tropical Storm Isidore and Hurricane Lili (USGS, 2007).

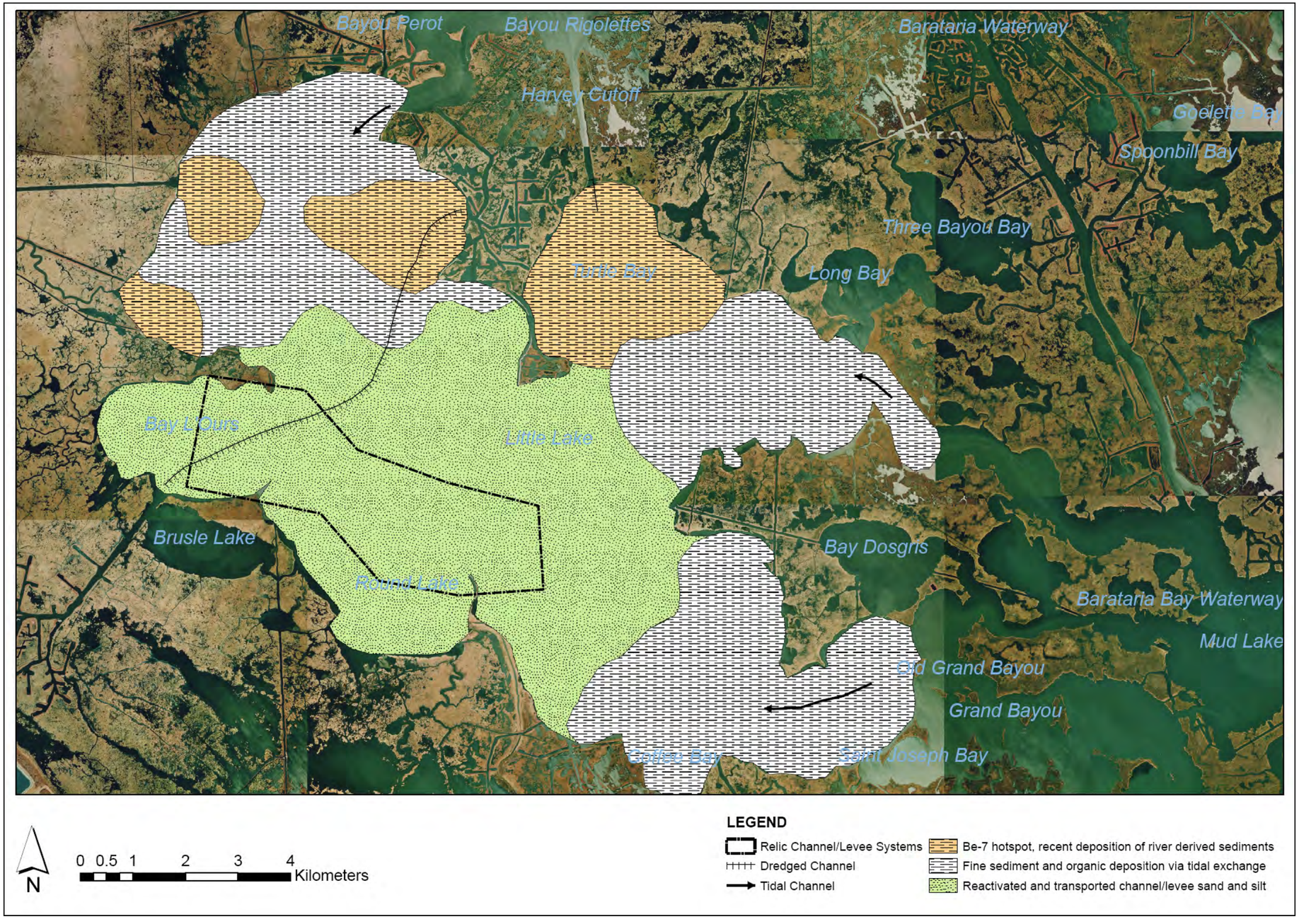

Figure 4.18. Overview of surface sediment deposition in Little Lake.

CHAPTER 5 LAKE BOTTOM SEDIMENT VARIABILITY AND ACOUSTIC IMAGERY

Introduction

Acoustic imagery generated by side scanning sonar has become a standard and essential tool for geological studies in the marine environment. Initially developed as a tool for naval purposes, side scanning sonar was first used for geological mapping in the 1960's and has been commercially available since 1970 (Roberts et al., 1999). The acoustic signal emitted from the sonar interacts with the seafloor and is scattered back to the sonar. The resultant backscatter is affected by the ensonification geometry, physical characteristics of the surface, and the nature of the seabed surface (such as composition and density) (Blondel and Murton, 1997). Generally speaking, different sediment types have distinct acoustic signatures. These acoustic signatures, coupled with seabed sampling and an experienced interpreter can be utilized to create a qualitative geologic interpretation. Acoustic images of the seafloor are regularly utilized for geologic mapping, marine habitat characterization, and obstacle/hazards detection.

Side scanning sonar systems are typically deployed hull-mounted, towed, or autonomously. Recent advancements in sonar and GPS instrumentation and data acquisition/processing methodologies coupled with a unique vessel configuration have made it possible to acquire acoustic imagery in the ultra-shallow coastal environment of Louisiana (Roberts et al., 2000; Roberts et al., 1999).

Prior to the late 1980's, most acoustic imagery was utilized in a qualitative way. More recently, automated acoustic imagery classification models are becoming more prevalent and numerous models are now commercially available. The intricate details regarding these classifications models are beyond the scope of this study, however, a simple statistical

correlation between the acoustic imagery and sediment properties of Little Lake has been tested as a part of this study.

Objectives

The objective of this portion of the study is to qualitatively identify acoustic lakebed features and determine if there is a statistical correlation between the side scan sonar acoustic characteristics and the sediment grain size for Little Lake.

Methods

Side scan sonar imagery was collected using dual-frequency (100 and 500 kHz) digital side scanning sonar during the same geophysical data acquisition cruise discussed in previous sections. Over 943 km of data were collected resulting in over 125 km^2 of coverage. The line spacing was approximately 150 m with a swath width of 200 m. The dual frequency (100 kHz and 500 kHz) sonar data was processed using standard sonar processing methods in ISIS. The sonar swath width was trimmed to 70 m on both port and starboard and a custom TVG table was implemented to remove any existing acoustic artifacts. All processed mosaics were exported as 0.2 m cell size, 8 bit geo-referenced image files and imported into a GIS. The imagery was smoothed with a 3x3 mean filter to remove spurious values due to noise or systematic problems which may occur during data acquisition (Blondel and Murton, 1997). The acoustic penetration depths were calculated for both sonar frequencies by dividing the sound velocity in water (1500 m/sec) by the sonar frequency resulting in a 0.3 to 1.5 cm skin depth.

In order to determine a correlation between sonar gray-scale backscatter values and the physical sediment properties, a 3 m buffer was created at all surface sediment sample locations. The buffer size was determined and limited by the horizontal accuracy of the GPS system

utilized for sediment sampling. Summary statistics within the 3 m buffer zones (min, max, mean, median, std, variety, majority, minority) were extracted from the 100 kHz and 500 kHz sonar at each sediment sample location. Simple linear regression analysis was used to correlate image gray scale intensity (acoustic backscatter values) to the sediment characteristics of the basin including sediment grain size, water content, organic content, and shell content. In addition, a visual interpretation of the sonar mosaic was conducted to delineate features on the lakebed and compare the presence of such features to surface sediment grain size.

Results

There were no statistical correlations between the 100 kHz and 500 kHz sonar backscatter values and the physical sediment properties. Given the lack of statistical correlation, a computer assisted classification/geologic map was not created for the sonar mosaic. However, a thorough visual interpretation of lakebed features was conducted. See Appendix B for large format side scan sonar mosaic and delineated lakebed feature maps.

Lakebed features identified on the side scan sonar mosaic included pipelines, channels, trawl and propeller scars, and shell beds. Moderate to intense bottom scars were prevalent in Little Lake accounting for approximately 25% of the total lakebed area. Intense bottom scars were identified near canal/stream entry points into the lake and are likely associated with high traffic, marine vessel routes. In addition, bottom scars were regularly found in shell bed regions. A pipeline network, delineated from the sonar mosaic, extended from a canal and channel in the North Basin and terminated at an oil well in the Central Basin.

A visual comparison of the lakebed features with surface sediment characteristics indicated a relationship between the frequency or presence of bottom scars and the predominant lakebed sediment grain size. Regions of high sand content (> 30%) are mostly devoid of bottom

scars (Fig. 5.1). In contrast, regions of high clay content (> 30%) show the greatest evidence and frequency of bottom scars (Fig. 5.2). In addition, it is evident from the sonar mosaic that regions that contain in excess of 15% estimated shell content appear to have associated high backscatter values (Fig. 5.3) regardless of the sediment matrix grain size.

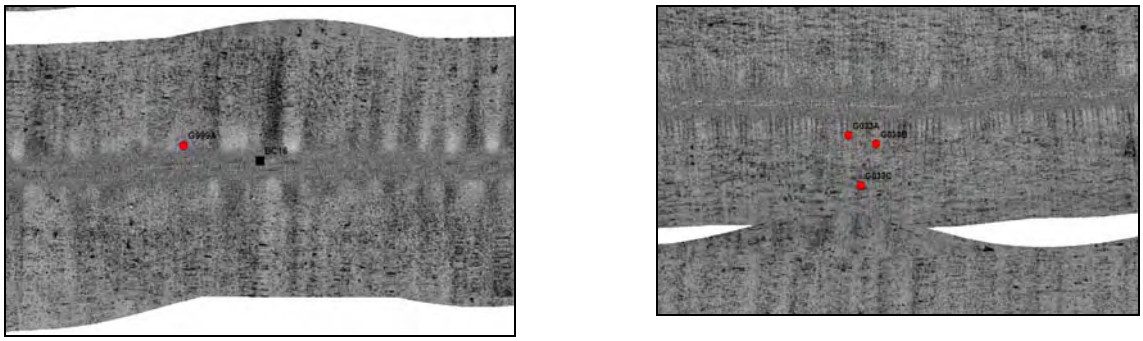

Figure 5.1. 500 kHz side scan sonar imagery in regions of high sand content.

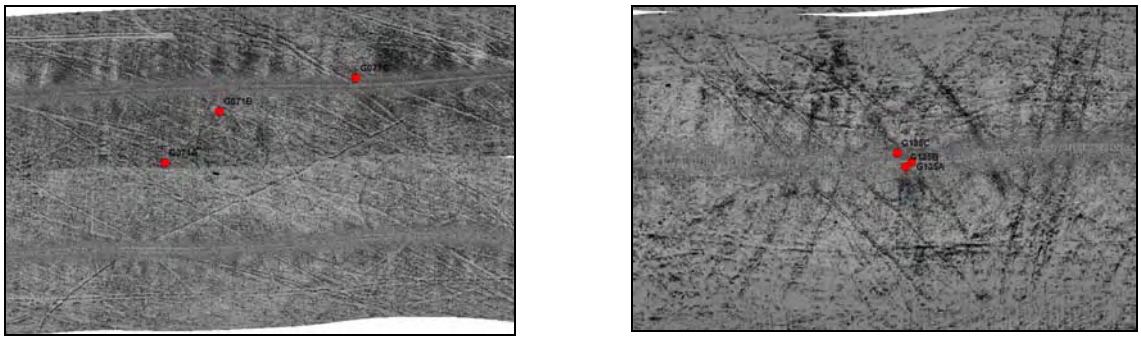

Figure 5.2. 500 kHz side scan sonar imagery in regions of high clay content.

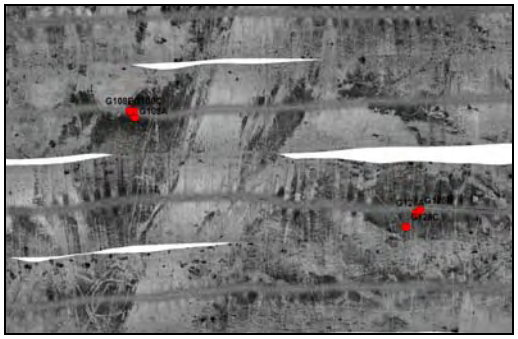

Figure 5.3. 500 kHz side scan sonar imagery in regions of high shell content.

Summary

Owing to the lack of a large grain size shift in the lake bottom sediments, there was no statistical (simple linear regression) correlation between the 100 kHz and 500 kHz side scan sonar imagery acoustic signal and the sediment grain size. This is a result of the homogenous nature of the lakebed sediments. More complex statistical models were not attempted and are beyond the scope of this study.

However, other lakebed features such as channels, trawl marks, prop scars, pipelines, and shell beds were apparent on the side scan sonar imagery. The prevalence of bottom scars appears to be related to marine activity (preferred navigation routes within Little Lake) and the predominant lakebed sediment grain size. Intense bottom scars were identified near main navigation channels. It was also noted that a large number of bottom scars occurred in regions where the lakebed sediments are high in clay content. Few or no bottom scars occurred in regions of high sand content (Fig. 5.4). The data suggest that trawl marks and prop scars are preserved better in clay-rich sediments. The preservation times are not known but would be critical to developing a clear understanding of benthic habitat conditions in coastal settings. The affects of marine activities on the resuspension and deposition of sediment and particulate matter in Little Lake should be determined in a more quantitative manner.

The side scan sonar data was a critical component of the lakebed baseline study and was utilized for determining sediment sampling locations and delineating lakebed features. In addition, the lake bottom sonar image will act as a baseline dataset for all future geologic studies in Little Lake.

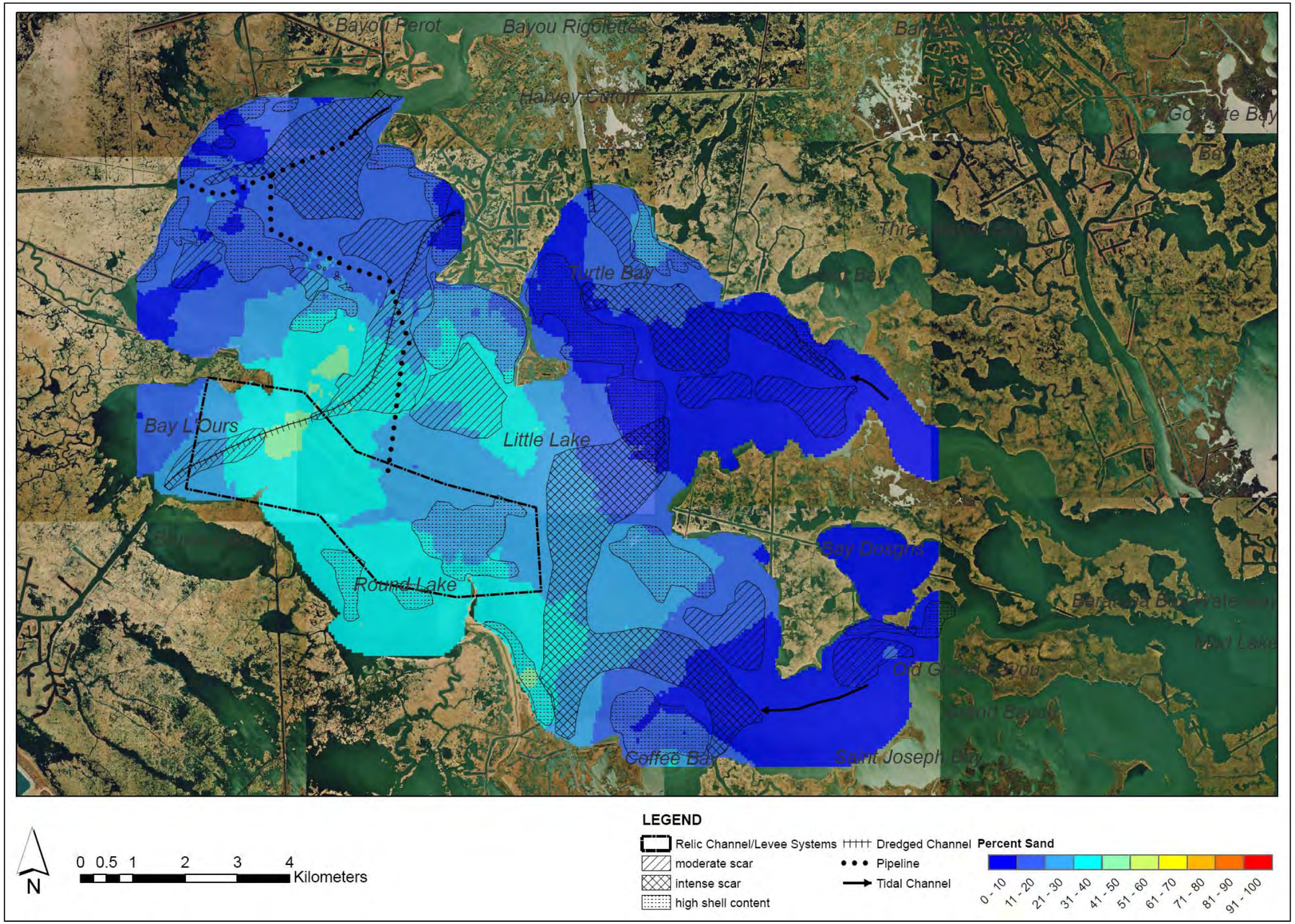

Figure 5.4 Seabed features from side scan sonar imagery. Note the lack of bottom scars in regions of high sand content.

CHAPTER 6 PROJECT CONCLUSIONS

The critical research questions outlined in the Introduction of this research paper were addressed by utilizing the geophysical data and sediment samples collected during this project. The project conclusions are as follows:

1) What is the origin of Little Lake and what is its lakebed morphology? Detailed bathymetric maps for the study site, derived from the single-beam echo sounder data, revealed three main deep tidal channels and one dredged canal leading into the lake. In addition, four main sub-basins with very little bathymetric variability were identified. The formation of Little Lake is interpreted to be the result of the combined effects of subsidence, lake margin erosion, and a regional decrease in sediment supply associated with Mississippi River avulsions. In addition, erosional forces and salt water intrusion lead to bank erosion, marshland deterioration and channel enlargement. Exposure to large storm events, including hurricanes, accelerates the natural enlargement processes. The sub-basins within Little Lake appear to have subsided, enlarged, fused and amalgamated to form the present lake perimeter.

2) How does the lakebed morphology control or influence the surface sediment properties of Little Lake? The integration of lakebed sediment samples with geophysical datasets (single-beam echo sounder, side scan sonar, and chirp subbottom sonar) revealed that both the lakebed morphology and in situ subsurface sediment deposits influence the current surface sediment distribution in Little Lake.

The three main tidal channels bring fine-grained, organic rich sediments into the lake during high water stages and tidal exchange by sloughing and entraining particulate matter from the lake-tidal channel perimeter and adjacent marshlands. In addition, the man-made canal (Harvey Cutoff), other canal/stream networks, and winnowing of lakebed sediments along the

SE-facing lake perimeter were interpreted as potential sources of silt rich sediments. Relic channel/levee deposits identified on the subbottom chirp sonar provide a source for the sandy sediments observed in the Central Basin and are reactivated by artificial dredging and redistributed in the localized region. A large fetch and increased exposure to forcing mechanisms in the Central Basin may account for some of the redistribution of the sand and the lack of fines content found in this area.

3) What are the sedimentary sequences, sediment accumulation characteristics (long and short-term), and the radionuclide signature of the surface sediments in Little Lake? Box core sampling and X-radiography revealed three distinct depositional sequences in Little Lake; a massive mud, an interbedded sequence, and sandy sequence. The mud sequence was observed near the tidal inlets while the interbedded sequence was identified near the lake perimeter. The sandy sequence occurred in regions where in situ sand and silt deposits are known to exist (relic channel/levee systems).

Utilizing the Be-7 and excess Pb-210 radionuclide profiles, a 3-layer accumulation sequence was identified. The topmost accumulation layer, identified as having detectable Be-7 activity, is interpreted as short-term (<200 days) sediment deposition associated with riverine derived sediment sources. The middle accumulation layer (constant excess Pb-210 activity with depth) signifies an event layer (rapid deposition, i.e. days or weeks) and is most likely a result of storm activity in the region (Tropical Storm Isidore and Hurricane Lili, 2002). The third accumulation layer demonstrates the characteristic radionuclide decay and the long-term excess Pb-210 derived accumulation rates for Little Lake range from 1-5mm/year.

Short-term sediment accumulation, determined utilizing surface sediment Be-7 activity, is occurring near point sources such as canal and stream networks along the perimeter of the

lake. These networks are indirectly linked to river water via the ICWW, Bayou Barataria, and Bayou Rigolettes and the increase in sediment load is likely linked to spring flooding. Both short-term and event deposition have occurred recently in Little Lake with slower accumulation records preserved below these deposits. Although a clear pattern of introduction of Mississippi River suspended sediment resulted from the study of Be-7 in the lake bottom sediments, the frequency of propeller scars and trawl marks suggest significant disruption of the natural sedimentation patterns. The residual times of propeller scars and trawl marks is unknown.

4) Given the sediment characteristics, is the region currently impacted by the Davis Pond River Diversion? The integration of geophysical datasets with seabed sampling techniques resulted in a comprehensive understanding of the surface sediment and accumulation characteristics of Little Lake. The similarities in the sediment characteristics around all major tidal channels leading into Little Lake and lack of evidence to support a distinct Be-7 activity emanating from the northern tidal channel are indications that the Davis Pond River Diversion project has not significantly affected Little Lake.

5) What acoustic features are present on the lakebed and do the acoustic characteristics of the lakebed correlate to the physical sediment properties? A qualitative interpretation of the side scan sonar mosaic revealed shell beds, trawl marks, propeller scars, pipelines, channels, and other subtle acoustic backscatter variations. Preliminary statistical analysis (simple linear regression) indicated no statistical correlation between the lakebed surface sediment grain size and the sonar acoustic characteristics. The homogenous nature of the lakebed does not allow for a unique acoustic signature of sediments in this region. A qualitative relationship was observed between bottom scar prevalence and the predominant lakebed sediment grain size; leading the author to link grain size to the preservation of such bottom features.

This study was the first comprehensive geologic assessment of an inter-distributary basin lake in the coastal deltaic plain of Louisiana. The geologic assessment of the lake bed surface for this study was determined by integrating seabed sample grain size and radionuclide analysis with high resolution hydrographic and geophysical datasets. Given the comprehensive results of the study and the lack of evidence to suggest that the surface geology of Little Lake has been affected by the Davis Pond River Diversion at the time the study, this research will indeed act as a baseline dataset for future geologic studies in this region. Baseline geologic datasets and a thorough assessment of pre-restorative conditions in the coastal bays/lakes are essential to evaluating the success of large scale coastal restoration projects in Louisiana.

REFERENCES

Allen, Y., 2003. Personal Communication, Baton Rouge.

Allison, M.A., Sheremet, A., Gon˜ i, M.A. and Stone, G.W., 2005. Storm layer deposition on the Mississippi–Atchafalaya subaqueous delta generated by Hurricane Lili in 2002. Continental Shelf Research, 25: 2213–2232.

Barras, J. et al., 2003. Historical and Projected Coastal Louisiana Land Changes: 1978-2050, USGS.

Barras, J.A., 2006. Land area change in coastal Louisiana after the 2005 hurricanes—a series of three maps: U.S. Geological Survey Open-File Report 06-1274.

Baskaran, M., Ravichandran, M. and Bianchi, T.S., 1997. Cycling of Beryllium-7 and Pb-210 in a High DOC, Shallow, Turbid Estuary of South-east Texas. Estuarine, Coastal, and Shelf Science, 45: 165-176.

Bentley, S.J., Keen, T.R., Blain, C.A. and Vaughan, W.C., 2002. The origin and preservation of a major hurricane event bed in the northern Gulf of Mexico: Hurricane Camille, 1969. Marine Geology, 186(3-4): 423-446.

Bentley, S.J. and Nittrouer, C.A., 1999. Physical and Biological Influences on the Formation of Sedimentary Fabric in an Oxygen-restricted Depositional Environment: Eckernforde Bay, Southwestern Baltic Sea. PALAIOS, 14: 585-600.

Berry, P.L. and Reid, D., 1987. An Introduction to Soil Mechanics. McGraw-Hill Book Company (UK) Limited, Maidenhead, Berkshire, 317 pp.

Blake, W.H., Walling, D.E. and He, Q., 2002. Using Cosmogenic Beryllium-7 as a Tracer in Sediment Budget Investigations. Geografiska Annaler, 84A: 89-102.

Blondel and Murton, 1997. Handbook of Seafloor Sonar Imagery. Wiley-Praxis Series in Remote Sensing. Praxis Publishing, Chichester, 314 pp.

Boesch, D. et al., 1994. Scientific Assessment of Coastal Wetland Loss, Restoration and Management in Louisiana. Journal of Coastal Research, Special Issue No. 20: 89.

Canuel, E.A., Martens, C.S. and Benninger, L., K., 1990. Seasonal variations in Be-7 activity in the sediments of Cape Lookout Bight, North Carolina. Geochimica et Cosmochimica Acta, 54: 237-245.

Coakley, J.P. and Syvitski, J.P.M., 1991. Sedigraph Technique, Principles, Methods, and Application of Particle Size Analysis. Cambridge University Press, Cambridge, pp. 368.

Coleman, J.M., 1966. Ecological changes in a massive fresh-water clay sequence. Transactions - Gulf Coast Association of Geological Societies, XVI: 159-174.

Coleman, J.M., Roberts, H.H. and Stone, G.W., 1998. Mississippi River Delta: an Overview. Journal of Coastal Research, 14(3): 698-716.

Compton, R.R., 1985. Geology in the Field. John Wiley & Sons, Inc., New York, 398 pp.

DeLaune, R.D., Whitcomb, J.H., Patrick, J., W.H., Pardue, J.H. and Pezeshki, S.R., 1989. Accretion and Canal Impacts in a Rapidly Subsiding Wetland: Cs-137 and Pb-210 Techniques. Estuaries, 12(4): 247-259.

Dellapenna, T.M., Kuehl, S.A. and Schaffner, L.C., 1998. Sea-bed Mixing and Particle Residence Times in Biologically and Physically Dominated Estuarine Systems: a Comparison of Lower Chesapeake Bay and the York River Subestuary. Estuarine, Coastal and Shelf Science, 46: 777-795.

Dyer, K.R., 1995. Sediment Transport Processes in Estuaries. In: G.M.E. Perillo (Editor), Geomorphology and Sedimentology of Estuaries . Developements in Sedimentology. Elsevier Sciences, B.V.

Frazier, D.E., 1967. Recent Deltaic Deposits of the Mississippi River: Their Development and Chronology. Transactions - Gulf Coast Association of Geological Societies, XVII: 287-311.

Fredine, J., 2003. Davis Pond Project Manager, USACE, New Orleans.

Frey, R.W. and Howard, J.D., 1986. Mesotidal Estuarine Sequences: A Perspective from the Georgia Bight. Journal of Sedimentary Petrology, 56(6): 911-924.

Gagliano, S.M., Kemp, E.B., Wicker, K.M. and Wiltenmuth, K.S., 2003. Active Geological Faults and Land Change in Southeastern Louisiana, Baton Rouge.

Hawley, N., Robbins, J.A. and Eadie, B.J., 1986. The partitioning of beryllium-7 in fresh water. Geochimica et Cosmochimica Acta, 50: 1127-1131.

Keucher, G.J., 1994. Geologic Framework and Consolidation Settlement Potential of the Lafourche Delta, Topstratum Valley Fill: Implications for Wetland Loss in Terrebonne and Lafourche Parishes, Louisiana. Ph.D. diss., Louisiana State University.

Lane, R., 2003. The Effect on Water Quality of Riverine Input into Coastal Wetlands. PhD Thesis, Louisiana State University, Baton Rouge, 153 pp.

Lane, R.R., Day, J.W. and Thibodeaux, B., 1999. Water quality analysis of a freshwater diversion at Caernarvon, Louisiana. Estuaries, 22: 327-336.

McCorquodale, J.A. and Georgiou, I., 2006. Three Dimensional Hydrodynamic Modeling of Barataria Estuary - Coastal Louisiana Ecosystem Assessment and Restoration (CLEAR) Model of Louisiana Coastal Area (LCA) Comprehensive Ecosystem Restoration Plan.

Milbert, D.G. and Hess, K.W., 2001. Combination of Topography and Bathymetry through Application of Calibrated Vertical Datum Transformations in the Tampa Bay Region, Proceedings of the 2nd Biennial Coastal GeoTools Conference, Charleston, SC.

Mullenbach, B.L. and Nittrouer, C.A., 2000. Rapid deposition of fluvial sediment in the Eel Canyon, northern California. Continental Shelf Research, 20: 2191-2212.

Nittrouer, C.A., Sternberg, R.W., Carpenter, R. and Bennett, J.T., 1979. The use of Pb-210 geochronology as a sedimentological tool: Application to the Washington continental shelf. Marine Geology, 31: 297-316.

NOAA, 2004. Vertical Datum Transformation Software Version 1.06.

NOAA, 2006. Tides & Currents. NOAA, pp. Tide and Current Data From NOAA website.

Park, D., 2002. Hydrodynamics and Freshwater Diversion within Barataria Basin. PhD Thesis, Louisiana State University, Baton Rouge, 107 pp.

Penland, S., Boyd, R. and Suttor, J.R., 1988. Transgressive Depositional Systems of the Mississippi Delta Plain: A Model for Barrier Shoreline and Shelf Sand Development. Journal of Sedimentary Petrology, 58(6): 932-949.

Pilkey, O.H., Morton, R.A., Kelley, J.T. and Penland, S., 1989. Coastal Land Loss. Short Course in Geology, 2. American Geophysical Union, Washington, DC, 73 pp.

Reyes, E., 2006. Geographical Data Acquisition and Basemap Development of historial Barataria Basin - Coastal Louisiana Ecosystem Assessment and Restoration (CLEAR) Model of Louisiana Coastal Area (LCA) Comprehensive Ecosystem Restoration Plan.

Roberts, H.H., 1997. Dynamic Changes of the Holocene Mississippi River Delta Plain: The Delta Cycle. Journal of Coastal Research, 13: 605-627.

Roberts, H.H., Wilson, C.A. and Supan, J., 2000. Acoustic Surveying of Ultra-Shallow Water Bottoms (<2.0m) for Both Engineering, and Environmental Applications, Offshore Technology Conference, Houston, Texas, pp. 1-10.

Roberts, H.H., Wilson, C.A., Supan, J. and Winans, W., 1999. New Technology for Characterizing Louisiana's Shallow Coastal Water Bottoms and Predicting Future Changes. Gulf Coast Association of Geological Societies Transactions, XLIX: 452-460.

Rotondo, K., 2004. Transport and Deposition of Fluid Mud Event Layers Along the Western Louisiana Inner Shelf. M.S. Thesis, Louisiana State University, Baton Rouge, 118 pp.

Sawlan, J., Borgeld, J., 1976. University of Washington Geological Oceanography Laboratory Manual, pp. 35.

Scrunton, P.C., 1960. Delta Building and the Deltaic Sequence. Recent Sediments, Northwest Gulf of Mexico, AAPG Symposium, 1960(82-102).

Snedden, G., 2006. River, Tidal, and Wind Interations in a Deltaic Estuarine System. PhD Thesis, Louisiana State University and Agricultural and Mechanical College, Baton Rouge, 104 pp.

Sommerfield, C.K., Nittrouer, C.A. and Alexander, C.R., 1999. Be-7 as a tracer of flood sedimentation on the northern California continental margin. Continental Shelf Research, 19: 335-361.

USACE, 2003. Project Fact Sheet, Davis Pond Freshwater Diversion Project.

USGS, 2007. USGS Real-Time Water Data for Louisiana.

Walling, D.E., He, Q. and Blake, W.H., 1999. Use of Be-7 and Cs-137 measurements to document short- and medium-term rates of water-induced soil erosion on agricultural land. Water Resources Research, 35: 3865-3874.

Wheelock, K.V., 2003. Pulsed River Flooding Effects on Sediment Deposition in Breton Sound Estuary, Louisiana. Master's Thesis, Louisiana State University, 159 pp.

APPENDIX A: RESULTS OF SEDIMENT ANALYSES

BOX CORE SEDIMENT SAMPLE LOCATIONS

Sample	Latitude Degrees N	Latitude Minutes N	Longitude Degrees W	Longitude Minutes W	Latitude Decimal Degrees North	Longitude Decimal Degrees West	General Comment	Total Sample Depth (cm)	Gamma Detector Utilized	Location Comment
BC01	29	34.123	090	11.111	29.568717	-90.185183	2 attempts	21	b3825	
BC02	29	33.639	090	12.274	29.560650	-90.204567	shell at bottom	21	b3825	
BC03	29	33.761	090	10.708	29.562683	-90.178467	3 attempts, 1st and 2nd shells	6	b3825	
BC04	29	32.937	090	10.447	29.548950	-90.174117	good core	25	b3825	
BC05	29	33.038	090	11.288	29.550633	-90.188133	2 attempts	14	b3825	
BC06	29	33.078	090	12.492	29.551300	-90.208200		15	2020	
BC07	29	32.404	090	13.215	29.540067	-90.220250	shell at bottom	15	2020	
BC08	29	32.552	090	12.023	29.542533	-90.200383		17	3825	
BC09	29	32.437	090	10.148	29.540617	-90.169133		28	3825	
BC10	29	31.741	090	09.702	29.529017	-90.161700	4 attempts, shell in subsurface	10	3825	
BC11	29	31.834	090	10.456	29.530567	-90.174267	shell bottom, NO SAMPLE			
BC12	29	31.364	090	12.179	29.532354	-90.205063	shell at bottom, shallow angled sample	15	3825	location from planned
BC13	29	31.580	090	12.293	29.532488	-90.220697		19	3825	location from planned
BC14	29	30.704	090	11.178	29.511733	-90.186300	shell bottom, NO SAMPLE			
BC15	29	30.079	090	09.962	29.501317	-90.166033		15	3825	
BC16	29	30.605	090	11.750	29.510083	-90.195833		11	3825	
BC17	29	30.586	090	07.595	29.509767	-90.126583	3 attempts	16	2020	
BC18	29	29.213	090	10.289	29.486883	-90.171483		10	2020	
BC19	29	29.328	090	08.703	29.488800	-90.145050	sand at base, core stopped penetration	11	2020	
BC20	29	28.594	090	07.703	29.476567	-90.128383	shell at base	13	2020	
BC22	29	27.885	090	06.667	29.464750	-90.111117	position moved due to oyster fisherman	20	3825	
BC23	29	28.266	090	04.577	29.471100	-90.076283	good core	26	2020	
BC24	29	32.535	090	07.639	29.538229	-90.130883		18	2020	location from planned
BC25	29	31.758	090	06.232	29.529300	-90.103867		23	b3825	
BC26	29	30.789	090	05.184	29.513150	-90.086400		21	2020	

SURFACE SEDIMENT SAMPLE LOCATIONS

Sample	Latitude Degrees N	Latitude Minutes N	Longitude Degrees W	Longitude Minutes W	Latitude Decimal Degrees North	Longitude Decimal Degrees West	Comment
G001A	29	33.992	90.00000	11.961	29.566533	-090.199350	shells
G001B	29	33.995	90.00000	11.963	29.566583	-090.199383	shells
G001C	29	33.988	90.00000	11.966	29.566467	-090.199433	shells
G002A	29	33.985	90.00000	11.945	29.566417	-090.199083	
G002B	29	33.982	90.00000	11.941	29.566367	-090.199017	
G002C	29	33.979	90.00000	11.947	29.566317	-090.199117	
G003A	29	33.596	90.00000	12.576	29.559933	-090.209600	shells
G003B	29	33.595	90.00000	12.582	29.559917	-090.209700	shells
G003C	29	33.586	90.00000	12.587	29.559767	-090.209783	
G004A	29	33.572	90.00000	12.028	29.559533	-090.200467	
G004B	29	33.573	90.00000	12.011	29.559550	-090.200183	
G004C	29	33.588	90.00000	12.023	29.559800	-090.200383	
G005A	29	33.649	90.00000	11.509	29.560817	-090.191817	
G005B	29	33.649	90.00000	11.512	29.560817	-090.191867	
G005C	29	33.647	90.00000	11.522	29.560783	-090.192033	
G006A	29	33.706	90.00000	11.008	29.561767	-090.183467	
G006B	29	33.706	90.00000	11.008	29.561767	-090.183467	
G006C	29	33.705	90.00000	11.018	29.561750	-090.183633	
G007A	29	33.466	90.00000	10.410	29.557767	-090.173500	
G007B	29	33.458	90.00000	10.417	29.557633	-090.173617	
G007C	29	33.449	90.00000	10.402	29.557483	-090.173367	
G008A	29	33.062	90.00000	10.400	29.551033	-090.173333	
G008B	29	33.057	90.00000	10.412	29.550950	-090.173533	
G008C	29	33.051	90.00000	10.419	29.550850	-090.173650	
G009A	29	32.837	90.00000	12.199	29.547283	-090.203317	
G009B	29	32.836	90.00000	12.211	29.547267	-090.203517	
G009C	29	32.836	90.00000	12.222	29.547267	-090.203700	
G010A	29	32.750	90.00000	12.572	29.545833	-090.209533	
G010B	29	32.752	90.00000	12.576	29.545867	-090.209600	
G010C	29	32.760	90.00000	12.589	29.546000	-090.209817	
G011A	29	32.728	90.00000	10.182	29.545467	-090.169700	
G011B	29	32.713	90.00000	10.195	29.545217	-090.169917	
G011C	29	32.703	90.00000	10.204	29.545050	-090.170067	
G012A	29	32.331	90.00000	11.083	29.538850	-090.184717	
G012B	29	32.312	90.00000	11.098	29.538533	-090.184967	
G012C	29	32.304	90.00000	11.092	29.538400	-090.184867	
G013A	29	32.322	90.00000	11.903	29.538700	-090.198383	
G013B	29	32.317	90.00000	11.905	29.538617	-090.198417	
G013C	29	32.311	90.00000	11.911	29.538517	-090.198517	
G014A	29	32.100	90.00000	13.128	29.535000	-090.218800	
G014B	29	32.112	90.00000	13.114	29.535200	-090.218567	
G014C	29	32.106	90.00000	13.117	29.535100	-090.218617	
G015A	29	32.074	90.00000	11.161	29.534567	-090.186017	shells
G015B	29	32.071	90.00000	11.163	29.534517	-090.186050	
G015C	29	32.063	90.00000	11.159	29.534383	-090.185983	
G016A	29	32.227	90.00000	10.160	29.537117	-090.169333	
G016B	29	32.223	90.00000	10.167	29.537050	-090.169450	
G016C	29	32.214	90.00000	10.177	29.536900	-090.169617	
G017A	29	31.992	90.00000	9.933	29.533200	-090.165550	
G017B	29	31.997	90.00000	9.934	29.533283	-090.165567	
G017C	29	32.002	90.00000	9.937	29.533367	-090.165617	

G018A	29.53322		90.15315		29.533220	-090.153150	
G018B	29.53315		90.15315		29.533150	-090.153150	
G018C	29.53310		90.15315		29.533100	-090.153150	
G019A	29.53075		90.15664		29.530750	-090.156640	shells
G019B	29.53084		90.15659		29.530840	-090.156590	shells
G019C	29.53094		90.15659		29.530940	-090.156590	
G020A	29.52908		90.16373		29.529080	-090.163730	check long coord
G020B	29.52900		90.16402		29.529000	-090.164020	
G020C	29.52892		90.16413		29.528920	-090.164130	
G021A	29	31.797	90.00000	10.424	29.529950	-090.173733	shells
G021B	29	31.798	90.00000	10.423	29.529967	-090.173717	shells
G021C	29	31.788	90.00000	10.429	29.529800	-090.173817	
G022A	29	31.744	90.00000	10.865	29.529067	-090.181083	
G022B	29	31.736	90.00000	10.852	29.528933	-090.180867	
G022C	29	31.728	90.00000	10.836	29.528800	-090.180600	
G023A	29	31.749	90.00000	11.414	29.529150	-090.190233	
G023B	29	31.746	90.00000	11.420	29.529100	-090.190333	
G023C	29	31.733	90.00000	11.419	29.528883	-090.190317	
G024A	29	31.729	90.00000	11.924	29.528817	-090.198733	
G024B	29	31.731	90.00000	11.934	29.528850	-090.198900	
G024C	29	31.750	90.00000	11.922	29.529167	-090.198700	
G025A	29	31.592	90.00000	11.382	29.526533	-090.189700	
G025B	29	31.596	90.00000	11.379	29.526600	-090.189650	
G025C	29	31.594	90.00000	11.382	29.526567	-090.189700	
G026A	29.52652		90.15746		29.526520	-090.157460	
G026B	29.52642		90.15740		29.526420	-090.157400	
G026C	29.52637		90.15738		29.526370	-090.157380	
G027A	29.52234		90.16208		29.522340	-090.162080	
G027B	29.52229		90.16192		29.522290	-090.161920	
G027C	29.52232		90.16188		29.522320	-090.161880	
G028A	29.52042		90.15340		29.520420	-090.153400	
G028B	29.52039		90.15340		29.520390	-090.153400	
G028C	29.52044		90.15338		29.520440	-090.153380	
G029A	29	31.316	90.00000	10.445	29.521933	-090.174083	
G029B	29	31.299	90.00000	10.470	29.521650	-090.174500	
G029C	29	31.304	90.00000	10.479	29.521733	-090.174650	
G030A	29	31.061	90.00000	10.769	29.517683	-090.179483	
G030B	29	31.051	90.00000	10.774	29.517517	-090.179567	
G030C	29	31.046	90.00000	10.776	29.517433	-090.179600	
G031A	29.51438		90.16265		29.514380	-090.162650	
G031B	29.51440		90.16246		29.514400	-090.162460	
G031C	29.51431		90.16268		29.514310	-090.162680	
G033A	29	30.676	90.00000	11.190	29.511267	-090.186500	
G033B	29	30.673	90.00000	11.180	29.511217	-090.186333	
G033C	29	30.660	90.00000	11.186	29.511000	-090.186433	
G035A	29	30.891	90.00000	13.420	29.514850	-090.223667	
G035B	29	30.881	90.00000	13.402	29.514683	-090.223367	
G035C	29	30.892	90.00000	13.397	29.514867	-090.223283	
G039A	29	30.039	90.00000	11.280	29.500650	-090.188000	
G039B	29	30.036	90.00000	11.289	29.500600	-090.188150	
G039C	29	30.036	90.00000	11.292	29.500600	-090.188200	
G041A	29.50508		90.16853		29.505080	-090.168530	
G041B	29.50492		90.16889		29.504920	-090.168890	
G041C	29.50499		90.16906		29.504990	-090.169060	
G042A	29	32.775	90.00000	9.747	29.546250	-090.162450	
G042B	29	32.776	90.00000	9.744	29.546267	-090.162400	

G042C	29	32.776	90.00000	9.748	29.546267	-090.162467
G043A	29	32.587	90.00000	9.719	29.543117	-090.161983
G043B	29	32.580	90.00000	9.731	29.543000	-090.162183
G043C	29	32.584	90.00000	9.740	29.543067	-090.162333
G044A	29	30.646	90.00000	8.713	29.510767	-090.145217
G044B	29	30.654	90.00000	8.723	29.510900	-090.145383
G044C	29	30.663	90.00000	8.712	29.511050	-090.145200
G045A	29.50175		90.14985		29.501750	-090.149850
G045B	29.50170		90.14975		29.501700	-090.149750
G045C	29.50171		90.14948		29.501710	-090.149480
G047A	29.50004		90.12743		29.500040	-090.127430
G047B	29.50000		90.12749		29.500000	-090.127490
G047C	29.50004		90.12756		29.500040	-090.127560
G048A	29	29.628	90.00000	8.566	29.493800	-090.142767
G048B	29	29.622	90.00000	8.571	29.493700	-090.142850
G048C	29	29.618	90.00000	8.575	29.493633	-090.142917
G050A	29	29.404	90.00000	10.219	29.490067	-090.170317
G050B	29	29.408	90.00000	10.223	29.490133	-090.170383
G050C	29	29.411	90.00000	10.225	29.490183	-090.170417
G052A	29	28.695	90.00000	10.824	29.478250	-090.180400
G052B	29	28.695	90.00000	10.831	29.478250	-090.180517
G052C	29	28.688	90.00000	10.812	29.478133	-090.180200
G055A	29.48975		90.13226		29.489750	-090.132260
G055B	29.48972		90.13229		29.489720	-090.132290
G055C	29.48970		90.13239		29.489700	-090.132390
G057A	29.48101		90.15106		29.481010	-090.151060
G057B	29.48108		90.15077		29.481080	-090.150770
G057C	29.48112		90.15069		29.481120	-090.150690
G061A	29.48304		90.12854		29.483040	-090.128540
G061B	29.48297		90.12859		29.482970	-090.128590
G061C	29.48286		90.12855		29.482860	-090.128550
G062A	29.47538		90.14697		29.475380	-090.146970
G062B	29.47526		90.14718		29.475260	-090.147180
G062C	29.47513		90.14733		29.475130	-090.147330
G064A	29.46801		90.14741		29.468010	-090.147410
G064B	29.46821		90.14725		29.468210	-090.147250
G064C	29.46814		90.14744		29.468140	-090.147440
G065A	29.46767		90.13975		29.467670	-090.139750
G065B	29.46759		90.13985		29.467590	-090.139850
G065C	29.46752		90.13992		29.467520	-090.139920
G067A	29.47390		90.11870		29.473900	-090.118700
G067B	29.47387		90.11869		29.473870	-090.118690
G067C	29.47396		90.11855		29.473960	-090.118550
G069A	29.46313		90.13270		29.463130	-090.132700
G069B	29.46316		90.13232		29.463160	-090.132320
G069C	29.46313		90.13189		29.463130	-090.131890
G070A	29.46532		90.12788		29.465320	-090.127880
G070B	29.46544		90.12740		29.465440	-090.127400
G070C	29.46514		90.12756		29.465140	-090.127560
G071A	29.46241		90.12033		29.462410	-090.120330
G071B	29.46281		90.11982		29.462810	-090.119820
G071C	29.46305		90.11856		29.463050	-090.118560
G072A	29.46492		90.11098		29.464920	-090.110980
G072B	29.46499		90.11070		29.464990	-090.110700
G072C	29.46500		90.11040		29.465000	-090.110400
G073A	29.46617		90.10865		29.466170	-090.108650
G073B	29.46620		90.10857		29.466200	-090.108570

G073C	29.46593		90.10861		29.465930	-090.108610
G074A	29.46733		90.10496		29.467330	-090.104960
G074B	29.46732		90.10497		29.467320	-090.104970
G074C	29.46723		90.10499		29.467230	-090.104990
G076A	29.45863		90.10848		29.458630	-090.108480
G076B	29.45856		90.10847		29.458560	-090.108470
G076C	29.45856		90.10836		29.458560	-090.108360
G077A	29.45850		90.11716		29.458500	-090.117160
G077B	29.45842		90.11720		29.458420	-090.117200
G077C	29.45843		90.11724		29.458430	-090.117240
G078A	29.45725		90.12641		29.457250	-090.126410
G078B	29.45733		90.12634		29.457330	-090.126340
G078C	29.45741		90.12633		29.457410	-090.126330
G079A	29.45253		90.12006		29.452530	-090.120060
G079B	29.45288		90.11988		29.452880	-090.119880
G079C	29.45292		90.11993		29.452920	-090.119930
G080A	29.45595		90.10307		29.455950	-090.103070
G080B	29.45589		90.10310		29.455890	-090.103100
G080C	29.45489		90.10305		29.454890	-090.103050
G098A	29	28.566	90.00000	4.013	29.476100	-090.066883
G098B	29	28.565	90.00000	4.017	29.476083	-090.066950
G098C	29	28.564	90.00000	4.021	29.476067	-090.067017
G099A	29	28.703	90.00000	4.018	29.478383	-090.066967
G099B	29	28.699	90.00000	4.024	29.478317	-090.067067
G099C	29	28.693	90.00000	4.025	29.478217	-090.067083
G102A	29	30.855	90.00000	7.566	29.514250	-090.126100
G102B	29	30.860	90.00000	7.567	29.514333	-090.126117
G102C	29	30.864	90.00000	7.567	29.514400	-090.126117
G105A	29	31.694	90.00000	8.545	29.528233	-090.142417
G105B	29	31.700	90.00000	8.543	29.528333	-090.142383
G105C	29	31.700	90.00000	8.559	29.528333	-090.142650
G108A	29	31.620	90.00000	8.163	29.527000	-090.136050
G108B	29	31.625	90.00000	8.164	29.527083	-090.136067
G108C	29	31.625	90.00000	8.168	29.527083	-090.136133
G110A	29	32.345	90.00000	8.415	29.539083	-090.140250
G110B	29	32.347	90.00000	8.418	29.539117	-090.140300
G110C	29	32.348	90.00000	8.423	29.539133	-090.140383
G112A	29	32.743	90.00000	8.148	29.545717	-090.135800
G112B	29	32.752	90.00000	8.146	29.545867	-090.135767
G112C	29	32.753	90.00000	8.148	29.545883	-090.135800
G114A	29	33.046	90.00000	7.986	29.550767	-090.133100
G114B	29	33.042	90.00000	7.980	29.550700	-090.133000
G114C	29	33.029	90.00000	7.982	29.550483	-090.133033
G116A	29	32.951	90.00000	7.686	29.549183	-090.128100
G116B	29	32.947	90.00000	7.689	29.549117	-090.128150
G116C	29	32.948	90.00000	7.690	29.549133	-090.128167
G118A	29	32.740	90.00000	7.393	29.545667	-090.123217
G118B	29	32.744	90.00000	7.394	29.545733	-090.123233
G118C	29	32.743	90.00000	7.379	29.545717	-090.122983
G120A	29	32.396	90.00000	7.255	29.539933	-090.120917
G120B	29	32.392	90.00000	7.280	29.539867	-090.121333
G120C	29	32.391	90.00000	7.260	29.539850	-090.121000
G123A	29	32.091	90.00000	6.967	29.534850	-090.116117
G123B	29	32.091	90.00000	6.971	29.534850	-090.116183
G123C	29	32.086	90.00000	6.971	29.534767	-090.116183
G125A	29	31.853	90.00000	7.116	29.530883	-090.118600
G125B	29	31.853	90.00000	7.118	29.530883	-090.118633

G125C	29	31.854	90.00000	7.100	29.530900	-090.118333	
G126A	29	31.533	90.00000	7.891	29.525550	-090.131517	
G126B	29	31.535	90.00000	7.887	29.525583	-090.131450	
G126C	29	31.521	90.00000	7.901	29.525350	-090.131683	
G129A	29	31.321	90.00000	7.444	29.522017	-090.124067	
G129B	29	31.324	90.00000	7.411	29.522067	-090.123517	
G129C	29	31.324	90.00000	7.408	29.522067	-090.123467	
G130A	29	31.622	90.00000	6.522	29.527033	-090.108700	
G130B	29	31.626	90.00000	6.530	29.527100	-090.108833	
G130C	29	31.630	90.00000	6.533	29.527167	-090.108883	
G135A	29.51464		90.11303		29.514640	-090.113030	
G135B	29.51462		90.11306		29.514620	-090.113060	
G135C	29.51468		90.11310		29.514680	-090.113100	
G136A	29	30.977	90.00000	6.274	29.516283	-090.104567	
G136B	29	30.981	90.00000	6.274	29.516350	-090.104567	
G136C	29	30.980	90.00000	6.276	29.516333	-090.104600	
G137A	29	31.316	90.00000	5.352	29.521933	-090.089200	
G137B	29	31.325	90.00000	5.344	29.522083	-090.089067	
G137C	29	31.326	90.00000	5.342	29.522100	-090.089033	
G143A	29	30.464	90.00000	5.307	29.507733	-090.088450	
G143B	29	30.462	90.00000	5.302	29.507700	-090.088367	
G143C	29	30.464	90.00000	5.310	29.507733	-090.088500	
G147A	29	33.107	90.00000	9.731	29.551783	-090.162183	
G147B	29	33.099	90.00000	9.739	29.551650	-090.162317	
G147C	29	33.095	90.00000	9.745	29.551583	-090.162417	
G148A	29.47900		90.12399		29.479000	-090.123990	
G148B	29.47909		90.12401		29.479090	-090.124010	
G148C	29.00000	28.72400	90.00000	12.447	29.479000	-090.124060	location from planned
G999A	29	30.610	90.00000	11.776	29.510167	-090.196267	

SEDIMENT GRAIN SIZE ANALYSIS

Sample	Method	Mean Grain Size (microns)	Median Grain Size (microns)	Mode	StDev	Percent Sand	Percent Silt	Percent Clay	Shells Present	Estimated Shell Percent	Retained on 250 micron seive	Water Content Percent	Mineral Content Percent	Organic Content Percent	Comment
G001A	surface	37.31	17.73	3.981	38.54	19	59	22	y	25	organics	57	33	10	shells
G001B	surface	31.94	30.89	0.531	35.39	20	64	17	y	5	organics	50	43	7	shells
G001C	surface	25.06	12.59	3.162	29.98	10	56	34	y	5	organics	58	31	11	shells
G002A	surface	39.75	34.64	47.32	32.53	21	61	18	y	10	shell	46	47	7	
G002B	surface	18.53	11.24	4.732	17.47	6	81	14	y	10		52	39	9	
G002C	surface	42.82	22.32	2.113	44.2	20	38	42	y	90	shell	36	60	4	
G003A	surface	23.84	15.98	5.957	23.52	6	86	8	y	1	organics	56	34	10	shells
G003B	surface	19.91	8.913	9.85	31.85	5	87	8	y	75	shell	40	55	5	shells
G003C	surface	28.03	7.767	5.623	32.71	7	83	10	y	75	shell	61	31	9	
G004A	surface	12.95	4.104	3.35	20.31	3	51	46	n	0	org/shell	67	22	12	
G004B	surface	17.78	5.868	3.981	17.36	5	69	27	n	0	shell	60	31	9	
G004C	surface	5.003	0.949	0.531	16.69	1	21	78	n	0	organics	71	14	16	
G005A	surface	34.97	19.54	5.012	36.04	20	72	8	n	0	shell	56	36	9	
G005B	surface	27.4	3.162	4.57	40.43	15	42	43	n	0	org/shell	58	33	10	
G005C	surface	14.93	3.095	2.239	22.18	6	38	56	n	0		58	31	11	
G006A	surface	31.04	9.168	2.985	39.85	18	46	36	y	50	shell	47	40	12	
G006B	surface	37.54	2.661	8.811	46.77	24	35	40	n	0	shell	59	31	10	
G006C	surface	34.1	1.585	17.26	41.03	18	47	36	n	0	organics	56	33	11	
G007A	surface	14.21	2.347	1.778	27.02	5	34	61	n	0	organics	69	16	14	
G007B	surface	21.82	3.204	1.585	32.12	12	36	52	y	5	organics	64	25	11	
G007C	surface	24.31	5.443	2.818	31.17	14	41	45	y	5	org/shell	57	32	11	
G008A	surface	26.26	15.35	1.995	29.95	13	48	39	y	10	organics	60	0	40	
G008B	surface	32.42	19	0.531	30.19	15	57	27	n	0	organics	57	28	14	
G008C	surface	30.31	2.239	13	32.16	13	47	40	y	5	organics	57	31	12	
G009A	surface	10.69	0.741	0.531	24.09	5	21	73	y	15	organics	66	22	12	
G009B	surface	5.259	4.246	0.531	13.72	4	51	45	y	10	organics	67	19	14	
G009C	surface	6.688	0.944	1.071	12.96	2	20	78	y	1	shell	71	18	11	
G010A	surface	20.72	1.413	5.14	25.79	5	47	48	n	0	org/shell	64	23	12	
G010B	surface	16.9	4.937	3.981	28.56	5	62	33	n	0	organics	69	21	10	
G010C	surface	12.59	5.066	1.995	0	1	50	49	n	0	shell	74	16	11	
G011A	surface	35.68	50.12	26.69	31.36	17	55	29	n	0	org/shell	59	33	7	
G011B	surface	44.67	35.86	53.09	37.18	21	58	21	n	0	org/shell	52	42	6	
G011C	surface	29.87	28.85	44.67	27.5	13	66	21	n	0	organics	63	33	4	
G012A	surface	24.05	8.426	2.661	26.56	12	49	39	n	0	org/shell	57	36	7	
G012B	surface	29.94	18.5	1.679	30.8	16	46	38	n	0	shell	63	31	6	
G012C	surface	31.43	22.62	3.35	31.39	16	63	22	n	0	org/shell	49	47	4	

G013A	surface	25.09	2.371	3.954	36.85	12	39	50	n	0	org/shell	60	31	9	
G013B	surface	30.62	13.28	1.679	40.91	16	46	38	n	0	shell	61	31	8	
G013C	surface	42.03	27.48	1.334	49.91	29	39	32	y	1	shell/sand	61	32	7	
G014A	surface	12.32	3.979	2.661	11.01	3	47	50	n	0		63	26	11	
G014B	surface	16.94	13.47	2.113	7.389	2	57	40	n	0	organics	71	21	9	
G014C	surface	20.74	11.07	3.548	22.79	4	63	33	n	0	shell	67	23	10	
G015A	surface	18.45	3.875	2.512	23.21	10	40	50	y	25	org/shell/sand	57	33	9	shells
G015B	surface	33.42	23.13	1.496	39.47	20	46	34	y	5	org/shell	59	33	8	
G015C	surface	27.06	14.5	1.259	32.23	10	53	37	y	5		61	28	11	
G016A	surface	31.88	21.96	2.239	34.02	15	53	33	n	0	organics	62	28	10	
G016B	surface	26.1	15.76	3.162	31.75	10	56	33	n	0	organics	74	11	15	
G016C	surface	29.8	17.03	2.985	32.12	11	53	36	n	0	organics	67	18	15	
G017A	surface	9.389	38.34	0.708	27.59	34	45	22	n	0	shell/sand	44	49	6	
G017B	surface	44.76	32.47	1.778	45.92	26	41	32	n	0	shell/sand	46	48	6	
G017C	surface	47.3	33.06	56.23	48.58	27	43	30	y	10	shell/sand	47	45	8	
G018A	surface	29.21	3.423	1.189	38.82	18	32	51	y	50	org/shell	75	3	22	
G018B	surface	36	16.48	2.512	41.42	21	44	36	y	20	org/shell	50	39	11	
G018C	surface	26.48	6.47	3.758	30.67	16	53	31	y	75	shell	36	55	9	
G019A	surface	11.08	3.201	2.661	20.2	4	35	61	y	90					100 percent shell
G019B	surface	25.07	10.01	2.661	28.91	12	48	40	y	80	organics	68	26	7	shells
G019C	surface	13.97	27.27	0.531	27.98	19	57	24	y	75	org/shell	62	29	10	
G020A	surface	53.39	45.05	89.13	51.47	38	52	11	y	10	shell/sand	41	52	6	
G020B	surface	52.26	41.62	105.9	50.97	39	35	27	n	0	shell/sand	52	41	7	
G020C	surface	15.34	3.644	2.818	25.59	7	40	53	y	100					100 percent shell
G021A	surface	14.35	2.961	2.371	25.94	7	32	61	y	25	shell	41	51	7	shells
G021B	surface	24.77	6.552	2.113	31.45	12	41	47	y	5	shell	64	27	10	shells
G021C	surface	12.2	2.096	1.778	22.94	4	28	68	n	0	shell	70	19	11	
G022A	surface	61.06	79.43	54.76	46.65	46	35	19	n	0	shell/sand	44	52	4	
G022B	surface	40.51	79.86	0.531	51.82	61	25	14	y	10	shell/sand	29	68	4	
G022C	surface	55.55	56.03	79.43	50.64	43	31	27	n	0	org/shell	37	58	5	
G023A	surface	45.27	38.52	53.09	41.83	27	61	12	n	0	shell/sand	36	60	4	
G023B	surface	22.59	49.43	0.531	41.13	38	43	18	n	0	shell/sand	39	55	6	
G023C	surface	63.06	57.36	63.1	49.01	44	45	12	n	0	shell/sand	32	64	4	
G024A	surface	26.84	15.24	2.512	29.94	13	50	37	y	1	shell	57	36	7	
G024B	surface	40.41	27.46	56.23	40.14	22	49	29	n	0	org/shell	54	38	8	
G024C	surface	14.96	28.74	0.531	29.42	23	46	31	n	0	shell	55	36	9	
G025A	surface	68.07	65.69	79.43	45.27	49	39	12	n	0	shell	34	60	5	
G025B	surface	63.02	52.82	84.14	47.68	42	41	17	y	1	shell	37	59	4	
G025C	surface	56.18	51.02	70.79	38.65	37	50	13	n	0	organics	43	52	5	
G026A	surface	46.29	41.84	53.09	41.24	28	66	7	y	5	org/shell	38	57	5	

G026B	surface	63.17	54.37	94.41	49.03	41	41	18	y	10	shell	35	62	4
G026C	surface	51.59	47.68	53.09	42.44	33	52	15	n	0	org/shell	38	59	3
G027A	surface	54.13	45.59	79.43	46.67	35	60	5	n	0	org/shell	38	58	4
G027B	surface	52.44	48.17	50.12	44.84	33	49	18	n	0	org/shell	50	41	9
G027C	surface	61.94	48.83	56.23	49.47	38	43	20	n	0	org/shell	39	57	4
G028A	surface	31.62	23.11	2.985	33.58	13	58	29	n	0	shell/sand	55	36	9
G028B	surface	57.24	59.73	66.83	46.84	43	38	19	n	0	org/shell	39	57	5
G028C	surface	62.85	61.98	70.79	40.44	46	38	16	y	5	shell	35	60	5
G029A	surface	40.58	27.9	3.35	42.29	26	49	24	n	0	org/shell	40	55	5
G029B	surface	24.5	65.34	0.531	42.87	50	32	18	n	0	shell	39	57	4
G029C	surface	50.44	40.19	1.413	51.7	34	38	28	n	0	shell/sand	55	37	8
G030A	surface	51.52	53.01	66.83	37.64	37	46	16	n	0	sand	40	56	5
G030B	surface	48.16	47.43	63.1	39.27	33	46	21	n	0	sand	58	35	7
G030C	surface	60.52	61.46	74.99	39.34	47	39	14	n	0	sand	44	51	5
G031A	surface	44.97	42.95	56.23	42.35	29	50	21	n	0	org/shell/sand	49	45	6
G031B	surface	44.78	41.02	1.778	48.15	29	41	30	n	0	shell/sand	50	44	6
G031C	surface	46.78	38.17	56.23	42.79	27	52	21	n	0	shell/sand	44	52	4
G033A	surface	44.22	40.94	1.884	44.16	29	41	29	n	0	shell/sand	44	50	6
G033B	surface	57.84	54.77	63.1	46.5	39	43	17	y	5	org/shell	41	55	4
G033C	surface	48.46	44.27	56.23	43.15	29	48	22	n	0	shell/sand	37	59	4
G035A	surface	25.58	13.85	19.95	32.77	8	75	17	n	0	org/shell	60	28	12
G035B	surface	17.84	7.661	5.012	25.35	4	79	16	n	0	org/shell	61	26	13
G035C	surface	19.05	8.583	5.623	28.08	3	83	14	n	0	org/shell	60	27	13
G039A	surface	51.9	53.06	66.83	40.79	36	43	21	n	0	shell/sand	40	56	4
G039B	surface	51.97	53.23	66.83	41.74	38	42	20	n	0	shell/sand	34	62	4
G039C	surface	51.47	52.87	59.57	39.57	36	47	17	y	1	shell/sand	40	56	4
G041A	surface	28.95	12.4	3.981	33.15	15	68	17	y	1	shell/sand	55	39	6
G041B	surface	29.51	21.14	2.239	31.15	15	50	36	n	0	shell/sand	55	38	6
G041C	surface	29.33	26.71	2.818	28.67	16	55	29	y	10	shell/sand	49	45	7
G042A	surface	20.97	2.239	3.222	33.62	8	40	51	n	0	organics	68	16	16
G042B	surface	25.49	16.79	1.496	29.04	13	54	34	n	0	organics	74	10	16
G042C	surface	21.31	16.97	1.679	11.3	10	56	34	n	0	organics	68	16	16
G043A	surface	17.82	4.323	3.35	26.86	7	48	45	y	25	organics	73	14	13
G043B	surface	14.64	4.753	2.818	22.04	4	50	46	y	15	shell	77	5	17
G043C	surface	18.84	10.22	2.239	25.2	5	52	43	n	0	organics	72	18	11
G044A	surface	43.02	31.5	3.548	45.06	24	61	15	y	5	shell/sand	39	58	4
G044B	surface	58.42	58.99	112.2	57.36	40	47	12	y	10	shell/sand	35	63	2
G044C	surface	69.14	81.3	0.531	60.59	56	29	15	n	0	shell/sand	26	72	2
G045A	surface	23.41	29.08	0.531	41.81	28	43	29	n	0	shell/sand	48	46	5
G045B	surface	52.71	39.43	2.661	54.16	36	36	28	y	10	shell/sand	51	43	6
G045C	surface	38.95	6.554	2.512	54.48	26	27	47	n	0	shell/sand	62	28	9

G047A	surface	16.17	3.126	2.512	28.14	7	34	59	y	10	org/shell	67	20	13
G047B	surface	24.17	8.983	3.548	29.71	13	56	31	n	0	org/shell	57	36	7
G047C	surface	28.52	23.34	3.162	31.83	18	57	25	n	0	org/shell/sand	53	41	6
G048A	surface	26.92	22.49	0.531	34.11	17	51	33	n	0	shell/sand	51	43	6
G048B	surface	34.57	36.27	0.531	39.72	22	51	27	n	0	shell/sand	45	50	5
G048C	surface	38.07	37.3	0.531	43.12	29	48	23	n	0	shell/sand	42	54	4
G050A	surface	16.75	47.32	0.531	30.33	31	48	21	n	0	org/shell	42	53	5
G050B	surface	47.24	56.85	66.83	43.75	42	45	13	n	0	org/shell	50	45	5
G050C	surface	46.16	58.58	0.531	42.55	44	43	13	n	0	org/shell	35	62	3
G052A	surface	25.32	1.836	66.83	0	20	28	53	y	20	organics	78	-1	23
G052B	surface	38.28	42.43	53.09	30.27	22	58	20	y	25	org/shell	45	50	5
G052C	surface	37.29	69.7	0.531	43.71	60	34	6	y	25	org/shell	34	62	4
G055A	surface	43.04	39.46	2.512	42.81	29	42	29	n	0	org/shell	45	50	5
G055B	surface	18.05	14.99	0.531	34.06	21	36	43	n	0	org/shell	43	52	5
G055C	surface	40.04	43.21	0.531	43.29	32	50	18	n	0	org/shell	48	46	6
G057A	surface	33.68	47.89	0.531	40.11	33	46	21	n	0	org/shell	37	59	4
G057B	surface	24.32	43.21	0.531	35.12	30	49	21	n	0	org/shell	41	55	4
G057C	surface	32.51	48.2	0.531	39.82	34	42	24	y	5	org/shell/sand	39	57	4
G061A	surface	39.63	35.47	3.162	38.76	27	48	25	y	10	org/shell	46	49	5
G061B	surface	33.8	23.57	2.512	35.84	21	45	34	y	5	org/shell	47	49	4
G061C	surface	38.17	31.86	1.995	38.61	24	44	32	y	5	org/shell/sand	43	52	5
G062A	surface	45.99	48.17	0.531	47.21	39	45	17	y	5	shell/sand	35	61	4
G062B	surface	22.55	41.57	0.531	40.78	37	37	26	n	0	org/shell/sand	42	53	5
G062C	surface	35.32	14.44	4.467	44.39	26	63	12	y	5	org/shell	39	56	4
G064A	surface	72.01	70.66	89.13	48.36	56	41	3	y	75	org/shell	39	58	3
G064B	surface	69.77	73.21	84.14	45.98	59	34	7	n	0	org/shell/sand	32	65	3
G064C	surface	68.42	68.96	79.43	43.34	56	39	5	n	0	org/shell/sand	30	68	2
G065A	surface	48.07	20.31	2.371	54.86	28	31	41	y	1	organics	60	29	11
G065B	surface	19.31	5.897	3.758	26.73	10	62	28	n	0	org/shell	44	51	6
G065C	surface	28.4	10.2	3.758	32.67	15	60	24	y	5	org/shell	44	50	7
G067A	surface	26.94	5.221	3.758	37.1	15	55	30	y	50	org/shell	56	35	9
G067B	surface	33.56	7.464	3.35	42.15	21	48	31	y	50	org/shell	53	41	7
G067C	surface	31.06	8.253	3.981	36.91	17	64	19	y	15	org/shell	51	43	6
G069A	surface	38.01	11.39	2.985	47.33	24	38	38	n	0	organics	59	33	8
G069B	surface	37.1	13.43	3.758	45.56	23	48	28	n	0	organics	58	35	7
G069C	surface	24.87	2.994	2.239	38.34	14	30	56	n	0	organics	57	32	11
G070A	surface	23.21	4.912	3.548	33.69	14	49	37	n	0	org/shell	52	41	7
G070B	surface	31.86	7.336	1.995	44.81	22	30	47	y	5	org/shell/sa	55	37	8

										nd					
G070C	surface	26.41	3.189	1.995	39.57	14	31	55	y	10	org/shell	51	41	8	
G071A	surface	3.613	0.71	0.668	16.44	1	5	94	y	35	organics	64	23	12	
G071B	surface	13.18	0.696	0.668	33.96	8	8	84	n	0	org/shell	67	19	14	
G071C	surface	6.881	0.553	0.531	30.66	2	3	95	n	0	organics	68	14	18	
G072A	surface	16.12	3.414	2.512	21.7	5	41	54	n	0	org/shell	60	32	8	
G072B	surface	20.1	10.88	3.35	10.92	11	58	30	n	0	org/shell	53	42	5	
G072C	surface	20.05	5.4	3.758	26.71	8	61	31	n	0	org/shell	57	36	7	
G073A	surface	5.079	1.744	1.679	15.83	2	11	87	y	75	org/shell	56	36	7	
G073B	surface	6.744	2.106	1.995	16.02	3	12	85	y	75	org/shell	44	50	6	
G073C	surface	1.572	0.742	0.75	7.077	1	2	97	n	0	organics	56	34	9	
G074A	surface	7.21	0.62	0.531	14.64	2	19	79	n	0	organics	75	9	16	
G074B	surface	8.464	0.715	0.531	23.71	3	22	75	n	0	org/shell	71	14	15	
G074C	surface	6.956	0.836	0.596	20.34	4	19	77	n	0	org/shell/sa	70	20	10	
										nd					
G076A	surface	14.7	1.14	0.944	29.86	8	26	66	n	0	org/shell	66	24	10	
G076B	surface	12.35	1.155	0.794	27.97	7	28	65	n	0	org/shell	57	35	8	
G076C	surface	20.59	3.501	2.512	30.69	10	36	54	n	0	organics	62	29	9	
G077A	surface	13.92	2.412	0.531	32.99	13	22	65	y	25	org/shell	58	34	8	
G077B	surface	10.97	0.938	0.841	33.32	7	10	83	y	50	org/shell	67	23	10	
G077C	surface	3.647	0.99	0.891	12.12	2	9	89	y	50	org/shell	53	42	5	
G078A	surface	4.645	0.799	0.531	19.78	4	6	91	y	75	org/shell	52	44	5	gray clay
G078B	surface	6.562	0.75	0.75	21.31	3	7	90	y	10	org/shell	54	40	6	
G078C	surface	6.087	0.825	0.531	19.73	6	6	88	y	1	org/shell	57	36	7	
G079A	surface	36.08	22.36	3.162	38.35	22	44	33	n	0	org/shell	48	47	6	
G079B	surface	31.15	79.76	0.531	47.38	62	26	11	n	0	org/shell	29	68	2	
G079C	surface	72.01	83.76	94.41	52.74	65	30	5	n	0	org/shell	31	67	2	
G080A	surface	17.21	0.516	0.531	47.28				n	0	organics	66	22	13	
G080B	surface	5.043	0.829	0.841	18.66	2	7	91	y	25	org/shell	71	16	13	
G080C	surface	9.374	0.832	0.708	22.49	4	20	76	y	10	organics	70	12	18	
G098A	surface	6.548	1.679	0.644	16.4	5	24	71	n	0	organics	72	13	15	
G098B	surface	18.55	2.993	2.371	25.47	8	35	58	n	0	organics	67	21	12	
G098C	surface	5.017	0.992	0.531	17.54	5	24	71	y	50	organics	73	12	16	
G099A	surface	7.59	0.616	0.531	25.03	2	15	84	y	15	org/shell	70	13	16	
G099B	surface	6.022	1.311	0.531	22.26	4	20	76	y	50	org/shell	70	17	13	
G099C	surface	13.47	1.15	0.841	26.71	7	28	65	y	5	organics	64	24	12	
G102A	surface	4.656	1.709	1.334	6.031	0	29	71	n	0	org/shell	62	28	10	
G102B	surface	9.171	3.259	2.818	16.71	3	35	62	n	0	organics	64	25	11	
G102C	surface	3.992	2.008	1.679	8.501	2	19	79	n	0	org/shell	56	36	8	
G105A	surface	24.85	7.714	4.732	28.73	11	76	13	n	0	organics	54	39	7	
G105B	surface	19.12	5.653	4.467	26.49	7	74	20	y	15	org/shell	55	37	8	
G105C	surface	22.8	6.125	4.217	27.46	10	67	23	y	10	org/shell	57	36	7	

G108A	surface	4.122	0.981	0.891	12.84	3	8	89	y	75	org/shell	62	28	10	
G108B	surface	6.539	1.968	1.585	12.88	2	27	71	y	10	org/shell	63	29	8	
G108C	surface	20.09	11.36	2.661	21.93	6	57	37	y	5	org/shell	46	48	6	
G110A	surface	22.82	8.23	4.732	27.41	7	81	12	y	25	org/shell	61	33	6	
G110B	surface	14.9	4.747	3.981	22.02	5	61	34	y	10	org/shell	61	29	9	
G110C	surface	19.82	5.579	3.758	27.19	8	61	31	y	10	org/shell	59	31	9	
G112A	surface	16.7	5.465	4.217	25.26	6	71	23	n	0	organics	63	28	9	
G112B	surface	30.79	15.04	4.217	32.34	16	70	13	y	50	org/shell	45	49	6	
G112C	surface	10.96	3.722	3.162	25.42	4	42	54	y	5	org/shell	59	32	9	
G114A	surface	14.64	2.238	1.585	25.42	6	35	59	y	30	org/shell	47	49	4	gray
G114B	surface	22.67	8.978	5.623	30.87	9	89	2	y	40	org/shell	35	61	4	gray
G114C	surface	14.81	1.449	0.944	31.34	8	33	60	y	40	org/shell	47	49	4	gray
G116A	surface	26.99	19	3.35	25.65	11	65	24	n	0	org/shell	54	37	9	
G116B	surface	26.09	7.765	4.467	30.61	13	74	13	n	0	org/shell	54	38	8	
G116C	surface	32.45	32.6	53.09	26.8	16	68	17	y	5	org/shell	52	42	6	
G118A	surface	32.97	39.89	0.531	29.68	21	62	17	y	15	org/shell	44	51	4	
G118B	surface	36.88	32.34	59.57	31.24	21	60	20	y	10	org/shell	49	46	5	
G118C	surface	0	0.516	66.83	0	42	58	0	y	25	org/shell	49	45	6	
G120A	surface	40.59	38.27	56.23	38.31	25	60	15	y	5	org/shell	38	58	4	
G120B	surface	25.75	46.86	0.531	38.3	33	42	24	y	25	org/shell	46	48	6	
G120C	surface	43.31	35.6	56.23	38.76	26	67	7	n	0	org/shell	46	49	4	
G123A	surface	24.93	12.19	3.35	27.69	9	62	29	y	5	org/shell	57	37	6	
G123B	surface	19.55	5.629	3.35	22.47	6	59	35	y	10	shell	58	35	7	
G123C	surface	24.38	15.01	2.512	29.97	7	56	37	y	25	shell	53	39	8	
G125A	surface	28.8	16.57	4.217	29.95	13	73	14	y	10	shell	52	43	5	
G125B	surface	27.38	17.75	3.981	25.85	12	73	15	y	25	shell	54	41	5	
G125C	surface	24.25	14.46	2.818	24.93	9	55	36	y	25	shell	53	41	7	
G126A	surface	26.92	14.44	3.35	31.12	11	62	27	y	50	org/shell	44	51	5	
G126B	surface	13.37	5.23	4.217	18.92	3	70	27	y	5	organics	49	46	5	
G126C	surface	3.414	0.854	0.708	4.887	2	15	83	y	10	org/shell	70	19	11	
G129A	surface	36.14	32.21	50.12	31.16	19	58	23	y	1	org/shell	55	38	7	
G129B	surface	7.719	2.23	1.778	16.95	3	27	70	n	0	org/shell	46	48	5	
G129C	surface	13	2.571	2.113	27.25	5	31	65	n	0	org/shell	61	33	6	
G130A	surface	10.64	3.372	2.985	16.89	2	36	61	y	1	org/shell	72	18	10	
G130B	surface	12.48	3.196	2.661	21.19	4	35	61	y	5	org/shell	58	33	9	
G130C	surface	3.771	0.907	0.75	11.03	2	14	84	y	5	org/shell	62	28	10	
G135A	surface	15.3	2.267	1.585	30.62	8	32	61	y	1	organics	61	29	10	
G135B	surface	12.23	1.842	1.585	21.13	5	26	69	y	1	org/shell	65	24	11	
G135C	surface	11.37	1.683	1.496	24.92	3	25	72	n	0	org/shell	65	25	10	
G136A	surface	12.76	2.433	2.113	19.92	4	29	66	n	0	org/shell	67	21	12	
G136B	surface	21.93	2.832	2.239	32.94	10	34	55	n	0	organics	70	17	12	
G136C	surface	24.73	4.632	2.985	36.36	10	45	46	n	0	organics	66	23	12	

G137A	surface	23.27	4.19	2.985	33.71	13	40	47	y	1	organics	62	29	9	
G137B	surface	4.105	0.846	0.794	14.22	2	5	93	y	75	org/shell	62	29	9	
G137C	surface	17.38	3.268	0.531	30.05	13	29	58	y	100	org/shell	84	6	11	
G143A	surface	8.642	1.105	0.944	19.56	3	22	76	n	0	org/shell	72	17	11	
G143B	surface	19.49	2.781	2.371	35.76	10	27	63	n	0	org/shell	68	21	11	
G143C	surface	9.16	0.735	0.531	11.04	1	29	69	n	0	organics	74	15	11	
G147A	surface	18.72	1.679	9.002	15.29	7	50	43	n	0	organics	68	22	11	
G147B	surface	16.86	2.804	1.995	26.45	7	35	58	n	0	shell	66	22	13	
G147C	surface	17.88	5.748	2.239	18.77	8	45	47	n	0	org/shell	67	21	12	
G148A	surface	26.2	45.67	0.531	35.19	31	40	29	y	5	org/shell	50	45	5	
G148B	surface	36.54	31.9	56.23	32.81	21	51	28	y	5	org/shell	47	48	4	
G148C	surface	25.89	6.509	2.818	31.8	11	48	41	y	25	org/shell	46	49	6	location from planned
G999A	surface	54.1	55.87	74.99	43.54	41	41	17	n	0	org/shell	39	58	3	
BC01	core	9.215	0.749	0.531	21.12	2	24	74	y		org/shell	73	11	17	
BC02	core	18.81	3.645	2.512	31	4	45	51	n		organics	67	20	13	
BC03	core	28.81	5.6	2.512	31.56	11	43	46				69	18	14	
BC04	core	27.69	23.5	0.531	31.12	16	50	33	y		org/shell	60	31	9	
BC05	core	29.31	20.45	2.661	36.59	26	42	32	y		org/shell	53	40	7	
BC06	core	13.72	54.73	0.668	31.15	43	57	0	y		org/shell	42	52	5	
BC07	core					21	79	0	y		org/shell	46	49	5	
BC08	core	19.21	4.926	3.35	23.56	7	53	40	y		shell @top org/shell	57	34	9	
BC09	core	21.05	5.048	3.162	27.12	8	49	43	y		org/shell	68	18	14	
BC10	core	16.68	53.58	0.75	31.59	39	43	18	y		org/shell	42	53	5	
BC12	core	14.14	13.43	0.531	28.34	13	47	39	y		org/shell	62	29	9	
BC13	core	15.51	4.543	3.35	19.92	7	52	41	y		org/shell	53	40	7	
BC15	core	10.66	25.18	0.531	30.87	28	40	32				45	49	6	
BC16	core	77.35	77.2	94.41	44.16	59	33	8	y		org/shell	37	59	4	
BC17	core	3.033	1.292	0.531	7.249	3	21	76	y		org/shell	60	30	10	
BC18	core	14.14	36.18	0.531	31.56	27	49	25	y		org/shell	46	48	6	
BC19	core	13.12	27.57	0.596	34.58	26	37	37	y		org/shell	45	49	7	
BC20	core	18.39	49.87	0.75	39.51	38	35	26	y		org/shell	34	61	4	
BC22	core	13.33	32.42	9.441	16	20	80	0	y		org/shell	47	48	5	
BC23	core	13.4	31.28	10	13.48	19	81	0	y		org/shell	55	37	8	
BC24	core	23.45	22.11	0.531	21.78	10	79	11	y		org/shell	43	52	5	
BC25	core	25.32	8.076	3.981	32.8	12	63	25	y		org/shell	51	42	7	
BC26	core	6.602	3.21	0.531	17.7	11	35	54	n		organics	59	31	10	

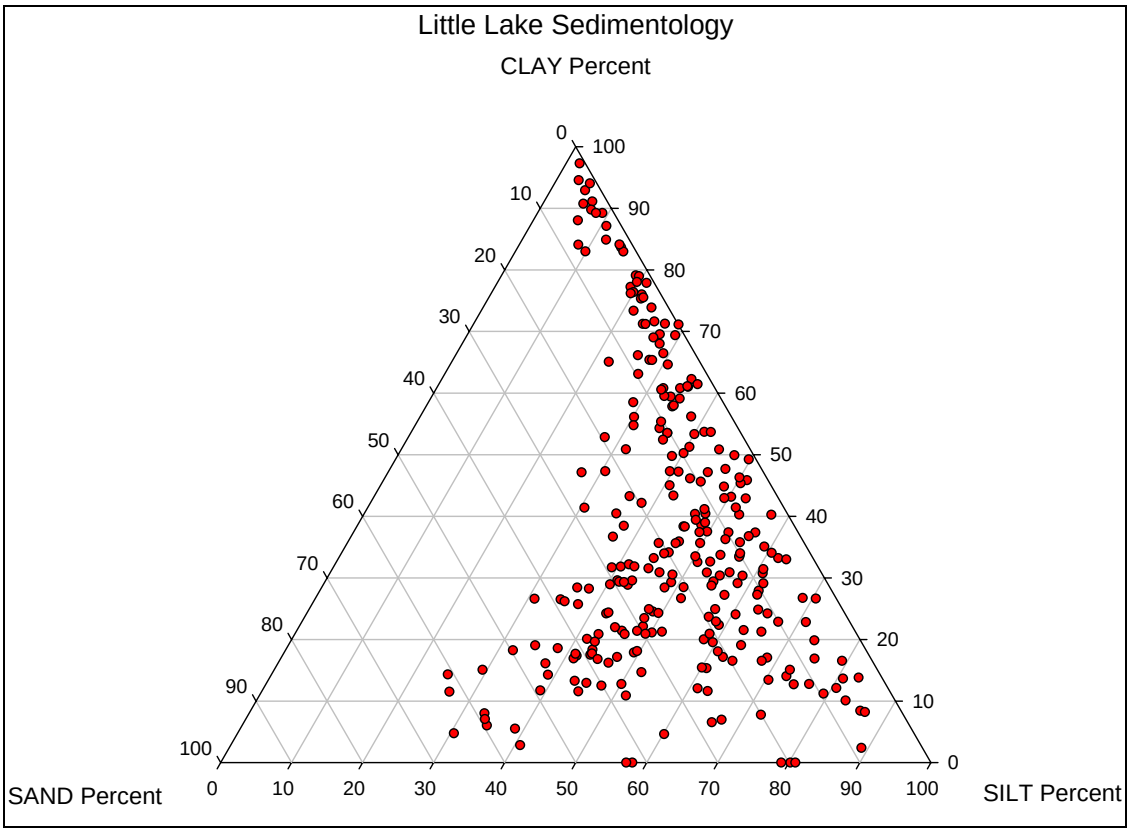
Little Lake Sedimentology
CLAY Percent
SAND Percent
SILT Percent
0
10
20
30
40
50
60
70
80
90
100

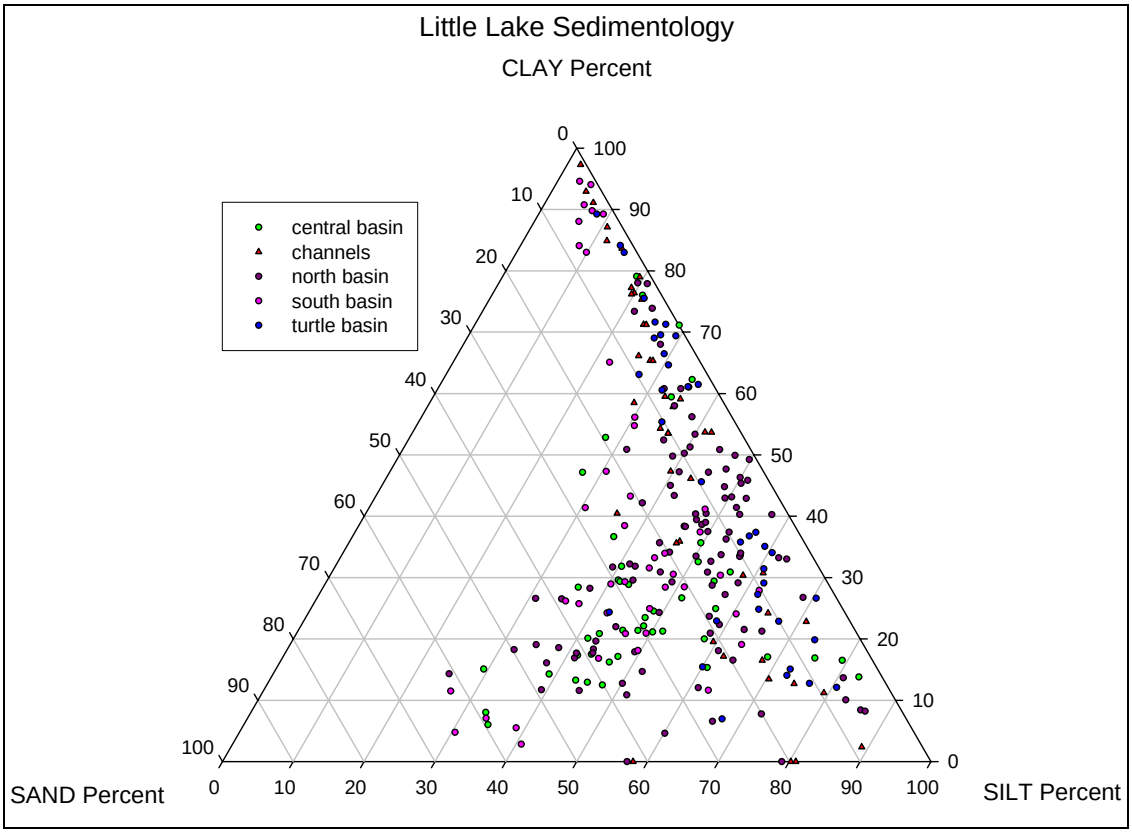
Little Lake Sedimentology
CLAY Percent
central basin
channels
north basin
south basin
turtle basin
SAND Percent
SILT Percent
0
10
20
30
40
50
60
70
80
90
100

SEDIMENT CORE LOG

PROJECT: Little Lake, Barataria Bay, LA **CORE ID:** BC01-B

Collection Date:	October 14, 2003	Logged By:	Michelle Greene	
Total Depth (cm):	21	Latitude (North)	29.568717	
Mudline Elevation MLLW (m):	Default Listing	Longitude (West)	-90.185183	Coordinate System: Geographic, WGS84

Core Depth (cm)	Sample ID	Photo	X-Radiograph	%Water	Be-7 Inventory (dpm/cm^2)	Be-7 (dpm/g)	Excess Pb-210 (dpm/g)	Excess Cs-137 (dpm/g)

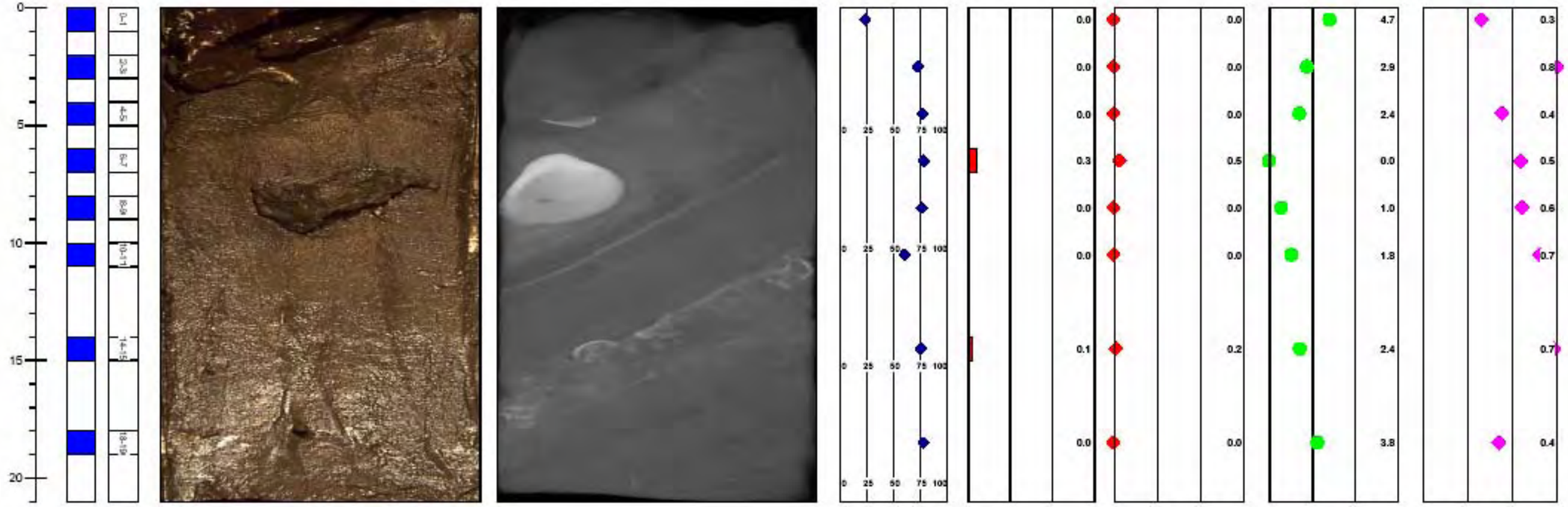

SEDIMENT CORE LOG

PROJECT: Little Lake, Barataria Bay, LA **CORE ID:** BC02-B

Collection Date:	October 14, 2003	Logged By:	Michelle Greene	
Total Depth (cm):	21	Latitude (North)	29.560650	
Mudline Elevation MLLW (m):	Default Listing	Longitude (West)	-90.204567	Coordinate System: Geographic, WGS84

Core Depth (cm)	Sample ID	Photo	X-Radiograph	%Water	Be-7 Inventory (dpm/cm^2)	Be-7 (dpm/g)	Excess Pb-210 (dpm/g)	Excess Cs-137 (dpm/g)

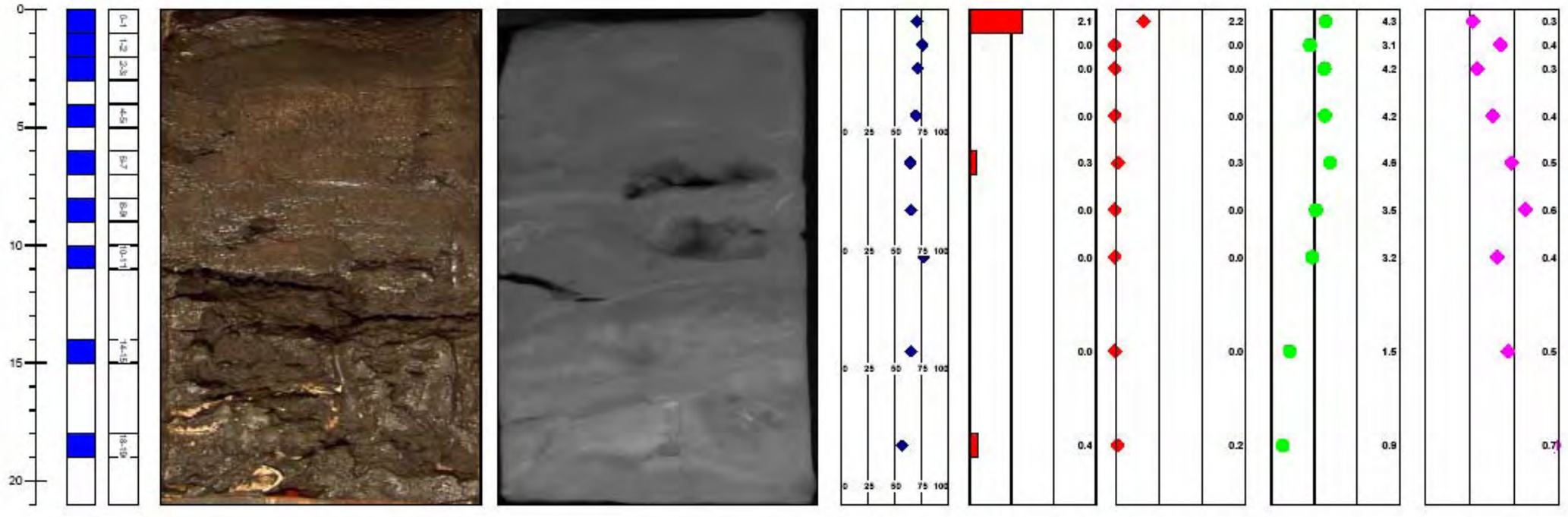

SEDIMENT CORE LOG

PROJECT: Little Lake, Barataria Bay, LA **CORE ID:** BC03-B

Collection Date:	October 14, 2003	Logged By:	Michelle Greene	
Total Depth (cm):	6	Latitude (North)	29.56268333	
Mudline Elevation MLLW (m):	Default Listing	Longitude (West)	-90.17846667	Coordinate System: Geographic, WGS84

Core Depth (cm)	Sample ID	Photo	X-Radiograph	%Water	Be-7 Inventory (dpm/cm^2)	Be-7 (dpm/g)	Excess Pb-210 (dpm/g)	Excess Cs-137 (dpm/g)
0					0.0	0.0	3.9	0.5
					0.0	0.0	3.3	0.3
5				0 25 50 75 100	0.2	0.1	1.8	0.2

SEDIMENT CORE LOG

PROJECT: Little Lake, Barataria Bay, LA **CORE ID:** BC04-B

Collection Date:	October 14, 2003	Logged By:	Michelle Greene	
Total Depth (cm):	25	Latitude (North)	29.548950	
Mudline Elevation MLLW (m):	Default Listing	Longitude (West)	-90.174117	Coordinate System: Geographic, WGS84

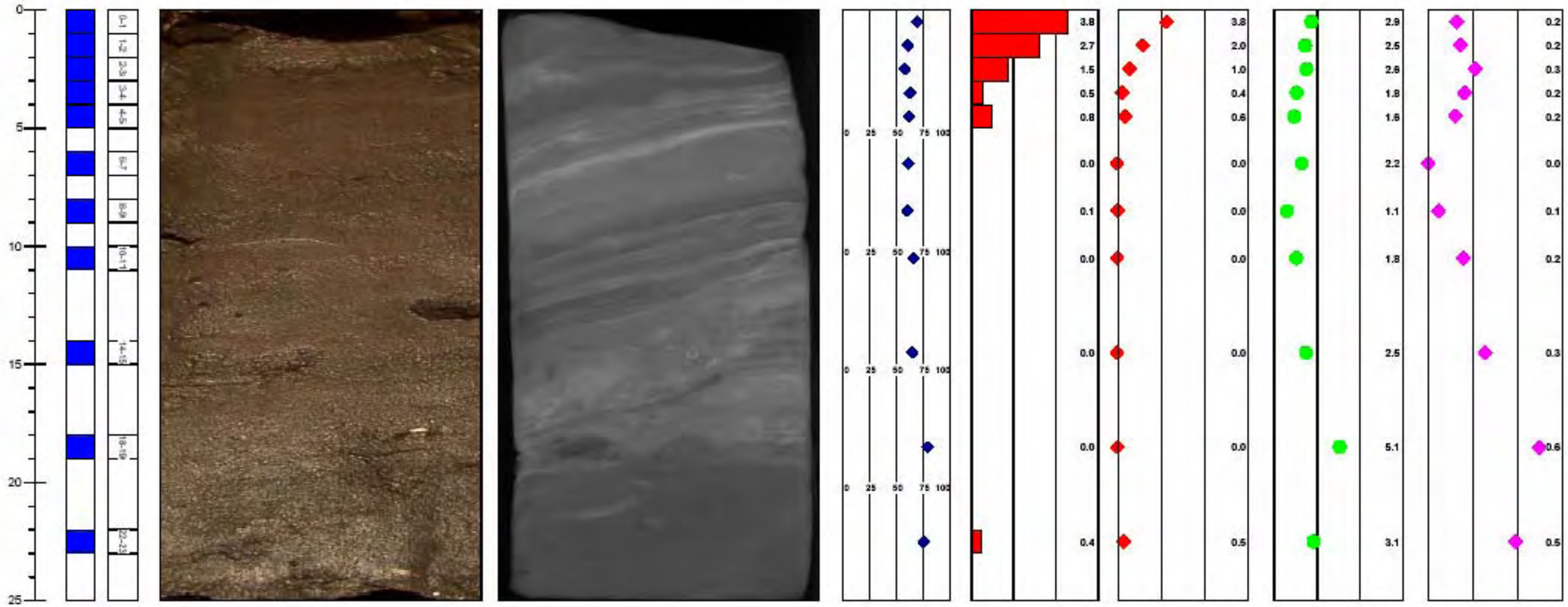

SEDIMENT CORE LOG

PROJECT: Little Lake, Barataria Bay, LA **CORE ID:** BC05-B

Collection Date:	October 14, 2003	Logged By:	Michelle Greene	
Total Depth (cm):	14	Latitude (North)	29.55063333	
Mudline Elevation MLLW (m):	Default Listing	Longitude (West)	-90.18813333	Coordinate System: Geographic, WGS84

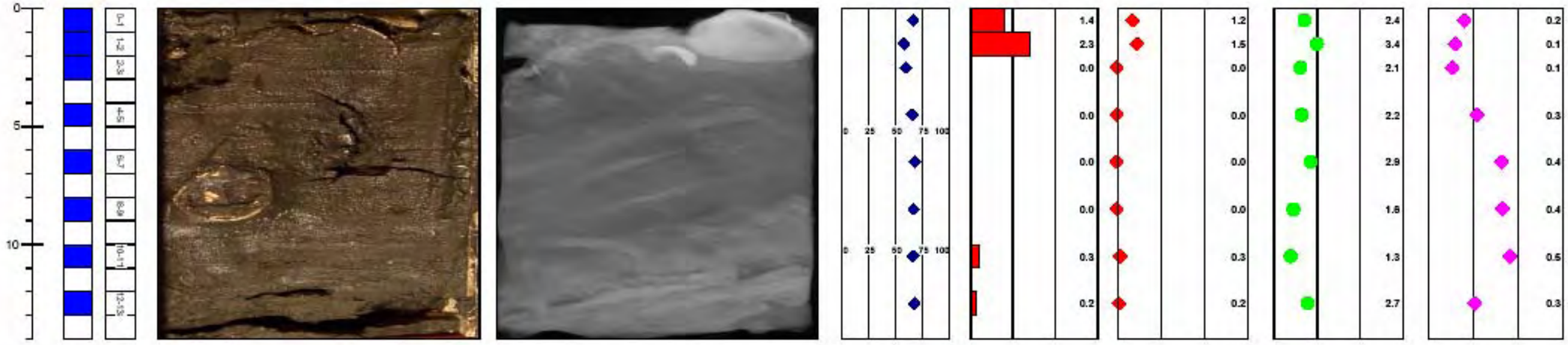

SEDIMENT CORE LOG

PROJECT: Little Lake, Barataria Bay, LA **CORE ID:** BC06-B

Collection Date:	October 14, 2003	Logged By:	Michelle Greene	
Total Depth (cm):	15	Latitude (North)	29.5513	
Mudline Elevation MLLW (m):	Default Listing	Longitude (West)	-90.2082	Coordinate System: Geographic, WGS84

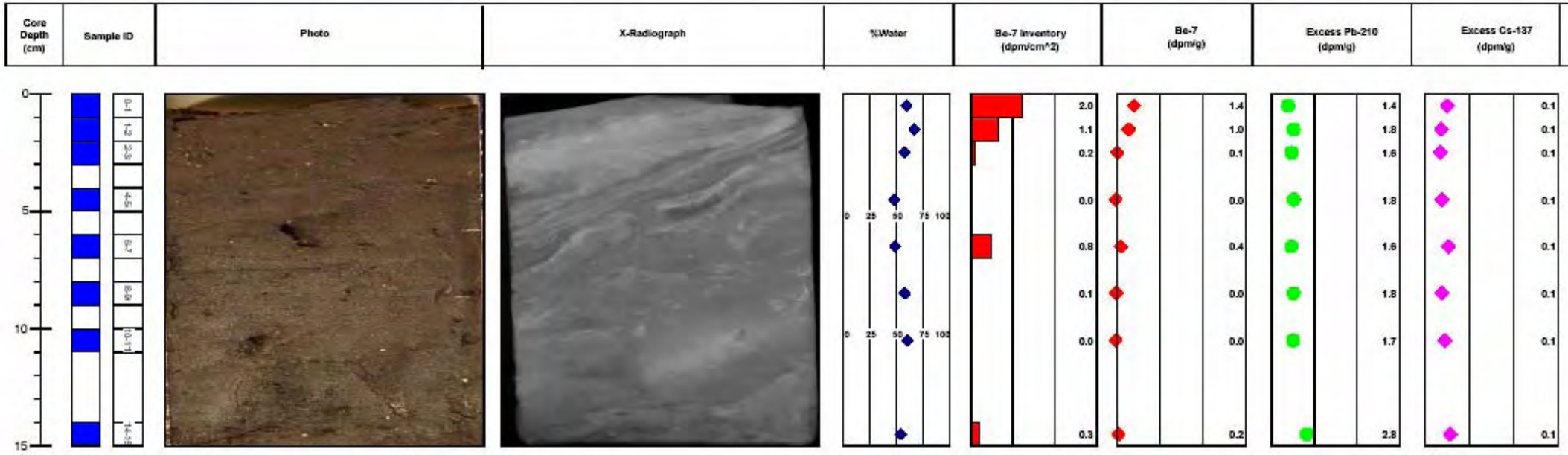

SEDIMENT CORE LOG

PROJECT: Little Lake, Barataria Bay, LA **CORE ID:** BC07-B

Collection Date:	October 14, 2003	Logged By:	Michelle Greene	
Total Depth (cm):	15	Latitude (North)	29.54006667	
Mudline Elevation MLLW (m):	Default Listing	Longitude (West)	-90.22025	Coordinate System: Geographic, WGS84

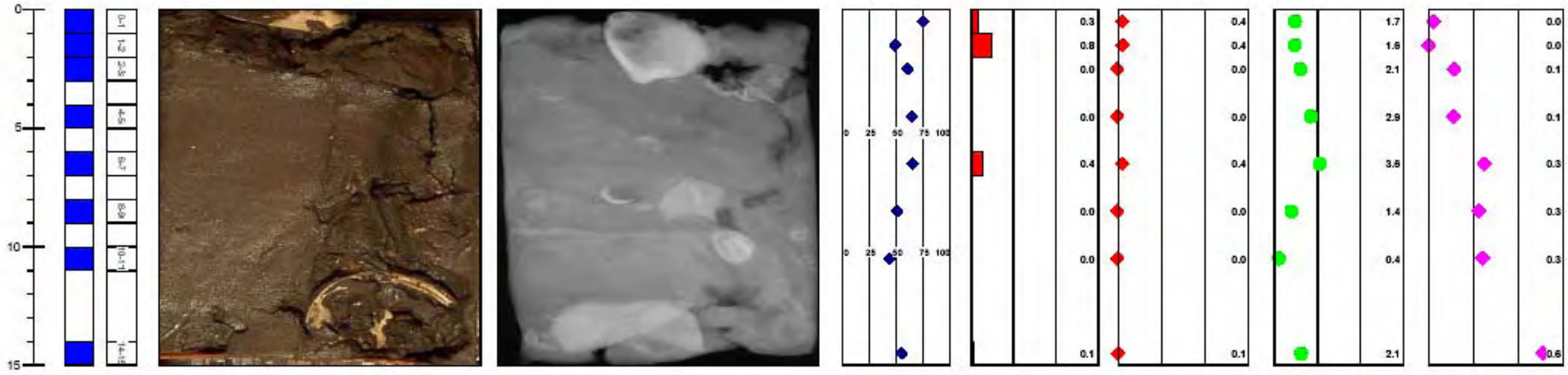

SEDIMENT CORE LOG

PROJECT: Little Lake, Barataria Bay, LA **CORE ID:** BC08-B

Collection Date:	October 14, 2003	Logged By:	Michelle Greene	
Total Depth (cm):	17	Latitude (North)	29.54253333	
Mudline Elevation MLLW (m):	Default Listing	Longitude (West)	-90.20038333	Coordinate System: Geographic, WGS84

Core Depth (cm)	Sample ID	Photo	X-Radiograph	%Water	Be-7 Inventory (dpm/cm^2)	Be-7 (dpm/g)	Excess Pb-210 (dpm/g)	Excess Cs-137 (dpm/g)
0 5 10 15	0-1 3-3 4-5 6-7 8-9 10-11 14-15			0 25 50 75 100 0 25 50 75 100 0 25 50 75 100	1.7 0.4 0.0 0.0 0.6 0.0 0.0	1.8 0.4 0.0 0.0 0.6 0.0 0.0	5.5 3.8 4.1 3.9 4.2 3.7 2.9	0.3 0.2 0.3 0.5 0.6 0.6 0.9

SEDIMENT CORE LOG

PROJECT: Little Lake, Barataria Bay, LA **CORE ID:** BC09-B

Collection Date:	October 14, 2003	Logged By:	Michelle Greene	
Total Depth (cm):	28	Latitude (North)	29.54061667	
Mudline Elevation MLLW (m):	elevation	Longitude (West)	-90.16913333	Coordinate System: Geographic, WGS84

Core Depth (cm)	Sample ID	Photo	X-Radiograph	%Water	Be-7 Inventory (dpm/cm^2)	Be-7 (dpm/g)	Excess Pb-210 (dpm/g)	Excess Cs-137 (dpm/g)

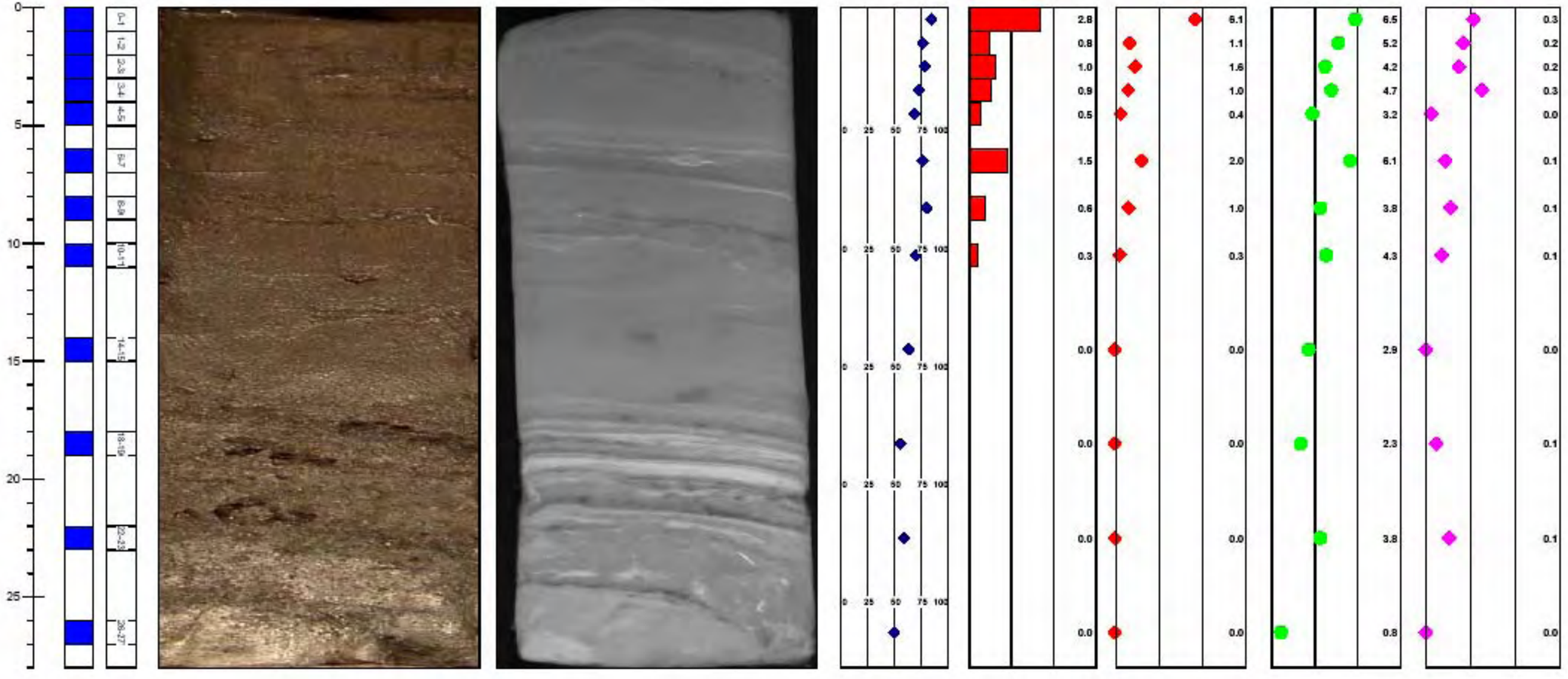

SEDIMENT CORE LOG

PROJECT: Little Lake, Barataria Bay, LA **CORE ID:** BC10-B

Collection Date:	October 14, 2003	Logged By:	Michelle Greene	
Total Depth (cm):	10	Latitude (North)	29.52901667	
Mudline Elevation MLLW (m):	Default Listing	Longitude (West)	-90.1617	Coordinate System: Geographic, WGS84

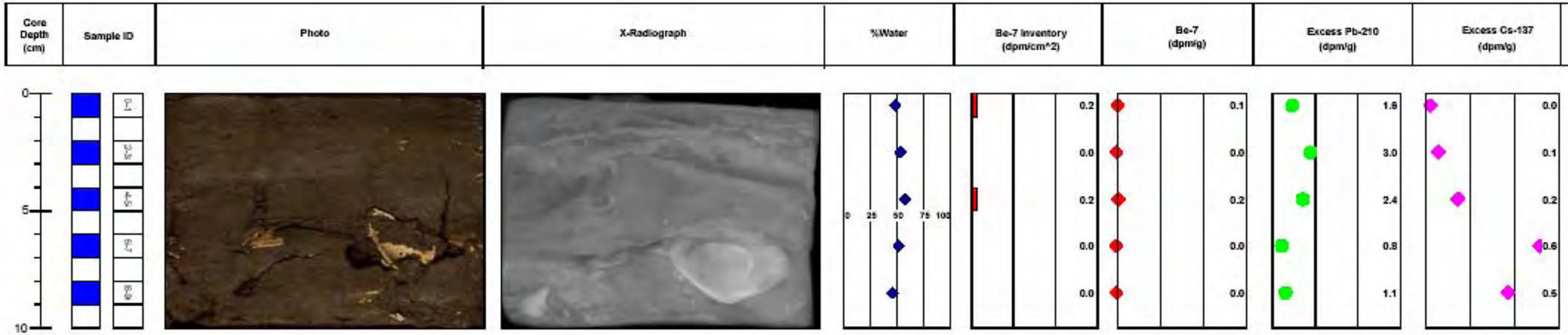

SEDIMENT CORE LOG

PROJECT: Little Lake, Barataria Bay, LA **CORE ID:** BC12-B

Collection Date:	October 14, 2003	Logged By:	Michelle Greene	
Total Depth (cm):	15	Latitude (North)	29.532354	
Mudline Elevation MLLW (m):	Default Listing	Longitude (West)	-90.205063	Coordinate System: Geographic, WGS84

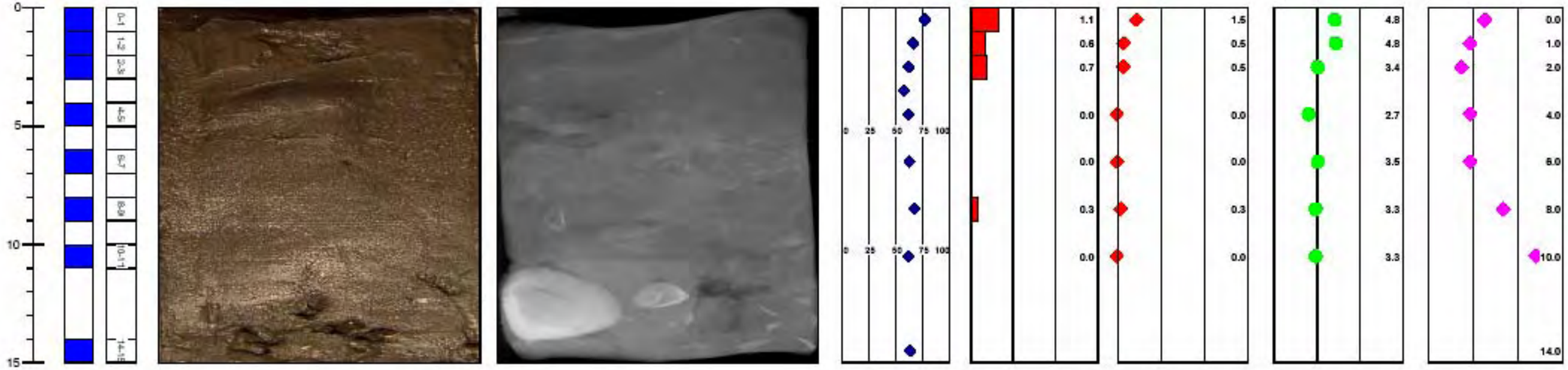

SEDIMENT CORE LOG

PROJECT: Little Lake, Barataria Bay, LA **CORE ID:** BC13-B

Collection Date:	October 14, 2003	Logged By:	Michelle Greene	
Total Depth (cm):	19	Latitude (North)	29.532488	
Mudline Elevation MLLW (m):	Default Listing	Longitude (West)	-90.220697	Coordinate System: Geographic, WGS84

Core Depth (cm)	Sample ID	Photo	X-Radiograph	%Water	Be-7 Inventory (dpm/cm^2)	Be-7 (dpm/g)	Excess Pb-210 (dpm/g)	Excess Cs-137 (dpm/g)
0 5 10 15	P1 2-3 4-5 6-7 8-9 10-11 14-15 18-19			0 25 50 75 100 0 25 50 75 100 0 25 50 75 100	2.8 4.0 2.4 2.3 0.8 0.2 0.0 6.8 0.0 0.7	3.9 4.6 3.3 3.0 0.7 0.2 0.0 5.0 0.0 0.7	5.0 6.4 6.8 4.9 2.3 1.5 1.9 1.8 2.8 3.3	0.1 0.2 0.1 0.2 0.1 0.1 0.5 0.7 1.0 1.4

SEDIMENT CORE LOG

PROJECT: Little Lake, Barataria Bay, LA **CORE ID:** BC15-B

Collection Date:	October 14, 2003	Logged By:	Michelle Greene	
Total Depth (cm):	15	Latitude (North)	29.50131667	
Mudline Elevation MLLW (m):	Default Listing	Longitude (West)	-90.16603333	Coordinate System: Geographic, WGS84

Core Depth (cm)	Sample ID	Photo	X-Radiograph	%Water	Be-7 Inventory (dpm/cm^2)	Be-7 (dpm/g)	Excess Pb-210 (dpm/g)	Excess Cs-137 (dpm/g)
0	1-2		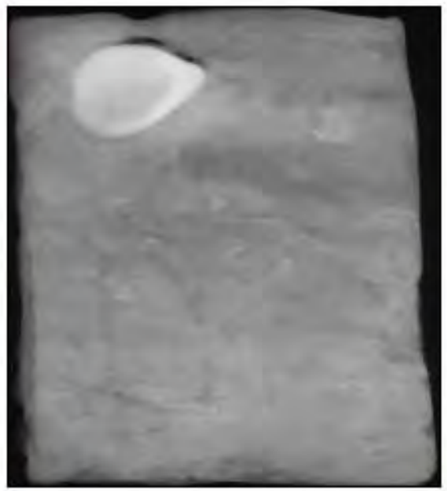	0 25 50 75 100	2.1 0.6 1.1 0.0 0.0	1.3 0.3 0.6 0.0 0.0	2.8 2.2 1.8 2.2 2.8	0.0 0.1 0.1 0.1 0.2
5	3-4			0 25 50 75 100	0.0 0.0 0.0 0.0 0.0	0.0 0.0 0.0 0.0 0.0	2.0 1.7 1.0 1.1	0.1 0.1 0.1 0.0
10	4-5							
	5-7							
	8-9							
	10-11							
15	14-15							

SEDIMENT CORE LOG

PROJECT: Little Lake, Barataria Bay, LA **CORE ID:** BC16-B

Collection Date:	October 14, 2003	Logged By:	Michelle Greene	
Total Depth (cm):	11	Latitude (North)	29.51008333	
Mudline Elevation MLLW (m):	Default Listing	Longitude (West)	-90.19583333	Coordinate System: Geographic, WGS84

Core Depth (cm)	Sample ID	Photo	X-Radiograph	%Water	Be-7 Inventory (dpm/cm^2)	Be-7 (dpm/g)	Excess Pb-210 (dpm/g)	Excess Cs-137 (dpm/g)
0 5 10	P-1 2-3 4-5 5-7 8-9 10-11		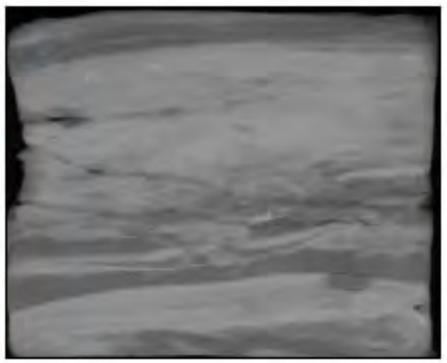	0 25 50 75 100 0 25 50 75 100	1.9 0.7 0.0 0.0 0.4 1.0	1.1 0.2 0.0 0.0 0.2 0.5	2.1 0.9 0.8 0.7 1.8 3.3	0.1 0.0 0.0 0.0 0.1 0.2

SEDIMENT CORE LOG

PROJECT: Little Lake, Barataria Bay, LA **CORE ID:** BC17-B

Collection Date:	October 14, 2003	Logged By:	Michelle Greene	
Total Depth (cm):	16	Latitude (North)	29.50976667	
Mudline Elevation MLLW (m):	Default Listing	Longitude (West)	-90.12658333	Coordinate System: Geographic, WGS84

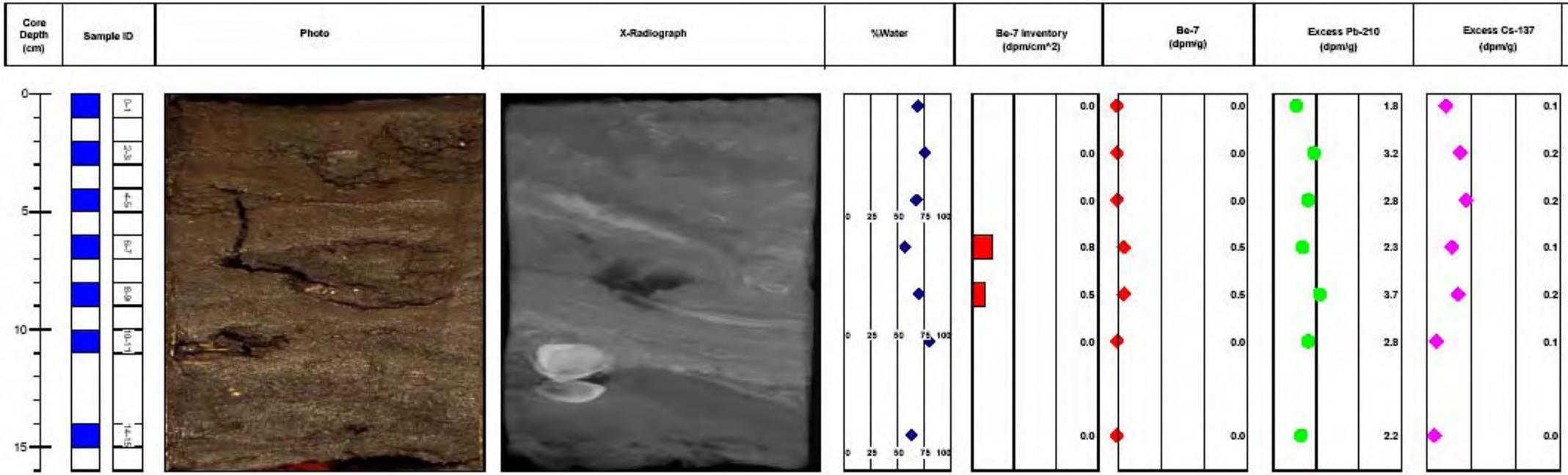

SEDIMENT CORE LOG

PROJECT: Little Lake, Barataria Bay, LA **CORE ID:** BC18-B

Collection Date:	October 16, 2003	Logged By:	Michelle Greene	
Total Depth (cm):	10	Latitude (North)	29.48688333	
Mudline Elevation MLLW (m):	Default Listing	Longitude (West)	-90.17148333	Coordinate System: Geographic, WGS84

Core Depth (cm)	Sample ID	Photo	X-Radiograph	%Water	Be-7 Inventory (dpm/cm^2)	Be-7 (dpm/g)	Excess Pb-210 (dpm/g)	Excess Cs-137 (dpm/g)	
0 5 10	PL 2.5 4.5 6.5 8.5		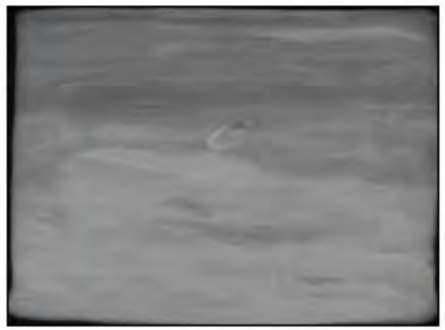	0 25 50 75 100	0.2 0.0 0.5 0.4 0.3	0.1 0.0 0.2 0.1 0.1	0.9 1.4 1.0 0.8 0.3	0.1 0.1 0.0 0.0 0.0	

SEDIMENT CORE LOG

PROJECT: Little Lake, Barataria Bay, LA **CORE ID:** BC19-B

Collection Date:	October 16, 2003	Logged By:	Michelle Greene	
Total Depth (cm):	11	Latitude (North)	29.4888	
Mudline Elevation MLLW (m):	BC19-B	Longitude (West)	-90.14505	Coordinate System: Geographic, WGS84

Core Depth (cm)	Sample ID	Photo	X-Radiograph	%Water	Be-7 Inventory (dpm/cm^2)	Be-7 (dpm/g)	Excess Pb-210 (dpm/g)	Excess Cs-137 (dpm/g)

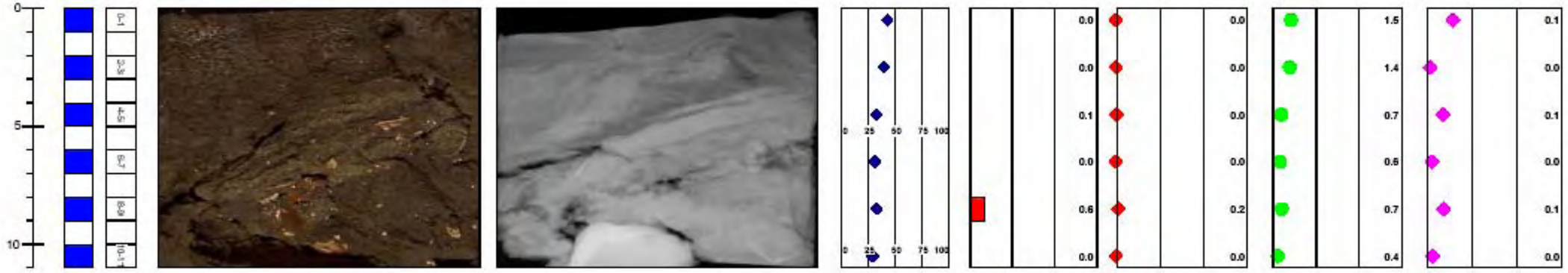

SEDIMENT CORE LOG

PROJECT: Little Lake, Barataria Bay, LA **CORE ID:** BC20-B

Collection Date:	October 16, 2003	Logged By:	Michelle Greene	
Total Depth (cm):	13	Latitude (North)	29.47656667	
Mudline Elevation MLLW (m):	Default Listing	Longitude (West)	-90.12838333	Coordinate System: Geographic, WGS84

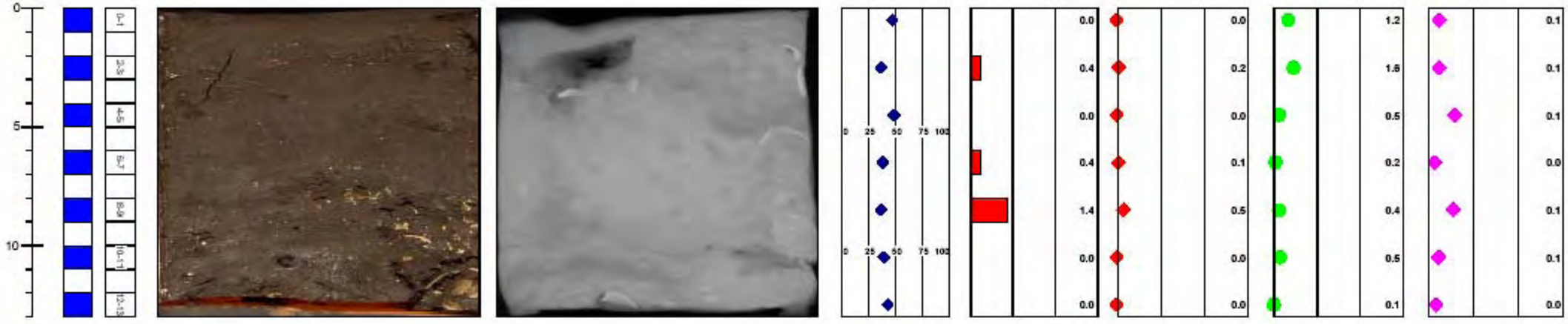

SEDIMENT CORE LOG

PROJECT: Little Lake, Barataria Bay, LA **CORE ID:** BC22-B

Collection Date:	October 16, 2003	Logged By:	Michelle Greene	
Total Depth (cm):	20	Latitude (North)	29.46475	
Mudline Elevation MLLW (m):	Default Listing	Longitude (West)	-90.11111667	Coordinate System: Geographic, WGS84

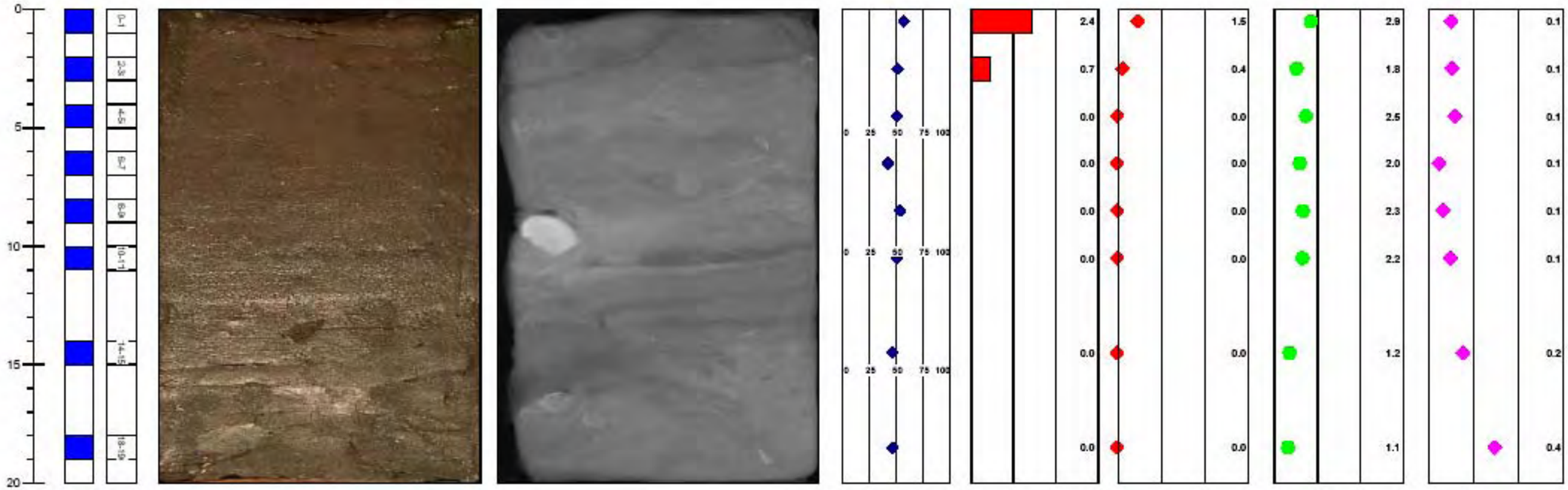

SEDIMENT CORE LOG

PROJECT: Little Lake, Barataria Bay, LA **CORE ID:** BC23-B

Collection Date:	October 16, 2003	Logged By:	Michelle Greene	
Total Depth (cm):	26	Latitude (North)	29.4711	
Mudline Elevation MLLW (m):	Default Listing	Longitude (West)	-90.07628333	Coordinate System: Geographic, WGS84

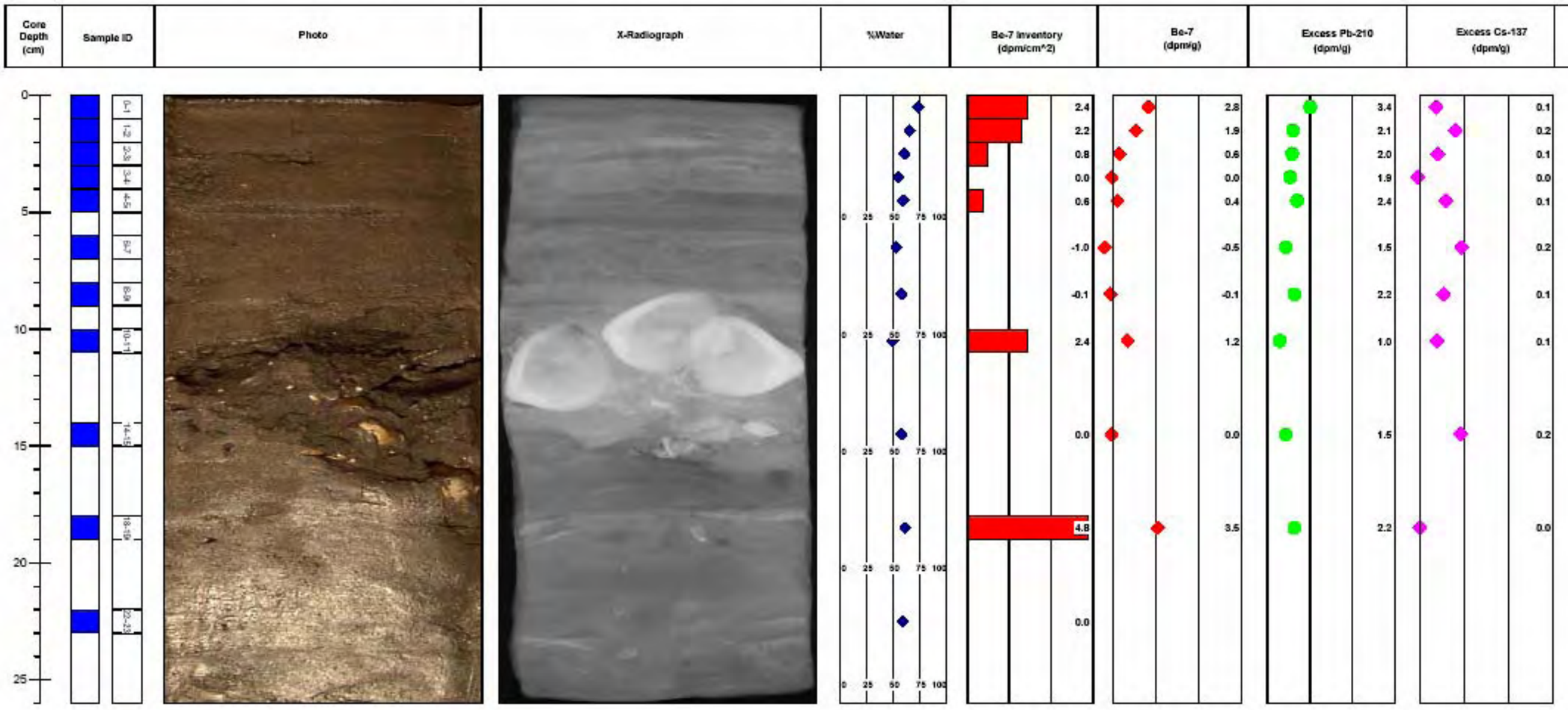

SEDIMENT CORE LOG

PROJECT: Little Lake, Barataria Bay, LA **CORE ID:** BC24-B

Collection Date:	October 14, 2003	Logged By:	Michelle Greene	
Total Depth (cm):	18	Latitude (North)	29.5382288	
Mudline Elevation MLLW (m):	Default Listing	Longitude (West)	-90.1308833	Coordinate System: Geographic, WGS84

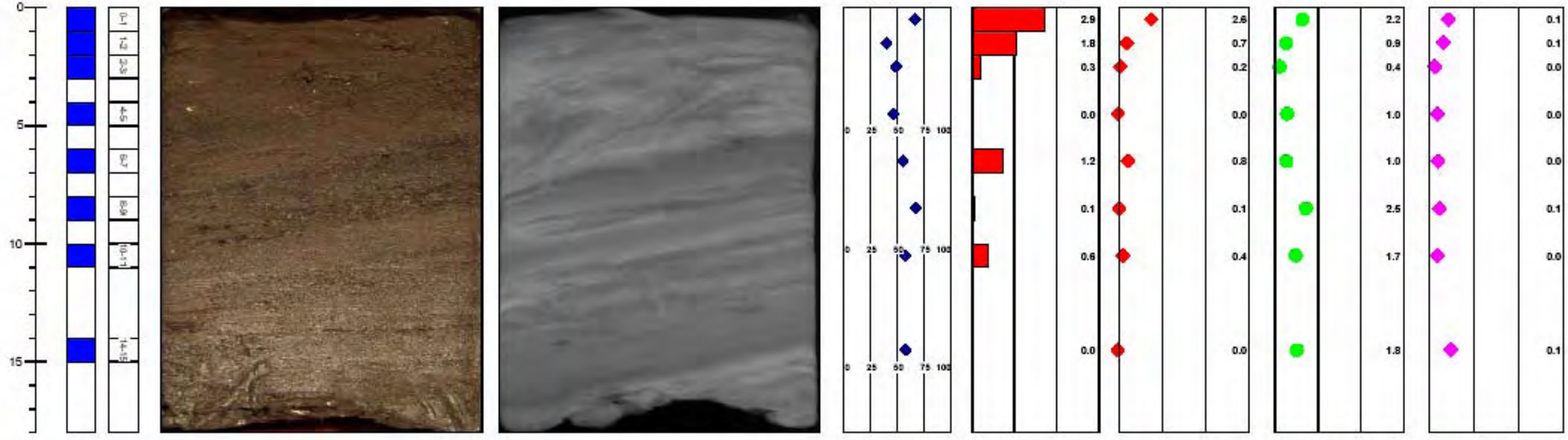

SEDIMENT CORE LOG

PROJECT: Little Lake, Barataria Bay, LA **CORE ID:** BC25-B

Collection Date:	October 14, 2003	Logged By:	Michelle Greene	
Total Depth (cm):	23	Latitude (North)	29.5293	
Mudline Elevation MLLW (m):	Default Listing	Longitude (West)	-90.10386667	Coordinate System: Geographic, WGS84

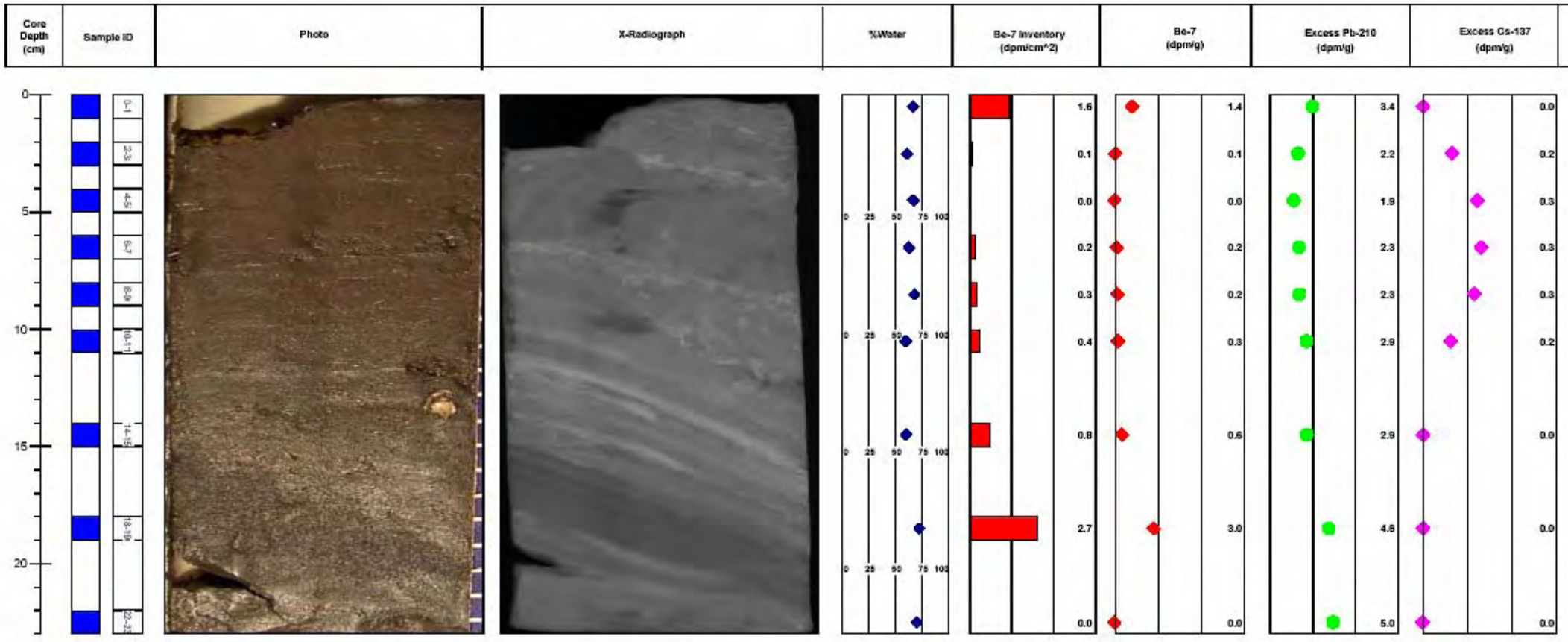

SEDIMENT CORE LOG

PROJECT: Little Lake, Barataria Bay, LA **CORE ID:** BC26-B

Collection Date:	October 14, 2003	Logged By:	Michelle Greene	
Total Depth (cm):	21	Latitude (North)	29.51315	
Mudline Elevation MLLW (m):	Default Listing	Longitude (West)	-90.0864	Coordinate System: Geographic, WGS84

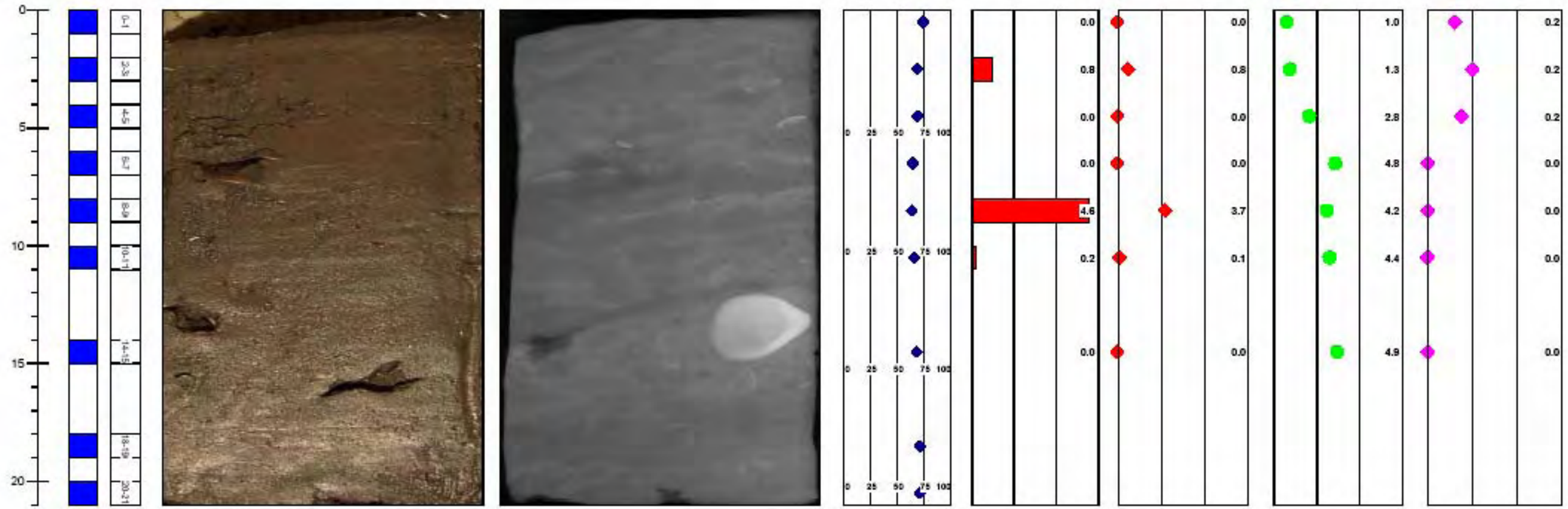

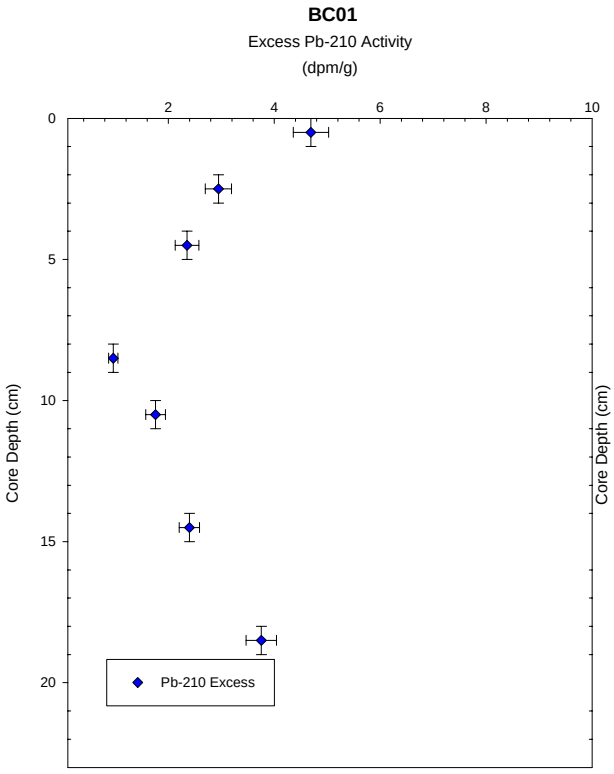
BC01
Excess Pb-210 Activity
(dpm/g)
Core Depth (cm)
Pb-210 Excess

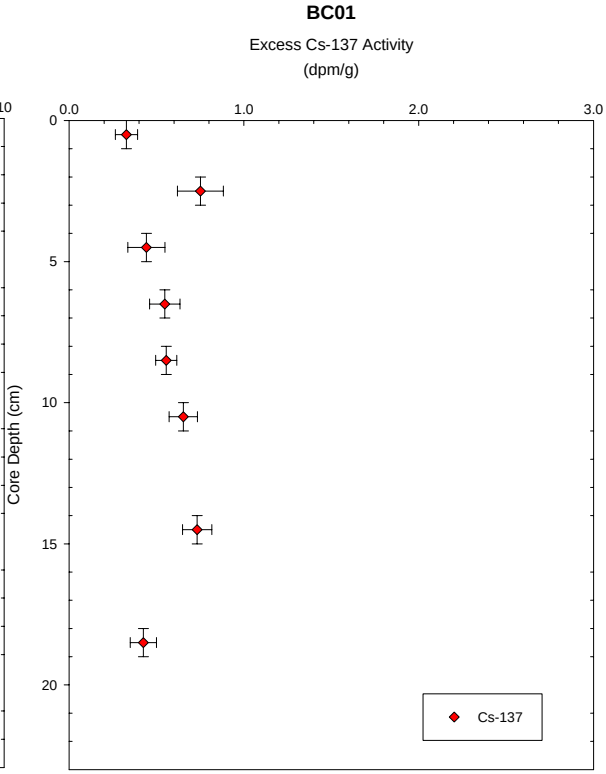
BC01
Excess Cs-137 Activity
(dpm/g)
Core Depth (cm)
Cs-137

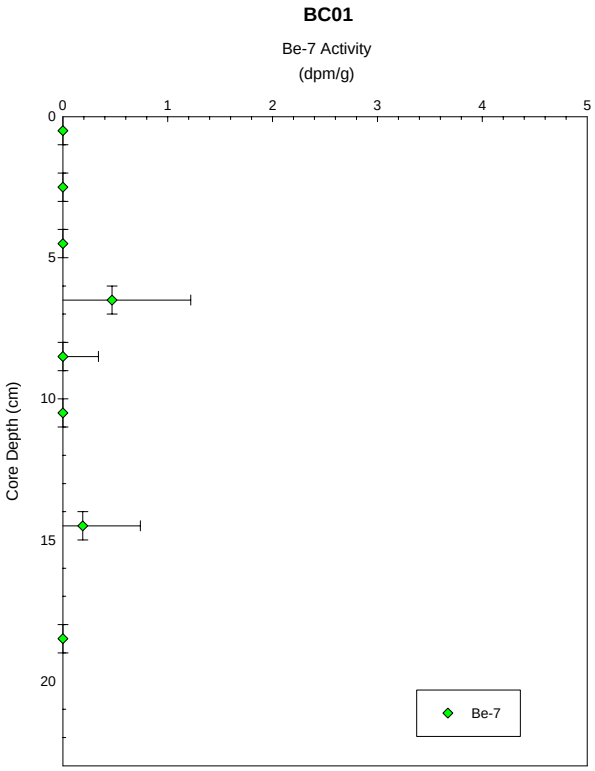
BC01
Be-7 Activity
(dpm/g)
Core Depth (cm)
Be-7

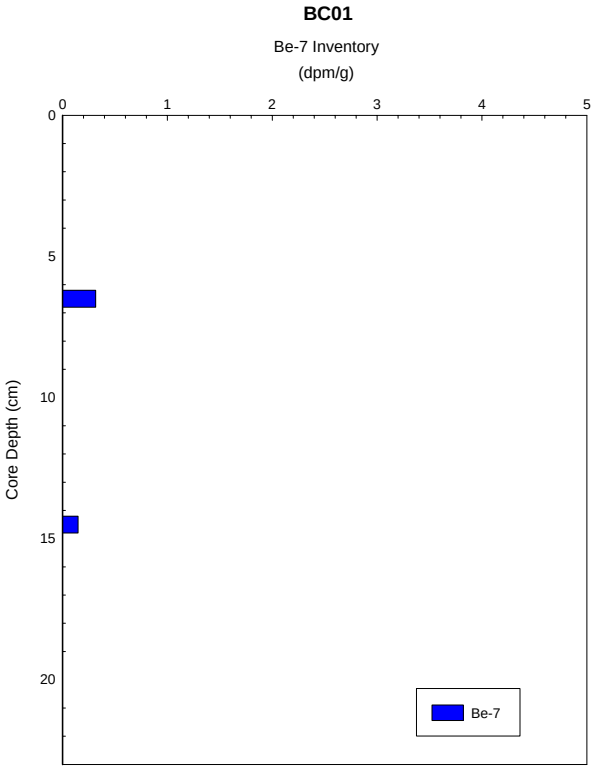
BC01
Be-7 Inventory
(dpm/g)
Core Depth (cm)
Be-7

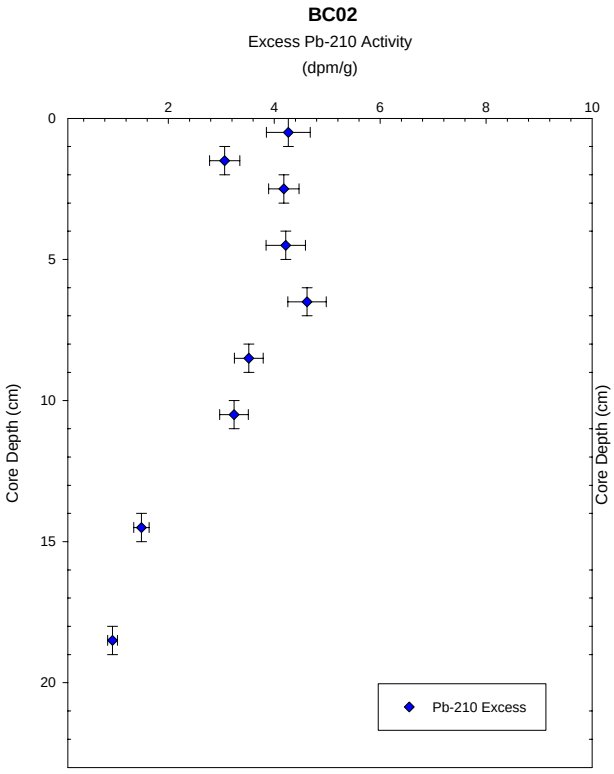
BC02
Excess Pb-210 Activity
(dpm/g)
Core Depth (cm)
Pb-210 Excess

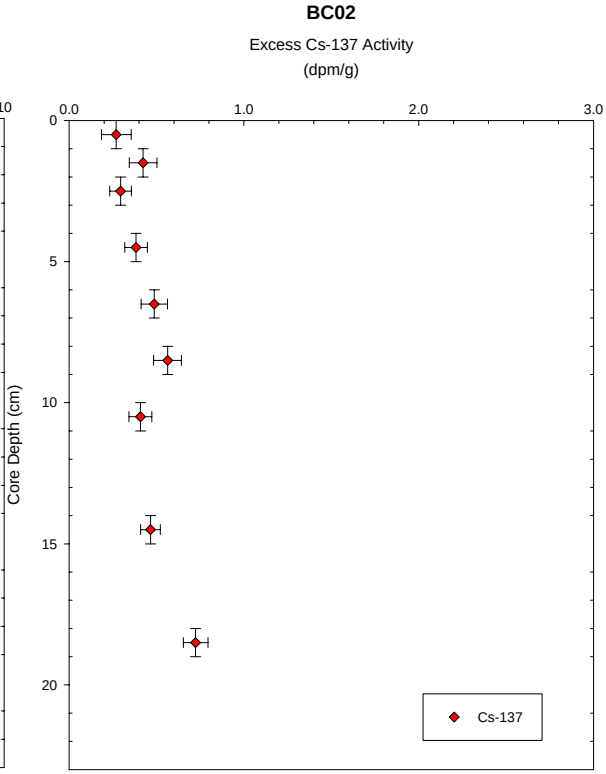
BC02
Excess Cs-137 Activity
(dpm/g)
Core Depth (cm)
Cs-137

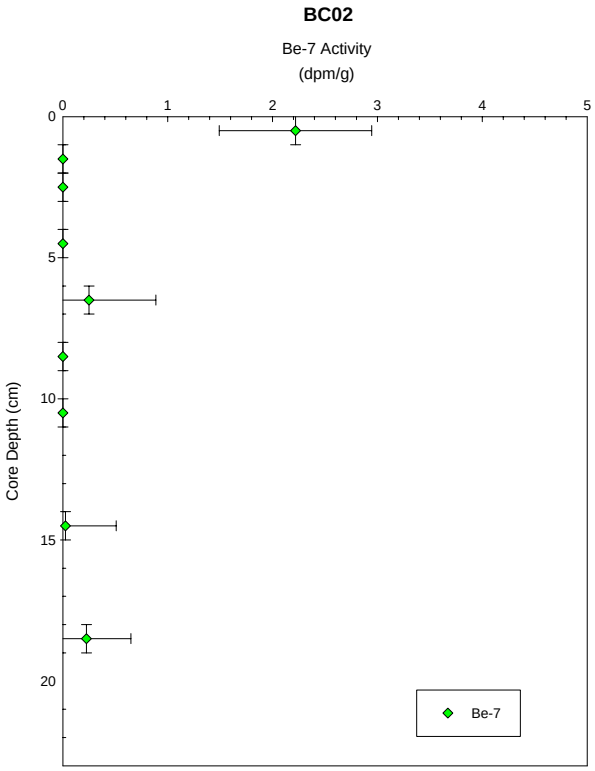
BC02
Be-7 Activity
(dpm/g)
Core Depth (cm)
Be-7

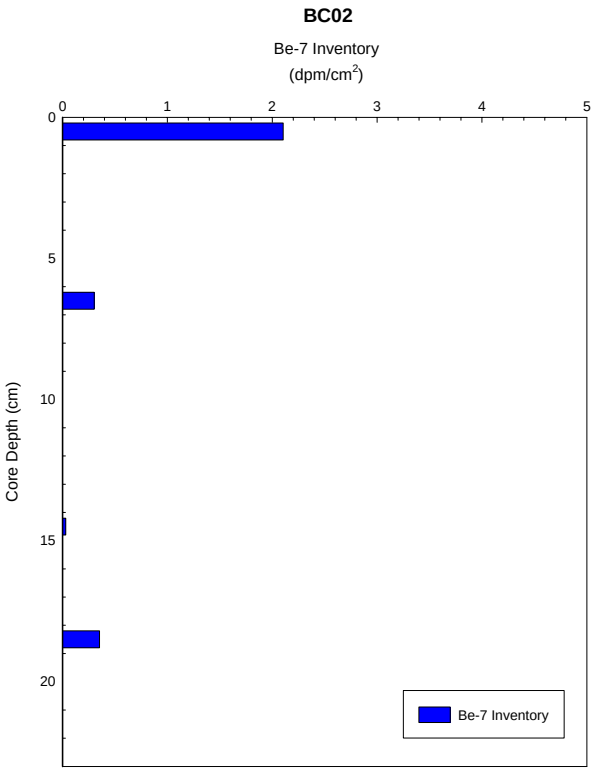
BC02
Be-7 Inventory
(dpm/cm2)
Core Depth (cm)
Be-7 Inventory

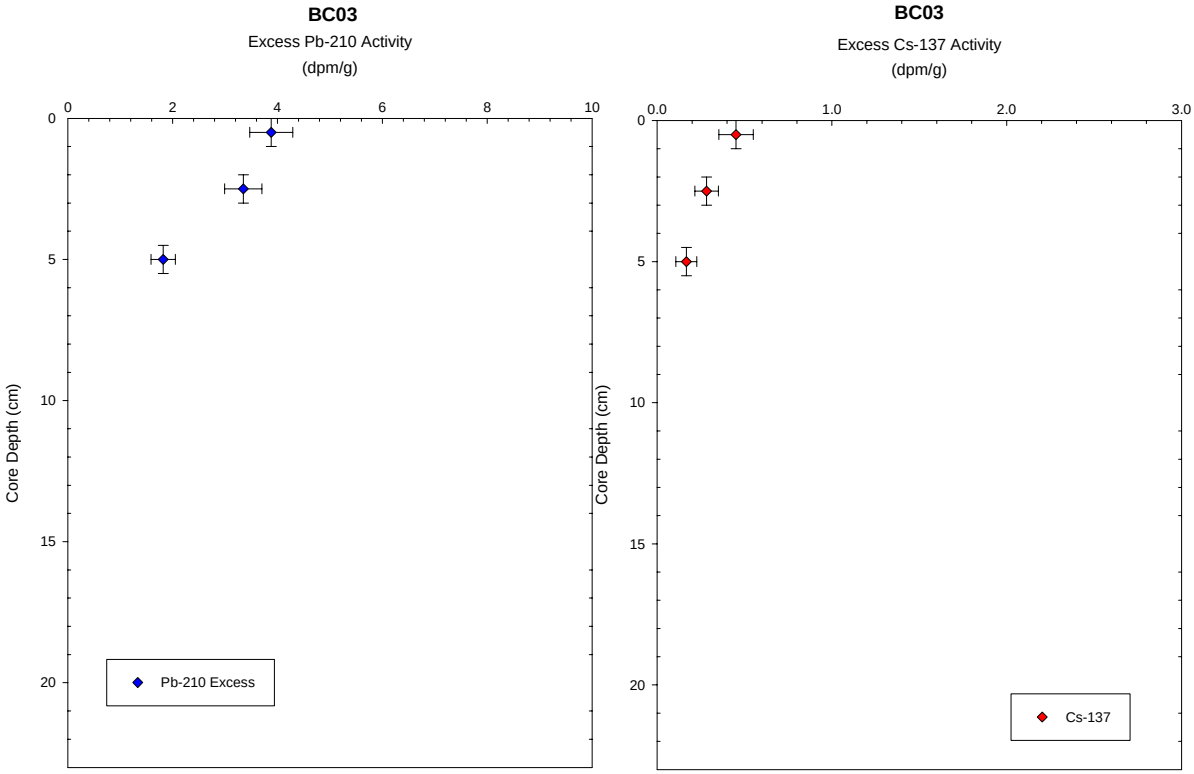
BC03
Excess Pb-210 Activity
(dpm/g)
Core Depth (cm)
Pb-210 Excess

BC03
Excess Cs-137 Activity
(dpm/g)
Core Depth (cm)
Cs-137

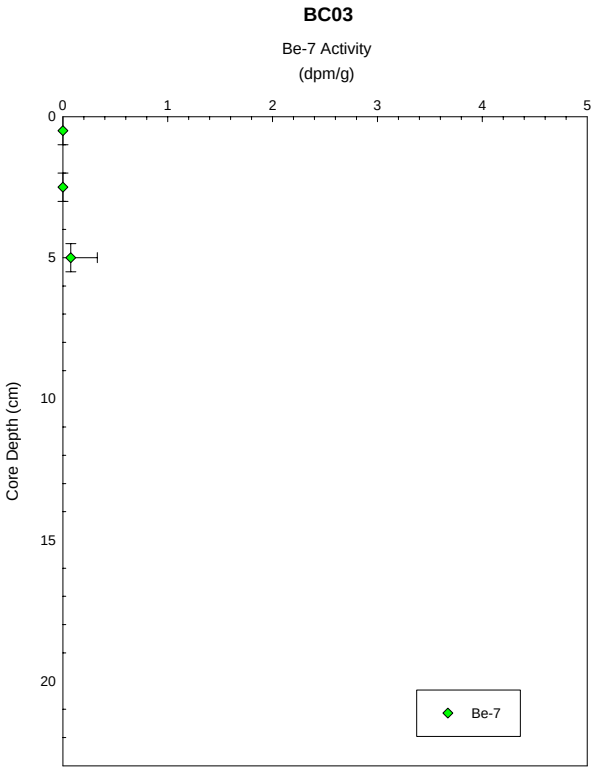
BC03
Be-7 Activity
(dpm/g)
Core Depth (cm)
Be-7

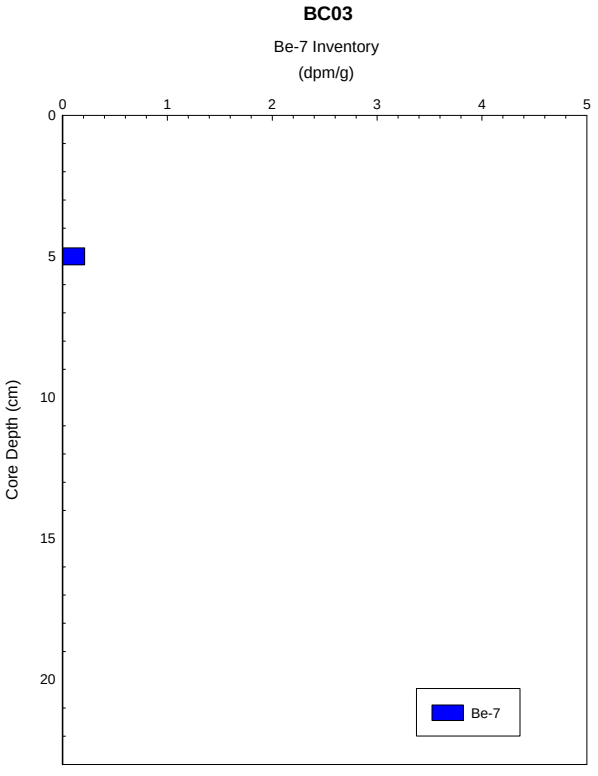
BC03
Be-7 Inventory
(dpm/g)
Core Depth (cm)
Be-7

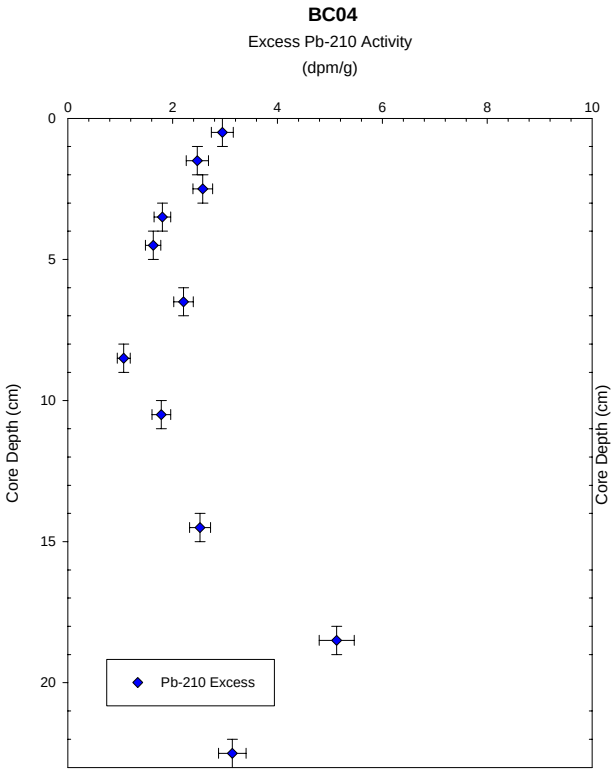
BC04
Excess Pb-210 Activity
(dpm/g)
Core Depth (cm)
Pb-210 Excess

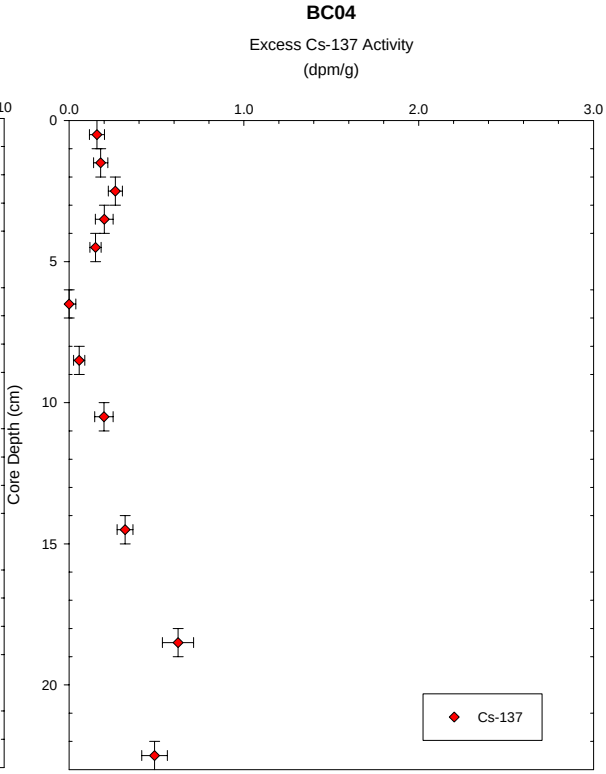
BC04
Excess Cs-137 Activity
(dpm/g)
Core Depth (cm)
Cs-137

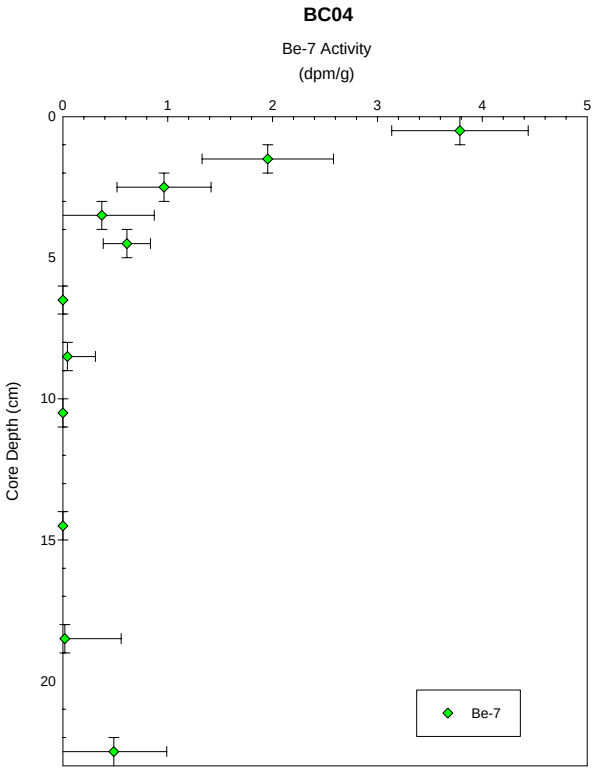
BC04
Be-7 Activity
(dpm/g)
Core Depth (cm)
Be-7

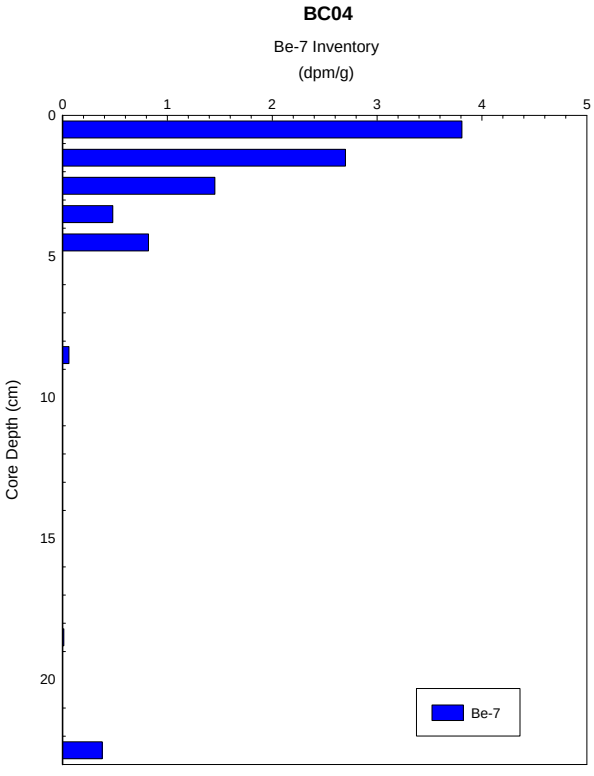
BC04
Be-7 Inventory
(dpm/g)
Core Depth (cm)
Be-7

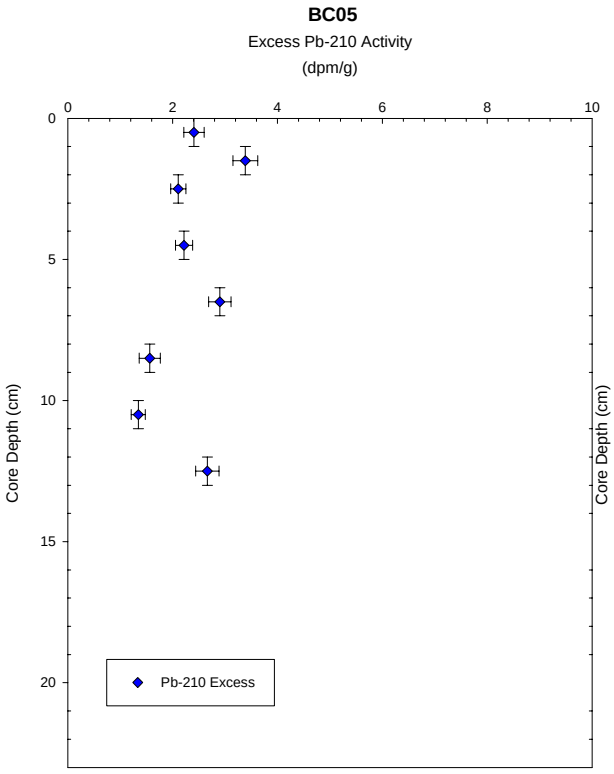
BC05
Excess Pb-210 Activity
(dpm/g)
Core Depth (cm)
Pb-210 Excess

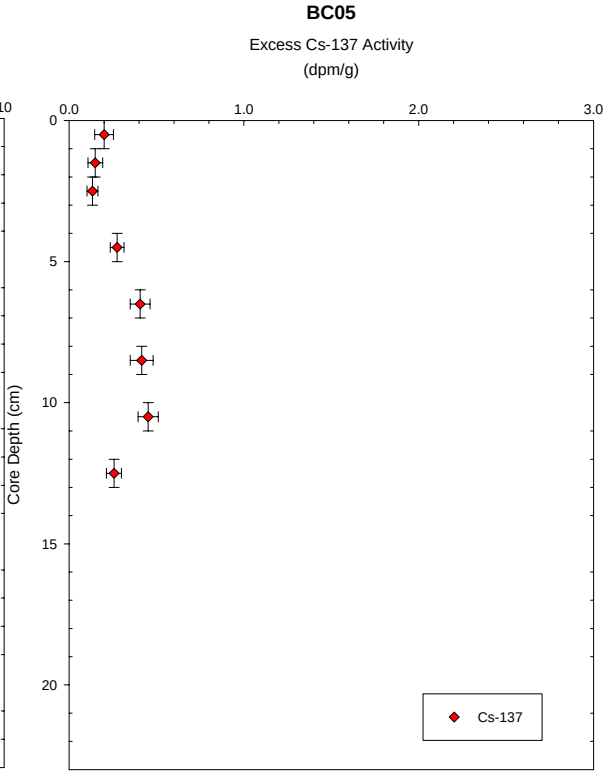
BC05
Excess Cs-137 Activity
(dpm/g)
Core Depth (cm)
Cs-137

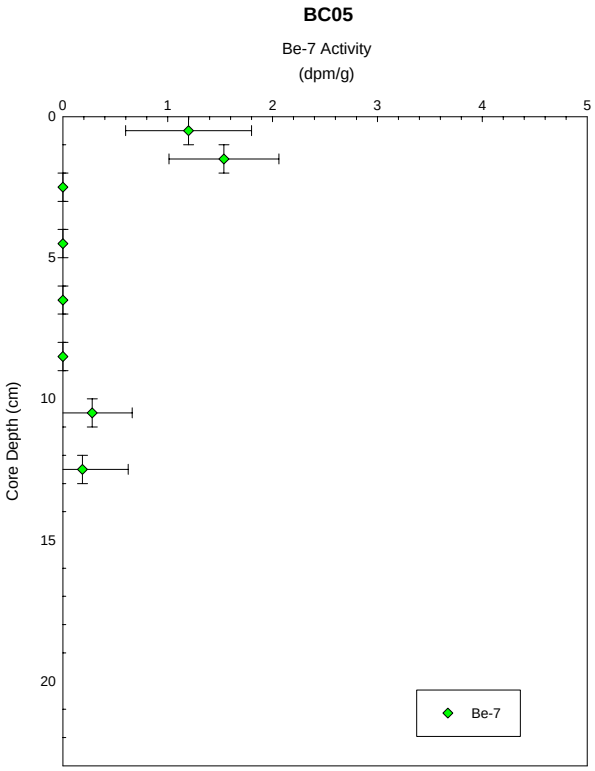
BC05
Be-7 Activity
(dpm/g)
Core Depth (cm)
Be-7

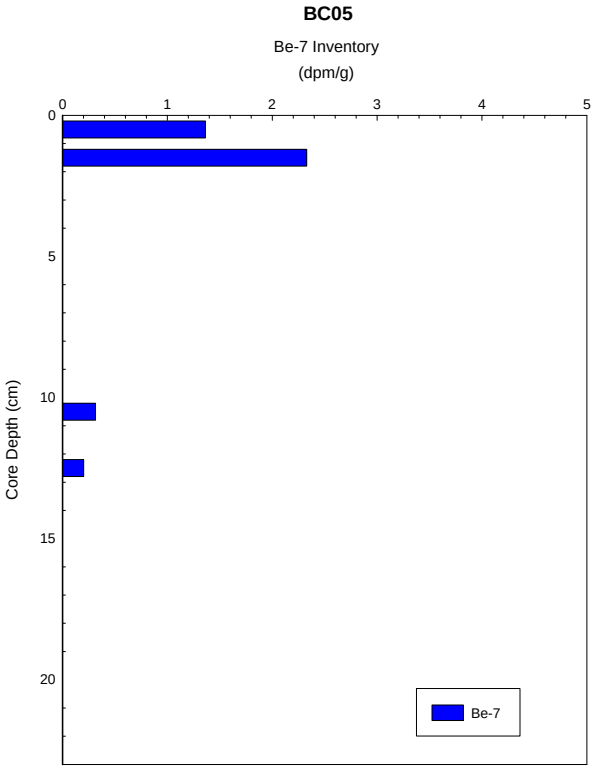
BC05
Be-7 Inventory
(dpm/g)
Core Depth (cm)
Be-7

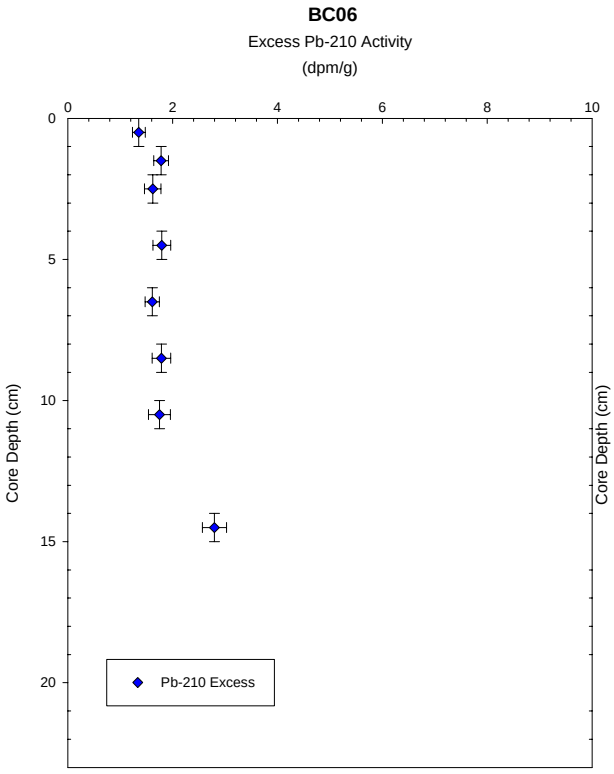
BC06
Excess Pb-210 Activity
(dpm/g)
Core Depth (cm)
Pb-210 Excess

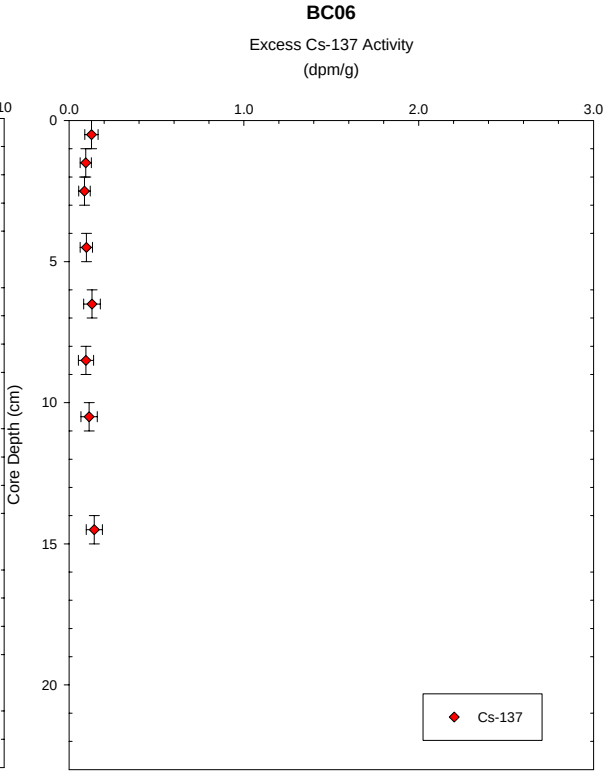
BC06
Excess Cs-137 Activity
(dpm/g)
Core Depth (cm)
Cs-137

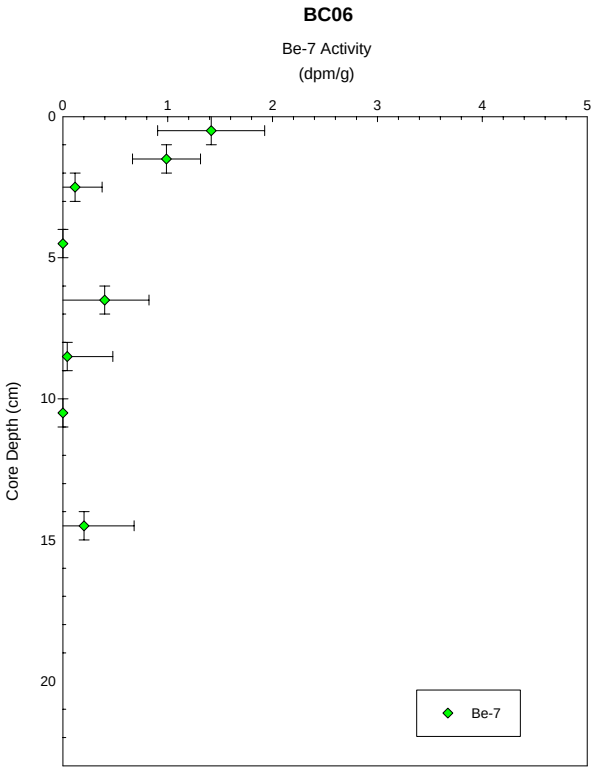
BC06
Be-7 Activity
(dpm/g)
Core Depth (cm)
Be-7

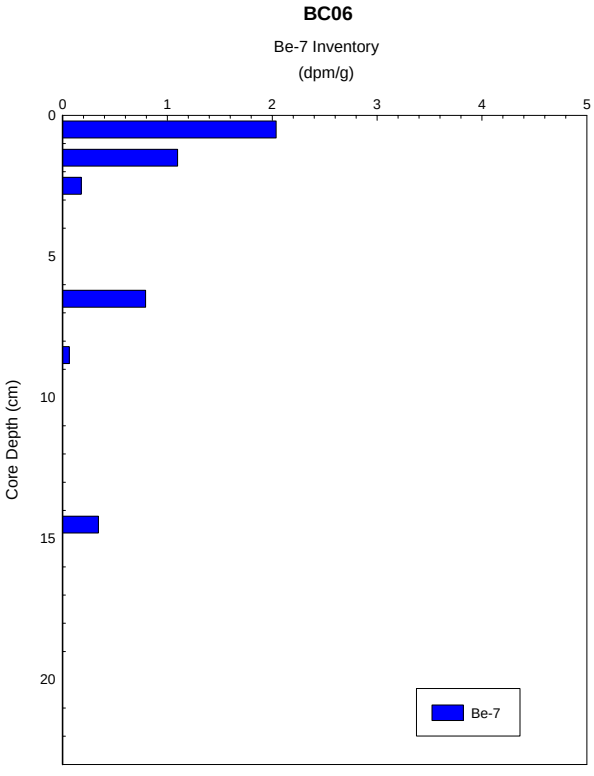
BC06
Be-7 Inventory
(dpm/g)
Core Depth (cm)
Be-7

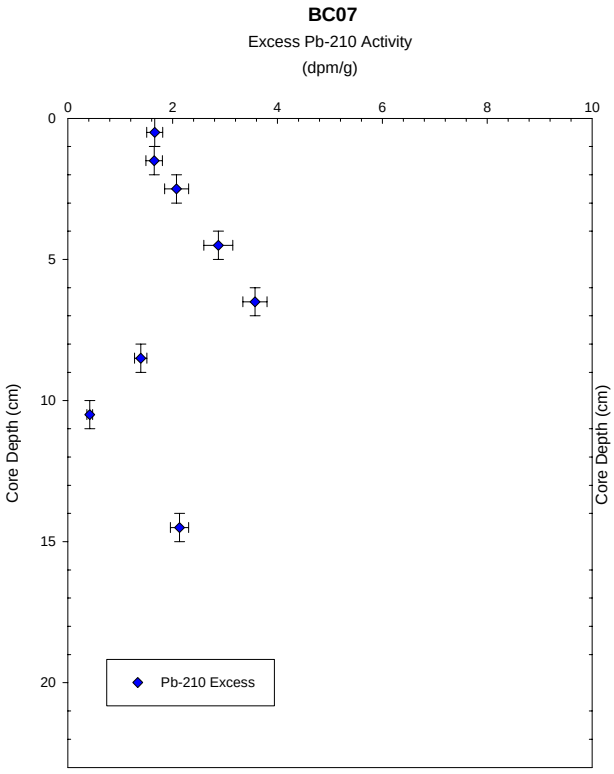
BC07
Excess Pb-210 Activity
(dpm/g)
Core Depth (cm)
Pb-210 Excess

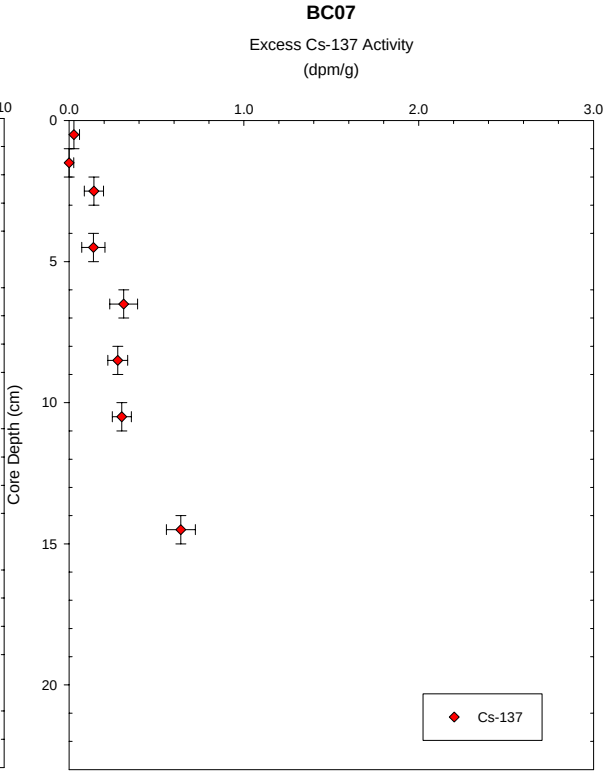
BC07
Excess Cs-137 Activity
(dpm/g)
Core Depth (cm)
Cs-137

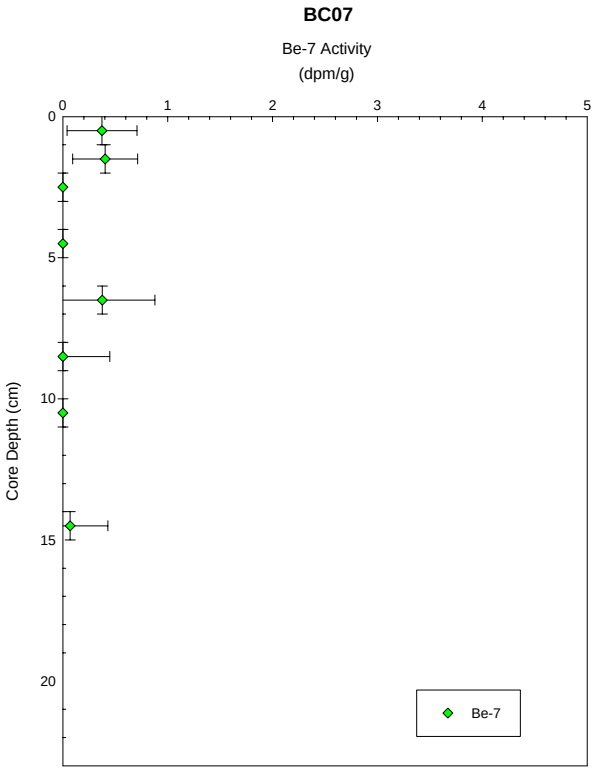
BC07
Be-7 Activity
(dpm/g)
Core Depth (cm)
Be-7

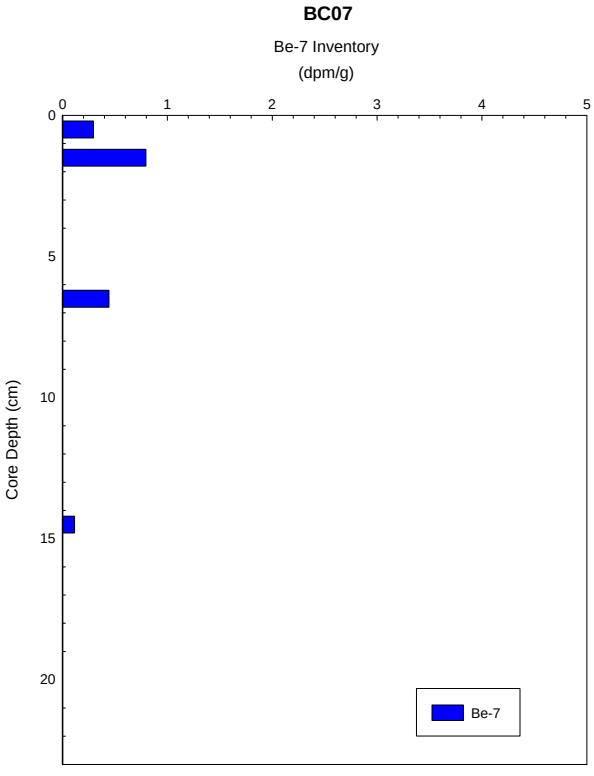
BC07
Be-7 Inventory
(dpm/g)
Core Depth (cm)
Be-7

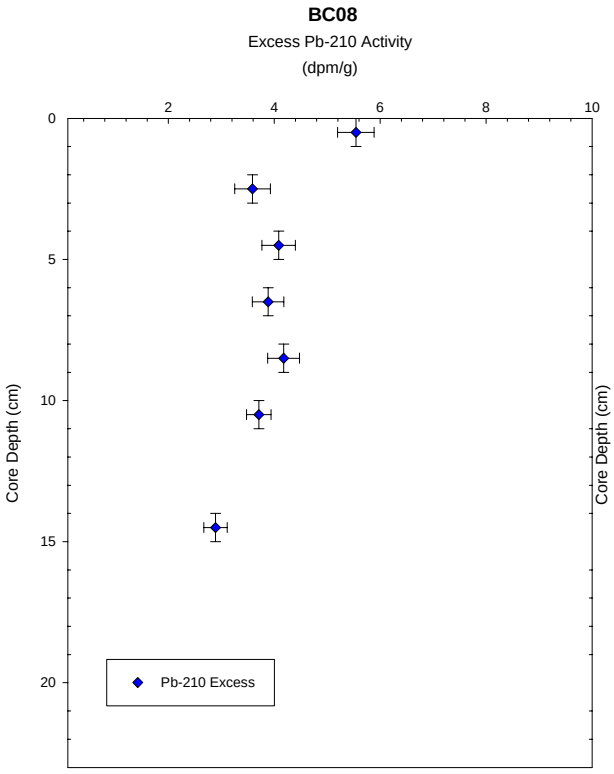
BC08
Excess Pb-210 Activity
(dpm/g)
Core Depth (cm)
Pb-210 Excess

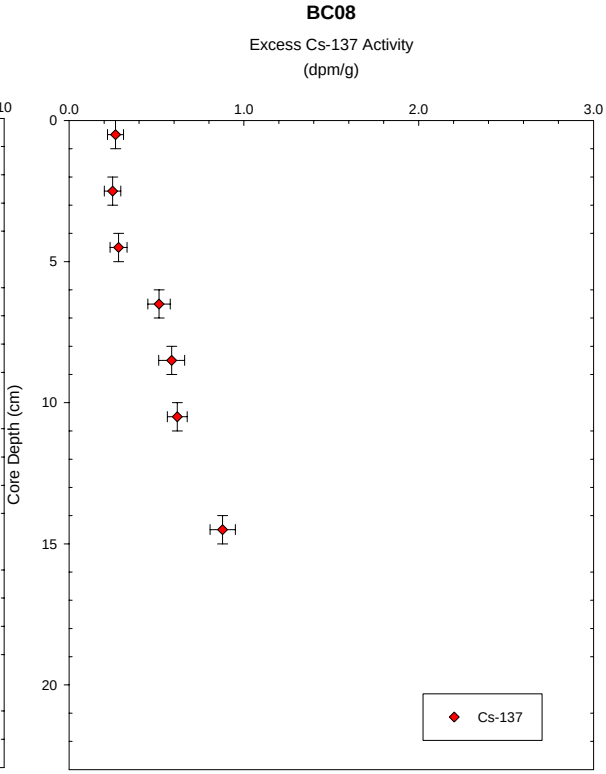
BC08
Excess Cs-137 Activity
(dpm/g)
Core Depth (cm)
Cs-137

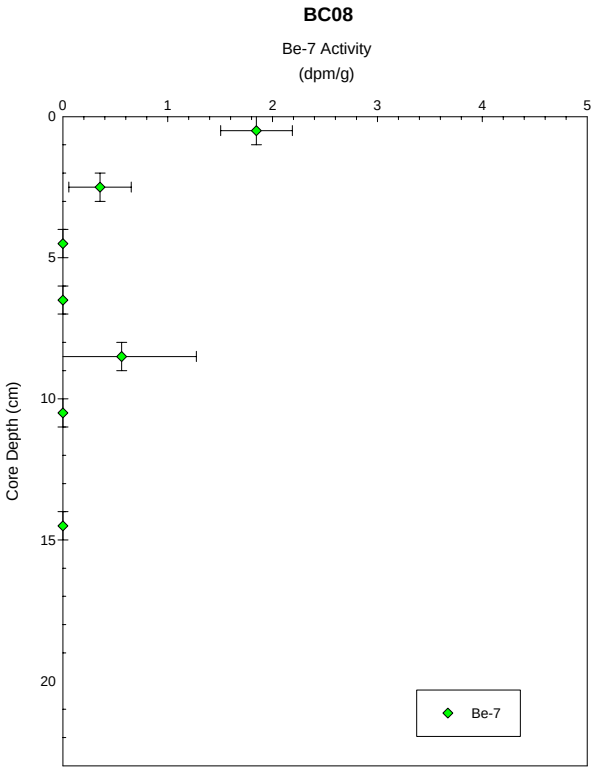
BC08
Be-7 Activity
(dpm/g)
Core Depth (cm)
Be-7

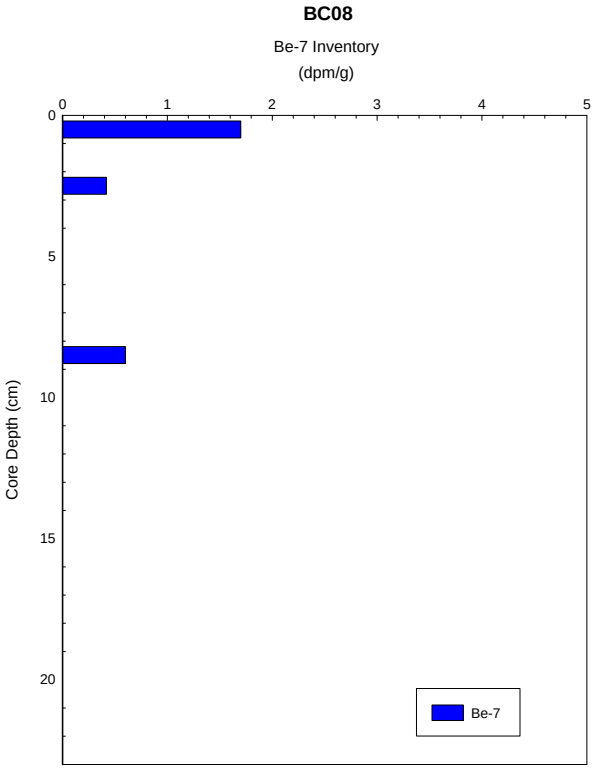
BC08
Be-7 Inventory
(dpm/g)
Core Depth (cm)
Be-7

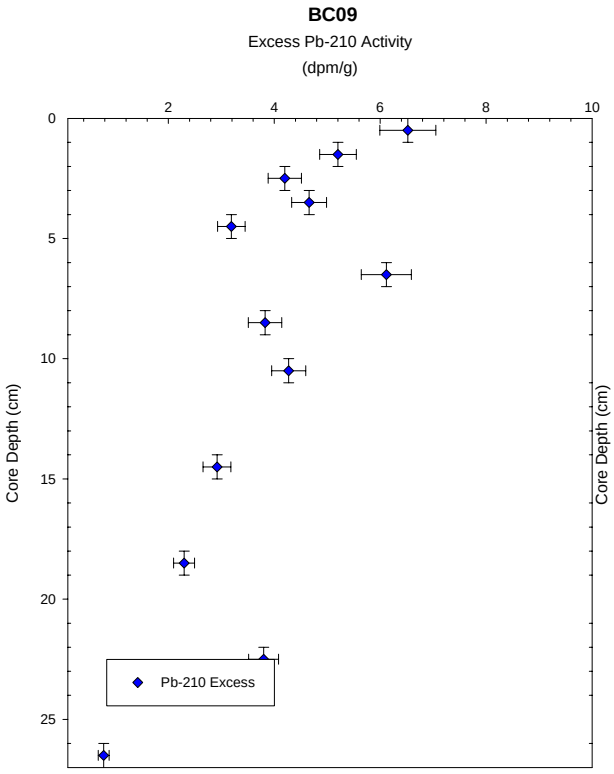
BC09
Excess Pb-210 Activity
(dpm/g)
Core Depth (cm)
Pb-210 Excess

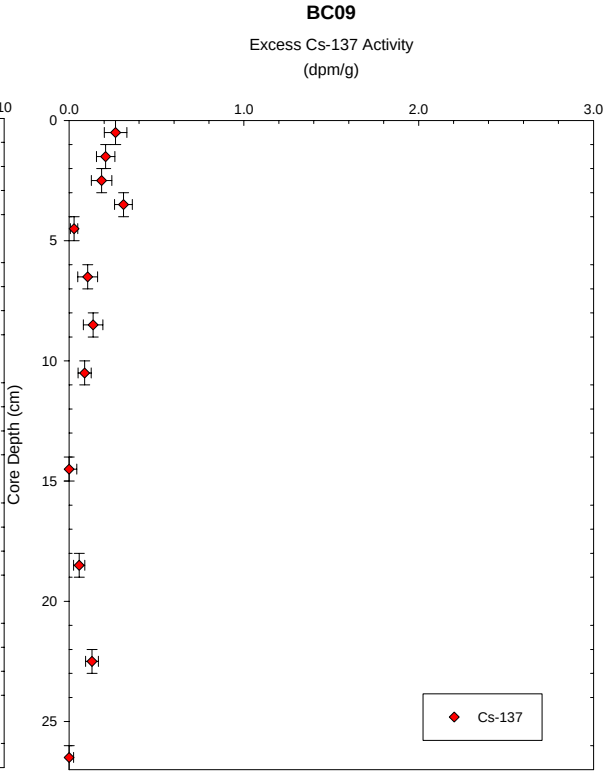
BC09
Excess Cs-137 Activity
(dpm/g)
Core Depth (cm)
Cs-137

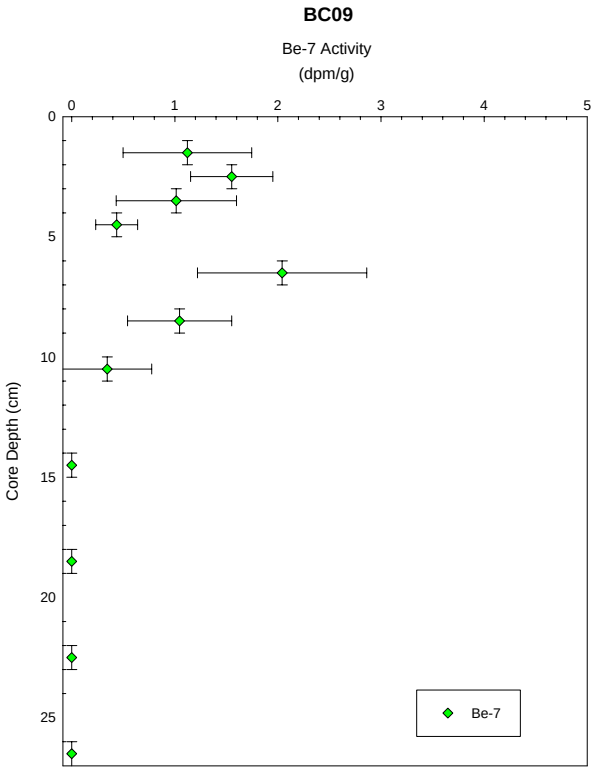
BC09
Be-7 Activity
(dpm/g)
Core Depth (cm)
Be-7

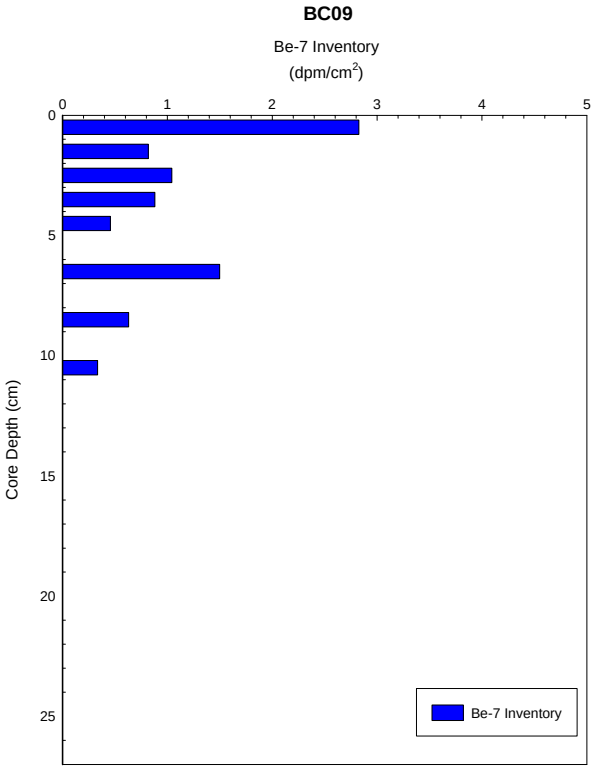
BC09
Be-7 Inventory
(dpm/cm2)
Core Depth (cm)
Be-7 Inventory

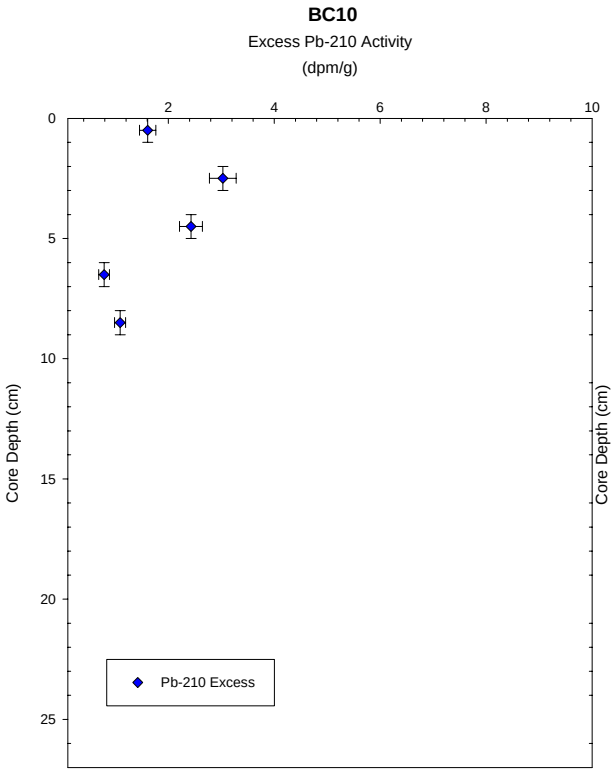
BC10
Excess Pb-210 Activity
(dpm/g)
Core Depth (cm)
Pb-210 Excess

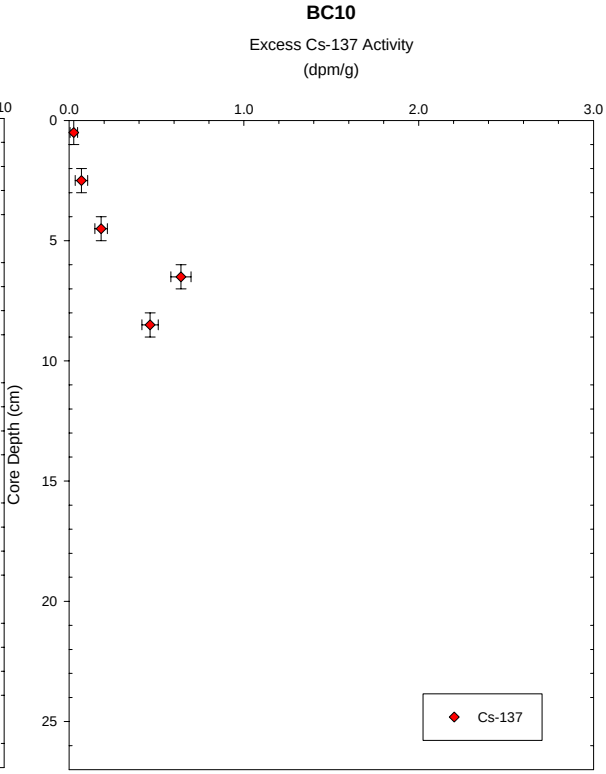
BC10
Excess Cs-137 Activity
(dpm/g)
Core Depth (cm)
Cs-137

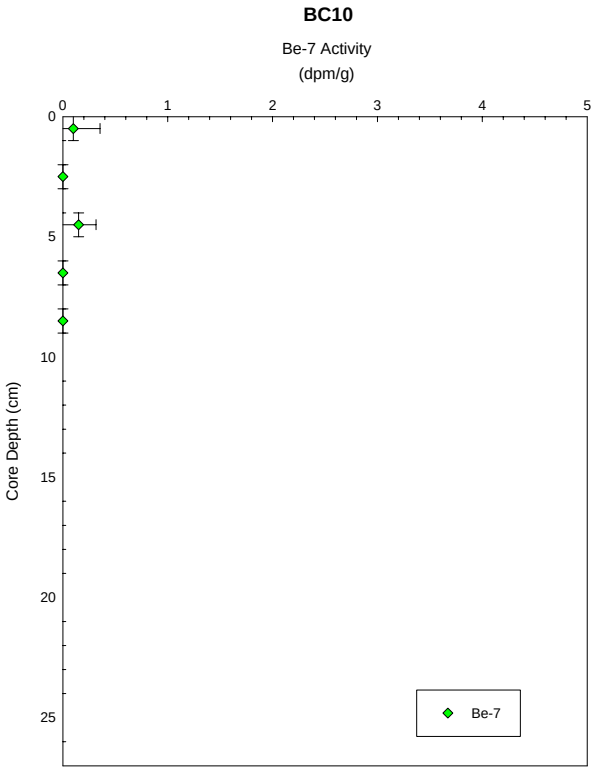
BC10
Be-7 Activity
(dpm/g)
Core Depth (cm)
Be-7

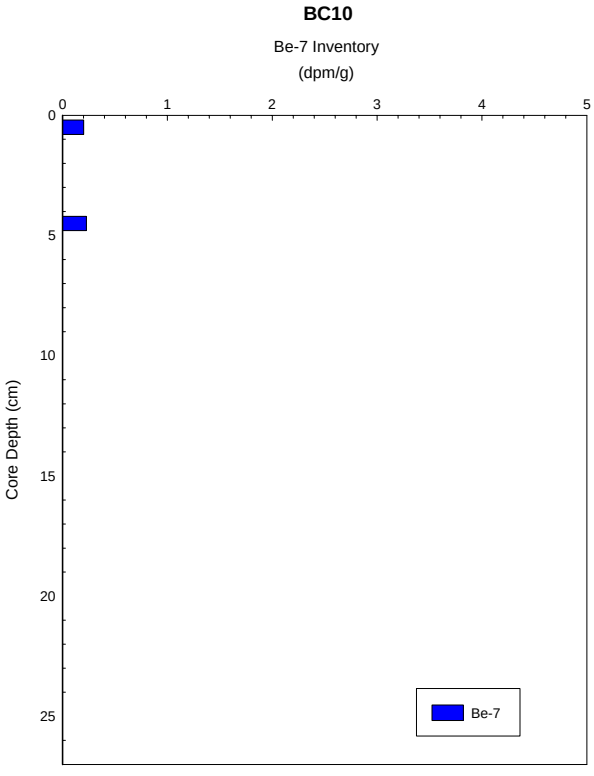
BC10
Be-7 Inventory
(dpm/g)
Core Depth (cm)
Be-7

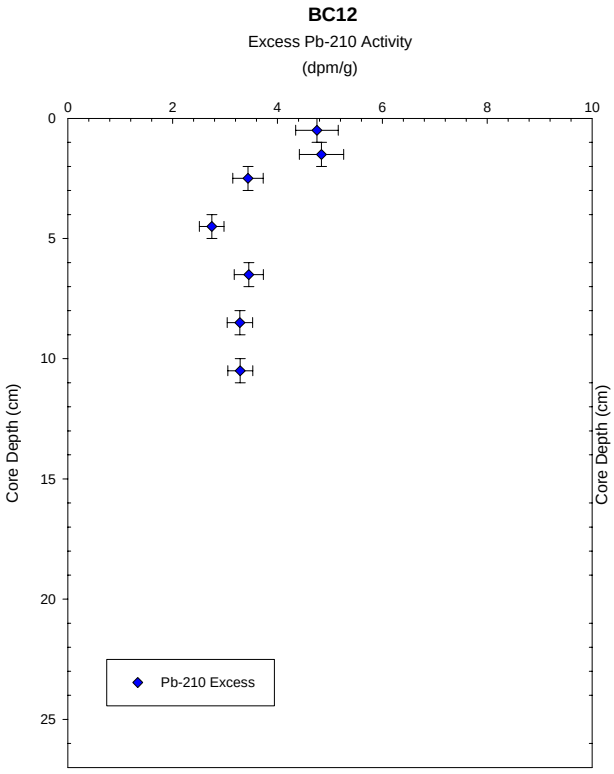
BC12
Excess Pb-210 Activity
(dpm/g)
Core Depth (cm)
Pb-210 Excess

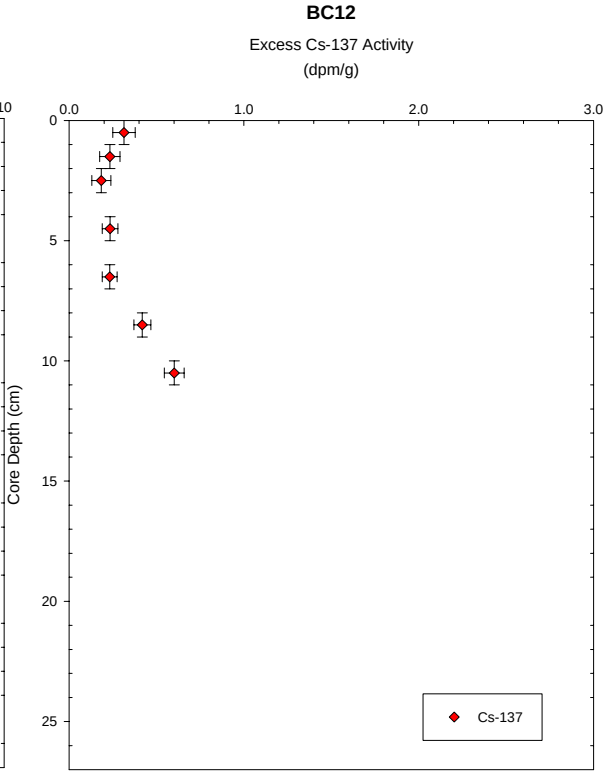
BC12
Excess Cs-137 Activity
(dpm/g)
Core Depth (cm)
Cs-137

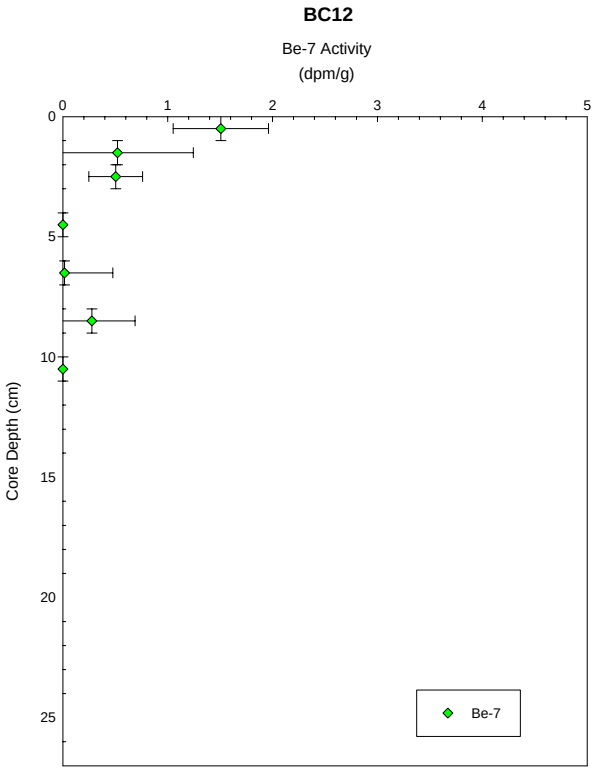
BC12
Be-7 Activity
(dpm/g)
Core Depth (cm)
Be-7

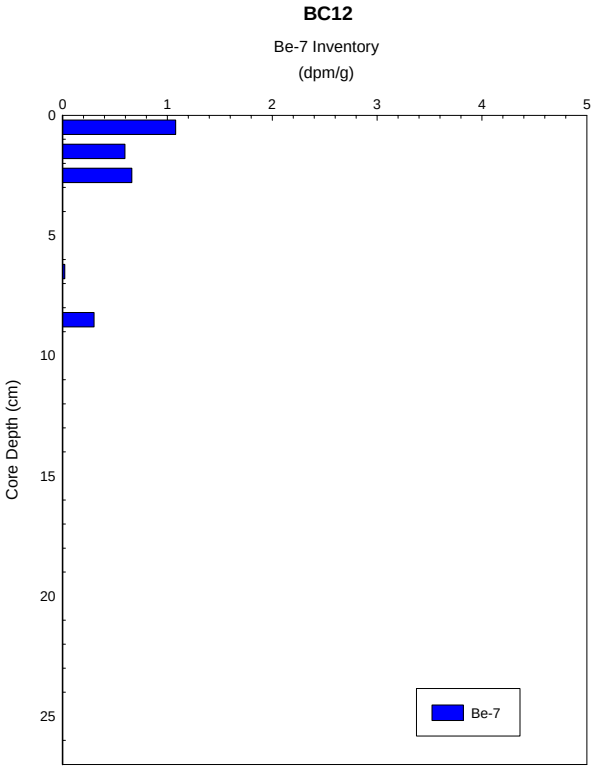
BC12
Be-7 Inventory
(dpm/g)
Core Depth (cm)
Be-7

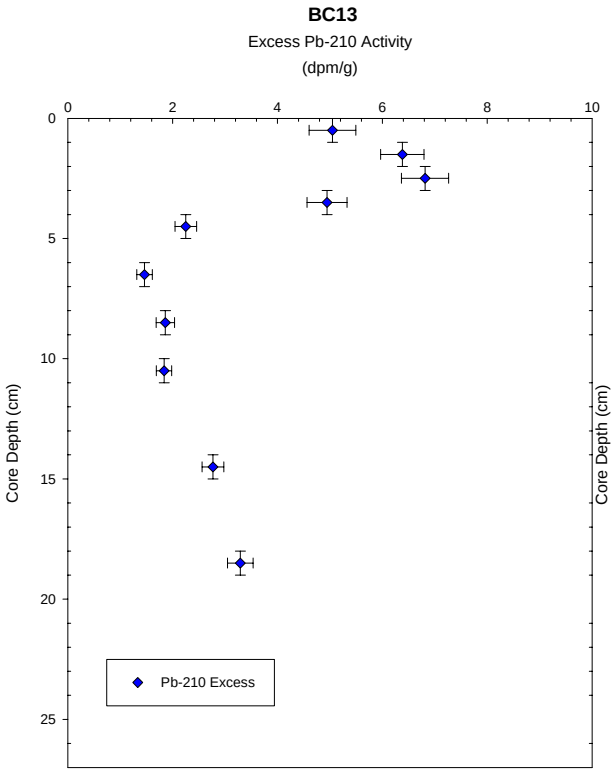
BC13
Excess Pb-210 Activity
(dpm/g)
Core Depth (cm)
Pb-210 Excess

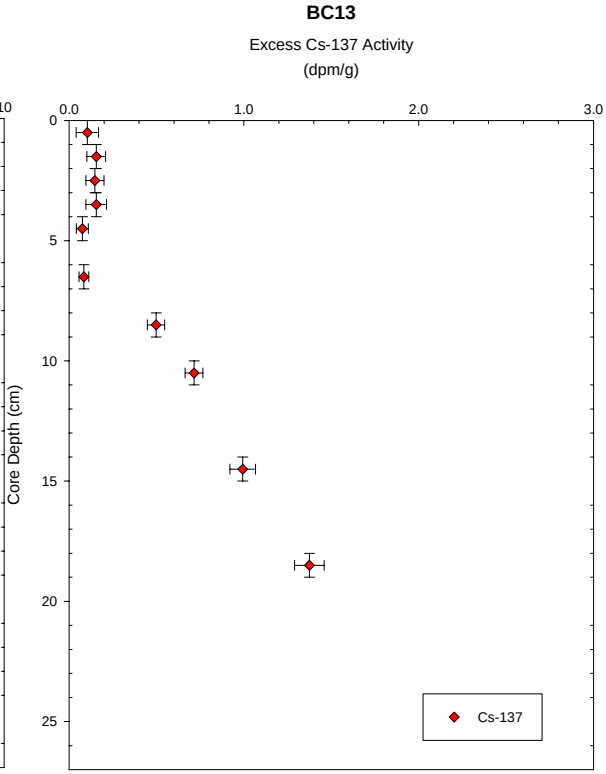
BC13
Excess Cs-137 Activity
(dpm/g)
Core Depth (cm)
Cs-137

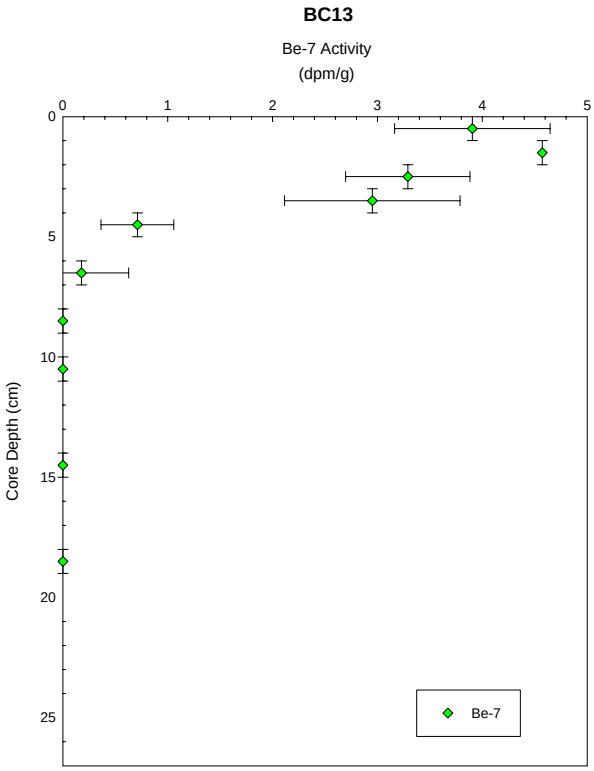
BC13
Be-7 Activity
(dpm/g)
Core Depth (cm)
Be-7

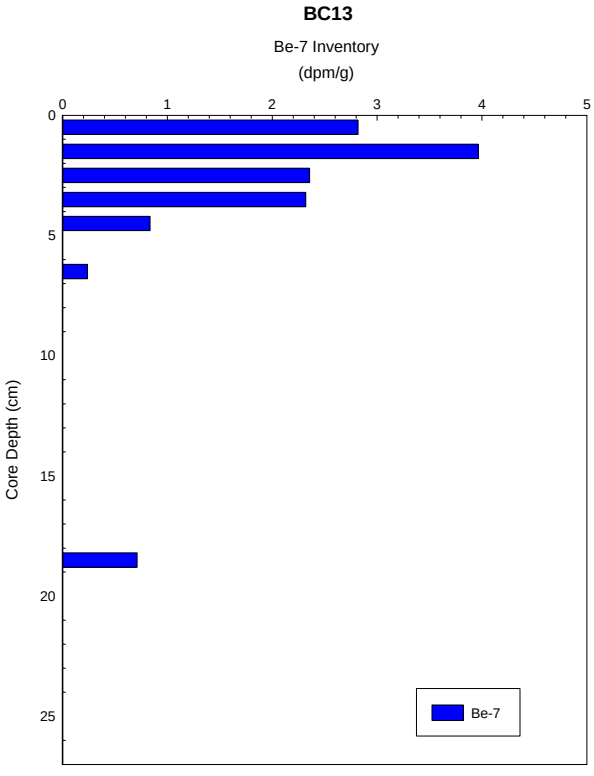
BC13
Be-7 Inventory
(dpm/g)
Core Depth (cm)
Be-7

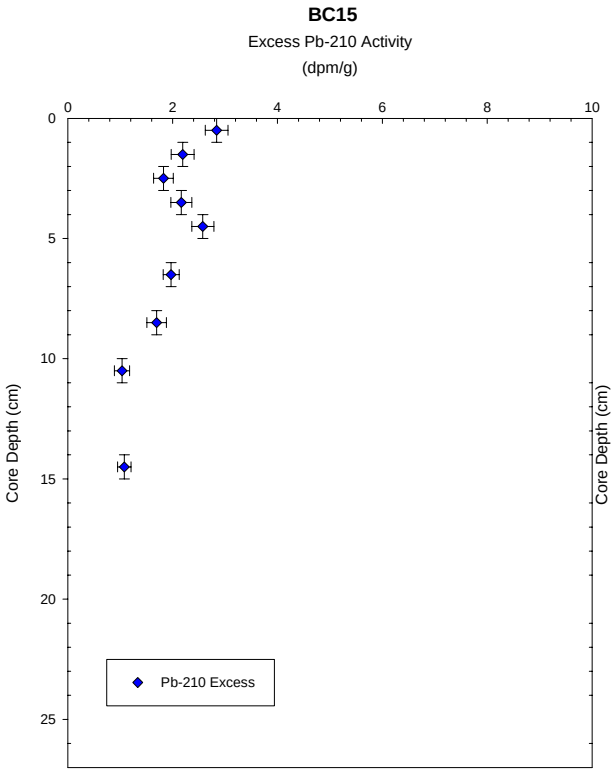
BC15
Excess Pb-210 Activity
(dpm/g)
Core Depth (cm)
Pb-210 Excess

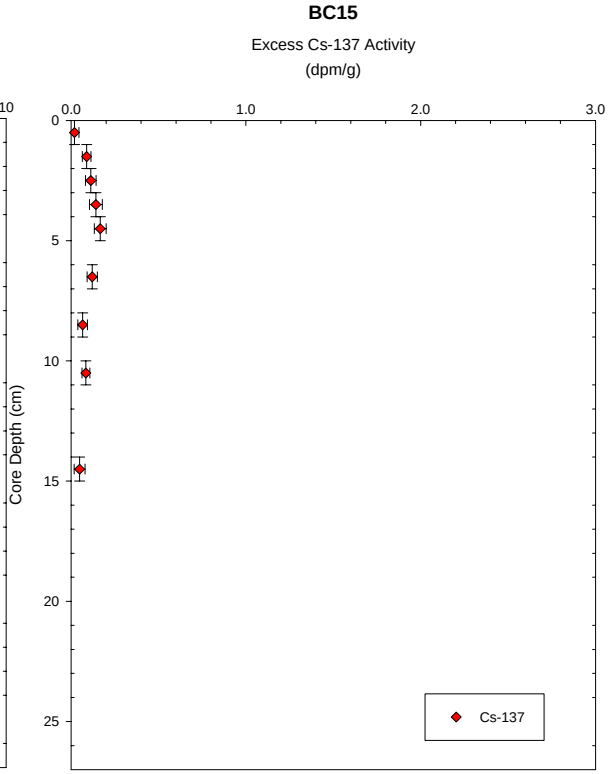
BC15
Excess Cs-137 Activity
(dpm/g)
Core Depth (cm)
Cs-137

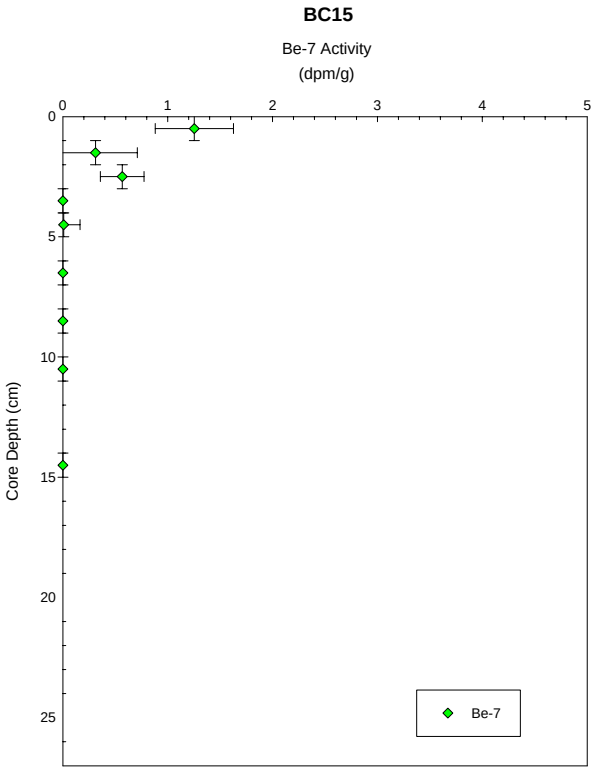
BC15
Be-7 Activity
(dpm/g)
Core Depth (cm)
Be-7

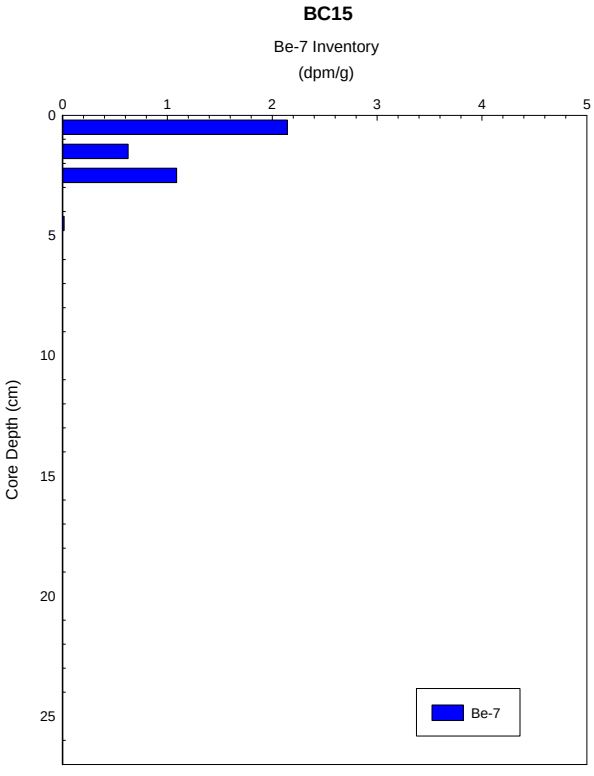
BC15
Be-7 Inventory
(dpm/g)
Core Depth (cm)
Be-7

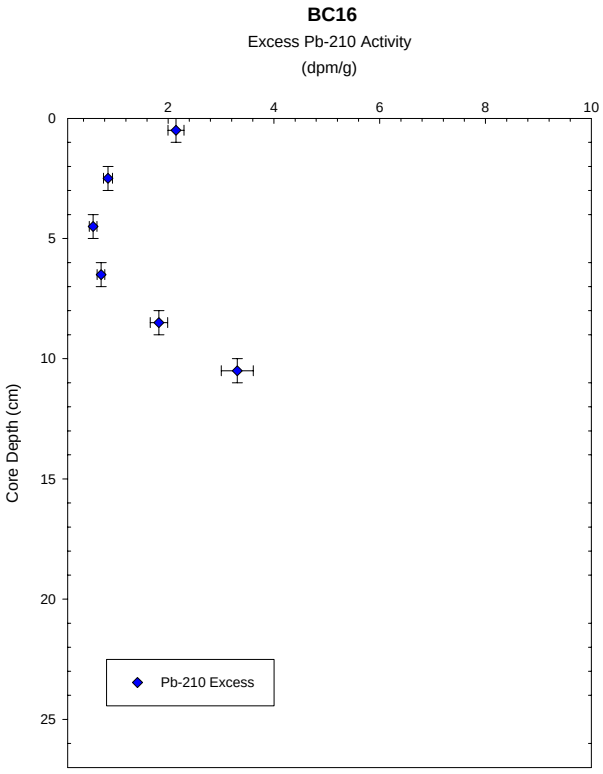
BC16
Excess Pb-210 Activity
(dpm/g)
Core Depth (cm)
Pb-210 Excess

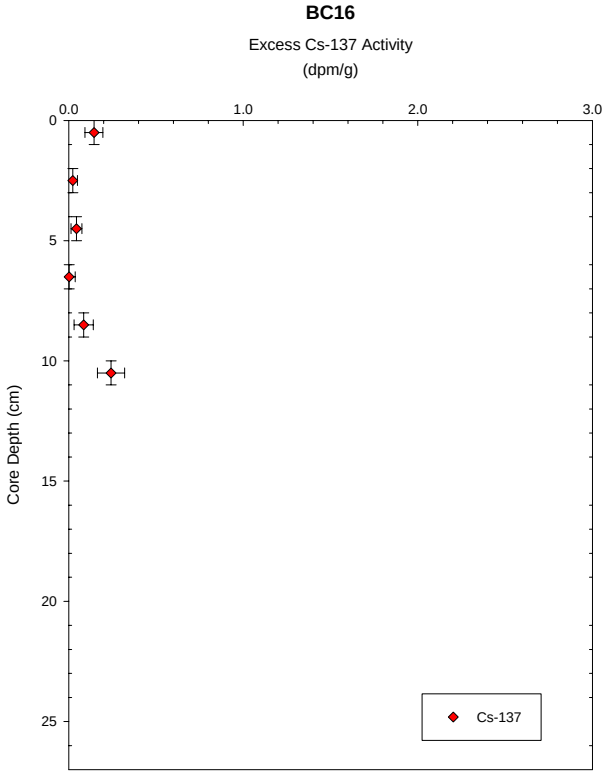
BC16
Excess Cs-137 Activity
(dpm/g)
Core Depth (cm)
Cs-137

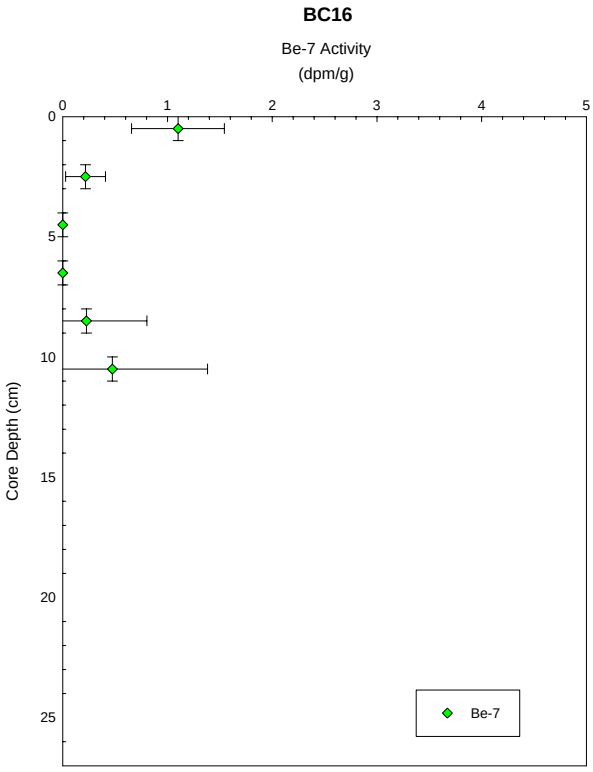
BC16
Be-7 Activity
(dpm/g)
Core Depth (cm)
Be-7

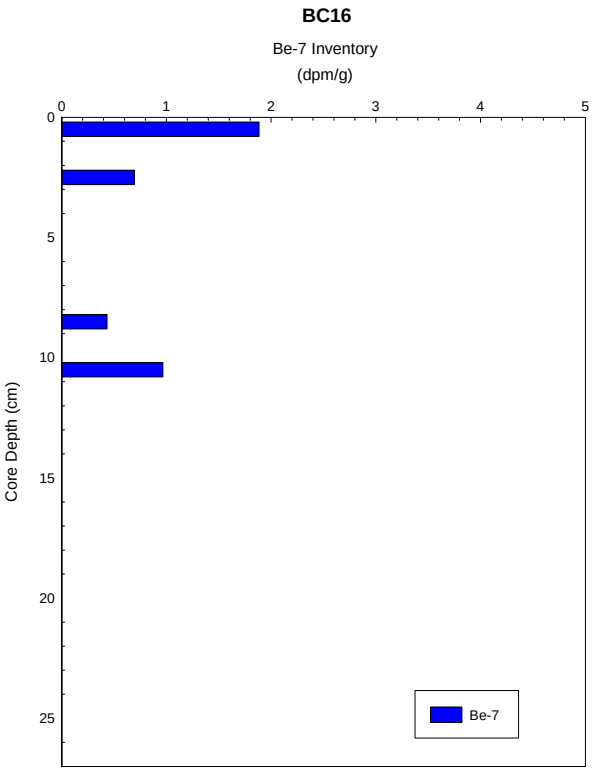
BC16
Be-7 Inventory
(dpm/g)
Core Depth (cm)
Be-7

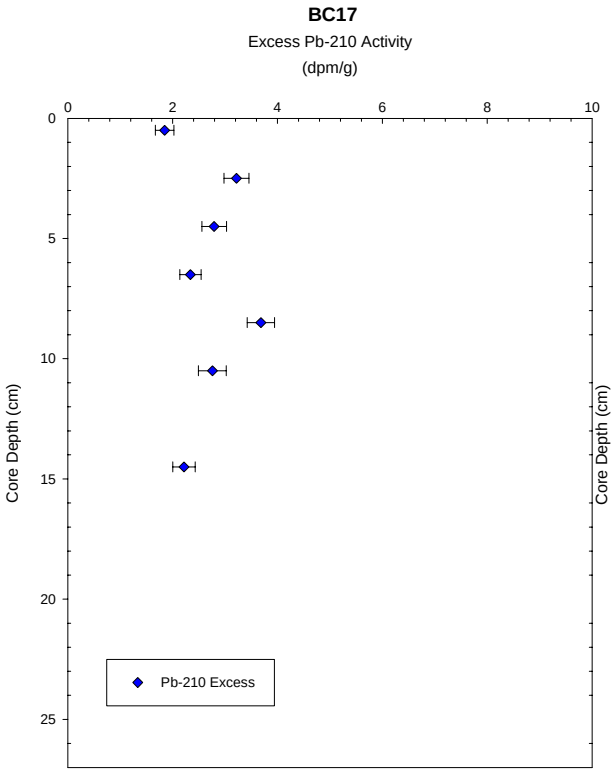
BC17
Excess Pb-210 Activity
(dpm/g)
Core Depth (cm)
Pb-210 Excess

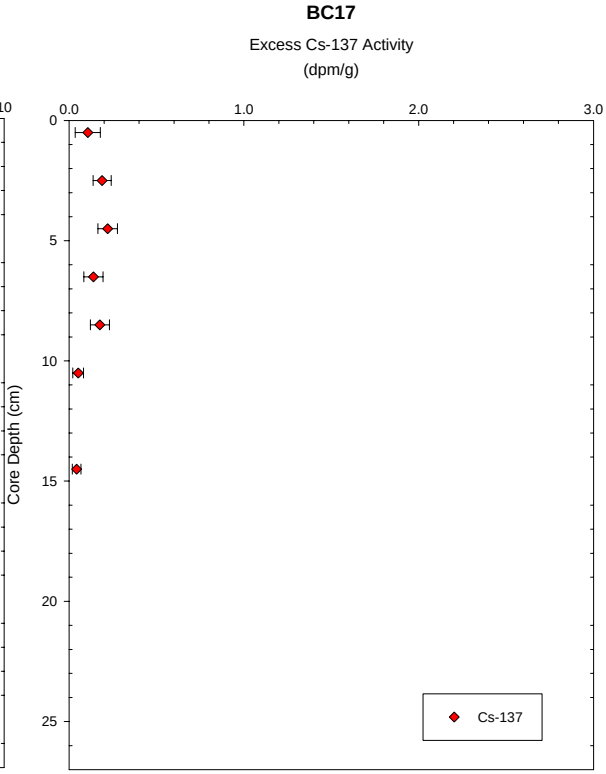
BC17
Excess Cs-137 Activity
(dpm/g)
Core Depth (cm)
Cs-137

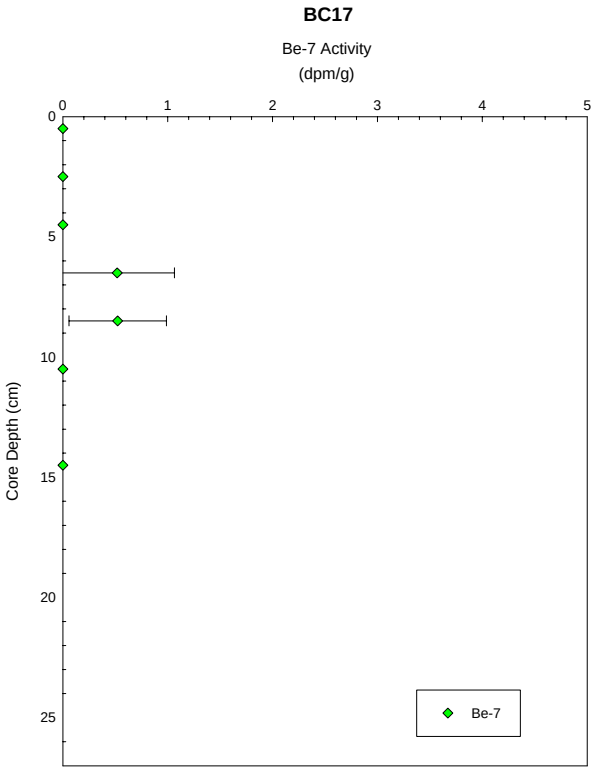
BC17
Be-7 Activity
(dpm/g)
Core Depth (cm)
Be-7

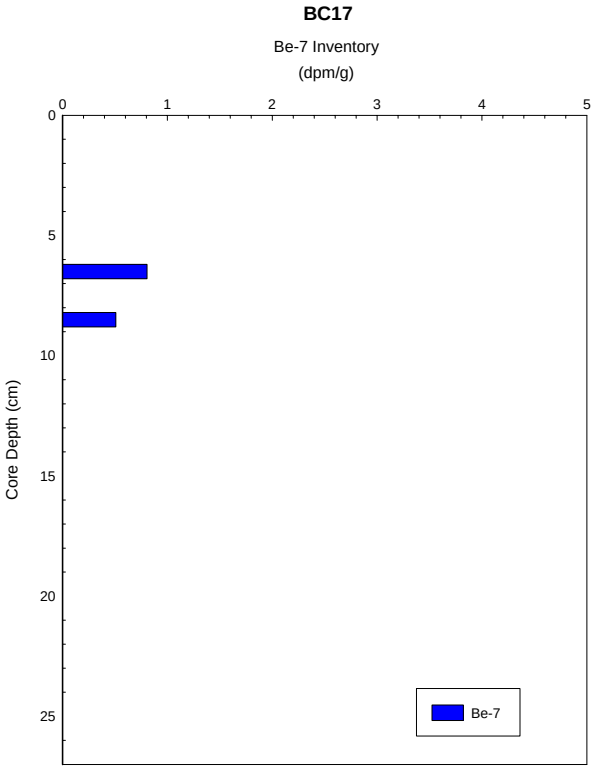
BC17
Be-7 Inventory
(dpm/g)
Core Depth (cm)
Be-7

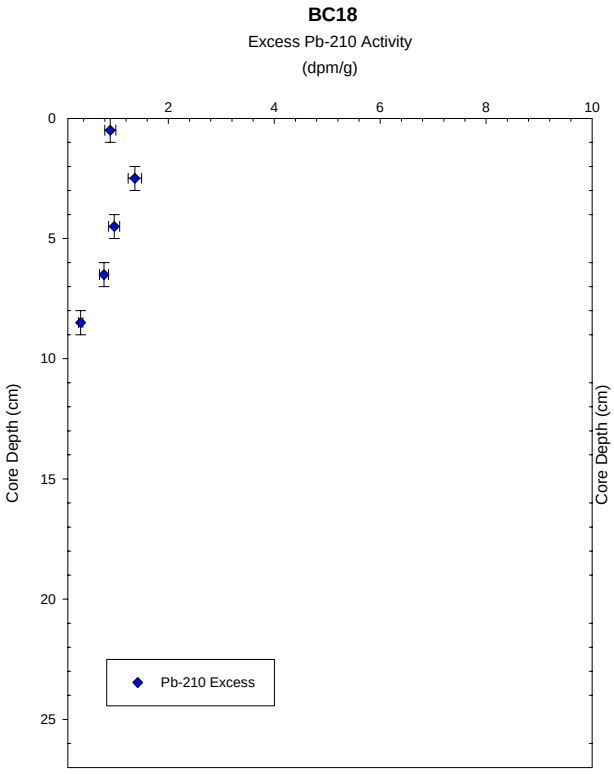
BC18
Excess Pb-210 Activity
(dpm/g)
Core Depth (cm)
Pb-210 Excess

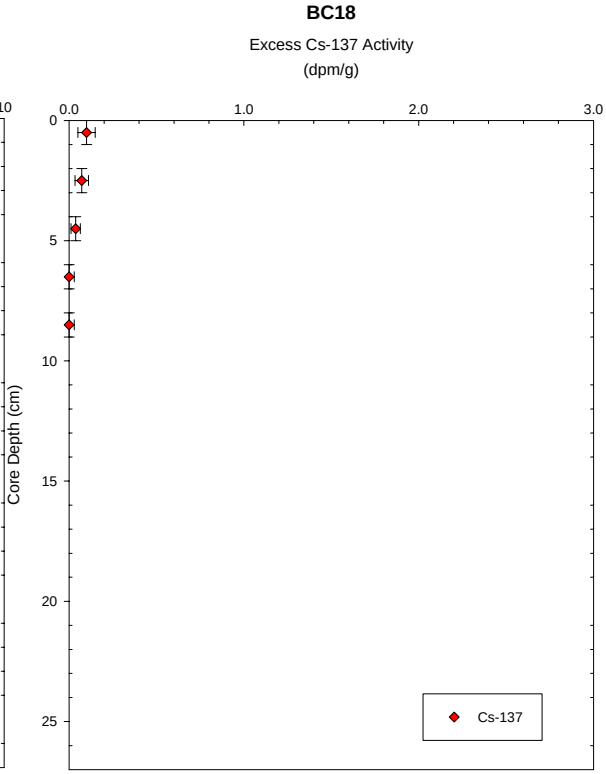
BC18
Excess Cs-137 Activity
(dpm/g)
Core Depth (cm)
Cs-137

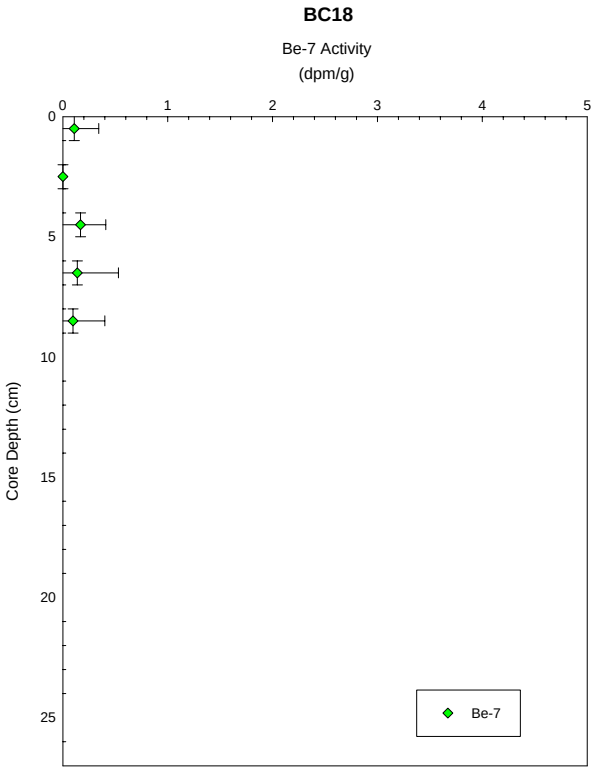
BC18
Be-7 Activity
(dpm/g)
Core Depth (cm)
Be-7

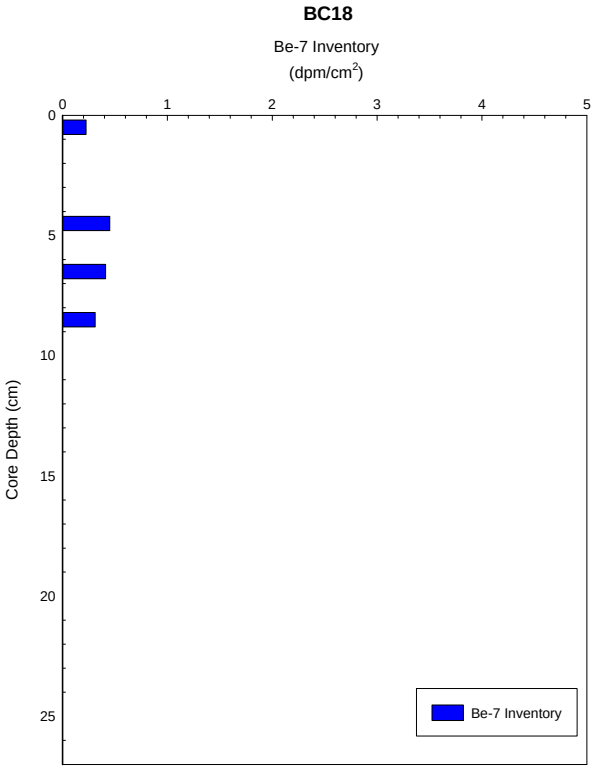
BC18
Be-7 Inventory
(dpm/cm2)
Core Depth (cm)
Be-7 Inventory

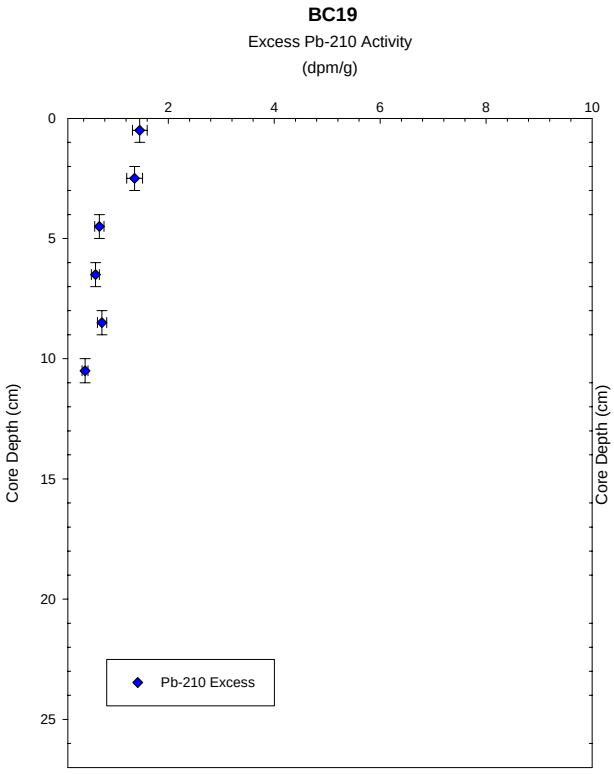
BC19
Excess Pb-210 Activity
(dpm/g)
Core Depth (cm)
Pb-210 Excess

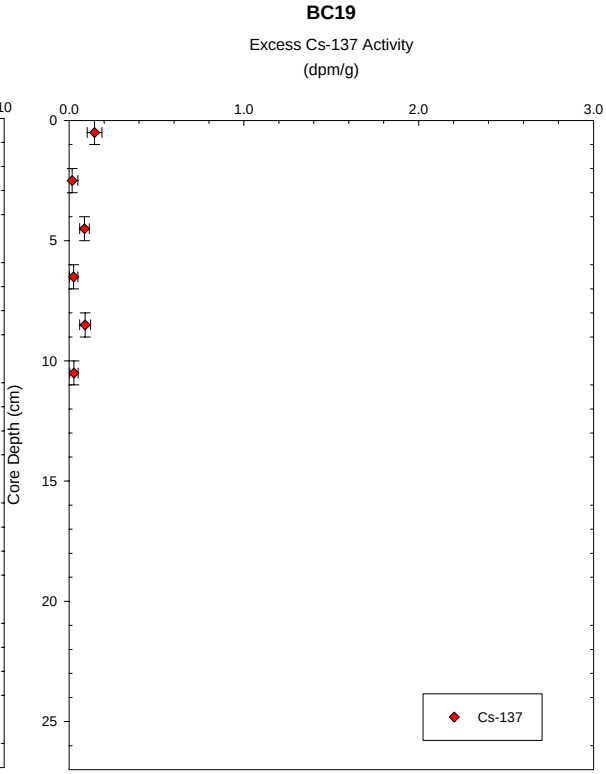
BC19
Excess Cs-137 Activity
(dpm/g)
Core Depth (cm)
Cs-137

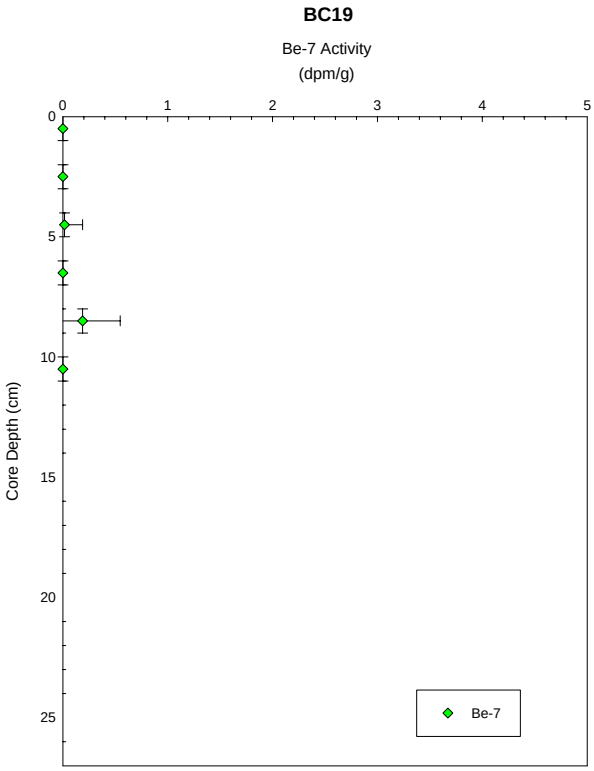
BC19
Be-7 Activity
(dpm/g)
Core Depth (cm)
Be-7

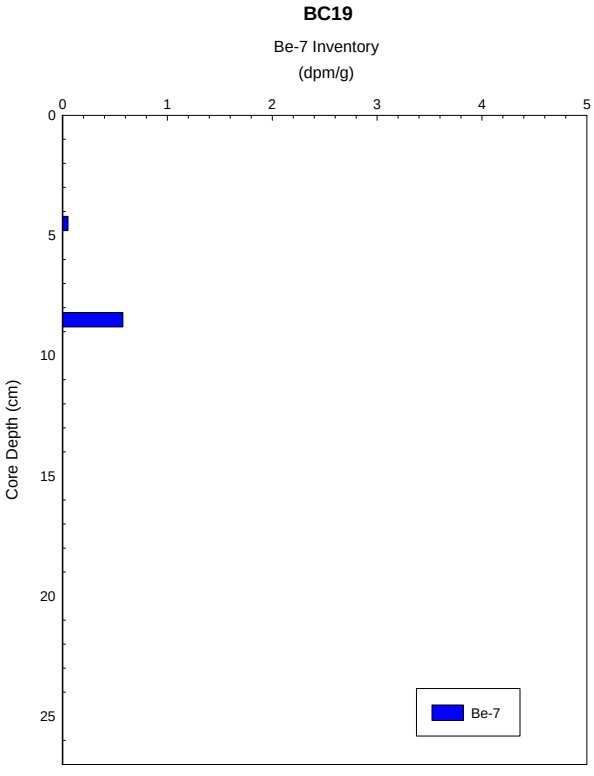
BC19
Be-7 Inventory
(dpm/g)
Core Depth (cm)
Be-7

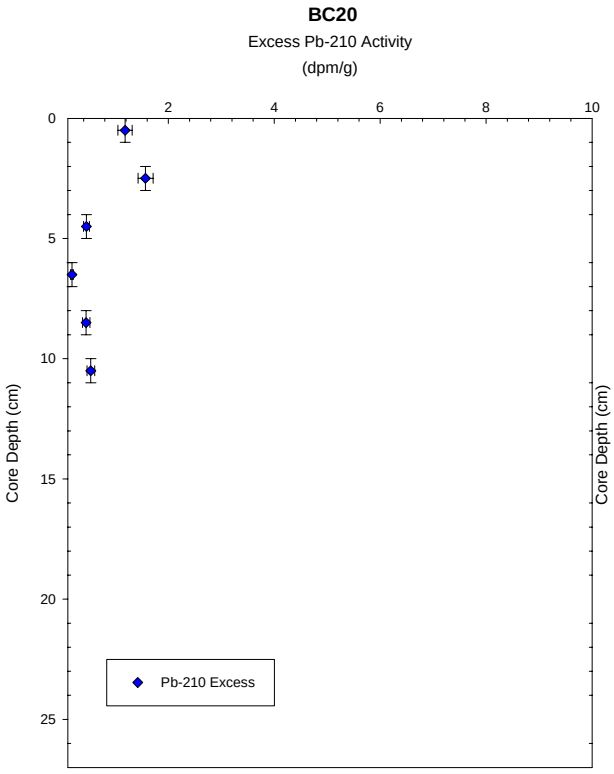
BC20
Excess Pb-210 Activity
(dpm/g)
Core Depth (cm)
Pb-210 Excess

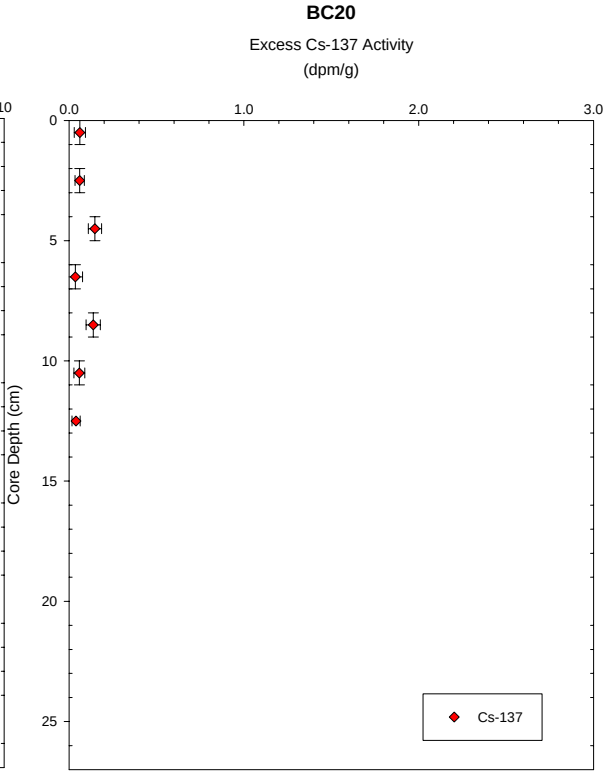
BC20
Excess Cs-137 Activity
(dpm/g)
Core Depth (cm)
Cs-137

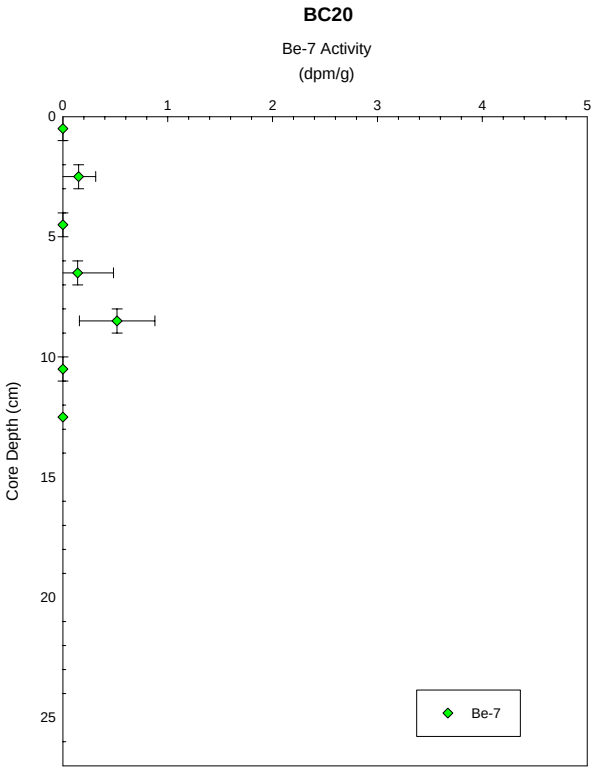
BC20
Be-7 Activity
(dpm/g)
Core Depth (cm)
Be-7

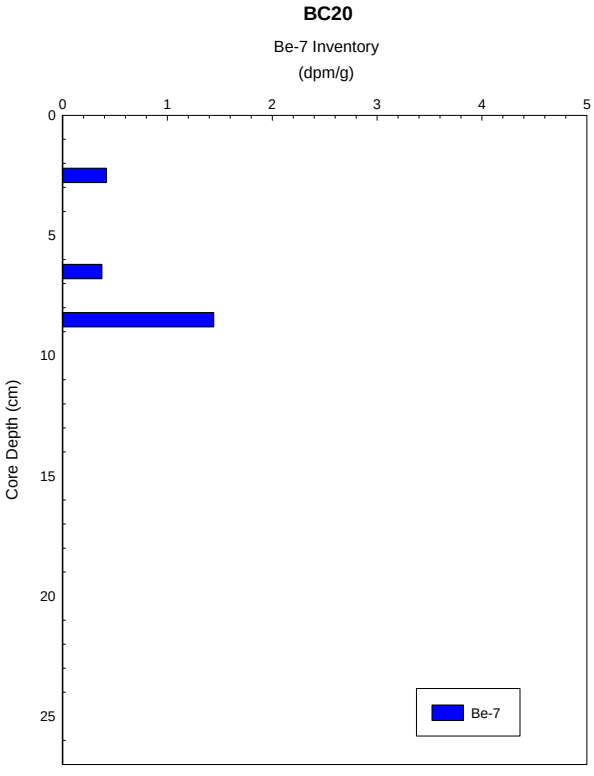
BC20
Be-7 Inventory
(dpm/g)
Core Depth (cm)
Be-7

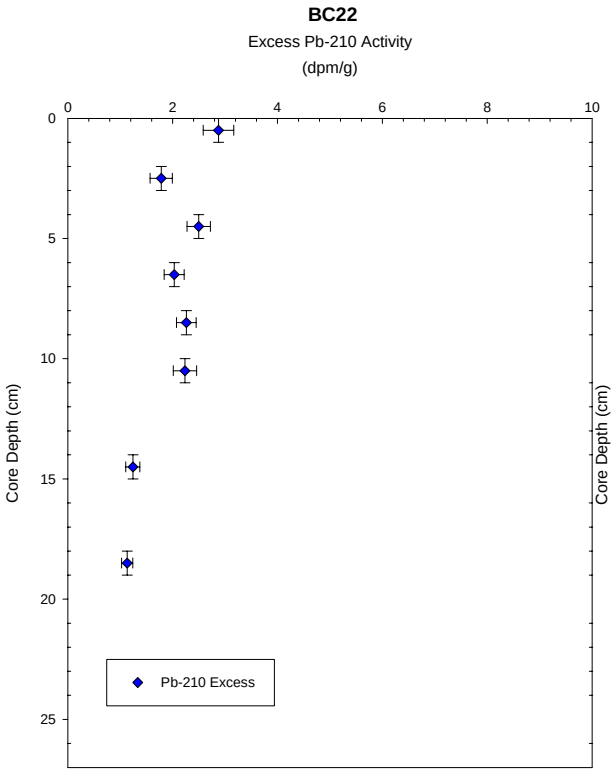
BC22
Excess Pb-210 Activity
(dpm/g)
Core Depth (cm)
Pb-210 Excess

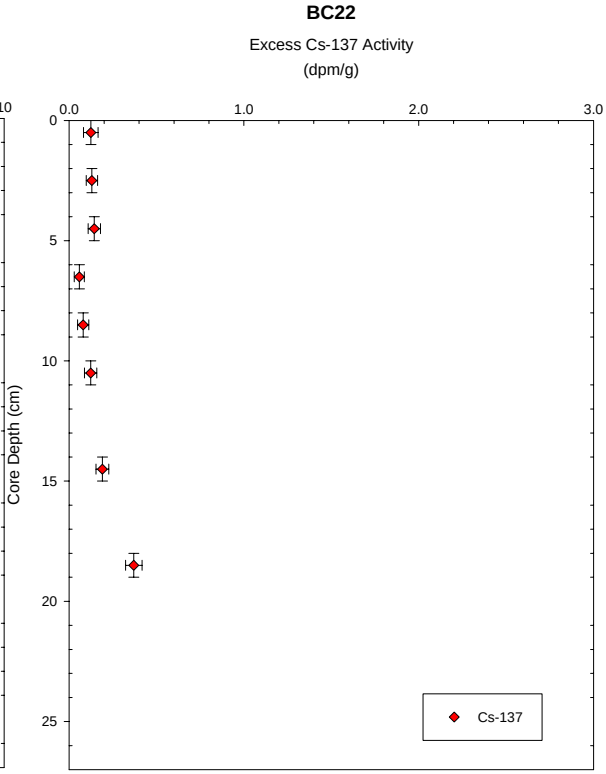
BC22
Excess Cs-137 Activity
(dpm/g)
Core Depth (cm)
Cs-137

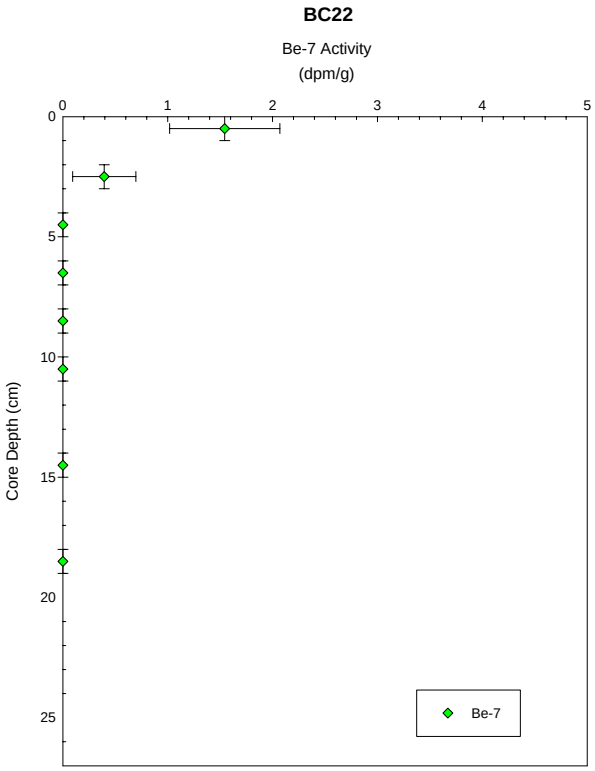
BC22
Be-7 Activity
(dpm/g)
Core Depth (cm)
Be-7

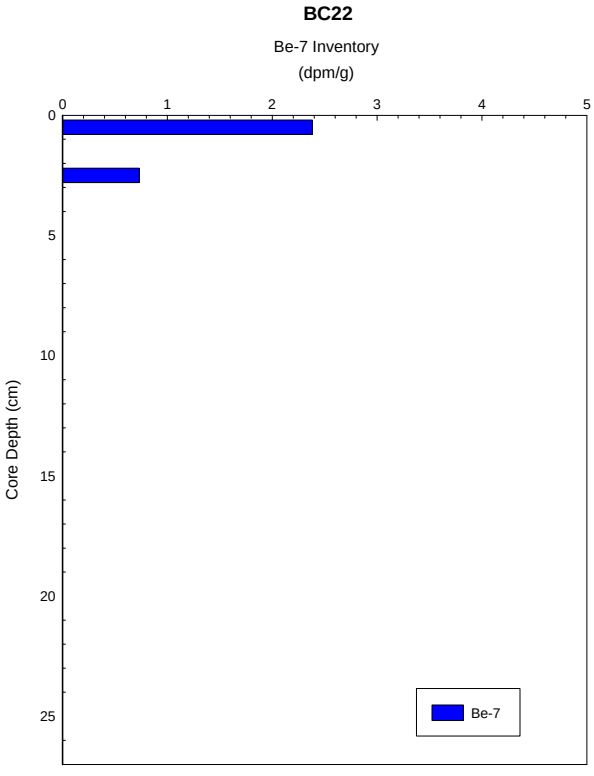
BC22
Be-7 Inventory
(dpm/g)
Core Depth (cm)
Be-7

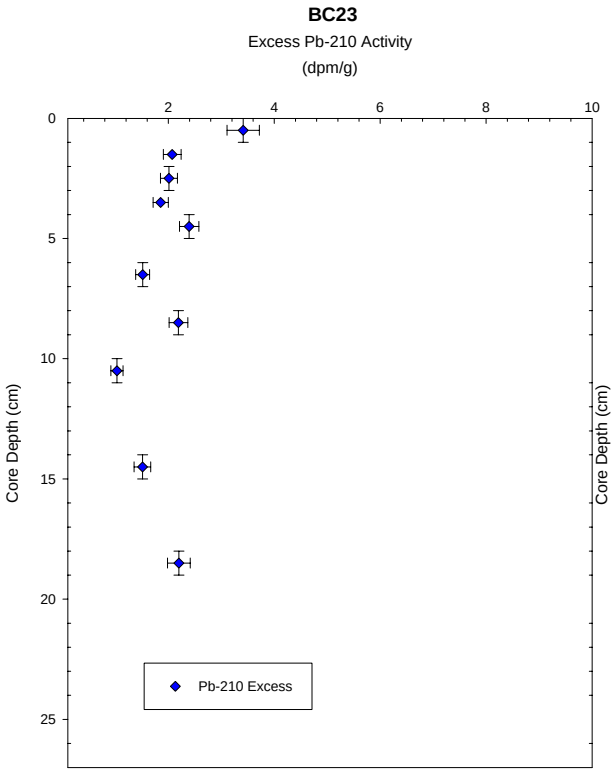
BC23
Excess Pb-210 Activity
(dpm/g)
Core Depth (cm)
Pb-210 Excess

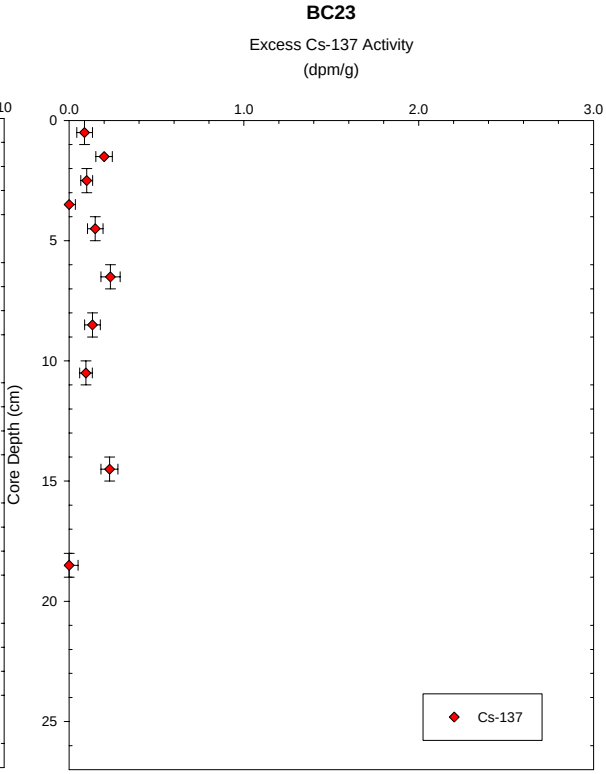
BC23
Excess Cs-137 Activity
(dpm/g)
Core Depth (cm)
Cs-137

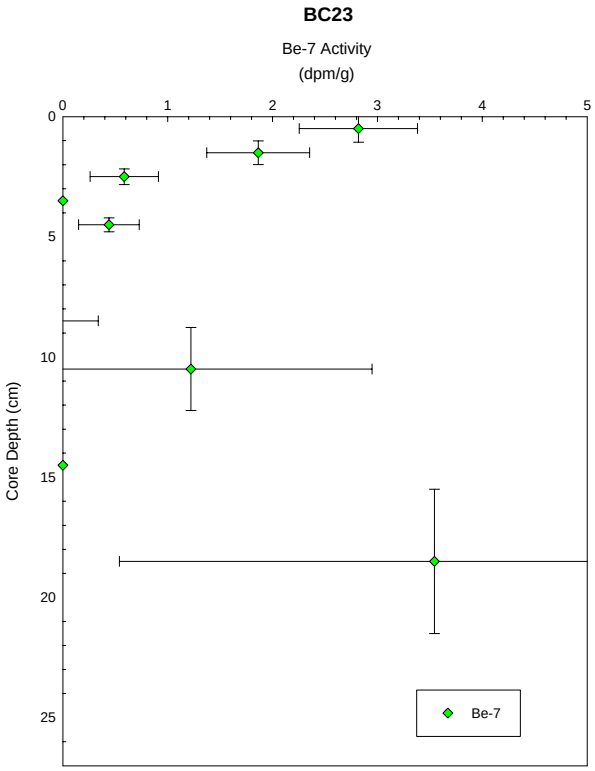
BC23
Be-7 Activity
(dpm/g)
Core Depth (cm)
Be-7

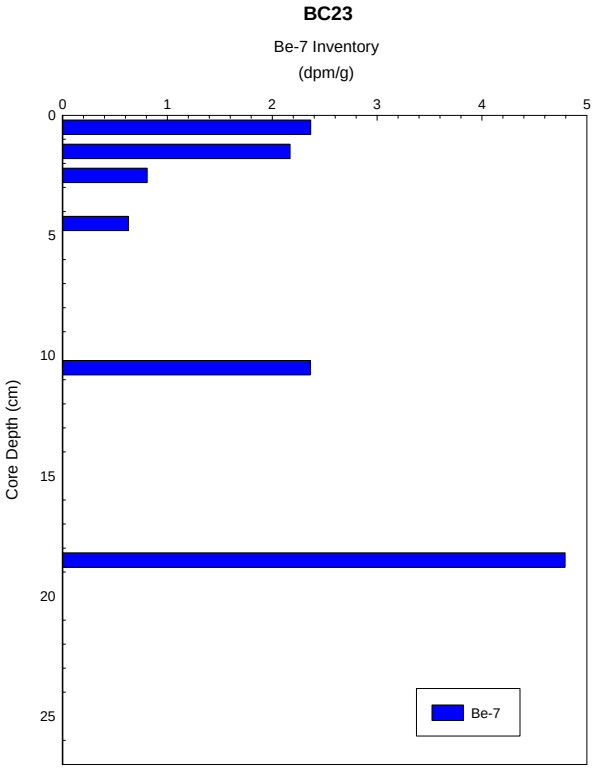
BC23
Be-7 Inventory
(dpm/g)
Core Depth (cm)
Be-7

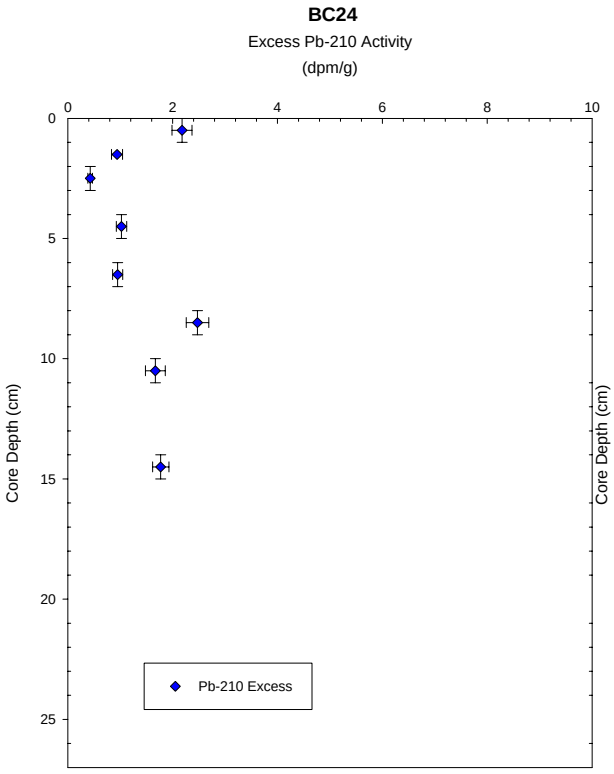
BC24
Excess Pb-210 Activity
(dpm/g)
Core Depth (cm)
Pb-210 Excess

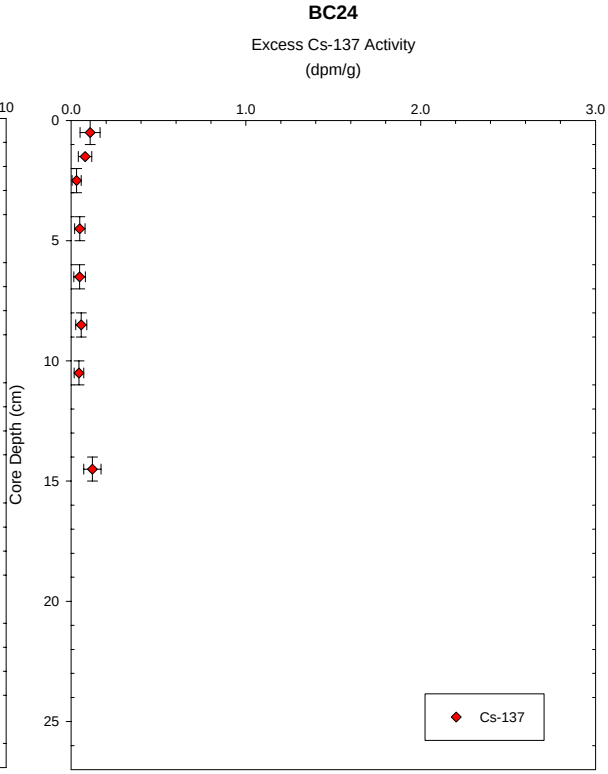
BC24
Excess Cs-137 Activity
(dpm/g)
Core Depth (cm)
Cs-137

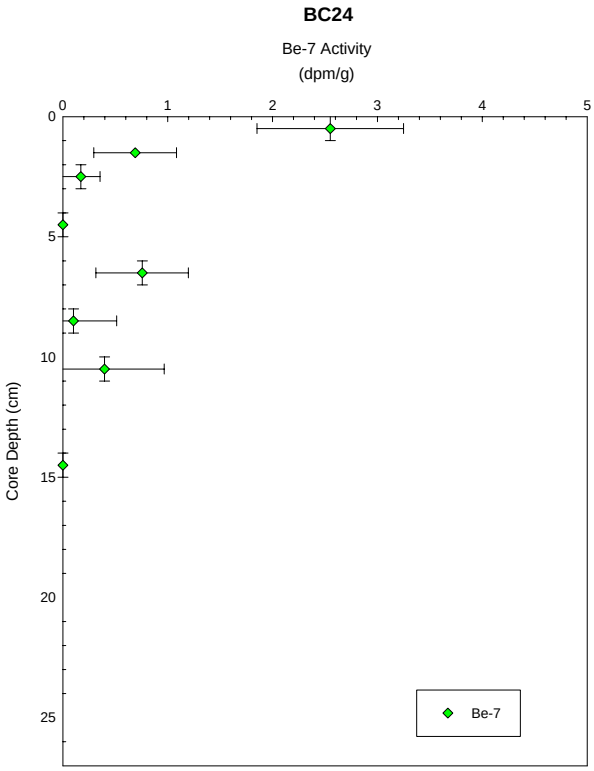
BC24
Be-7 Activity
(dpm/g)
Core Depth (cm)
Be-7

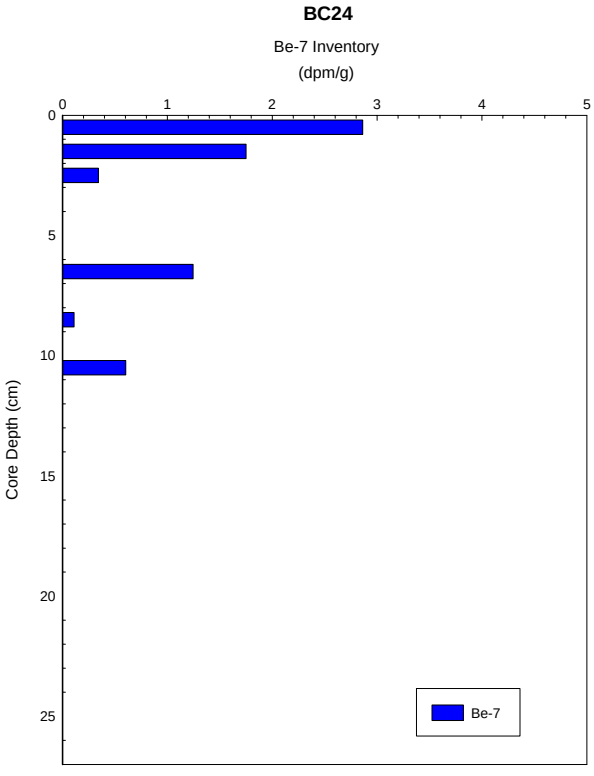
BC24
Be-7 Inventory
(dpm/g)
Core Depth (cm)
Be-7

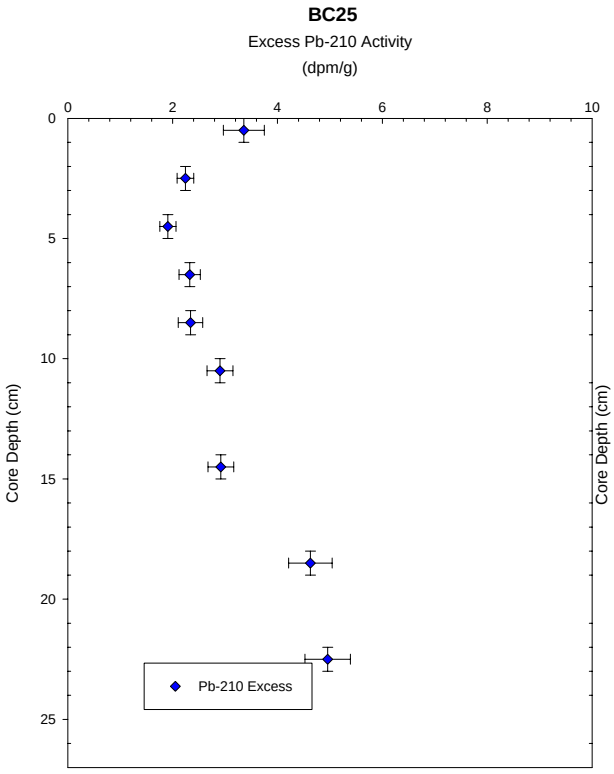
BC25
Excess Pb-210 Activity
(dpm/g)
Core Depth (cm)
Pb-210 Excess

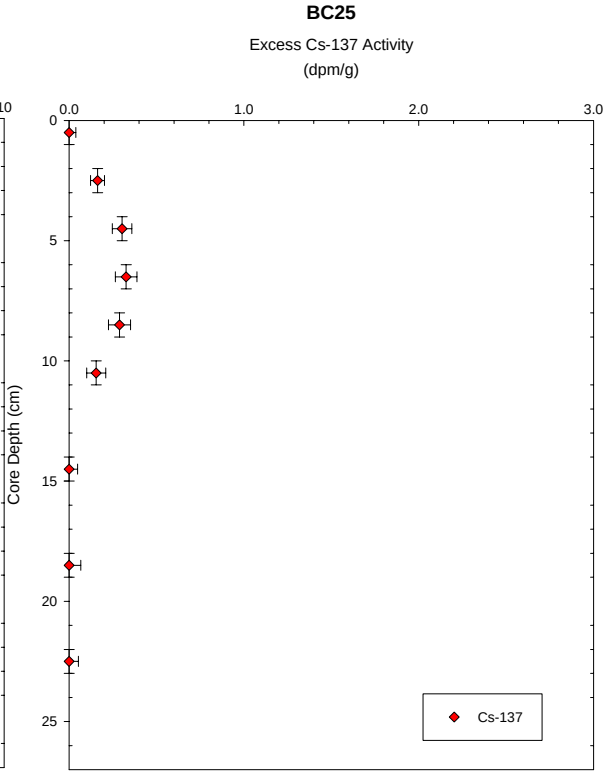
BC25
Excess Cs-137 Activity
(dpm/g)
Core Depth (cm)
Cs-137

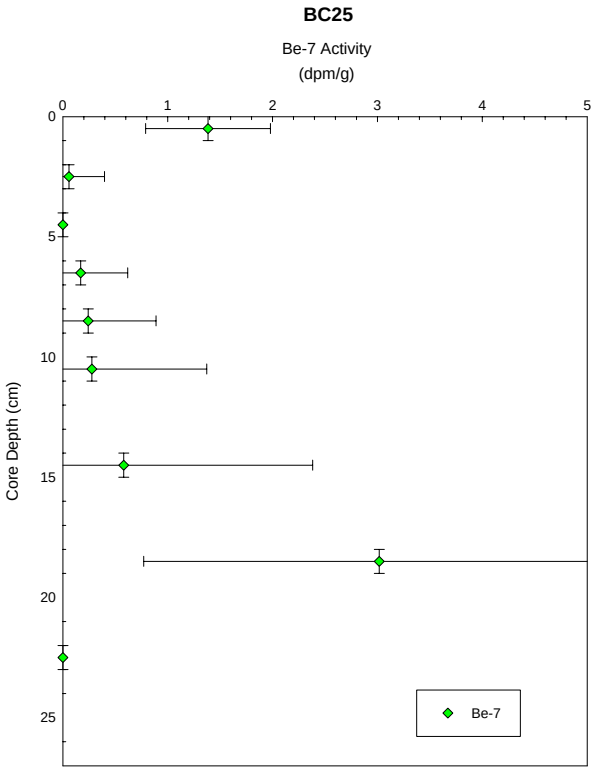
BC25
Be-7 Activity
(dpm/g)
Core Depth (cm)
Be-7

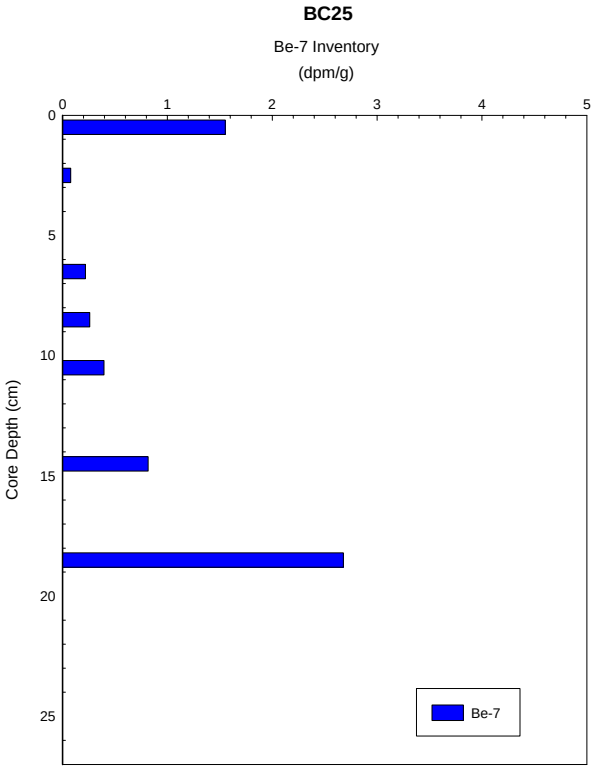
BC25
Be-7 Inventory
(dpm/g)
Core Depth (cm)
Be-7

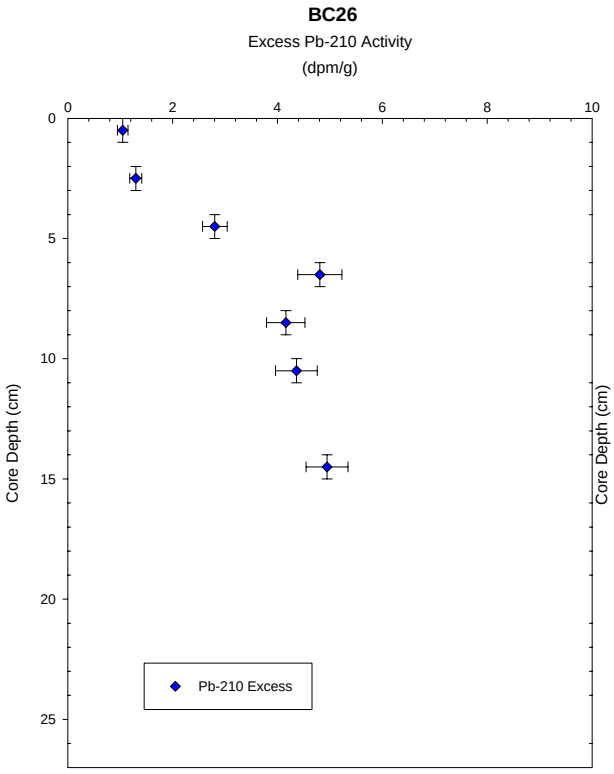
BC26
Excess Pb-210 Activity
(dpm/g)
Core Depth (cm)
Pb-210 Excess

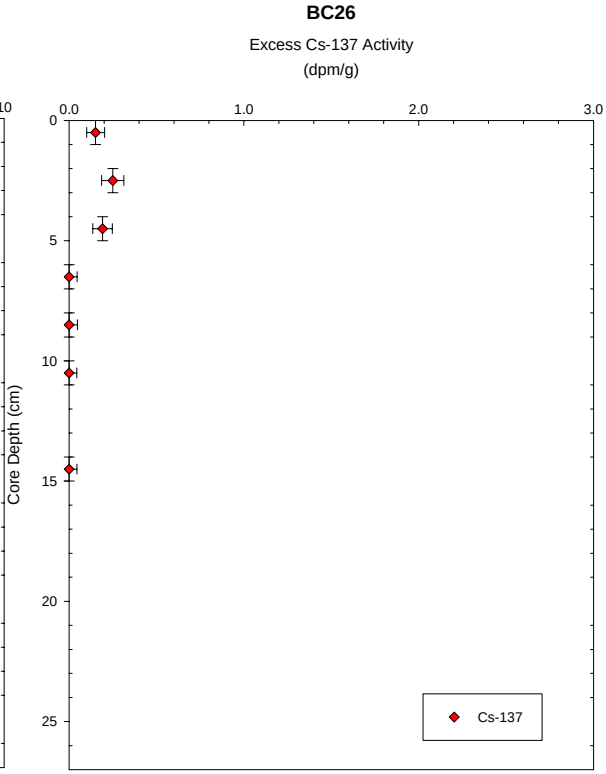
BC26
Excess Cs-137 Activity
(dpm/g)
Core Depth (cm)
Cs-137

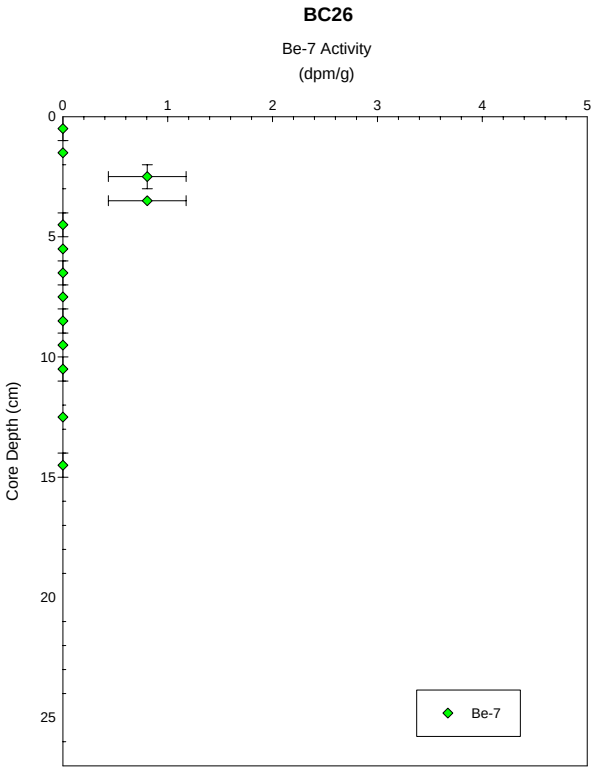
BC26
Be-7 Activity
(dpm/g)
Core Depth (cm)
Be-7

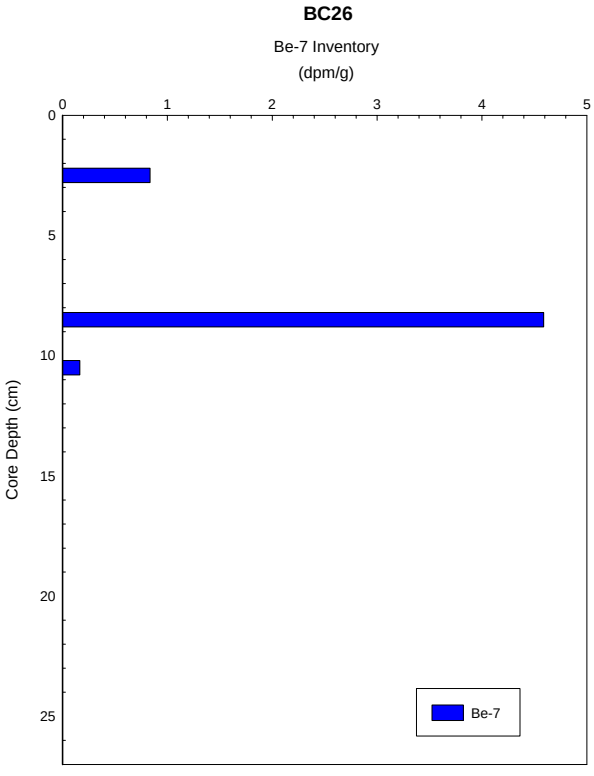
BC26
Be-7 Inventory
(dpm/g)
Core Depth (cm)
Be-7

RADIONUCLIDE DATA

Sample	Detector	Collection Date	Sample Depth (cm)	Sample Interval (cm)	Percent Solids	Percent Water	Porosity	Dry Bulk Density	Pb-210 Excess (dpm/g)	Pb-210 Excess Error (dpm/g)	LN Pb-210 Excess (dpm/g)	LN Pb-210 Excess Error (dpm/g)	Cs-137 Excess (dpm/g)	Cs-137 Error (dpm/g)	Be-7 Activity (dpm/g)	Be-7 Activity Error (dpm/g)	Be-7 Inventory (dpm/cm^2)
BC01	B382514/10/2003		0.5	0-1	76.99	23.01	0.44	1.46	4.6919	0.3324	1.5458	-1.1015	0.3287	0.0635	0.0000	0.0000	0.0000
BC01	B382514/10/2003		2.5	2-3	27.67	72.33	0.87	0.33	2.9449	0.2469	1.0801	-1.3987	0.7513	0.1312	0.0000	0.0000	0.0000
BC01	B382514/10/2003		4.5	4-5	23.06	76.94	0.90	0.27	2.3527	0.2237	0.8556	-1.4976	0.4423	0.1061	0.0000	0.0000	0.0000
BC01	B382514/10/2003		6.5	6-7	21.95	78.05	0.90	0.25	-0.6150	-0.0944	0.0000	0.0000	0.5476	0.0869	0.4699	0.7497	0.3160
BC01	B382514/10/2003		8.5	8-9	23.74	76.26	0.89	0.28	0.9615	0.0881	-0.0393	-2.4295	0.5560	0.0605	-0.1059	0.3406	-0.0780
BC01	B382514/10/2003		10.5	10-11	40.28	59.72	0.79	0.54	1.7587	0.1860	0.5646	-1.6818	0.6537	0.0807	0.0000	0.0000	0.0000
BC01	B382514/10/2003		14.5	14-15	24.86	75.14	0.89	0.29	2.3964	0.1910	0.8740	-1.6553	0.7330	0.0840	0.1907	0.5490	0.1484
BC01	B382514/10/2003		18.5	18-19	22.22	77.78	0.90	0.26	3.7552	0.2859	1.3231	-1.2522	0.4250	0.0749	0.0000	0.0000	0.0000
BC02	B382514/10/2003		0.5	0-1	29.32	70.68	0.86	0.36	4.2645	0.4141	1.4503	-0.8817	0.2699	0.0848	2.2188	0.7262	2.1038
BC02	B382514/10/2003		1.5	1-2	24.46	75.54	0.89	0.29	3.0635	0.2836	1.1196	-1.2602	0.4231	0.0791	0.0000	0.0000	0.0000
BC02	B382514/10/2003		2.5	2-3	28.61	71.39	0.87	0.35	4.1819	0.2874	1.4308	-1.2469	0.2942	0.0621	0.0000	0.0000	0.0000
BC02	B382514/10/2003		4.5	4-5	30.46	69.54	0.86	0.37	4.2149	0.3718	1.4386	-0.9894	0.3829	0.0644	0.0000	0.0000	0.0000
BC02	B382514/10/2003		6.5	6-7	35.67	64.33	0.82	0.46	4.6172	0.3635	1.5298	-1.0120	0.4872	0.0756	0.2502	0.6377	0.3030
BC02	B382514/10/2003		8.5	8-9	34.94	65.06	0.83	0.45	3.5172	0.2728	1.2577	-1.2989	0.5635	0.0793	0.0000	0.0000	0.0000
BC02	B382514/10/2003		10.5	10-11	23.66	76.34	0.89	0.28	3.2388	0.2688	1.1752	-1.3136	0.4081	0.0651	0.0000	0.0000	0.0000
BC02	B382514/10/2003		14.5	14-15	35.04	64.96	0.83	0.45	1.4923	0.1434	0.4003	-1.9425	0.4659	0.0563	0.0264	0.4817	0.0312
BC02	B382514/10/2003		18.5	18-19	43.31	56.69	0.77	0.59	0.9459	0.0897	-0.0557	-2.4111	0.7241	0.0704	0.2257	0.4241	0.3532
BC03	B382514/10/2003		0.5	0-1	28.14	71.86	0.87	0.34	3.8802	0.4109	1.3559	-0.8894	0.4520	0.0985	0.0000	0.0000	0.0000
BC03	B382514/10/2003		2.5	2-3	35.40	64.60	0.83	0.45	3.3497	0.3556	1.2089	-1.0340	0.2834	0.0670	0.0000	0.0000	0.0000
BC03	B382514/10/2003		5	4-6	63.35	36.65	0.60	1.04	1.8200	0.2321	0.5988	-1.4605	0.1671	0.0598	0.0769	0.2521	0.2117
BC04	B382514/10/2003		0.5	0-1	30.77	69.23	0.85	0.38	2.9479	0.2084	1.0811	-1.5682	0.1594	0.0428	3.7869	0.6508	3.8090
BC04	B382514/10/2003		1.5	1-2	39.45	60.55	0.80	0.52	2.4711	0.2131	0.9047	-1.5459	0.1808	0.0406	1.9544	0.6270	2.6981
BC04	B382514/10/2003		2.5	2-3	42.11	57.89	0.78	0.57	2.5750	0.1870	0.9459	-1.6765	0.2646	0.0406	0.9649	0.4485	1.4531
BC04	B382514/10/2003		3.5	3-4	37.54	62.46	0.81	0.49	1.8049	0.1587	0.5905	-1.8408	0.2013	0.0504	0.3719	0.4992	0.4811
BC04	B382514/10/2003		4.5	4-5	38.59	61.41	0.81	0.51	1.6297	0.1459	0.4884	-1.9248	0.1515	0.0316	0.6108	0.2247	0.8193
BC04	B382514/10/2003		6.5	6-7	38.98	61.02	0.80	0.51	2.2092	0.1868	0.7926	-1.6778	0.0000	0.0388	0.0000	0.0000	0.0000
BC04	B382514/10/2003		8.5	8-9	40.04	59.96	0.80	0.53	1.0672	0.1242	0.0651	-2.0862	0.0581	0.0323	0.0434	0.2666	0.0611
BC04	B382514/10/2003		10.5	10-11	34.39	65.61	0.83	0.44	1.7846	0.1782	0.5792	-1.7251	0.1996	0.0523	0.0000	0.0000	0.0000
BC04	B382514/10/2003		14.5	14-15	35.48	64.52	0.83	0.45	2.5237	0.2005	0.9257	-1.6069	0.3199	0.0453	0.0000	0.0000	0.0000
BC04	B382514/10/2003		18.5	18-19	21.17	78.83	0.91	0.24	5.1289	0.3347	1.6349	-1.0946	0.6230	0.0891	0.0200	0.5363	0.0129
BC04	B382514/10/2003		22.5	22-23	25.00	75.00	0.89	0.30	3.1394	0.2624	1.1440	-1.3379	0.4888	0.0736	0.4860	0.5055	0.3805
BC05	B382514/10/2003		0.5	0-1	33.94	66.06	4.79	-9.85	2.4081	0.1932	0.8788	-1.6441	0.2001	0.0533	1.1995	0.6009	1.3639
BC05	B382514/10/2003		1.5	1-2	42.29	57.71	-2.27	8.51	3.3870	0.2370	1.2200	-1.4395	0.1499	0.0421	1.5373	0.5243	2.3291
BC05	B382514/10/2003		2.5	2-3	40.36	59.64	-5.27	16.30	2.1086	0.1432	0.7460	-1.9433	0.1341	0.0311	0.0000	0.0000	0.0000

BC05	B382514/10/2003	4.5	4-5	34.80	65.20	5.71	-12.26	2.2182	0.1637	0.7967	-1.8095	0.2751	0.0390	0.0000	0.0000	0.0000
BC05	B382514/10/2003	6.5	6-7	32.11	67.89	3.70	-7.02	2.9006	0.2131	1.0649	-1.5459	0.4067	0.0570	0.0000	0.0000	0.0000
BC05	B382514/10/2003	8.5	8-9	33.33	66.67	4.33	-8.67	1.5660	0.2015	0.4485	-1.6020	0.4152	0.0658	0.0000	0.0000	0.0000
BC05	B382514/10/2003	10.5	10-11	33.66	66.34	4.56	-9.26	1.3455	0.1343	0.2968	-2.0079	0.4531	0.0578	0.2803	0.3809	0.3154
BC05	B382514/10/2003	12.5	12-13	32.56	67.44	3.90	-7.54	2.6628	0.2228	0.9794	-1.5015	0.2568	0.0433	0.1867	0.4375	0.2015
BC06	202014/10/2003	0.5	0-1	40.72	59.28	0.79	0.54	1.3566	0.1216	0.3050	-2.1068	0.1281	0.0377	1.4145	0.5096	2.0366
BC06	202014/10/2003	1.5	1-2	33.33	66.67	0.84	0.42	1.7803	0.1408	0.5768	-1.9607	0.0954	0.0321	0.9882	0.3241	1.0982
BC06	202014/10/2003	2.5	2-3	42.61	57.39	0.78	0.58	1.6211	0.1573	0.4831	-1.8498	0.0883	0.0330	0.1171	0.2581	0.1792
BC06	202014/10/2003	4.5	4-5	52.03	47.97	0.71	0.77	1.7947	0.1691	0.5848	-1.7772	0.0989	0.0349	0.0000	0.0000	0.0000
BC06	202014/10/2003	6.5	6-7	51.28	48.72	0.71	0.75	1.6117	0.1342	0.4773	-2.0085	0.1314	0.0476	0.3993	0.4217	0.7928
BC06	202014/10/2003	8.5	8-9	42.39	57.61	0.78	0.57	1.7872	0.1760	0.5806	-1.7371	0.0966	0.0431	0.0425	0.4356	0.0645
BC06	202014/10/2003	10.5	10-11	39.46	60.54	0.80	0.52	1.7481	0.2087	0.5586	-1.5666	0.1148	0.0468	0.0000	0.0000	0.0000
BC06	202014/10/2003	14.5	14-15	46.04	53.96	0.75	0.64	2.7990	0.2312	1.0292	-1.4646	0.1440	0.0462	0.2015	0.4788	0.3430
BC07	202014/10/2003	0.5	0-1	25.17	74.83	0.89	0.30	1.6589	0.1527	0.5062	-1.8794	0.0280	0.0318	0.3737	0.3332	0.2949
BC07	202014/10/2003	1.5	1-2	51.04	48.96	0.71	0.74	1.6483	0.1561	0.4998	-1.8570	0.0000	0.0269	0.4036	0.3097	0.7958
BC07	202014/10/2003	2.5	2-3	39.44	60.56	0.80	0.52	2.0764	0.2285	0.7306	-1.4761	0.1421	0.0547	0.0000	0.0000	0.0000
BC07	202014/10/2003	4.5	4-5	35.66	64.34	0.82	0.46	2.8710	0.2754	1.0547	-1.2895	0.1388	0.0668	0.0000	0.0000	0.0000
BC07	202014/10/2003	6.5	6-7	34.85	65.15	0.83	0.44	3.5704	0.2316	1.2727	-1.4627	0.3127	0.0799	0.3773	0.5020	0.4436
BC07	202014/10/2003	8.5	8-9	49.22	50.78	0.73	0.71	1.3932	0.1173	0.3316	-2.1433	0.2788	0.0567	-0.4376	0.4483	-0.8190
BC07	202014/10/2003	10.5	10-11	56.19	43.81	0.67	0.86	0.4201	0.0542	-0.8672	-2.9156	0.3014	0.0542	0.0000	0.0000	0.0000
BC07	202014/10/2003	14.5	14-15	45.00	55.00	0.76	0.62	2.1325	0.1747	0.7573	-1.7446	0.6394	0.0829	0.0699	0.3597	0.1152
BC08	382514/10/2003	0.5	0-1	28.64	71.36	0.87	0.35	5.5401	0.3436	1.7120	-1.0683	0.2659	0.0460	1.8467	0.3414	1.7012
BC08	382514/10/2003	2.5	2-3	34.95	65.05	0.83	0.45	3.5896	0.3348	1.2780	-1.0941	0.2489	0.0479	0.3547	0.2975	0.4185
BC08	382514/10/2003	4.5	4-5	32.33	67.67	0.84	0.40	4.0829	0.3157	1.4068	-1.1530	0.2834	0.0482	0.0000	0.0000	0.0000
BC08	382514/10/2003	6.5	6-7	31.21	68.79	0.85	0.39	3.8833	0.2977	1.3567	-1.2118	0.5146	0.0640	0.0000	0.0000	0.0000
BC08	382514/10/2003	8.5	8-9	32.35	67.65	0.84	0.40	4.1762	0.2999	1.4294	-1.2044	0.5873	0.0745	0.5610	0.7124	0.6006
BC08	382514/10/2003	10.5	10-11	28.74	71.26	0.87	0.35	3.7083	0.2301	1.3106	-1.4692	0.6186	0.0568	0.0000	0.0000	0.0000
BC08	382514/10/2003	14.5	14-15	25.65	74.35	0.88	0.30	2.8912	0.2195	1.0617	-1.5165	0.8787	0.0727	0.0000	0.0000	0.0000
BC09	382514/10/2003	0.5	0-1	15.70	84.30	0.93	0.17	6.5214	0.5279	1.8751	-0.6388	0.2659	0.0648	6.1398	0.7578	2.8269
BC09	382514/10/2003	1.5	1-2	23.52	76.48	0.89	0.27	5.2011	0.3473	1.6489	-1.0576	0.2093	0.0521	1.1223	0.6241	0.8177
BC09	382514/10/2003	2.5	2-3	21.93	78.07	0.90	0.25	4.1982	0.3124	1.4346	-1.1634	0.1858	0.0587	1.5522	0.3994	1.0428
BC09	382514/10/2003	3.5	3-4	27.24	72.76	0.87	0.33	4.6576	0.3307	1.5385	-1.1065	0.3112	0.0510	1.0146	0.5841	0.8801
BC09	382514/10/2003	4.5	4-5	31.78	68.22	0.85	0.40	3.1891	0.2594	1.1597	-1.3493	0.0287	0.0210	0.4363	0.2032	0.4568
BC09	382514/10/2003	6.5	6-7	23.68	76.32	0.89	0.28	6.1150	0.4727	1.8107	-0.7494	0.1062	0.0567	2.0412	0.8203	1.4997
BC09	382514/10/2003	8.5	8-9	19.95	80.05	0.91	0.23	3.8244	0.3146	1.3414	-1.1566	0.1376	0.0560	1.0463	0.5057	0.6305
BC09	382514/10/2003	10.5	10-11	29.98	70.02	0.86	0.37	4.2710	0.3218	1.4518	-1.1338	0.0890	0.0373	0.3447	0.4312	0.3358
BC09	382514/10/2003	14.5	14-15	36.87	63.13	0.82	0.48	2.9187	0.2632	1.0711	-1.3349	0.0000	0.0437	0.0000	0.0000	0.0000
BC09	382514/10/2003	18.5	18-19	44.51	55.49	0.76	0.61	2.2967	0.1975	0.8315	-1.6218	0.0581	0.0317	0.0000	0.0000	0.0000
BC09	382514/10/2003	22.5	22-23	40.86	59.14	0.79	0.55	3.7980	0.2826	1.3345	-1.2638	0.1312	0.0361	0.0000	0.0000	0.0000
BC09	382514/10/2003	26.5	26-27	50.46	49.54	0.72	0.73	0.7794	0.1018	-0.2492	-2.2847	0.0000	0.0262	0.0000	0.0000	0.0000
BC10	382514/10/2003	0.5	0-1	51.88	48.12	0.71	0.76	1.6097	0.1543	0.4761	-1.8689	0.0268	0.0215	0.1001	0.2553	0.2020

BC10	382514/10/2003	2.5	2-3	47.15	52.85	0.74	0.66	3.0279	0.2518	1.1079	-1.3793	0.0706	0.0351	0.0000	0.0000	0.0000
BC10	382514/10/2003	4.5	4-5	42.42	57.58	0.78	0.57	2.4255	0.2158	0.8860	-1.5334	0.1836	0.0355	0.1508	0.1670	0.2293
BC10	382514/10/2003	6.5	6-7	48.61	51.39	0.73	0.69	0.7873	0.1014	-0.2392	-2.2885	0.6405	0.0579	0.0000	0.0000	0.0000
BC10	382514/10/2003	8.5	8-9	54.51	45.49	0.68	0.82	1.0886	0.1032	0.0849	-2.2714	0.4631	0.0472	0.0000	0.0000	0.0000
BC12	3825 37908	0.5	0-1	23.15	76.85	0.90	0.27	4.7526	0.4052	1.5587	-0.9033	0.3144	0.0641	1.5071	0.4547	1.0783
BC12	3825 37908	1.5	1-2	34.06	65.94	0.83	0.43	4.8398	0.4232	1.5769	-0.8599	0.2333	0.0576	0.5218	0.7231	0.5957
BC12	3825 37908	2.5	2-3	37.97	62.03	0.81	0.50	3.4373	0.2905	1.2347	-1.2360	0.1846	0.0548	0.5039	0.2560	0.6616
BC12	3825 37908	4.5	4-5	38.51	61.49	0.81	0.50	2.7471	0.2355	1.0106	-1.4461	0.2345	0.0451	0.0000	0.0000	0.0000
BC12	3825 37908	6.5	6-7	37.52	62.48	0.81	0.49	3.4523	0.2786	1.2390	-1.2781	0.2321	0.0427	0.0174	0.4599	0.0225
BC12	3825 37908	8.5	8-9	32.81	67.19	0.84	0.41	3.2837	0.2430	1.1890	-1.4146	0.4193	0.0482	0.2771	0.4118	0.3019
BC12	3825 37908	10.5	10-11	38.25	61.75	0.81	0.50	3.2900	0.2381	1.1909	-1.4352	0.6017	0.0564	0.0000	0.0000	0.0000
BC12	3825 37908	14.5	14-15	36.80	63.20	0.82	0.48									
BC13	382514/10/2003	0.5	0-1	23.33	76.67	0.90	0.27	5.0478	0.4467	1.6189	0.8059	0.1042	0.0642	3.9051	0.7414	2.8195
BC13	382514/10/2003	1.5	1-2	27.24	72.76	0.87	0.33	6.3804	0.4129	1.8532	0.8846	0.1557	0.0538	4.5714	910.1742	3.9645
BC13	382514/10/2003	2.5	2-3	23.17	76.83	0.90	0.27	6.8155	0.4503	1.9192	0.7979	0.1481	0.0512	3.2900	0.5930	2.3561
BC13	382514/10/2003	3.5	3-4	25.09	74.91	0.89	0.30	4.9445	0.3821	1.5983	0.9621	0.1556	0.0593	2.9506	0.8367	2.3203
BC13	382514/10/2003	4.5	4-5	34.82	65.18	0.83	0.44	2.2512	0.2060	0.8114	1.5797	0.0756	0.0342	0.7112	0.3476	0.8353
BC13	382514/10/2003	6.5	6-7	38.48	61.52	0.81	0.50	1.4643	0.1482	0.3814	1.9095	0.0850	0.0273	0.1791	0.4490	0.2393
BC13	382514/10/2003	8.5	8-9	37.85	62.15	0.81	0.49	1.8617	0.1746	0.6215	1.7452	0.4980	0.0492	0.0000	0.0000	0.0000
BC13	382514/10/2003	10.5	10-11	38.95	61.05	0.80	0.51	1.8367	0.1477	0.6080	1.9128	0.7147	0.0507	4.9899	6.2484	6.7748
BC13	382514/10/2003	14.5	14-15	26.15	73.85	0.88	0.31	2.7681	0.2071	1.0182	1.5747	0.9933	0.0735	0.0000	0.0000	0.0000
BC13	382514/10/2003	18.5	18-19	29.57	70.43	0.86	0.36	3.2910	0.2446	1.1912	1.4082	1.3750	0.0848	0.7430	8.8376	0.7118
BC15	382514/10/2003	0.5	0-1	46.17	53.83	0.75	0.64	2.8393	0.2157	1.0436	-1.5340	0.0193	0.0253	1.2544	0.3724	2.1440
BC15	382514/10/2003	1.5	1-2	51.70	48.30	0.71	0.76	2.1923	0.2184	0.7849	-1.5214	0.0891	0.0249	0.3111	0.3989	0.6251
BC15	382514/10/2003	2.5	2-3	50.11	49.89	0.72	0.72	1.8247	0.1887	0.6014	-1.6678	0.1132	0.0301	0.5667	0.2088	1.0883
BC15	382514/10/2003	3.5	3-4	49.06	50.94	0.73	0.70	2.1667	0.1981	0.7732	-1.6188	0.1420	0.0367	0.0000	0.0000	0.0000
BC15	382514/10/2003	4.5	4-5	46.55	53.45	0.75	0.65	2.5760	0.2115	0.9462	-1.5534	0.1670	0.0338	0.0087	0.1565	0.0151
BC15	382514/10/2003	6.5	6-7	45.92	54.08	0.75	0.64	1.9727	0.1523	0.6794	-1.8822	0.1210	0.0293	0.0000	0.0000	0.0000
BC15	382514/10/2003	8.5	8-9	63.50	36.50	0.60	1.04	1.6967	0.1861	0.5287	-1.6817	0.0664	0.0274	0.0000	0.0000	0.0000
BC15	382514/10/2003	10.5	10-11	67.65	32.35	0.55	1.16	1.0356	0.1441	0.0350	-1.9369	0.0848	0.0224	0.0000	0.0000	0.0000
BC15	382514/10/2003	14.5	14-15	63.28	36.72	0.60	1.04	1.0807	0.1276	0.0776	-2.0589	0.0485	0.0309	0.0000	0.0000	0.0000
BC16	382514/10/2003	0.5	0-1	46.24	53.76	0.75	0.65	2.1475	0.1530	0.7643	-1.8775	0.1451	0.0512	1.1007	0.4440	1.8850
BC16	382514/10/2003	2.5	2-3	69.33	30.67	0.53	1.21	0.8636	0.0840	-0.1467	-2.4765	0.0232	0.0268	0.2172	0.1905	0.6960
BC16	382514/10/2003	4.5	4-5	67.77	32.23	0.55	1.16	0.5835	0.0731	-0.5387	-2.6160	0.0447	0.0312	0.0000	0.0000	0.0000
BC16	382514/10/2003	6.5	6-7	67.96	32.04	0.55	1.17	0.7305	0.0730	-0.3140	-2.6174	0.0032	0.0345	0.0000	0.0000	0.0000
BC16	382514/10/2003	8.5	8-9	49.93	50.07	0.72	0.72	1.8259	0.1636	0.6021	-1.8102	0.0861	0.0544	0.2266	0.5768	0.4328
BC16	382514/10/2003	10.5	10-11	52.16	47.84	0.70	0.77	3.3068	0.3015	1.1960	-1.1989	0.2427	0.0778	0.4745	0.9083	0.9658
BC17	202014/10/2003	0.5	0-1	31.33	68.67	0.85	0.39	1.8474	0.1761	0.6138	-1.7365	0.1071	0.0716	0.0000	0.0000	0.0000
BC17	202014/10/2003	2.5	2-3	24.50	75.50	0.89	0.29	3.2179	0.2387	1.1687	-1.4327	0.1889	0.0520	0.0000	0.0000	0.0000
BC17	202014/10/2003	4.5	4-5	32.28	67.72	0.85	0.40	2.7932	0.2354	1.0272	-1.4465	0.2205	0.0561	0.0000	0.0000	0.0000
BC17	202014/10/2003	6.5	6-7	43.04	56.96	0.77	0.59	2.3388	0.2027	0.8497	-1.5961	0.1393	0.0548	0.5194	0.5445	0.8058

BC17	202014/10/2003	8.5	8-9	29.98	70.02	0.86	0.37	3.6831	0.2606	1.3038	-1.3449	0.1764	0.0540	0.5230	0.4652	0.5095
BC17	202014/10/2003	10.5	10-11	20.45	79.55	0.91	0.23	2.7580	0.2640	1.0145	-1.3318	0.0526	0.0307	0.0000	0.0000	0.0000
BC17	202014/10/2003	14.5	14-15	37.03	62.97	0.82	0.48	2.2174	0.2123	0.7964	-1.5500	0.0427	0.0250	0.0000	0.0000	0.0000
BC18	202016/10/2003	0.5	0-1	52.61	47.39	0.70	0.78	0.9032	0.1036	-0.1019	-2.2669	0.0998	0.0499	0.1087	0.2343	0.2242
BC18	202016/10/2003	2.5	2-3	48.47	51.53	0.73	0.69	1.3674	0.1264	0.3129	-2.0683	0.0724	0.0381	0.0000	0.0000	0.0000
BC18	202016/10/2003	4.5	4-5	61.90	38.10	0.62	1.00	0.9770	0.1047	-0.0232	-2.2571	0.0380	0.0269	0.1701	0.2398	0.4509
BC18	202016/10/2003	6.5	6-7	66.41	33.59	0.57	1.12	0.7849	0.0848	-0.2422	-2.4680	-0.0161	0.0294	0.1380	0.3922	0.4108
BC18	202016/10/2003	8.5	8-9	69.53	30.47	0.53	1.22	0.3440	0.0406	-1.0673	-3.2034	-0.0074	0.0297	0.0967	0.3038	0.3113
BC19	202016/10/2003	0.5	0-1	57.40	42.60	0.66	0.89	1.4601	0.1400	0.3785	-1.9660	0.1457	0.0422	0.0000	0.0000	0.0000
BC19	202016/10/2003	2.5	2-3	60.69	39.31	0.63	0.97	1.3623	0.1498	0.3092	-1.8987	0.0171	0.0329	0.0000	0.0000	0.0000
BC19	202016/10/2003	4.5	4-5	67.74	32.26	0.55	1.16	0.6965	0.0885	-0.3617	-2.4251	0.0885	0.0274	0.0172	0.1718	0.0530
BC19	202016/10/2003	6.5	6-7	68.97	31.03	0.54	1.20	0.6222	0.0749	-0.4745	-2.5913	0.0263	0.0242	0.0000	0.0000	0.0000
BC19	202016/10/2003	8.5	8-9	67.32	32.68	0.56	1.15	0.7475	0.0857	-0.2910	-2.4569	0.0919	0.0312	0.1887	0.3585	0.5747
BC19	202016/10/2003	10.5	10-11	71.08	28.92	0.51	1.26	0.4264	0.0562	-0.8525	-2.8784	0.0278	0.0236	0.0000	0.0000	0.0000
BC20	202016/10/2003	0.5	0-1	53.21	46.79	0.70	0.79	1.1828	0.1334	0.1679	-2.0146	0.0618	0.0316	0.0000		0.0000
BC20	202016/10/2003	2.5	2-3	63.67	36.33	0.60	1.05	1.5689	0.1434	0.4504	-1.9423	0.0607	0.0267	0.1507	0.1628	0.4181
BC20	202016/10/2003	4.5	4-5	51.55	48.45	0.71	0.76	0.4525	0.0552	-0.7930	-2.8961	0.1479	0.0383	0.0000	0.0000	0.0000
BC20	202016/10/2003	6.5	6-7	62.00	38.00	0.61	1.00	0.1800	0.0247	-1.7148	-3.6996	0.0356	0.0412	0.1414	0.3423	0.3756
BC20	202016/10/2003	8.5	8-9	63.80	36.20	0.60	1.05	0.4488	0.0685	-0.8012	-2.6809	0.1381	0.0408	0.5177	0.3607	1.4412
BC20	202016/10/2003	10.5	10-11	61.12	38.88	0.62	0.98	0.5368	0.0716	-0.6222	-2.6371	0.0590	0.0313	0.0000	0.0000	0.0000
BC20	202016/10/2003	12.5	12-13	57.40	42.60	0.66	0.89	0.0622	0.0106	-2.7782	-4.5512	0.0399	0.0233	0.0000	0.0000	0.0000
BC22	382516/10/2003	0.5	0-1	42.86	57.14	0.78	0.58	2.8733	0.2902	1.0555	-1.2370	0.1245	0.0410	1.5441	0.5263	2.3819
BC22	382516/10/2003	2.5	2-3	48.89	51.11	0.73	0.70	1.7843	0.2116	0.5790	-1.5533	0.1302	0.0324	0.3953	0.3012	0.7325
BC22	382516/10/2003	4.5	4-5	49.83	50.17	0.72	0.72	2.4983	0.2215	0.9156	-1.5073	0.1444	0.0358	0.0000	0.0000	0.0000
BC22	382516/10/2003	6.5	6-7	57.80	42.20	0.65	0.90	2.0292	0.1914	0.7077	-1.6532	0.0589	0.0289	0.0000	0.0000	0.0000
BC22	382516/10/2003	8.5	8-9	46.49	53.51	0.75	0.65	2.2615	0.1873	0.8160	-1.6749	0.0805	0.0317	0.0000	0.0000	0.0000
BC22	382516/10/2003	10.5	10-11	49.73	50.27	0.72	0.72	2.2351	0.2226	0.8043	-1.5024	0.1236	0.0350	0.0000	0.0000	0.0000
BC22	382516/10/2003	14.5	14-15	53.68	46.32	0.69	0.80	1.2423	0.1348	0.2170	-2.0039	0.1906	0.0361	0.0000	0.0000	0.0000
BC22	382516/10/2003	18.5	18-19	53.60	46.40	0.69	0.80	1.1326	0.1063	0.1245	-2.2418	0.3705	0.0471	0.0000	0.0000	0.0000
BC23	202016/10/2003	0.5	0-1	26.52	73.48	0.88	0.32	3.4116	0.3045	1.2272	-1.1892	0.0888	0.0447	2.8188	0.5638	2.3670
BC23	202016/10/2003	1.5	1-2	34.60	65.40	0.83	0.44	2.0729	0.1673	0.7289	-1.7879	0.2002	0.0473	1.8633	0.4912	2.1707
BC23	202016/10/2003	2.5	2-3	39.39	60.61	0.80	0.52	2.0107	0.1597	0.6985	-1.8344	0.1010	0.0336	0.5858	0.3261	0.8072
BC23	202016/10/2003	3.5	3-4	45.31	54.69	0.76	0.63	1.8556	0.1435	0.6182	-1.9411	-0.0102	0.0357	0.0000	0.0000	0.0000
BC23	202016/10/2003	4.5	4-5	40.50	59.50	0.79	0.54	2.3928	0.1833	0.8724	-1.6968	0.1498	0.0441	0.4402	0.2895	0.6293
BC23	202016/10/2003	6.5	6-7	47.20	52.80	0.74	0.67	1.5159	0.1322	0.4160	-2.0238	0.2369	0.0546	-0.5476	0.3976	-0.9653
BC23	202016/10/2003	8.5	8-9	42.08	57.92	0.78	0.57	2.1907	0.1781	0.7842	-1.7257	0.1339	0.0448	-0.0978	0.4356	-0.1471
BC23	202016/10/2003	10.5	10-11	50.37	49.63	0.72	0.73	1.0295	0.1163	0.0291	-2.1513	0.0967	0.0361	1.2214	1.7272	2.3629
BC23	202016/10/2003	14.5	14-15	42.17	57.83	0.78	0.57	1.5115	0.1572	0.4131	-1.8502	0.2314	0.0484	0.0000	0.0000	0.0000
BC23	202016/10/2003	18.5	18-19	38.84	61.16	0.80	0.51	2.1972	0.2136	0.7872	-1.5438	0.0000	0.0523	3.5431	3.0032	4.7926
BC23	202016/10/2003	22.5	22-23	41.47	58.53	0.79	0.56									
BC24	202014/10/2003	0.5	0-1	33.59	66.41	0.84	0.42	2.1801	0.1905	0.7794	-1.6584	0.1085	0.0573	2.5506	0.6982	2.8617

BC24	202014/10/2003	1.5	1-2	60.25	39.75	0.63	0.96	0.9395	0.1054	-0.0624	-2.2502	0.0800	0.0383	0.6903	0.3949	1.7518
BC24	202014/10/2003	2.5	2-3	51.30	48.70	0.71	0.75	0.4276	0.0448	-0.8496	-3.1061	0.0319	0.0258	0.1723	0.1819	0.3424
BC24	202014/10/2003	4.5	4-5	53.51	46.49	0.69	0.80	1.0247	0.1000	0.0244	-2.3024	0.0496	0.0301	0.0000	0.0000	0.0000
BC24	202014/10/2003	6.5	6-7	44.92	55.08	0.76	0.62	0.9533	0.0949	-0.0478	-2.3549	0.0482	0.0328	0.7573	0.4407	1.2461
BC24	202014/10/2003	8.5	8-9	32.87	67.13	0.84	0.41	2.4747	0.2163	0.9061	-1.5309	0.0585	0.0316	0.1017	0.4110	0.1111
BC24	202014/10/2003	10.5	10-11	42.42	57.58	0.78	0.57	1.6718	0.1887	0.5139	-1.6673	0.0452	0.0276	0.3970	0.5696	0.6039
BC24	202014/10/2003	14.5	14-15	42.39	57.61	0.78	0.57	1.7737	0.1561	0.5731	-1.8570	0.1220	0.0492	0.0000	0.0000	0.0000
BC25	B382514/10/2003	0.5	0-1	33.57	66.43	0.84	0.42	3.3576	0.3911	1.2112	-0.9388	0.0000	0.0389	1.3848	0.5948	1.5525
BC25	B382514/10/2003	2.5	2-3	39.05	60.95	0.80	0.51	2.2452	0.1595	0.8088	-1.8358	0.1629	0.0396	0.0585	0.3394	0.0797
BC25	B382514/10/2003	4.5	4-5	33.46	66.54	0.84	0.42	1.9103	0.1546	0.6473	-1.8668	0.3036	0.0563	0.0000	0.0000	0.0000
BC25	B382514/10/2003	6.5	6-7	37.25	62.75	0.81	0.48	2.3257	0.2026	0.8440	-1.5964	0.3268	0.0616	0.1708	0.4474	0.2188
BC25	B382514/10/2003	8.5	8-9	32.41	67.59	0.84	0.40	2.3413	0.2341	0.8507	-1.4521	0.2883	0.0632	0.2420	0.6472	0.2597
BC25	B382514/10/2003	10.5	10-11	40.50	59.50	0.79	0.54	2.9033	0.2473	1.0659	-1.3971	0.1554	0.0547	0.2775	1.0944	0.3967
BC25	B382514/10/2003	14.5	14-15	39.97	60.03	0.80	0.53	2.9196	0.2461	1.0714	-1.4019	0.0000	0.0483	0.5813	1.8006	0.8165
BC25	B382514/10/2003	18.5	18-19	27.77	72.23	0.87	0.33	4.6291	0.4150	1.5324	-0.8794	0.0000	0.0670	3.0175	2.2458	2.6778
BC25	B382514/10/2003	22.5	22-23	30.46	69.54	0.86	0.37	4.9567	0.4321	1.6007	-0.8391	0.0000	0.0537	0.0000	0.0000	0.0000
BC26	202014/10/2003	0.5	0-1	26.03	73.97	0.88	0.31	1.0499	0.1006	0.0487	-2.2966	0.1519	0.0510	0.0000	0.0000	0.0000
BC26	202014/10/2003	2.5	2-3	31.59	68.41	0.85	0.39	1.2975	0.1154	0.2604	-2.1593	0.2497	0.0632	0.8048	0.3704	0.8365
BC26	202014/10/2003	4.5	4-5	30.87	69.13	0.85	0.38	2.8040	0.2354	1.0311	-1.4465	0.1915	0.0558	0.0000	0.0000	0.0000
BC26	202014/10/2003	6.5	6-7	35.70	64.30	0.82	0.46	4.8076	0.4214	1.5702	-0.8643	0.0000	0.0454	0.0000	0.0000	0.0000
BC26	202014/10/2003	8.5	8-9	36.50	63.50	0.82	0.47	4.1590	0.3669	1.4253	-1.0028	0.0000	0.0472	3.6783	4.1748	4.5881
BC26	202014/10/2003	10.5	10-11	34.29	65.71	0.83	0.43	4.3606	0.3984	1.4726	-0.9204	0.0000	0.0442	0.1438	4.1383	0.1656
BC26	202014/10/2003	14.5	14-15	31.98	68.02	0.85	0.40	4.9465	0.3997	1.5987	-0.9170	0.0000	0.0453	0.0000	0.0000	0.0000

LEAD 210 DERIVED SEDIMENT ACCUMULATION RATES

Sample	Y	X	Sequence	Depth Range	Accumulation Rate mm/year	R_Squared
BC01	29.568717	-90.185183	massive mud with shells	0-6.5	1.0	0.9396
BC02	29.560650	-90.204567	massive mud with shells	6.5-18.5	2.0	0.9817
BC03	29.56268333	-90.17846667	interbedded sand and mud	0-5.5	2.0	0.9504
BC04	29.548950	-90.174117	interbedded sand and mud	none	none	none
BC05	29.55063333	-90.18813333	interbedded sand and mud	none	none	none
BC06	29.5513	-90.2082	interbedded sand and mud	none	none	none
BC07	29.54006667	-90.22025	massive mud with shells	none	none	none
BC08	29.54253333	-90.20038333	massive mud with shells	8.5-14.5	5.0	0.9999
BC09	29.54061667	-90.16913333	interbedded sand and mud	10.5-26.5	3.0	0.9755
BC10	29.52901667	-90.1617	thick sand	none	none	none
BC12	29.532354	-90.205063	massive mud with shells	none	none	none
BC13	29.532488	-90.220697	interbedded sand and mud	none	none	none
BC15	29.50131667	-90.16603333	thick sand	none	none	none
BC16	29.51008333	-90.19583333	thick sand	none	none	none
BC17	29.50976667	-90.12658333	interbedded sand and mud	none	none	none
BC18	29.48688333	-90.17148333	thick sand	none	none	none
BC19	29.4888	-90.14505	thick sand	none	none	none
BC20	29.47656667	-90.12838333	thick sand	none	none	none
BC22	29.46475	-90.11111667	massive mud with shells	10.5-18.5	4.0	0.8499
BC23	29.4711	-90.07628333	interbedded sand and mud	none	none	none
BC24	29.5382288	-90.1308833	interbedded sand and mud	none	none	none
BC25	29.5293	-90.10386667	interbedded sand and mud	none	none	none
BC26	29.51315	-90.0864	massive mud with shells	none	none	none

APPENDIX B: SIDE SCAN SONAR DATA/MAPS

SIDE SCAN SONAR IMAGERY ZONAL STATISTICS

100kHz and 500kHz Side Scan Sonar Backscatter Imagery Grayscale (8bit) Summary/Zonal Statistics in 3m Buffer Zone																								
Sample	100kHz COUNT	100kHz AREA	100kHz MIN	100kHz MAX	100kHz RANGE	100kHz MEAN	100kHz STD	100kHz SUM	100kHz VARIETY	100kHz MAJORITY	100kHz MINORITY	100kHz MEDIAN	500kHz COUNT	500kHz AREA	500kHz MIN	500kHz MAX	500kHz RANGE	500kHz MEAN	500kHz STD	500kHz SUM	500kHz VARIETY	500kHz MAJORITY	500kHz MINORITY	500kHz MEDIAN
BC01	32	32	41	152	111	80.03	25.08	2561.00	26	56	41	75	32	32	47	97	50	73.03	12.54	2337.00	25	68	47	73
BC02	29	29	138	188	50	162.62	11.95	4716.00	23	168	138	163	29	29	102	192	90	144.69	22.65	4196.00	23	127	102	145
BC03	28	28	0	224	224	20.50	59.85	574.00	4	0	157	0	28	28	0	205	205	39.25	69.70	1099.00	8	0	108	0
BC04	26	26	107	198	91	153.31	21.15	3986.00	22	151	107	151	26	26	123	169	46	146.31	12.77	3804.00	20	132	123	146
BC05	29	29	88	194	106	125.90	24.58	3651.00	23	113	88	119	29	29	95	177	82	121.62	23.34	3527.00	25	95	96	115
BC06	29	29	115	174	59	142.52	13.05	4133.00	20	147	115	143	29	29	119	200	81	151.35	20.32	4389.00	23	156	119	150
BC07	27	27	56	160	104	103.96	24.81	2807.00	25	85	56	101	27	27	90	191	101	140.82	27.92	3802.00	25	115	90	137
BC08	28	28	104	214	110	175.04	24.81	4901.00	25	158	104	174	28	28	119	225	106	176.39	21.44	4939.00	22	165	119	177
BC09	28	28	88	223	135	151.25	32.17	4235.00	25	131	88	147	28	28	123	204	81	153.75	20.85	4305.00	23	142	123	146
BC10	29	29	95	188	93	123.14	18.67	3571.00	26	108	95	120	29	29	96	149	53	120.86	13.98	3505.00	23	125	96	121
BC12	28	28	80	219	139	131.07	36.46	3670.00	25	80	82	123	28	28	76	220	144	139.93	32.57	3918.00	26	123	76	132
BC13	29	29	67	208	141	114.38	39.54	3317.00	26	93	67	95	29	29	81	193	112	122.83	31.83	3562.00	27	105	81	113
BC15	27	27	89	181	92	122.41	20.01	3305.00	23	101	89	117	27	27	111	154	43	127.59	11.44	3445.00	19	121	111	124
BC16	29	29	53	203	150	122.62	32.90	3556.00	25	128	53	123	29	29	114	174	60	146.97	15.63	4262.00	21	153	114	144
BC17	28	28	78	203	125	116.71	30.98	3268.00	26	111	78	111	28	28	94	185	91	135.14	24.93	3784.00	25	103	94	129
BC18	28	28	78	169	91	105.82	22.21	2963.00	24	86	78	100	28	28	90	121	31	103.79	6.64	2906.00	17	99	96	104
BC19	28	28	90	253	163	150.54	43.54	4215.00	22	109	90	132	28	28	116	186	70	140.54	16.28	3935.00	23	133	116	134
BC20	29	29	79	200	121	139.24	24.56	4038.00	26	122	79	139	29	29	100	222	122	141.83	20.67	4113.00	23	141	100	141
BC22	26	26	46	240	194	100.62	43.64	2616.00	25	86	46	87	26	26	63	158	95	90.65	22.93	2357.00	19	79	63	84
BC23	27	27	74	252	178	156.89	62.02	4236.00	27	74	74	140	32	32	72	216	144	120.41	41.05	3853.00	29	78	72	103
BC24	28	28	84	232	148	152.93	32.70	4282.00	23	116	84	152	28	28	110	210	100	134.50	22.78	3766.00	23	124	110	125
BC26	27	27	69	235	166	151.41	45.40	4088.00	24	115	69	151	27	27	63	183	120	122.07	33.87	3296.00	23	95	63	121
G001C	30	30	0	249	249	141.63	102.13	4249.00	20	0	152	202	30	30	0	137	137	74.07	52.86	2222.00	16	0	102	104
G002A	28	28	179	246	67	211.21	17.40	5914.00	24	204	179	212	28	28	100	188	88	129.64	24.87	3630.00	24	109	100	117
G002B	28	28	129	244	115	190.54	35.02	5335.00	27	223	129	199	28	28	131	229	98	174.82	27.50	4895.00	24	164	131	166
G002C	29	29	78	184	106	112.03	28.55	3249.00	25	87	79	105	29	29	93	239	146	153.17	39.82	4442.00	26	111	93	139
G003A	32	32	104	173	69	128.06	15.26	4098.00	25	116	104	124	32	32	104	193	89	134.47	24.36	4303.00	25	117	109	128
G003B	28	28	115	187	72	139.93	16.46	3918.00	23	126	115	137	28	28	124	221	97	163.32	28.49	4573.00	25	130	124	155
G003C	28	28	99	172	73	129.25	16.54	3619.00	21	113	99	130	28	28	104	158	54	123.18	15.15	3449.00	21	110	104	116
G004A	28	28	116	234	118	172.32	30.33	4825.00	23	163	116	173	28	28	95	227	132	148.68	35.61	4163.00	26	110	95	139
G004B	26	26	111	178	67	147.65	17.29	3839.00	23	133	111	147	26	26	95	180	85	131.08	23.10	3408.00	24	107	95	127
G004C	28	28	131	193	62	150.07	13.28	4202.00	22	143	131	145	28	28	113	178	65	135.46	17.87	3793.00	24	117	113	128
G005A	25	25	49	221	172	129.96	53.67	3249.00	25	49	49	130	25	25	79	242	163	156.00	51.11	3900.00	24	211	79	153
G005B	27	27	56	170	114	91.00	30.49	2457.00	22	67	56	81	27	27	73	172	99	103.00	22.71	2781.00	21	77	73	103
G005C	28	28	70	200	130	134.75	31.19	3773.00	26	106	70	131	28	28	79	163	84	117.86	21.85	3300.00	22	137	80	122
G006B	27	27	34	117	83	53.56	16.49	1446.00	18	39	34	48	27	27	38	94	56	59.89	15.34	1617.00	23	45	38	58
G006C	28	28	37	121	84	75.21	24.31	2106.00	25	53	37	72	28	28	50	146	96	85.25	27.56	2387.00	24	58	50	78
G007A	26	26	125	237	112	180.42	30.57	4691.00	24	162	125	171	26	26	114	214	100	138.96	22.05	3613.00	22	133	114	133
G007B	28	28	103	194	91	137.79	20.88	3858.00	22	131	103	131	28	28	120	156	36	135.07	9.87	3782.00	19	127	122	132
G007C	28	28	0	165	165	101.57	59.75	2844.00	18	0	119	127	28	28	0	189	189	109.21	64.19	3058.00	17	0	128	138
G008A	28	28	100	160	60	133.50	17.89	3738.00	24	117	100	129	28	28	99	212	113	122.43	21.00	3428.00	22	119	99	117
G008B	29	29	105	145	40	117.48	11.00	3407.00	22	110	105	115	29	29	103	159	56	122.07	13.87	3540.00	23	116	103	118
G008C	29	29	99	187	88	122.24	20.87	3545.00	23	99	100	115	29	29	114	190	76	136.55	18.67	3960.00	23	119	114	132
G009A	30	30	89	242	153	174.20	45.34	5226.00	28	219	89	178	30	30	85	247	162	196.57	47.13	5897.00	24	236	85	216
G009B	27	27	66	231	165	114.56	39.56	3093.00	22	79	66	106	27	27	80	187	107	114.78	24.66	3099.00	24	90	80	115
G009C	28	28	81	236	155	172.25	43.81	4823.00	27	175	81	175	28	28	89	244	155	183.57	38.47	5140.00	27	191	89	189
G010A	32	32	64	166	102	100.66	31.34	3221.00	28	68	64	90	32	32	86	219	133	127.47	35.18	4079.00	26	86	89	120
G010B	27	27	73	207	134	107.93	28.94	2914.00	25	95	73	99	27	27	76	203	127	105.67	30.26	2853.00	21	107	76	98
G010C	29	29	72	183	111	107.03	28.53	3104.00	24	84	72	100	29	29	81	144	63	98.24	14.82	2849.00	21	90	81	94
G011A	29	29	128	208	80	160.45	19.10	4653.00	24	143	128	160	29	29	106	188	82	137.41	22.20	3985.00	25	120	106	131
G011B	29	29	93	189	96	136.55	21.25	3960.00	24	120	93	134	29	29	87	219	132	131.41	26.29	3811.00	26	117	87	124

G011C	29	29	94	180	86	128.41	17.56	3724.00	20	114	94	125	29	29	118	172	54	146.76	15.02	4256.00	22	155	118	145
G012A	29	29	126	195	69	152.17	19.43	4413.00	26	136	126	151	29	29	116	204	88	170.48	20.07	4944.00	22	168	116	171
G012B	29	29	83	148	65	112.48	19.14	3262.00	26	103	83	108	29	29	122	186	64	145.35	14.23	4215.00	23	138	122	144
G012C	28	28	90	198	108	134.64	27.28	3770.00	22	105	90	144	28	28	90	190	100	138.00	28.47	3864.00	27	124	90	131
G013A	31	31	132	208	76	159.81	16.55	4954.00	26	153	132	157	31	31	110	173	63	142.55	12.05	4419.00	24	142	110	142
G013B	28	28	86	167	81	111.68	18.35	3127.00	24	94	86	108	28	28	85	163	78	123.04	16.17	3445.00	25	115	85	119
G013C	27	27	122	246	124	169.41	33.28	4574.00	26	213	122	166	27	27	127	208	81	152.19	21.11	4109.00	23	152	130	149
G014A	28	28	50	153	103	74.07	28.53	2074.00	21	55	50	64	28	28	59	114	55	77.43	15.52	2168.00	20	70	59	71
G014B	27	27	46	150	104	72.81	21.23	1966.00	21	49	46	69	27	27	58	112	54	77.52	14.52	2093.00	20	72	58	73
G014C	29	29	76	206	130	142.97	37.55	4146.00	28	132	76	152	29	29	76	178	102	119.90	27.35	3477.00	26	122	76	123
G015A	29	29	158	240	82	210.28	23.25	6098.00	27	209	158	212	29	29	141	247	106	211.48	27.50	6133.00	26	218	141	218
G015B	28	28	132	230	98	177.68	24.31	4975.00	22	152	132	177	28	28	146	237	91	195.36	25.75	5470.00	25	165	146	198
G015C	27	27	139	249	110	200.44	25.88	5412.00	21	206	139	206	27	27	137	249	112	194.37	34.26	5248.00	25	225	137	196
G016A	29	29	105	230	125	146.14	38.79	4238.00	27	108	105	134	29	29	103	202	99	134.24	30.33	3893.00	25	110	103	124
G016B	29	29	99	215	116	128.48	36.20	3726.00	23	103	99	112	29	29	106	224	118	132.35	28.24	3838.00	22	106	109	123
G016C	30	30	0	121	121	69.00	47.26	2070.00	19	0	1	98	30	30	0	163	163	83.83	57.67	2515.00	20	0	1	118
G017A	27	27	59	164	105	101.04	29.67	2728.00	25	81	59	99	27	27	70	204	134	109.33	36.05	2952.00	23	91	70	92
G017B	29	29	75	233	158	113.76	35.91	3299.00	27	83	75	100	29	29	68	174	106	105.00	27.41	3045.00	26	70	68	99
G017C	29	29	61	138	77	88.72	19.75	2573.00	23	96	61	80	29	29	95	189	94	120.76	21.60	3502.00	25	97	95	118
G018A	29	29	79	225	146	143.66	40.50	4166.00	26	118	79	137	29	29	67	219	152	128.07	48.53	3714.00	28	67	73	119
G018B	26	26	89	244	155	149.89	39.94	3897.00	23	143	89	143	26	26	82	251	169	162.85	42.43	4234.00	24	144	82	158
G018C	29	29	74	223	149	152.86	33.28	4433.00	28	159	74	151	29	29	96	211	115	146.03	34.81	4235.00	27	145	96	143
G019A	28	28	140	223	83	181.50	21.74	5082.00	25	151	140	183	28	28	116	176	60	150.32	15.83	4209.00	18	155	116	153
G019B	29	29	141	215	74	179.21	20.26	5197.00	25	157	141	181	29	29	101	201	100	149.03	22.39	4322.00	27	137	101	144
G019C	28	28	125	233	108	178.71	26.97	5004.00	24	155	125	177	28	28	100	220	120	168.71	29.10	4724.00	24	149	100	171
G020A	29	29	136	253	117	182.00	38.32	5278.00	25	136	142	175	29	29	116	249	133	166.90	38.09	4840.00	25	130	116	164
G020B	26	26	151	249	98	205.54	25.39	5344.00	20	221	151	214	26	26	115	253	138	188.46	30.13	4900.00	22	174	115	190
G020C	27	27	149	254	105	215.33	30.75	5814.00	23	189	149	224	27	27	135	254	119	210.44	37.44	5682.00	25	216	135	219
G021A	12	12	67	218	151	109.50	43.72	1314.00	11	107	67	96	12	12	70	174	104	104.58	28.24	1255.00	11	99	70	99
G021B	29	29	47	160	113	88.66	24.04	2571.00	26	84	47	86	29	29	69	158	89	89.72	20.66	2602.00	22	85	69	85
G021C	29	29	101	216	115	144.35	32.39	4186.00	26	119	101	136	29	29	62	182	120	123.07	32.22	3569.00	27	117	62	120
G022A	29	29	93	148	55	112.28	13.13	3256.00	20	106	93	107	29	29	107	166	59	132.52	13.13	3843.00	19	126	107	130
G022B	27	27	103	166	63	128.59	14.36	3472.00	25	124	103	128	27	27	119	168	49	137.82	13.96	3721.00	20	130	123	136
G022C	29	29	105	165	60	123.55	14.07	3583.00	21	113	105	121	29	29	103	163	60	117.38	12.86	3404.00	21	112	103	115
G023A	29	29	116	202	86	153.28	23.37	4445.00	22	145	120	152	29	29	137	224	87	174.62	24.19	5064.00	28	162	137	177
G023B	29	29	90	162	72	129.55	19.13	3757.00	24	130	90	130	29	29	126	190	64	160.83	19.33	4664.00	25	126	129	159
G023C	27	27	120	201	81	157.59	18.20	4255.00	25	147	120	153	27	27	141	195	54	160.74	12.15	4340.00	20	153	141	158
G024A	27	27	0	182	182	130.59	40.22	3526.00	23	0	112	138	27	27	0	171	171	124.19	36.61	3353.00	19	133	107	133
G024B	29	29	114	149	35	129.79	9.63	3764.00	19	114	115	131	29	29	127	169	42	136.55	9.44	3960.00	18	132	128	134
G024C	29	29	101	149	48	122.48	12.82	3552.00	24	114	101	121	29	29	114	150	36	129.55	9.34	3757.00	22	114	115	131
G025A	18	18	98	210	112	177.22	27.18	3190.00	16	168	98	184	18	18	122	212	90	176.00	19.06	3168.00	14	155	122	182
G025B	29	29	119	169	50	146.41	11.05	4246.00	21	130	119	147	29	29	115	165	50	139.62	12.64	4049.00	26	145	115	140
G025C	28	28	95	168	73	144.82	16.63	4055.00	23	142	95	145	28	28	121	171	50	141.43	12.72	3960.00	23	151	124	142
G026A	28	28	88	133	45	98.00	9.69	2744.00	18	94	88	94	28	28	85	115	30	93.79	7.48	2626.00	14	87	85	91
G026B	29	29	87	117	30	100.24	7.81	2907.00	19	95	87	99	29	29	94	112	18	103.28	5.15	2995.00	16	106	94	103
G026C	29	29	0	136	136	73.41	53.87	2129.00	15	0	99	104	29	29	0	156	156	72.97	53.86	2116.00	14	0	101	105
G027A	28	28	101	195	94	137.57	24.60	3852.00	21	142	101	138	28	28	109	177	68	125.54	14.34	3515.00	21	114	109	123
G027B	26	26	114	209	95	161.54	24.56	4200.00	24	143	114	160	26	26	116	182	66	150.08	21.47	3902.00	25	181	116	142
G027C	28	28	84	181	97	124.96	26.11	3499.00	23	85	84	128	28	28	104	156	52	124.29	15.00	3480.00	24	111	104	120
G028A	8	8	93	174	81	125.00	29.45	1000.00	8	93	93	109	8	8	93	153	60	122.63	21.05	981.00	8	93	93	116
G028B	30	30	88	156	68	112.47	17.36	3374.00	24	112	88	110	30	30	94	174	80	116.40	18.43	3492.00	25	102	95	111
G028C	29	29	91	166	75	124.00	19.26	3596.00	22	108	91	120	29	29	96	183	87	118.79	18.48	3445.00	24	103	96	116
G029A	29	29	66	124	58	89.10	16.52	2584.00	19	110	66	88	29	29	83	133	50	101.38	12.32	2940.00	22	94	83	99
G029B	27	27	55	137	82	85.63	21.50	2312.00	21	62	55	77	27	27	84	148	64	110.78	17.24	2991.00	23	89	84	106
G029C	28	28	63	145	82	94.64	23.32	2650.00	21	82	63	89	28	28	70	154	84	99.07	19.47	2774.00	23	90	70	93
G030A	28	28	95	227	132	146.00	37.25	4088.00	27	95	96	138	28	28	88	189	101	125.50	25.95	3514.00	24	97	88	116
G030B	28	28	73	196	123	112.00	32.30	3136.00	26	87	73	97	28	28	70	186	116	101.68	27.55	2847.00	24	79	70	92

G030C	28	28	67	215	148	90.50	28.89	2534.00	20	80	67	80	28	28	58	145	87	96.18	26.50	2693.00	22	75	59	93
G031A	29	29	72	167	95	123.41	21.04	3579.00	26	129	72	125	29	29	112	178	66	146.93	16.30	4261.00	21	147	112	147
G031B	27	27	97	158	61	124.89	17.06	3372.00	18	129	100	129	27	27	113	168	55	141.59	14.32	3823.00	24	133	113	142
G031C	28	28	76	168	92	127.18	23.48	3561.00	26	112	76	125	28	28	109	179	70	141.57	15.39	3964.00	25	123	109	141
G033A	28	28	87	155	68	122.07	16.92	3418.00	23	121	87	121	28	28	103	165	62	131.07	19.54	3670.00	25	116	103	125
G033B	28	28	102	218	116	147.04	28.90	4117.00	26	119	102	144	28	28	90	165	75	129.07	16.62	3614.00	21	118	90	127
G033C	32	32	110	251	141	171.25	37.65	5480.00	31	130	110	174	32	32	104	229	125	170.75	35.30	5464.00	26	131	104	173
G035A	32	32	81	216	135	137.25	37.83	4392.00	28	96	81	123	32	32	122	205	83	161.56	25.22	5170.00	24	160	125	160
G035B	28	28	79	254	175	145.89	48.35	4085.00	24	79	83	126	28	28	110	207	97	140.89	22.22	3945.00	23	128	110	134
G035C	29	29	78	230	152	143.24	36.84	4154.00	27	109	78	145	29	29	113	181	68	138.07	16.61	4004.00	24	133	113	133
G039A	29	29	0	195	195	98.07	39.73	2844.00	25	0	61	93	29	29	95	211	116	131.21	22.44	3805.00	26	110	95	128
G039B	25	25	61	254	193	121.60	49.18	3040.00	23	77	61	111	25	25	96	157	61	116.12	14.45	2903.00	21	101	96	116
G039C	27	27	0	254	254	114.93	71.57	3103.00	22	0	52	99	27	27	101	177	76	120.33	15.71	3249.00	22	107	101	117
G041A	29	29	111	154	43	124.41	12.25	3608.00	19	112	114	119	29	29	122	211	89	146.72	20.84	4255.00	22	134	122	139
G041B	28	28	105	196	91	142.79	24.40	3998.00	24	115	105	137	28	28	117	192	75	146.54	19.50	4103.00	22	146	117	140
G041C	28	28	102	195	93	133.18	24.88	3729.00	25	103	102	123	28	28	116	179	63	141.04	17.51	3949.00	23	117	116	139
G042A	12	12	42	70	28	55.00	7.51	660.00	9	52	42	53	12	12	61	114	53	79.25	15.84	951.00	11	71	61	71
G042B	29	29	44	171	127	75.69	27.10	2195.00	25	51	44	73	29	29	71	185	114	99.86	25.53	2896.00	23	75	71	95
G042C	27	27	55	190	135	101.78	46.41	2748.00	26	62	55	82	27	27	73	210	137	114.93	38.49	3103.00	26	78	73	100
G043A	27	27	106	197	91	156.04	19.91	4213.00	21	148	106	154	27	27	115	217	102	151.26	22.87	4084.00	25	141	115	147
G043B	32	32	108	232	124	165.00	26.33	5280.00	25	174	108	163	32	32	118	216	98	160.09	25.36	5123.00	26	134	118	154
G043C	29	29	111	224	113	167.48	29.34	4857.00	27	163	111	163	29	29	119	216	97	161.93	21.13	4696.00	21	161	119	158
G044A	29	29	135	244	109	195.45	25.24	5668.00	23	197	135	197	29	29	149	233	84	187.35	22.41	5433.00	26	149	167	185
G044B	28	28	93	238	145	160.96	36.42	4507.00	28	93	93	150	28	28	117	226	109	159.21	30.65	4458.00	22	128	117	154
G044C	28	28	0	199	199	46.64	75.01	1306.00	9	0	127	0	28	28	0	182	182	42.68	66.98	1195.00	12	0	4	0
G045A	30	30	80	204	124	138.80	28.34	4164.00	29	128	80	136	30	30	125	168	43	141.30	10.18	4239.00	20	138	125	143
G045B	29	29	55	236	181	139.31	45.87	4040.00	25	148	55	149	29	29	106	168	62	139.17	15.29	4036.00	25	133	106	138
G045C	28	28	91	215	124	140.86	36.22	3944.00	24	103	91	133	28	28	108	182	74	145.57	18.51	4076.00	23	131	108	147
G047A	29	29	70	132	62	91.72	18.25	2660.00	23	71	70	85	29	29	72	140	68	93.03	17.33	2698.00	23	85	72	86
G047B	29	29	79	167	88	103.45	22.46	3000.00	22	81	79	96	29	29	84	139	55	97.24	12.47	2820.00	21	88	86	93
G047C	27	27	66	125	59	85.33	14.76	2304.00	20	66	68	84	27	27	74	141	67	91.04	14.49	2458.00	20	77	74	88
G048A	27	27	81	233	152	119.22	32.93	3219.00	24	81	88	108	27	27	79	178	99	107.41	25.59	2900.00	25	83	79	98
G048B	29	29	92	202	110	145.48	30.77	4219.00	25	139	92	143	29	29	71	181	110	112.93	23.87	3275.00	23	103	71	111
G048C	27	27	81	214	133	133.11	32.87	3594.00	24	101	81	132	27	27	101	157	56	133.78	16.04	3612.00	19	126	101	136
G050A	28	28	64	121	57	83.18	16.54	2329.00	21	73	64	77	28	28	94	127	33	100.96	7.11	2827.00	13	96	94	98
G050B	29	29	76	144	68	90.21	13.41	2616.00	20	79	76	88	29	29	104	146	42	115.07	8.85	3337.00	19	109	104	113
G050C	29	29	76	145	69	94.00	15.52	2726.00	20	82	79	91	29	29	109	133	24	115.66	4.98	3354.00	14	112	109	115
G052A	29	29	95	183	88	144.10	27.24	4179.00	23	183	95	142	29	29	113	230	117	156.55	26.10	4540.00	25	152	113	152
G052B	29	29	90	227	137	147.48	30.67	4277.00	27	108	90	145	29	29	103	230	127	154.00	26.33	4466.00	26	141	103	149
G052C	29	29	91	194	103	141.62	27.38	4107.00	25	129	91	134	29	29	99	227	128	169.69	26.77	4921.00	27	159	99	168
G055A	22	22	84	178	94	137.91	29.20	3034.00	20	166	84	137	22	22	107	177	70	131.18	15.83	2886.00	20	121	107	126
G055B	32	32	70	254	184	132.09	38.71	4227.00	29	120	70	121	32	32	95	167	72	125.72	17.39	4023.00	26	109	95	123
G055C	28	28	66	211	145	135.50	38.99	3794.00	26	125	66	126	28	28	85	163	78	110.04	15.89	3081.00	23	92	85	107
G057A	28	28	62	197	135	116.68	34.23	3267.00	25	88	62	107	28	28	87	166	79	126.89	17.32	3553.00	24	110	87	128
G057B	29	29	67	192	125	119.38	33.03	3462.00	28	81	67	114	29	29	97	170	73	136.28	22.46	3952.00	24	142	97	142
G057C	27	27	60	240	180	140.59	53.40	3796.00	27	60	60	132	27	27	85	252	167	167.37	52.43	4519.00	25	167	85	167
G061A	28	28	94	179	85	137.50	24.43	3850.00	23	123	94	136	28	28	100	199	99	136.75	24.48	3829.00	24	109	100	134
G061B	29	29	105	200	95	144.21	24.24	4182.00	25	143	105	145	29	29	106	203	97	138.21	25.13	4008.00	23	111	106	129
G061C	27	27	110	199	89	137.22	24.07	3705.00	23	117	110	125	27	27	116	177	61	137.00	16.84	3699.00	19	127	116	130
G062A	30	30	82	220	138	138.93	30.69	4168.00	28	125	82	133	30	30	102	194	92	139.63	16.66	4189.00	24	142	102	138
G062B	28	28	88	200	112	131.32	31.49	3677.00	24	117	88	121	28	28	97	158	61	121.14	14.56	3392.00	20	115	97	116
G062C	28	28	89	192	103	128.11	29.44	3587.00	23	92	89	122	28	28	88	156	68	120.39	18.39	3371.00	24	128	88	120
G064A	28	28	158	254	96	213.54	27.54	5979.00	27	238	158	217	28	28	165	243	78	211.07	16.51	5910.00	21	221	165	209
G064B	28	28	90	202	112	145.43	33.05	4072.00	27	93	90	141	28	28	108	177	69	143.71	17.90	4024.00	25	151	108	145
G064C	28	28	137	254	117	196.68	32.84	5507.00	25	151	137	202	28	28	137	228	91	191.82	20.88	5371.00	23	194	137	194
G065A	27	27	78	193	115	123.48	29.31	3334.00	25	135	78	125	27	27	78	174	96	119.04	24.12	3214.00	21	113	78	112
G065B	28	28	81	199	118	123.93	35.08	3470.00	26	96	81	110	28	28	91	154	63	119.96	16.47	3359.00	25	109	91	118

G065C	28	28	68	195	127	127.89	30.44	3581.00	23	134	68	134	28	28	83	145	62	108.54	14.04	3039.00	22	113	83	109
G067A	20	20	84	164	80	119.65	24.02	2393.00	18	103	84	110	20	20	114	199	85	156.45	24.62	3129.00	17	114	130	154
G067B	28	28	82	210	128	135.36	36.30	3790.00	26	120	82	122	28	28	96	191	95	140.00	20.09	3920.00	23	114	96	139
G067C	28	28	88	241	153	138.29	40.76	3872.00	25	89	88	127	28	28	125	185	60	156.04	16.05	4369.00	24	136	125	159
G069A	29	29	71	154	83	107.41	20.31	3115.00	22	106	71	106	29	29	77	127	50	101.28	12.47	2937.00	21	102	77	102
G069B	29	29	56	128	72	92.10	18.92	2671.00	23	94	56	94	29	29	55	83	28	68.55	7.10	1988.00	19	66	55	68
G069C	28	28	63	189	126	118.11	30.71	3307.00	25	88	63	116	28	28	79	152	73	112.25	15.45	3143.00	25	100	79	111
G070A	29	29	64	186	122	99.21	30.78	2877.00	25	64	75	91	29	29	75	211	136	116.90	36.25	3390.00	27	78	75	108
G070B	28	28	58	220	162	120.18	43.67	3365.00	27	99	58	112	28	28	61	172	111	104.29	26.07	2920.00	26	107	61	107
G070C	30	30	72	177	105	108.97	22.35	3269.00	25	119	77	106	30	30	101	198	97	127.37	20.19	3821.00	24	113	101	123
G071A	28	28	95	246	151	140.64	37.39	3938.00	25	97	95	134	28	28	122	238	116	167.61	30.57	4693.00	23	157	122	158
G071B	27	27	57	198	141	115.93	36.26	3130.00	25	74	57	122	27	27	103	191	88	135.37	23.68	3655.00	24	111	103	131
G071C	32	32	79	243	164	157.16	41.21	5029.00	27	157	79	157	32	32	131	182	51	157.53	14.18	5041.00	26	154	131	154
G072A	28	28	72	144	72	103.32	20.22	2893.00	26	88	72	96	28	28	88	144	56	106.18	11.46	2973.00	20	101	88	103
G072B	28	28	75	140	65	100.25	19.54	2807.00	21	93	75	93	28	28	96	128	32	112.54	9.12	3151.00	20	117	96	112
G072C	29	29	69	142	73	88.83	15.91	2576.00	22	82	76	85	29	29	93	120	27	102.24	6.95	2965.00	13	98	101	101
G073A	29	29	115	227	112	164.79	29.97	4779.00	26	132	115	161	29	29	121	204	83	160.83	22.78	4664.00	26	129	121	157
G073B	28	28	119	235	116	165.54	30.74	4635.00	25	131	119	161	28	28	124	204	80	168.00	24.20	4704.00	27	140	124	169
G073C	28	28	130	221	91	176.57	24.44	4944.00	22	144	130	175	28	28	142	197	55	170.29	13.23	4768.00	22	157	142	170
G074A	8	8	42	128	86	75.25	24.37	602.00	8	42	42	66	8	8	62	114	52	85.13	20.34	681.00	6	62	81	73
G074B	29	29	49	152	103	93.93	22.57	2724.00	25	88	49	89	29	29	83	166	83	116.90	18.12	3390.00	23	106	83	117
G074C	30	30	77	138	61	103.00	15.48	3090.00	24	93	77	103	30	30	89	149	60	118.17	14.30	3545.00	26	107	89	115
G076A	30	30	51	115	64	66.97	16.71	2009.00	19	57	55	60	30	30	55	106	51	65.43	10.41	1963.00	17	61	55	62
G076B	28	28	62	107	45	78.07	13.13	2186.00	18	65	62	75	28	28	62	117	55	77.68	12.95	2175.00	21	66	62	73
G076C	28	28	69	164	95	94.64	20.89	2650.00	23	77	69	87	28	28	59	93	34	76.36	6.75	2138.00	18	76	59	76
G077A	29	29	111	235	124	172.14	30.38	4992.00	25	162	111	167	29	29	107	215	108	157.24	25.17	4560.00	26	152	107	155
G077B	22	22	111	254	143	166.32	36.32	3659.00	20	191	111	158	22	22	94	215	121	159.86	28.64	3517.00	22	94	94	156
G077C	29	29	101	240	139	169.48	32.42	4915.00	24	176	101	176	29	29	117	207	90	146.72	18.08	4255.00	23	141	117	142
G078A	29	29	80	254	174	171.62	48.06	4977.00	27	105	80	175	29	29	73	230	157	137.59	33.80	3990.00	24	136	73	137
G078B	29	29	74	227	153	146.62	37.73	4252.00	27	148	74	157	29	29	96	199	103	151.07	23.88	4381.00	25	138	96	150
G078C	26	26	103	218	115	151.54	33.58	3940.00	22	103	105	147	26	26	119	202	83	155.42	17.39	4041.00	20	156	119	156
G079A	28	28	73	152	79	117.61	18.51	3293.00	23	105	73	114	28	28	76	141	65	102.43	14.10	2868.00	22	100	76	100
G079B	29	29	75	220	145	131.55	35.85	3815.00	27	121	75	121	29	29	78	165	87	116.35	23.11	3374.00	25	106	78	113
G079C	27	27	72	160	88	115.56	24.27	3120.00	21	112	72	112	27	27	75	148	73	101.70	17.12	2746.00	21	108	75	100
G080A	26	26	82	205	123	145.39	33.67	3780.00	23	116	82	137	26	26	93	200	107	145.19	25.12	3775.00	22	118	93	140
G080B	29	29	81	224	143	135.38	41.98	3926.00	27	92	81	123	29	29	75	205	130	135.72	27.81	3936.00	27	100	75	136
G080C	27	27	80	241	161	156.78	38.84	4233.00	26	139	80	154	27	27	94	191	97	140.78	20.98	3801.00	24	127	94	144
G098A	27	27	65	146	81	77.52	16.88	2093.00	18	71	65	73	28	28	90	165	75	99.93	13.80	2798.00	17	93	90	95
G098B	30	30	64	236	172	79.40	30.40	2382.00	19	69	64	71	27	27	90	166	76	98.52	14.28	2660.00	14	93	91	95
G098C	29	29	64	119	55	72.38	10.39	2099.00	15	68	64	69	29	29	86	96	10	91.79	2.60	2662.00	8	92	86	92
G099A	30	30	96	254	158	172.30	44.05	5169.00	27	105	96	167	28	28	106	236	130	148.71	30.01	4164.00	22	130	106	136
G099B	27	27	106	209	103	142.70	29.94	3853.00	24	110	106	134	28	28	119	210	91	161.93	23.21	4534.00	24	166	119	161
G099C	29	29	114	238	124	181.66	33.46	5268.00	27	129	114	182	29	29	139	236	97	182.90	22.72	5304.00	26	163	139	186
G102A	27	27	116	189	73	150.37	21.54	4060.00	23	157	116	147	27	27	103	182	79	127.30	18.68	3437.00	22	129	103	122
G102B	28	28	100	246	146	146.75	35.31	4109.00	25	100	105	142	28	28	91	215	124	147.00	27.07	4116.00	23	132	91	144
G102C	30	30	92	217	125	146.10	37.73	4383.00	26	151	92	143	30	30	90	203	113	138.97	27.98	4169.00	28	124	90	136
G105A	29	29	87	236	149	158.17	36.12	4587.00	24	144	87	160	29	29	149	218	69	173.00	16.18	5017.00	20	158	150	172
G105B	28	28	82	201	119	154.86	27.42	4336.00	24	129	82	149	28	28	121	166	45	143.89	10.93	4029.00	22	126	121	144
G105C	29	29	93	183	90	140.52	21.77	4075.00	23	137	93	137	29	29	134	174	40	151.79	11.14	4402.00	21	160	134	151
G108A	28	28	91	254	163	200.57	32.81	5616.00	26	173	91	205	28	28	157	233	76	189.29	17.15	5300.00	24	183	157	189
G108B	27	27	142	254	112	187.63	24.43	5066.00	23	172	142	183	27	27	117	161	44	140.89	10.81	3804.00	20	149	117	142
G108C	28	28	110	227	117	177.68	26.45	4975.00	28	110	110	175	28	28	117	172	55	143.68	13.61	4023.00	23	137	117	140
G110A	30	30	86	241	155	170.70	37.09	5121.00	27	156	86	167	30	30	107	232	125	166.83	28.24	5005.00	22	154	107	166
G110B	27	27	97	215	118	148.33	32.57	4005.00	24	107	97	142	27	27	102	180	78	142.96	21.43	3860.00	21	130	102	141
G110C	29	29	103	253	150	158.83	39.20	4606.00	26	113	103	157	29	29	97	233	136	162.21	35.39	4704.00	25	134	97	162
G112A	28	28	62	200	138	122.36	30.27	3426.00	26	123	62	118	28	28	103	179	76	131.43	18.21	3680.00	23	128	106	129
G112B	21	21	72	183	111	111.52	35.03	2342.00	21	72	72	105	21	21	74	160	86	111.81	19.48	2348.00	16	94	74	106

G112C	27	27	65	246	181	135.67	48.13	3663.00	24	97	65	133	27	27	81	172	91	119.07	25.10	3215.00	21	87	81	112
G114A	28	28	147	254	107	224.29	33.37	6280.00	17	254	147	233	28	28	175	244	69	219.32	17.48	6141.00	23	216	175	217
G114B	29	29	55	254	199	234.35	40.19	6796.00	12	254	55	254	29	29	163	254	91	217.52	26.36	6308.00	24	178	163	228
G114C	27	27	102	108	6	104.67	1.81	2826.00	7	104	108	104	27	27	107	131	24	117.48	6.23	3172.00	15	121	107	118
G116A	28	28	101	228	127	150.39	31.34	4211.00	24	129	101	143	28	28	112	234	122	139.25	27.31	3899.00	23	126	113	133
G116B	16	16	109	189	80	151.06	19.10	2417.00	13	129	109	148	16	16	105	140	35	117.31	10.50	1877.00	13	111	105	113
G116C	29	29	105	228	123	166.21	24.33	4820.00	27	167	105	167	29	29	105	148	43	121.35	10.08	3519.00	20	108	105	123
G118A	29	29	75	213	138	130.45	33.78	3783.00	22	94	75	131	29	29	120	169	49	140.66	12.88	4079.00	22	129	120	138
G118B	28	28	78	239	161	143.86	35.66	4028.00	25	116	78	138	28	28	128	179	51	147.36	12.70	4126.00	21	148	128	146
G118C	29	29	72	216	144	151.76	34.76	4401.00	27	132	72	151	29	29	121	164	43	142.55	11.60	4134.00	24	142	121	142
G120A	27	27	106	254	148	183.93	37.11	4966.00	26	180	106	176	27	27	123	246	123	186.00	35.57	5022.00	25	132	123	194
G120B	29	29	125	250	125	178.83	33.76	5186.00	24	139	125	178	29	29	122	252	130	167.35	32.50	4853.00	25	122	132	156
G120C	28	28	134	254	120	202.32	32.86	5665.00	24	181	134	200	28	28	138	237	99	189.54	24.55	5307.00	23	206	138	193
G123A	27	27	94	204	110	140.85	32.53	3803.00	25	108	94	139	27	27	94	189	95	121.93	20.00	3292.00	22	108	94	117
G123B	28	28	96	226	130	141.29	32.01	3956.00	27	111	96	132	28	28	95	201	106	146.75	27.22	4109.00	23	139	95	139
G123C	28	28	101	202	101	141.21	29.51	3954.00	23	126	101	126	28	28	108	204	96	142.21	24.84	3982.00	23	115	108	134
G125A	19	19	89	204	115	133.21	32.85	2531.00	19	89	89	132	19	19	98	203	105	147.90	30.59	2810.00	18	161	98	148
G125B	27	27	64	220	156	121.07	36.27	3269.00	21	75	64	114	27	27	84	204	120	130.96	31.05	3536.00	23	113	84	122
G125C	27	27	72	233	161	137.41	49.14	3710.00	25	80	72	126	27	27	91	200	109	137.52	28.00	3713.00	24	96	91	135
G126A	28	28	93	234	141	168.04	35.79	4705.00	24	147	93	160	28	28	105	205	100	155.75	22.47	4361.00	23	151	105	153
G126B	28	28	111	217	106	172.68	22.69	4835.00	23	180	111	177	28	28	128	196	68	163.89	14.43	4589.00	23	164	128	163
G126C	29	29	107	236	129	155.41	35.57	4507.00	28	126	107	145	29	29	134	233	99	182.00	23.46	5278.00	18	164	134	179
G129A	26	26	56	213	157	124.23	40.76	3230.00	24	125	56	121	26	26	74	182	108	105.46	25.56	2742.00	21	87	74	98
G129B	26	26	53	163	110	105.73	26.64	2749.00	21	78	53	101	26	26	74	143	69	103.85	18.93	2700.00	21	83	74	97
G129C	26	26	52	169	117	99.38	29.27	2584.00	22	78	52	90	26	26	74	149	75	103.77	20.48	2698.00	23	87	74	98
G130A	28	28	82	247	165	158.54	46.86	4439.00	27	157	82	151	28	28	117	234	117	177.71	32.03	4976.00	27	171	117	174
G130B	29	29	114	234	120	177.14	28.39	5137.00	27	168	114	178	29	29	136	242	106	190.93	26.13	5537.00	27	176	136	196
G130C	30	30	109	201	92	162.27	25.70	4868.00	27	129	109	164	30	30	121	188	67	155.57	18.11	4667.00	21	124	121	151
G135A	19	19	126	254	128	171.47	37.69	3258.00	17	126	129	160	19	19	112	205	93	149.32	23.02	2837.00	18	150	112	148
G135B	28	28	81	254	173	150.57	49.17	4216.00	22	82	81	143	28	28	115	169	54	137.93	16.50	3862.00	23	134	115	134
G135C	27	27	84	242	158	122.96	30.40	3320.00	23	97	84	117	27	27	114	189	75	155.33	18.30	4194.00	24	167	114	158
G136A	29	29	99	185	86	121.69	23.40	3529.00	21	105	99	115	29	29	94	218	124	138.10	31.64	4005.00	26	126	94	135
G136B	21	21	75	131	56	100.86	17.39	2118.00	18	80	75	96	21	21	106	186	80	135.05	18.72	2836.00	17	120	106	132
G136C	29	29	76	254	178	121.35	39.88	3519.00	28	95	76	110	29	29	103	194	91	135.97	21.72	3943.00	26	137	103	132
G137A	28	28	80	248	168	144.25	46.66	4039.00	26	90	80	128	28	28	88	207	119	154.43	28.94	4324.00	24	141	88	146
G137B	20	20	78	254	176	138.20	60.22	2764.00	19	79	78	112	20	20	94	221	127	137.35	36.68	2747.00	18	132	94	128
G137C	28	28	66	245	179	133.89	50.90	3749.00	26	74	66	111	28	28	94	207	113	140.93	29.20	3946.00	25	123	94	133
G143A	25	25	77	243	166	138.84	44.96	3471.00	23	100	77	133	25	25	86	148	62	118.68	19.35	2967.00	20	103	86	112
G143B	27	27	72	207	135	101.22	26.66	2733.00	21	78	72	96	27	27	79	198	119	117.07	24.74	3161.00	23	89	79	119
G143C	28	28	75	229	154	104.75	32.79	2933.00	23	95	75	95	28	28	80	183	103	123.11	27.91	3447.00	26	92	80	129
G147A	29	29	119	245	126	166.52	27.67	4829.00	26	152	119	162	29	29	108	247	139	175.14	41.04	5079.00	27	135	108	174
G147B	29	29	119	224	105	174.66	34.22	5065.00	27	199	119	174	29	29	91	238	147	180.79	43.12	5243.00	27	174	91	187
G147C	30	30	106	244	138	192.20	33.19	5766.00	26	159	106	193	30	30	115	249	134	191.70	34.00	5751.00	24	141	115	189
G148A	28	28	78	166	88	119.25	28.48	3339.00	24	81	78	113	28	28	91	186	95	126.82	24.45	3551.00	25	100	91	126
G148B	29	29	85	238	153	139.59	36.92	4048.00	26	103	85	133	29	29	95	168	73	133.79	15.77	3880.00	25	123	95	134
G148C	29	29	75	196	121	122.45	35.08	3551.00	25	91	75	113	29	29	84	171	87	121.31	19.12	3518.00	26	115	84	118
G999A	27	27	105	214	109	134.74	25.48	3638.00	24	105	107	138	27	27	116	166	50	137.63	13.66	3716.00	21	154	116	138

768000 772000 776000 780000 784000 788000

3273000 3270000 3267000 3264000 3261000

Harvey Cutoff

Spoonbill Bay

Three Bayou Bay

Turtle Bay

Long Bay

Bay L'Ours

Little Lake

Brusle Lake

Round Lake

Bay Dosgris

Old Grand Bayou

Grand Bayou

Coffee Bay

Saint Joseph Bay

768000 772000 776000 780000 784000 788000

3273000 3270000 3267000 3264000 3261000

N

0 0.5 1 2 3 4 Kilometers

Notes:
1998 DOQQ Imagery from LAGIS website
Side scan sonar collected June & July 1999
UTM Zone 15 North, NAD83

500 kHz Side Scan Sonar
Little Lake, Barataria Bay, LA

768000 772000 776000 780000 784000 788000

3273000 3270000 3267000 3264000 3261000

Harvey Cutoff

Spoonbill Bay

Three Bayou Bay

Turtle Bay

Long Bay

Bay L'Ours

Little Lake

Brusle Lake

Round Lake

Bay Dosgris

Old Grand Bayou

Grand Bayou

Coffee Bay

Saint Joseph Bay

N

0 0.5 1 2 3 4 Kilometers

Notes:
1998 DOQQ Imagery from LAGIS website
Side scan sonar collected June & July 1999
UTM Zone 15 North, NAD83

LEGEND

- Potential Shell Bed
- Intense Prop/Trawl Scar
- Moderate Prop/Trawl Scar
- Relic Channel/Levee Systems
- Dredged Channel
- Pipeline
- Tidal Channel

Lakebed Features
500 kHz Side Scan Sonar
Little Lake, Barataria Bay, LA

VITA

Michelle Greene was born in Salt Lake City, Utah. She is the daughter of Chad and Linda Greene and the sister of Catherine Gardner and Stephan Douglas Greene. She graduated from Olympic High School in 1989 and attended the University of Washington starting in the Fall of 1989. In the Summer of 1995, Michelle received her Bachelor of Science degree with a double major in oceanography and geology. She has worked in the professional oceanographic field for the past six years for the United States Geological Survey Marine and Coastal Surveys, and two divisions within the Fugro Group (Seafloor Surveys International and Fugro Chance). Michelle also worked as a Student Research Assistant at Louisiana State University for Dr. Harry Roberts of the Coastal Studies Institute. Michelle recently married Sean McDonald of Halifax, Nova Scotia, Canada, where they currently reside with their son Liam Indigo McDonald.